Title
Land Use in Renewable Energy Planning

Author
Wu, Grace C

Publication Date
2018

Peer reviewed|Thesis/dissertation

Land Use in Renewable Energy Planning

by

Grace C Wu

A dissertation submitted in partial satisfaction of the

requirements for the degree of

Doctor of Philosophy

in

Energy and Resources

in the

Graduate Division

of the

University of California, Berkeley

Committee in charge:

Professor Margaret S. Torn, Chair
Professor Duncan Callaway
Professor Jeffrey Q. Chambers

Spring 2018

Land Use in Renewable Energy Planning

Abstract

Land Use in Renewable Energy Planning

by

Grace C Wu

Doctor of Philosophy in Energy and Resources

University of California, Berkeley

Professor Margaret S. Torn, Chair

All forms of energy generation can have intensive or extensive land use requirements, causing habitat and biodiversity loss in sensitive and diverse ecosystems globally. With the rapid transformation and growth of the energy sector in countries worldwide, understanding the impacts of past practices and charting the trajectory of future development projects is imperative for preventing negative environmental consequences. This dissertation contributes modeling strategies for integrating environmental impacts in renewable energy planning processes and spatially-explicit empirical methods for identifying and quantifying land use and land cover impacts related to renewable energy development.

To explore land use and energy conflicts in a jurisdiction that is in the midst of a large-scale low-carbon energy transition, I ask the following: (1) is it possible to meet California's ambitious renewable energy targets without using high conservation-value land? (2) what are the system costs of low-impact renewable energy development? I find that while trade-offs between conservation value and renewable resource quality exist, restricting development to low-impact land is not only possible, but incurs only negligible economic cost increases. Given this possibility, I use California as a case study to identify decision-making opportunities in energy planning processes for integrating conservation and land use values and avoiding conservation-climate conflicts.

Extending the spatial methods developed for California to countries in Africa that are planning renewable energy expansion, I ask, what is the potential for low-environmental-impact, socially-responsible, and cost-effective development of wind and solar energy in emerging economies in Africa? Using a multi-criteria analysis approach, I find that "no-regrets" options—specifically areas that are low-cost, low-environmental impact, and highly accessible—exist such that significant fractions of demand can be quickly served with low-impact resources without large additional cost.

Despite the magnitude and pace of hydropower expansion in highly biodiverse aquatic and terrestrial ecosystems in Southeast Asia, Africa, and Latin America, the potential indirect land use and land cover change resulting from hydropower development is poorly understood. To fill this gap, I ask, what are the indirect deforestation and land use impacts of utility-scale

hydropower development in the Brazilian Amazon? Do siting choices and pre-existing land use and land cover affect the extent of the impact? Using scalable remote sensing and spatial econometric methods for causal inference, I find a 11-59% increase in indirect deforestation due to hydropower development. These findings can contribute to estimates of potential future terrestrial impacts from the hundreds of hydropower plants planned and proposed in relatively intact areas of the Brazilian Amazon.

To my teachers, advisers, and mentors

"What I stand for is what I stand on" – Wendell Berry
"Never lose a holy curiosity" – Albert Einstein

Contents

List of Figures

List of Tables

Acknowledgments

It has often been said that ERG is a place of steadfast self-determination. Yet, there is little doubt in my mind that I would have had little to self-determine if it were not for the essential opportunities, support, and guidance I received from so many mentors, colleagues, and friends at ERG, UC Berkeley, and beyond.

This dissertation would not have been possible without the encouragement and advice of my dissertation committee members—Margaret Torn, Duncan Callaway, and Jeff Chambers. I am immensely grateful to Margaret for her generosity in sharing her time, expansive knowledge, deep wisdom. I remember many brainstorming strolls in the hills of North Berkeley during which she would graciously and seriously entertain my myriad, ambitious—and sometimes, wild—research ideas. I benefited from her knack for asking the right questions and never forgetting the forest for the trees. Like a true ERGie, Margaret always demonstrated deep curiosity and concern about topics far afield from her own. With a rare ability to balance big-picture policy impact with scientific rigor and depth, Margaret's embodiment of the ERGie spirit has and continues to be my inspiration that it is possible to successfully wear multiple hats.

I have always been amazed and impressed with Duncan's cautious enthusiasm. From Duncan, I learned the art of crafting projects around a central, accessible storyline, but maintaining grounding in a clear academic contribution. Duncan somehow grasped my perennial (ERGie) struggle between the practical and the academically novel and always provided advice with the right blend of skepticism and excitement—leading to both scientific rigor and practical, game-changing potential.

I have Jeff to thank for introducing me to the wonder, power, and pitfalls of remote sensing. He set me on course for fruitful experimentation in a vast new research area. Jeff's enthusiasm for interesting questions and focus on devising the most elegant and parsimonious methods for answering them has been a constant reminder that the reward of research lies beyond the weeds.

I owe special thanks to Jim Williams, who teamed up with Margaret to introduce me to the land use and energy dilemma in California. Thanks to Jim, Margaret, and colleagues at E3, I cultivated a fruitful collaboration with The Nature Conservancy and was exposed to an array of topics that will keep me busy throughout my postdoctoral years and beyond. Because of Jim's candid feedback on my first paper, he set me on the path to writing with the audience, and not my ego, in mind.

Each project in my dissertation benefited from the keen insight of several collaborators. Erica Brand at the Nature Conservancy helped me to devise a project that would have practical policy value and encouraged me to think both strategically and rigorously. Others at The Nature Conservancy—Dick Cameron, Brian Cohen, Laura Crane, and more recently Emily Leslie—have shown me how the right blend of science and policy can lead to practical action. I have very fond memories of working with Kudakwashe Ndhlukula and Tijana Radjoicic during their time at IRENA. From them, I learned about the difficult but important work of persistent stakeholder engagement. For the last chapter, I am indebted to Van Butsic,

who I wish I had met much earlier in my time at UC Berkeley, for generously and patiently teaching me econometrics and for sharing his deep knowledge of land use change and its drivers. I am grateful to Nick Clinton and others from the Google Earth Engine (GEE) team who generously offered advice and GEE asset space, enabling remote sensing analysis at scales that would not have been possible otherwise. Nearly every project I have worked on in my time at ERG has benefited from Ranjit Deshmukh's encouragement and insightful thinking. His optimism and creativity have saved many a project from a morass of paralyzing confusion and complexity.

Throughout my time at UC Berkeley, I am lucky to have received generous financial support from many funders, including NSF Graduate Research Fellowship Program, UC Berkeley, International Energy Studies Group at LBNL, International Renewable Energy Agency, International Rivers, Philomathia Foundation, and The Nature Conservancy.

Many people played important roles in bringing me to ERG. Pomona Professors Rick Hazlett and Jonathan Wright, whose combination of academic rigor, holy curiosity, and deep love of the natural world inspired me to pursue and create knowledge to preserve the intrinsic value of all living and non-living things, and without whom I would never have considered undertaking a PhD. Jessica Hellmann recognized the potential in me and encouraged me to pursue graduate studies. Her ability to make science accessible and meaningful for the public was my first exposure to scholar activism.

I have been very lucky to have a community of friends and colleagues who have rooted for me, believed in me, and inspired me. Thanks to my fellow ERG '13 cohort—Sasha, JP, Dan, Deepa, Heidi, Ranjit, Nikhil, Justin, Mark—for camaraderie and friendship. Other ERGies friends include Jess Reilly, Diego Ponce de Leon Barido, Veronica Jacome, Kripa Jagannathan, Nikky Avila, Chris Hyun, Michaelangelo Tabone, Rebekah Shirley, Danielle Svehla Christanson. Their friendship has given the day-to-day a sense of meaning and satisfaction more enduring than the frenetic ebbing and waning of work and research. Sharada Prasad deserves special thanks for making sure that I occasionally soaked in the joy of the PhD journey, knowing that I had a strong tendency to fixate on the final outcome. His indomitable spirit, indiscriminate eating habits, zeal for life, and ability to get into trouble have no equals (though the "Sharadas" of subsequent cohorts—Justin, Diego, Vero—do come strikingly close). Throughout these years, "Sharada" has become synonymous with "friendship" for me. Kay Burns deserves special recognition because she is the reason the ERG community feel like family for me. Kay's the glue that keeps us all together.

In my first year at ERG, I discovered meditation, which proved to be my most reliable antidote for grad-school-induced neurosis. I slowly cultivated my practice over these last several years with help and encouragement from the community at the Berkeley Buddhist Monastery (BBM). I am grateful to BBM for Friday night sutra lectures, quiet meditation mornings, and pointing the Way.

My parents—Jessie and Jeffrey—taught me persistence, patience, and fortitude, all of which proved essential in making it through this PhD journey. Their love and desire for me to have a better future propelled them on a journey from Taiwan to California almost exactly 28 years ago. I have only started to realize the extent of their sacrifice. Their constant

care and support—though often expressed in unorthodox ways by Western standards—never wavered.

My final words of appreciation go to Ranjit Deshmukh, without whom this PhD journey would have been far less joyous, humorous, and wondrous. Thank you, Ranjit, for being my partner, friend, and colleague, and for giving my life meaning beyond measure.

Chapter 1

Land use in renewable energy planning

"Buy land, they're not making it anymore" — Mark Twain

"Location, location, location" — Unknown

1.1 The scale and extent of land-energy connections

To date, the greatest drivers of land use change and habitat loss have been agriculture, forestry, mining, and urbanization (Ellis, 2011); energy land-use requirements have thus far been low—standing at about 2% of land globally (Fritsche et al., 2017). Yet, ambitious low-carbon transitions are underway in many developed countries—requiring expansion of renewable energy generation facilities—and the growth in energy demand in emerging economies is being met with rapid energy development—increasingly of renewable technologies such as wind, solar, and bionergy. These recent developments suggest the potential for "energy sprawl" (McDonald et al., 2009) to be another significant driver of habitat and biodiversity loss world-wide (Trainor, McDonald, and Fargione, 2016). From 2011 to 2016, the amount of renewable energy capacity additions exceeded fossil fuel generating capacity globally (IEA, 2017). In 2016, the share of newly installed renewable capacity (biomass, geoethermal, hydropower, solar, wind) was 61.5% of the total in the U.S. (FERC, 2016). Studies suggest that if the U.S. is to meet deep decarbonization targets of 80% reduction in greenhouse gas emissions by 2050, the transition will require approximately 1500 GW of wind capacity and 750 MW of solar photovoltaic (PV) capacity—or about the land area of South Dakota including spacing between turbines and assuming all ground-mounted solar PV (Williams, Haley, et al., 2014). Thanks in large part to declining wind and solar costs and its widespread potential, the future of energy looks to be increasingly renewable (IEA, 2017).

In anticipation of the rapid rise of renewable technologies globally, an understanding of renewable energy's potential for changing large-scale land use patterns will be critical for mitigating any negative impacts. The direct land requirements of energy facilities is often used in life-cycle studies that compare the environmental impacts of energy systems (Fthenakis and Kim, 2009; Berrill et al., 2016). However, the direct land footprint of energy

facilities and feedstocks is an imperfect proxy for ecological impacts. It does not account for habitat fragmentation, microclimatic modifications, or indirect land use changes. For all technologies, siting of energy facilities to avoid or reduce impacts to important wildlife migration routes and critical habitat will largely dictate its impact to biodiversity (Lovich and Ennen, 2011). Proper siting, design, and operation of energy facilities are imperative for avoiding and mitigating negative impacts to biodiversity and other ecosystem services (UNEP, 2017). The case for responsible siting practices must consider and account for the trade-offs between conservation and other ecosystem values and project costs. Yet little is known about the degree to which potential high quality renewable energy—and hence, lower cost—resource areas conflict with high conservation value land.

The location of renewable energy facilities determine multiple important dimensions of renewable energy integration, including the performance, operations, direct costs, and system-wide costs. First, the total amount of electricity generated on an annual or longer-term basis is determined by an area's long-run average resource quality, which could vary significantly over geographic space. For example, the average wind speed (e.g., m/sec), insolation (e.g., $MWh/m^2/day$), or stream flow and hydraulic head (e.g., m^3/sec and meters) dictates how much absolute MWh of electricity can be extracted. Given that revenue from selling electricity is directly tied to quantity generated, project developers consider average resource quality one of the most important siting criteria. Second, the amount of renewable energy generation can vary considerably in time at multiple time scales (e.g., minutes, hourly, daily, or seasonally). Temporal variability of renewable resources plays an important role in large-scale renewable energy integration because the supply of electricity must be temporally balanced with the demand for electricity. Lastly, the location of generators—specifically, whether or not they are close to the place where electricity is ultimately consumed—determine the amount of other supporting infrastructure projects such as transmission lines and roads. Several studies have found that electricity systems with higher shares of variable renewable energy have more transmission capacity requirements (MacDonald et al., 2016; Berrill et al., 2016).

The choice of siting criteria could lead to dramatically different project locations, each having their own set of land-use and conservation impacts. In some cases, areas with the highest average resource quality may not be those whose temporal generation patterns are favorably matched with the temporal pattern of demand. In other cases, the highest average resource quality areas may be much further away from existing transmission infrastructure. Depending on the distribution of wildlife and important habitat across the landscape, conservation considerations can reinforce or conflict with energy-planning criteria. The balancing of siting criteria nuance the argument that scaling up renewable energy is only a matter of balancing risks between climate change threats to biodiversity and direct threats of habitat loss from infrastructure siting (Allison, Root, and Frumhoff, 2014). Frameworks proposed to address the conflicts between conservation, land use, and large-scale renewable energy has thus far failed to leverage the fact that different siting criteria are important to different energy planners and actors. This dissertation attempts to chart the missing linkages between multiple siting criteria including direct costs, system costs, land use, and conservation

impacts. It provides approaches for examining if and where energy development decision criteria are compatible with conservation criteria.

Human transformation of the landscape through energy extraction and its impacts on key ecosystem services are poorly understood and accounted for in the energy planning process. As regions undergo large-scale transitions from conventional and fossil fuel energy to renewable resources, information about environmental impacts and electricity generation trade-offs and synergies will be necessary to avoid environmentally damaging outcomes while meeting climate change goals. **The goal of this dissertation is to characterize and quantify past and possible future consequences of renewable energy power plant siting on land use and electricity-system costs.** This dissertation quantitatively assesses and compares the land use requirements and conservation-energy trade-offs of various low-carbon pathways (Chapter 2); develops an approach to integrate conservation considerations into existing renewable energy planning processes (Chapter 3); provides a methodology for examining the impact of various siting criteria for wind and solar energy on system-wide costs (Chapter 4); and evaluates the importance of difficult-to-quantify dimensions of indirect land use and land cover impact from hydropower development (Chapter 5).

The dissertation is focused on three key utility-scale technologies for renewable electricity generation—wind, solar, and hydropower. The chapters cover multiple geographic areas at various regional (Eastern and Southern Africa in Chapter 4) and subnational scales (California in Chapters 2-3, Brazilian Amazon in Chapter 5), with the choice of study area largely determined by the stage, ambition, and most prominent technologies in each jurisdiction's renewable energy transition. All study areas are on the cusp of either a significant growth in new energy development via renewable technologies (African countries, Brazil) or an ambitious fossil-to-renewable transition (California). Chapters 2-4 are modeling studies that combine geospatial information systems (GIS) approaches with renewable energy and power systems methods to anticipate the scale of land use impacts of future renewable energy systems (Chapters 2,3) and to examine the interlinkages of land use and energy-systems investment costs (Chapters 3,4). Chapter 5 is an empirical study using remote sensing and statistical, econometric techniques to estimate land use impacts of large-scale hydroelectricity generation in the Brazilian Amazon, a biodiversity and hydropower development hotspot. Taken together, the dissertation aims to inform the early stages of energy planning processes so as to simultaneously reduce land use and land cover impacts of renewable energy infrastructure and reduce siting barriers to achieving lower impact renewable energy development.

1.2 Land use of low-carbon electricity pathways and integrating land use in energy planning

The large-scale transition from conventional to low-carbon generation technologies presents new non-GHG environmental challenges. Historically, under a conventional-generation-dominated power system, land use and electricity occupied separate planning spheres. This

may have been due to the operational phase for conventional generation being spatially disaggregated, with the siting of power plants typically independent of the location of upstream processes such as mining (Kaza and Curtis, 2014; Smil, 2005). Because the land use footprint of a conventional power plant is minuscule relative to the energy it generates (Fthenakis and Kim, 2009), large-capacity conventional power plants could be sited with few constraints (primarily air quality related). Renewable energy technologies, on the other hand, spatially concentrate their operational phases, making their power plant footprints larger, and have generation characteristics that are inherently tied to location and siting choices, making their rapid growth as much a landscape integration problem as it does a grid integration problem (Smil, 2005; Outka, 2011). These new challenges of renewable energy development require revisions to the way that land use is considered in energy planning. Chapters 2 and 3 provide one way to integrate land use and conservation considerations in the energy planning process and identify key challenges and tradeoffs between land use and energy planning.

Limited land in areas where low-carbon electricity will be in high demand could constrain cost-effective or ecologically sound energy infrastructure development. Chapter 2 contributes an understanding of land-use related constraints and challenges of achieving low-carbon transitions. With legally binding renewable energy generation targets of 33% by 2020 and 50% by 2030, and a target currently in legislation of 100% by 2050, California is used as a case study because of the strong policy imperative. The large number of failed permit applications for siting utility-scale solar and wind energy projects in California due to a broad range of aesthetic and ecological siting concerns strengthens the need for strategies to balance competing land uses (Kahn, 2000; Shirley, Shmidt, and Rogers, 2012). In a study conducted by the Division of Ratepayer Advocates, the average contract failure rate for renewable projects in California was 23% from 2002-2009, with siting and permitting reported as the cause for one-third of these failures (Shirley, Shmidt, and Rogers, 2012). Renewable resource patchiness in ways that poorly coincide with electricity load centers will require transmission line and substation expansion that have their own aesthetic and ecological challenges (Vajjhala and Fischbeck, 2007). California, with a human population of nearly 40 million, more species and more endemic species than any other state in the U.S., and the largest share of agricultural profits in the U.S., is ripe for land use competition related conflicts. In this chapter, I ask the following: (1) how much land is required to achieve different low-carbon generation scenarios in 2050 for California and is it possible to achieve renewable energy targets by avoiding land of conservation value? (2) To what extent do economic costs and conservation value conflict in these future scenarios? (3) To what extent will high resource quality land overlap between technologies?

Chapter 3 extends the scope and nearer-term policy value of Chapter 2 by asking whether and how California can simultaneously meet its conservation and climate goals by 2030 and importantly, explores the system cost implications of possible solutions. It develops a framework for integrating and evaluating land use and conservation considerations into a decision-support tool—the Renewable Portfolio Standard (RPS) Calculator—used by the California Public Utilities Commission (CPUC) for planning renewable energy projects. Chapter 3's analytical approach was developed after an informal charting of the multiple decision-making

points in renewable energy development in California, the key stakeholders, and their main decision criteria. An understanding of how energy development projects are conceived is necessary for better understanding how and why siting-related environmental impacts succeed or fail in being factored into the planning process (Mulvaney, 2017).

The initial charting process identified the critical role of transmission planning in the siting of new renewable energy projects in California. The portfolios of future generation projects necessary to meet California's renewable energy targets dictated where investments in transmission extensions and upgrades would be made. The RPS Calculator stood out as a key modeling tool for facilitating transmission planning efforts between multiple California energy agencies and actors. Without detailed environmental constraints on the renewable resources available for development, the RPS Calculator created energy portfolios with the majority of new solar PV projects sited in the desert southwest of California, an ecologically intact area relative to other suitable sites for development. These overall observations from the RPS Calculator—that unconstrained energy build-outs are more concentrated in the desert—are consistent with results from Chapter 2 regarding the possible locations of future renewable energy power plants. The goal of Chapter 3 is to understand how environmental constraints impact renewable resource availability, the spatial distribution of resources, and overall system costs, as well as assess the land-use related conservation impacts of entire energy portfolios, which can be used in the portfolio selection process.

1.3 Strategic siting of wind and solar projects to meet multiple objectives

Chapter 4 examines to what extent key challenges to renewables integration can be addressed by strategic, low-impact, and equitable siting of wind and solar power plants. In Chapter 4, I ask the following: (1) what is the potential for low-impact or cost-effective renewable energy development in Southern and Eastern Africa? (2) How does the consideration of multiple siting criteria—including land use—affect direct and system-wide costs? (3) What is the role of an international energy market in enabling optimal site selection and lowering system costs?

The case for multi-objective renewable energy siting in the African context rests on system costs and efficiency. In capital-strapped developing countries, the analysis, tools, and capacity to implement 'soft' and information-driven solutions to address the challenge of variable renewable energy integration, such as strategic siting and resource sharing through integrated electricity markets, are severely lacking yet much needed. As a region, Africa is in an unparalleled energy crisis rife with electricity deficiency, lack of access, and high costs (World Bank, 2014). How African countries and the international community tackle this crisis in the coming decades will have large social, environmental, and climate implications. One route is to continue financing large hydropower dams and fossil fuel power plants. Another route is to pursue renewable alternatives like wind and solar power in earnest. But

what will it take for wind and solar energy to be credible, lower-impact, and cost-competitive alternatives? Chapter 4 determines whether countries in the Eastern and Southern African Power Pools can pursue low-carbon electricity development in a cost-effective and low-impact way, and if so, where and how. Using a unique spatially- and temporally-explicit supply and demand dataset, the chapter evaluates solar and wind resource potential and its siting trade-offs for 21 countries in the Southern and Eastern Africa region.

1.4 Indirect land use impacts of hydropower siting

Chapter 5 examines the indirect deforestation and agricultural land use expansion impacts of utility-scale hydropower development, using the Brazilian Amazon as a case study region. Brazil has the second largest installed capacity of hydropower in the world, and energy planning since the mid 2000s has identified the Amazon as Brazil's final frontier for hydropower development (EPE, 2016). However, development of hundreds of planned hydropower plants in the Amazon could have severe and long-term unintended indirect environmental consequences. The siting of relatively "greenfield" hydropower plants and ancillary transmission and road infrastructure in areas of intact primary or secondary forest cover can play an important role in the opening up of the frontier for other land uses such as logging and agriculture (Barber et al., 2014). The vast majority of the existing literature on hydropower's freshwater and terrestrial impacts examines the direct loss of habitat resulting from flooding or river flow modifications (Benchimol and Peres, 2015; Alho, 2011), but little is known about the scale of indirect land use impacts of greenfield hydropower development projects. In Chapter 5, I ask the following question: How much indirect deforestation has resulted from hydropower development in the Brazilian Amazon?

Interest in drivers of indirect land use change (LUC) from energy development has thus far been restricted to bioenergy. Yet, the definition of indirect LUC from bioenergy is restrictive in that it specifically refers to LUC that occurs elsewhere (distal, not proximal) due to bioenergy crops displacing food crops, and LUC impacts are primarily driven by price effects or are market mediated. In the case of hydropower, indirect LUC could occur close to or far from the project location, depending on the mechanism, which may nor may not be market mediated. Previous studies on deforestation drivers in the Brazilian Amazon have shown that migrant workers who enter into short-term contracts during the construction phase of a hydropower project engage in exploitative activities such as illegal logging following project completion (Fearnside, 2008). As an example of displacement driven land use change, other studies have shown that reservoirs or flooding around the river could cause indirect land use change due to re-settlements or the substitution of river-based livelihoods disrupted by hydropower development (Orr et al., 2012; Tefera and Sterk, 2008).

Indirect LULC impacts of resource extractive activities such as mining and hydropower (Sonter, Barrett, et al., 2015) have been poorly quantified beyond single case study examples, precluding their use in quantitative estimates of proposed projects' impacts (see Sonter, Herrera, et al., 2017 for an exception). A consistent weakness of environmental im-

pact assessments (EIAs) is lack of quantitative projections for negative ecological and social consequences, particularly as dams are known to have spatially diffuse impacts that are only observable in the medium to long term (Andrade Meireles et al., 2013). Research of past projects is needed to support EIAs. Projections are most reliable when based on regionally generalizable trends situated within geographic contexts and trends best determined through analysis of large samples of past projects, which is typically cost or computationally prohibitive.

Large-scale spatial analysis and data collection from remotely sensed imagery is now possible due to the revolution in parallel computer processing and data storage on the cloud. Google Earth Engine (GEE) is one such scalable remote sensing analysis and image repository platform that allows rapid preprocessing and analysis of entire satellite mission archives (Gorelick et al., 2017). GEE overcomes desktop processing, storage, and human labor limitations, making it now possible to generate dense satellite image time series datasets over multiple, large areas. These datasets enable researchers to leverage spatial causal inference methods that are powerful yet data-intensive—requiring long time series, large samples, and/or matched controls. In Chapter 5, I use GEE and econometric methods to quantify deforestation and land use impacts of utility-scale hydropower plants in the Brazilan Amazon developed from 1984 to 2017, or within the Landsat mission time frame.

Chapter 2

Land use of low-carbon electricity pathways for California [1]

The land-use implications of deep decarbonization of the electricity sector (e.g., 80% below 1990 emissions) have not been well-characterized quantitatively or spatially. We assessed the operational-phase land-use requirements of different low-carbon scenarios for California in 2050 and found that most scenarios have comparable direct land footprints. While the per MWh footprint of renewable energy (RE) generation is initially higher, that of fossil and nuclear generation increases over time with continued fuel use. We built a spatially-explicit model to understand the interactions between resource quality and environmental constraints in a high RE scenario (>70% of total generation). We found that there is sufficient land within California to meet the solar and geothermal target, but areas with the highest quality wind and solar resources also tend to be those with high conservation value. Development of land with lower conservation value results in lower average capacity factors and higher generation costs, but also provides opportunity for co-location of different generation technologies, which could significantly improve land-use efficiency and reduce permitting, leasing, and transmission infrastructure costs. Basing siting decisions on long-term RE build-out requirements produces significantly different results, including better conservation outcomes, than implied by the current piecemeal approach to planning.

[1] This chapter was originally published as:

Wu, G.C., M.S. Torn, J. Williams. 2015. Incorporating Land-Use Requirements and Environmental Constraints in Low-Carbon Electricity Planning for California. *Environmental Science and Technology.* 10.1021/es502979v

The main content of the published paper has been placed in its entirety in the main body of the dissertation and the supporting information has been placed in its entirety in the Appendix of the dissertation.

2.1 Introduction

Recent studies indicate that incorporating very high (>70%) penetrations of low-carbon generation into the electricity grid by 2050 is both necessary to achieve deep economy-wide greenhouse gas (GHG) reductions, and feasible from a technical and cost perspective (Nelson et al., 2012; Williams, DeBenedictis, et al., 2012; Mai et al., 2012; Fripp, 2012; [EWIS] European Wind Integration Study, 2010; Bird and Milligan, 2012). However, these studies have not systematically explored the resource requirements and non-GHG environmental impacts of these scenarios, including land use.

Current land-use planning for electricity

Several energy resource potential and zoning studies have been conducted in the U.S. to anticipate and coordinate transmission expansion requirements in the next 10-15 years and also to increase the efficiency and speed of renewable energy (RE) development (California Public Utilities Commission [CPUC], 2009; Black & Veatch Corp. and NREL, 2009; Electricity Reliability Council of Texas (ERCOT), 2008; U.S. BLM and U.S. DOE, 2012. To facilitate "environmentally responsible" development on public land, several federal agencies have collectively produced a Solar Programmatic Environmental Impact Statement (Solar PEIS) for southwestern states (U.S. BLM and U.S. DOE, 2012). For strategic resource and load centers, efforts have recently been focused on higher resolution, regional studies, such as the landmark Desert Renewable Energy Conservation Plan (DRECP), a joint initiative charged with overseeing the siting of 22 GW-worth of RE projects in Southern California (Desert Renewable Conservation Plan, 2012). Stoms, Dashiell, and Davis (2013) developed an energy "compatibility index" metric based on degree of habitat degradation as a proxy for identifying valuable ecological resources (Stoms, Dashiell, and Davis, 2013). Although these and other studies (Stoms, Dashiell, and Davis, 2013; Kiesecker et al., 2011; Cameron, Cohen, and Morrison, 2012) have advanced integrated energy planning, their short-to-medium term planning horizon is a significant limitation in light of more recent, long-term deep-decarbonization goals. With few associated physical constraints, five to fifteen year implementation plans have historically been the norm in the electricity sector.

Low-carbon studies of California point to the electrification of many uses, especially in transportation, such that even with unprecedented energy efficiency, total electricity demand could increase by 50-100% (Williams, DeBenedictis, et al., 2012; Wei et al., 2013). For example, if this electricity demand is met with mostly RE, installed capacity of utility-scale photovoltaic (PV) and thermal concentrating solar power (CSP) could be 30 - 35 GW and 20 - 90 GW by 2050, respectively (Williams, DeBenedictis, et al., 2012; Mai et al., 2012). Based on published ranges for solar land-use factors (Ong, Campbell, and Heath, 2012; Ong, Campbell, Denholm, et al., 2013; R. R. Hernandez, Hoffacker, and Field, 2014), or the installed capacity per unit area, this would call for the conversion of 1400 to 3570 km^2 of land. Given the potential land-use impacts of solar and wind generation (Copeland et al., 2009; R. Hernandez et al., 2014; National Research Council, 2007) the integration

of such large quantities of new generation into the landscape, combined with competing demands for residential and agricultural land plus the conservation imperative for diverse and unique ecosystems, poses a challenge for ecologically sensitive land-use and electricity planning (Shirley, Shmidt, and Rogers, 2012; Kahn, 2000). Having one of the most ambitious RE targets in the U.S., California must be able to anticipate long-term land-use challenges and the dynamics of scaling up generation technologies to identify robust solutions. Policy and siting strategies that address potential conflicts in advance could expedite low-carbon development and reduce environmental impacts.

Given that deep-decarbonization goals will require sector-wide transformation, it is crucial that analyses treat the electricity sector as part of an integrated system, which calls for spatially incorporating multiple generation technologies, other electricity infrastructure, and conservation priorities into a single model. Previous publications on land-use impacts have treated technologies in isolation (Aydin, Kentel, and Duzgun, 2010; Dawson and Schlyter, 2012). In contrast, an integrated, scenario-based approach would allow evaluation of alternative build-outs—reflecting not only trade-offs and complementarity among technologies, but also different conservation value and land-use prioritization according to different stakeholders.

Objectives

The goal of this paper is to develop an integrated assessment of the land-use requirements for deep-decarbonization electricity scenarios and anticipate the land-use implementation challenges and opportunities of a high RE build-out in a spatially-explicit manner. We apply this approach to address three questions that have broad technical and policy relevance for any region that is planning high RE integration. California is used as the case study because of data availability and the policy imperative.

First, how much land is required to meet different low-carbon generation scenarios, and can California's goals be met primarily by RE without developing on environmentally sensitive lands? To understand the extent to which land could be a constraining factor, we estimate electricity land-use using operational-phase land-use factors and compare them with land availabilities modeled under different environmental constraint scenarios using a multi-criteria geographic information system (GIS) approach.

Second, how spatially distinct are RE development areas selected based on economic versus environmental criteria? Using resource quality and transmission distance as an indicator for economic costs, we assess the degree to which conservation and cost-effective development goals may conflict by characterizing differences in environmental constraint scenarios and the spatial relationship between resource quality, environmental sensitivity, and transmission and road connectivity. This analysis determines whether meeting conservation goals could warrant more proactive planning or if additional land may be needed for development.

Third, to what extent do suitable development areas for different technologies overlap under various sets of environmental constraints? We explore if and where areas can support deployment of multiple technologies, which could inform the choice of generation technology

Table 2.1: Environmental scoring classification scheme based on the WECC classification system for transmission30 and environmental constraint scenarios

"Ex" indicates scores excluded from each scenario.

Scoring Scheme		Environmental Constraint scenarios			
Score	Description	Least Stringent	3rd most	2nd most	Most Stringent
4	Legal Exclusions: Areas with legal restrictions against energy development, regardless of GAP status. This score strictly follows exclusions from previous planning studies.7,8,30,31	Ex	Ex	Ex	Ex
3.5	High Biodiversity Risk: All remaining GAP status 1 or 2 areas not included under Score 4 (private or public).		Ex	Ex	Ex
3	High Environmental Risk: Areas with some restrictions on energy development in order to maintain natural characteristics, areas of important cultural or historical value (mixed natural and human landscapes), and prime agricultural land. This score includes some GAP statuses 3 and 4 areas, and all "avoid" and "Category 2" areas identified in WREZ8 and RETI7 studies, respectively.			Ex	Ex
2	Medium Environmental Risk: Lands not listed as avoidance or Score 2 but have ecological or social value, including recreational areas, national forest land, other agricultural land, important bird areas (for wind only).				Ex
1	No known restrictions on energy development.				

or motivate innovative strategies such as co-location of technologies to produce hybrid wind-solar power plants.

2.2 Methods

Operational land-use requirements

We selected one recent study with which to examine probable electricity build-out scenarios for California in 2050 (Williams, DeBenedictis, et al., 2012). The study estimates generation and installed capacity using aggressive learning curves for the following corner scenarios: Baseline, Mixed, High Nuclear, High Renewables (RE), and High Carbon Capture and Sequestration (CCS). All low-carbon scenarios achieve 80% CO_{2e} reduction from 1990 levels (or a reduction to 85 Mt CO_{2e} from Baseline emissions of 875 Mt CO_{2e}) and are comparable in total generation, but produce at least an additional 120 TWh yr^{-1} of electricity over Baseline primarily due to the electrification of transportation (Williams, DeBenedictis, et al., 2012). Installed capacity is similar across the low-carbon scenarios, but is highest in the High RE scenario. See Supporting Information (Appendix A) Figure A.1 for estimates of

generation and installed capacity (Williams, DeBenedictis, et al., 2012). Appendix A Figure A.2 provides a visual overview of the methods in the present study.

To estimate annual average, operational-phase land requirements of the nine largest electricity generation technologies (Figure 2.1), we used annual generation estimates under each build-out scenario2 and empirical land transformation land-use factors for electricity generated (m^2 GWh^{-1}) assuming a 30-year plant lifetime (Appendix Table A.1; highlighted in yellow) (Fthenakis and Kim, 2009; Ong, Campbell, and Heath, 2012; Denholm, Hand, et al., 2009; Jordaan, 2010). All land-use factors represent operational-phase activities, which excludes indirect land impacts associated with energetic inputs or the production, manufacturing, or transportation of capital goods. Included are direct land use associated with the power plant; mining, drilling, and extraction of fuels; and the pipeline transport of the fuel. For non-bioenergy renewable technologies, the power plant's land use represents the entire operational-phase land use. All reported values in this present study represent "land transformation," or land that is "altered from a reference state" per unit of electricity generation (m^2 GWh^{-1}) or installed capacity (m^2 GW^{-1}). We do not apply land occupation metrics, which account for the duration that the land is under use (e.g. m^2 y GWh^{-1}), due to the highly variable assumptions regarding recovery periods (Fthenakis and Kim, 2009).

The renewable technologies land-use literature distinguishes between "direct" and "total" land use, with the former being land that is transformed from one state to another, and the latter being the entire area of the power plant. Available Life Cycle Assessment (LCA) literature provide estimates of "land transformation" for conventional generation, which suggests that these are estimates of "direct" land use (Fthenakis and Kim, 2009; Jordaan, 2010; National Energy Technology Laboratory, 2014). Given this lack of specificity for natural gas, coal, and nuclear, conventional generation estimates are compared with both direct and total land use of renewable technologies (Figure 2.2).

Generation potential of renewable technologies

To estimate available land for RE development in California under various environmental constraints, we developed suitability models for geothermal, PV, CSP, and wind technologies using Python, ArcGIS 10.1, and the following types of datasets: physical (slope, elevation, water), socio-economic (population, military, airports), technical (resource), natural disasters (flood, earthquake, landslide), agricultural (cropland, prime farmland), environmental (ecological, cultural, historic areas) (Appendix Tables A.2-A.4). Using specifications for thresholds and buffer distances from previous studies (Appendix Tables A.2, A.3) (California Public Utilities Commission [CPUC], 2009; Black & Veatch Corp. and NREL, 2009; WECC EDTF, 2011; Lopez et al., 2012), we applied GIS map algebra techniques to create binary maps of areas that meet the technical, socio-economic, and environmental criteria for energy development.

To construct environmental constraint scenarios, we assigned each land type one of four environmental impact scores (Table 2.1) based on its conservation interest, biodiversity management designations, and legal restrictions against energy development (Table A.4). The

scoring scheme is loosely based on risk categories in the Western Electricity Coordinating Council's (WECC) Environmental Recommendations for Transmission Planning (ERTP) report (WECC EDTF, 2011). We modified the land area classifications in previous stakeholder-based studies using the U.S. Geological Survey's (USGS) National Gap Analysis Program (GAP) status code system that ranks the biodiversity management intention for protected areas, to serve as a proxy for areas with conservation interest that have legal recognition (Table 2.1, Table A.4). Statuses 1 and 2 have legal protection against permanent natural land cover disturbance and also meet the definition of "protected" by the International Union for Conservation of Nature (Appendix A). However, land areas with GAP statuses 3 or 4 may still have conservation interest and are scored based on previously reported stakeholder-agreed categories. See Table A.4 for all land areas included in the analysis, their environmental scores, and classifications used in previous studies. The four environmental scenarios that result from this are Least Stringent, Second-most Stringent, Third-most Stringent, and Most Stringent (Table 2.1). The Third- and Most-stringent scenarios, in particular, represent different degrees of land conservation above and beyond legal and biodiversity management protections. See Figure A.3A for locations of environmental scores across WECC for solar.

To refine the suitability maps (Figure A.4), potential areas in each environmental scenario were divided to represent utility-scale "development areas" between 100 and 1-1.2 GW in capacity, which serve as a spatial unit of analysis consistent with sizes of potential RE zones (Table A.2). The potential installed capacity of each development area was estimated using total operational-phase capacity-based land-use factors (MW km^{-2}) for the four RE technologies (Table A.1; highlighted in blue). Our initial results from modeling nuclear, coal, and natural gas land availability revealed vast suitable areas to site power plants within California that greatly exceeded demand, which is consistent with a previous study (Omitaomu et al., 2012). However, the site suitability of conventional power plants' is not the same as its "potential capacity", as is the case for renewable energy (excluding biomass), because the land footprint of fuel is distinct from that of the power plant (Omitaomu et al., 2012). Although operational-stage land-use factors exist for extraction and mining (Fthenakis and Kim, 2009), we do not spatially model the potential of coal, natural gas, and nuclear because we lack sufficient information to estimate the energy extracted per unit of land with the degree of confidence comparable to estimates for wind and solar resources. The fuel cycles of these technologies also lie largely outside of the California study area. We have included geothermal in our analysis because it does not have upstream and geographically distinct fuel stages, and spatial data on "geothermal feasibility" were publicly available (Table A.3).

Multi-criteria selection

To select development areas that meet 2050 demand, we developed a multi-criteria selection process that maximizes resource quality (e.g., insolation) and minimizes environmental impact of additional transmission and road connection, a process that minimizes km^2 MWh^{-1}. Using a transmission "cost surface" based on WECC's ERTP (WECC EDTF, 2011), we calculated the optimal, least-environmental-cost path connecting each development area to the

nearest road and transmission corridor (see Figure A.3B for the transmission cost surface map and Appendix A for more details about transmission calculations). For each development area, we calculated the average annual electricity generation by multiplying the installed capacity by 8760 hours and the capacity factor, which was calculated from the area-weighted average resource quality (equations in Appendix A). We ranked each criterion (resource quality, environmental impacts of transmission and road connection) and summed the individual ranks to calculate an equally weighted, multi-criteria score with which to choose the best overall development areas that meet demand.

Spatial interactions

To estimate the proportion of resource quality classes within each environmental constraint scenario, we sampled the resource quality value of each 500m cell and classified values into representative ranges. For solar, these ranges were based on quartiles of resource quality in the Least Stringent environmental scenario. We classified wind classes into the following classes: 3, 4-6, and 7. Since geothermal suitability assessment considered two classes, values were classified into feasibility scores of 9 and 10. For each class, we calculated the total area and the potential installed capacity.

To assess co-location potential and possible siting trade-offs between technologies, we quantified the pairwise overlapping area between technologies within each build-out and environmental constraint scenario. To assess the divergence of build-outs between environmental constraint scenarios, we calculated the overlapping area between scenarios for each technology.

2.3 Results

Land-use requirements in build-out scenarios

Direct land-use estimates are similar between High RE, High CCS, and Mixed scenarios, but High Nuclear and Baseline scenarios require about 20% and 25% less land, respectively (Figure 2.1). The Baseline scenario requires the least land because its total installed capacity is lowest due to the lack of transportation electricity demand, and the majority of capacity comprises of natural gas-combined cycle, which has high average land-use efficiency. The High Nuclear scenario is the second-least land-intensive because of nuclear's higher land-use efficiency (140 m^2 GWh^{-1} vs. approx. 400 m2 GWh^{-1} for solar, NGCC-CCS, and coal). However, values reported here are for land transformation; land occupation values for the operational phase of nuclear power is very high (300, 000 m^2 y GWh^{-1}) because of the assumed recovery times of land from nuclear waste (Fthenakis and Kim, 2009). Due to the reliance on out-of-state deposits of coal, natural gas, and uranium—fuels that dominate the Baseline and High Nuclear scenarios—and since the land requirements for natural gas and coal dwarf those for power plants, the vast majority of the land requirements in these two

scenarios would be outside California (Fthenakis and Kim, 2009). Total land use estimates are significantly greater than direct land use in the High RE build-out, primarily as a result of wind power (Figure 2.1B).

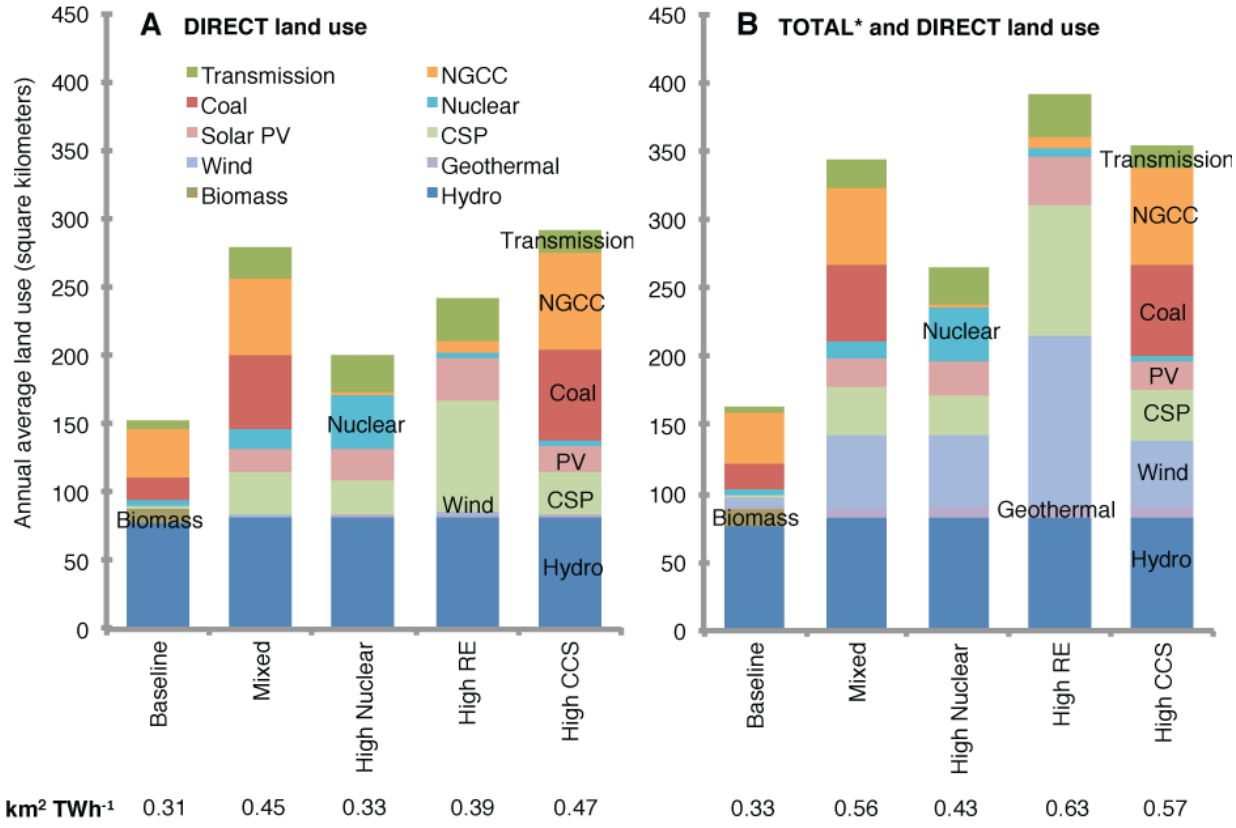

Figure 2.1: Direct and total energy land use requirements for California. Annual average direct (A)and total (B) land use change for electricity generation necessary to meet the 2050 demand for 30 years (the assumed power plant lifetime) for each low-carbon scenario and its average land area (km2) per unit generation (TWh) weighted across all technologies. *Figure 2.1 (B) shows total power plant land use (transformation) for only wind, PV, CSP, and geothermal technologies and direct land use for all other technologies since no total land-use factors could be confidently identified in the literature for conventional generation technologies. Land transformation land-use factors applied here do not account for duration of land recovery from uses associated with electricity generation, as is typically captured in land occupation metrics. Land occupation estimates are not reported in this present study.

Renewable generation potential of environmental constraint scenarios

We compared each technology's potential installed capacity with its expected capacity in 2050 (Figure 2.2) for different sets of environmental constraints. Although the amount of land available for development decreases with increasingly stringent environmental constraints, we found that generation potential within California is sufficient to meet 2050 demand under all build-out scenarios for PV and geothermal technologies. Wind development in California is constrained by the availability of suitable areas in all low-carbon build-out scenarios, using the current average total land-use factor assumed here (Table A.1); higher land-use factors, which would allow sufficient wind energy to be generated in-state, are theoretically achievable (Denholm, Hand, et al., 2009). Figure 2.2A also shows the amount of wind potential in the WECC under the Most Stringent environmental constraint scenario, which vastly exceeds California's requirement for wind energy, though out-of-state resources would have greater transmission needs.

In these results, technologies are not required to have mutually exclusive areas of resource potential. If co-location cannot be achieved, these capacity estimates here would be lower. Notably, because wind and CSP suitable areas overlap, if all suitable areas for wind are developed exclusively for wind generation, the most stringent environmental constraints could preclude the development of approximately 10 GW of CSP, and wind development in California would still be insufficient to meet 2050 High RE scenario targets (Figure 2.2A).

Interactions between conservation value and renewable resource quality

With increasing environmental constraints, the available land with the highest resource quality for all technologies decreases (Figure 2.2). Although all technologies show a reduction in available land with increasing environmental stringency, this trend is stronger for wind and solar technologies because a disproportionate percentage of the reduction occurs in areas with the highest resource quality (Figure 2.2B). The covariance of resource and environmental quality is also reflected in the spatial distribution of modeled build-outs for solar. For CSP and PV development areas under the High RE build-out, there is 45% and 33% overlap, respectively, between the Least and Most Stringent environmental scenarios; thus, 55% and 67% of all development areas selected for high resource quality and low transmission and road impact are sited in different locations, depending on the stringency of environmental constraints (Figures 2.3, 2.4). Under the Least Stringent scenario, CSP and PV are mostly concentrated in the Mojave Desert and east of the Sierra Nevada (Figure 2.4A), whereas under the Most Stringent scenario, relatively more development is located in the Southeast and Colorado Desert, where PEIS Solar Energy Zones have been identified (Figure 2.4B) (U.S. BLM and U.S. DOE, 2012). In the Most Stringent scenario and at high RE penetration, the system-wide capacity factor will be lower and diurnal generation profiles likely different compared with the Least Stringent scenario.

Table 2.2: Characteristics of the multi-criteria model-selected development areas that meet demand in three electricity build-out cases and under the Least (L) and Most (M) Stringent environmental scenarios.

		Mean environmental impact[2]		Mean resource quality [3]		Total transmission environmental impact [4]		Total road environmental impact		In-state generation area (km^2)	
		L	M	L	M	L	M	L	M	L	M
Wind	Baseline	1.7	1	5.25	4.51	0	0	0	0	248	272
	High CCS	2.35	1	3.88	3.60d	0	0	0	0	2403	1465d
	High RE [5]	2.29	1	3.67	3.6	565,500	365,300	6000	5000	4600	1465
CSP	Baseline	3.05	1	8.58	8.39	0	0	0	0	13	13
	High CCS	2.34	1	8.22	8.04	2000	124,900	0	0	1253	1281
	High RE	2.09	1	8.08	7.81	358,900	4,827,200	0	0	3259	3371
PV	Baseline	-	-	-	-	-	-	-	-	-	-
	High CCS	2.63	1	5.93	5.9	0	0	0	0	797	802
	High RE	2.29	1	5.92	5.88	0	500	0	0	1399	1408
Geothermal	Baseline	1.36	1	10	10	0	2500	0	0	76	76
	High CCS	1.33	1	9.59	9.6	23,800	94,300	0	0	240	240
	High RE	1.34	1	9.61	9.62	23,800	93,300	0	0	233	233

The overall generation area and transmission impacts for CSP differ between Least and Most Stringent scenarios. While the Most Stringent, High RE build-out requires only 112 km^2 (3% of total CSP area) more land than the Least Stringent scenario to generate the same amount of electricity due to exclusion of higher insolation areas, it has an order of magnitude greater transmission impact due to the need to develop some CSP in locations far from existing lines (Table 2.2).

[2]Environmental impact values were calculated using the scoring scheme detailed in Table 2.1

[3]wind expressed in units of wind classes (1-lowest, 7-highest); CSP expressed in units of solar direct normal radiation (DNI), kWh m^{-2} day^{-1}; PV expressed in units of solar global horizontal radiation (GHI), kWh m^{-2} day^{-1}, geothermal expressed in units of geothermal feasibility score.

[4]Transmission and road costs are in units of environmental impact score (Table 2.1) and area of land. The total impact reported constitutes the impact per grid cell of transmission (0.25 km^2) summed across all lengths of additional transmission required under each scenario following classifications in Table A.4.

[5]Demand exceeds supply; all criteria reported are for all potential sites in California (no project selection was performed) after applying environmental exclusions.

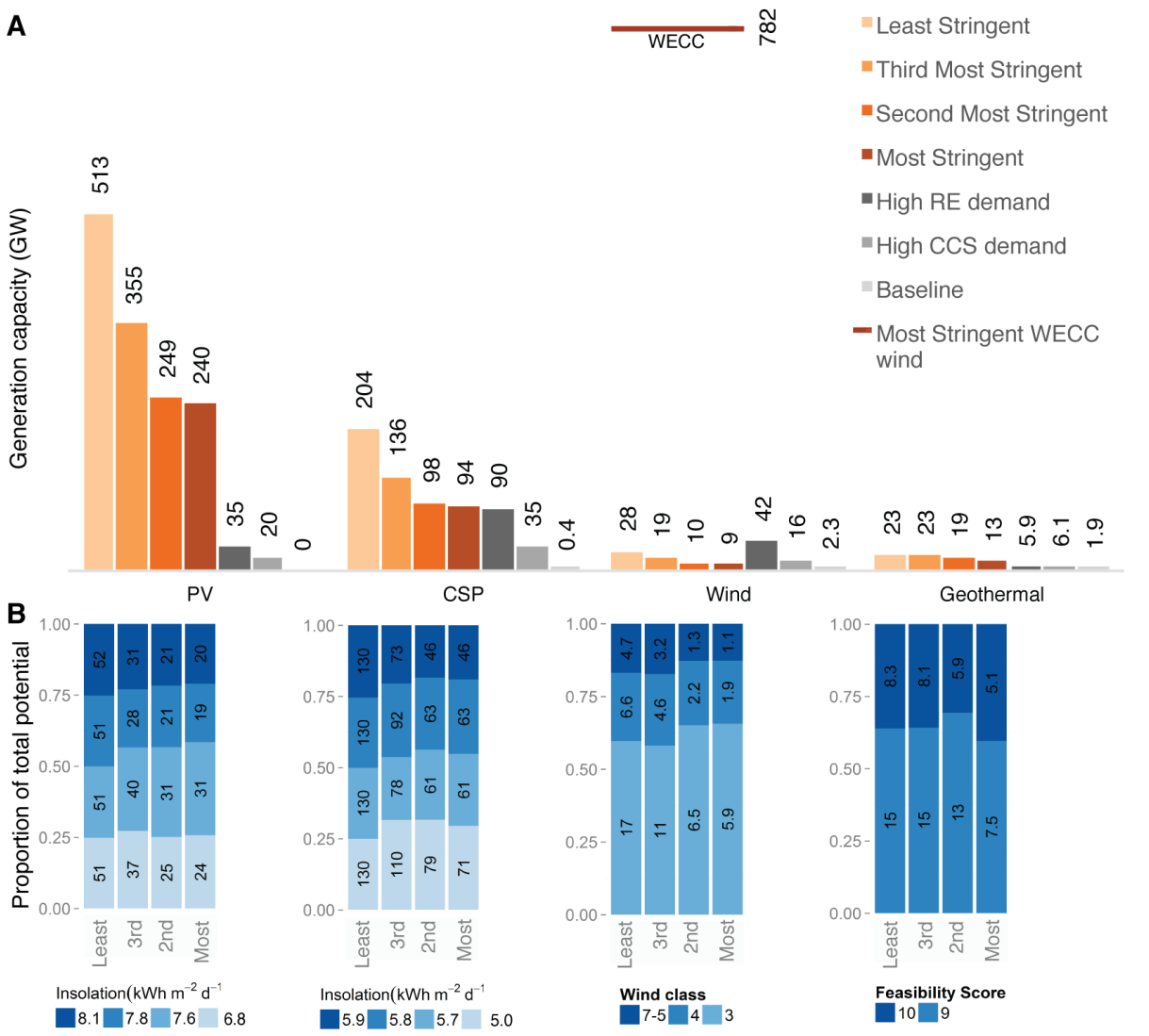

Figure 2.2: Renewable energy generation potential across environmental constraint scenarios. (A) Renewable electricity generation capacity potential (GW) under various environmental constraint scenarios (orange bars) compared with scenarios of California's technology-specific generation in 20502 (grey bars). The horizontal line shows the estimated potential of wind power capacity under the Most Stringent environmental scenario for the entire Western Electricity Coordinating Council (WECC) within the U.S. (B) Stacked blue bars show the relative proportion of renewable energy generation capacity that falls within each resource quality class (vertical axis) under each environmental constraint scenario (horizontal axis; Table 2.1). Values in each stacked bar indicate the potential in gigawatts (GW). For PV and CSP technologies, the class sizes follow quartiles of resource quality values under the Least Stringent environmental scenario. Due to the skewed distribution of wind classes, classes are approximate quartiles for wind capacity, and for geothermal, percentage of installed capacity is shown by the two highest geothermal feasibility scores (9, 10).

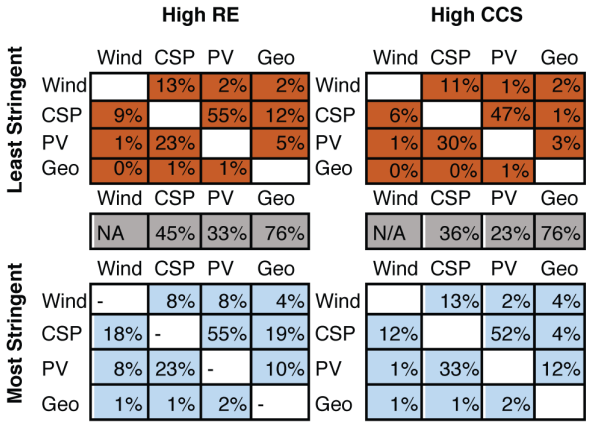

Figure 2.3: Percentage overlap of multi-criteria, model-selected development areas between electricity generation technologies and environmental constraint scenarios for the High Renewable Energy (RE) and High CCS build-outs.
Values indicate percentage overlap between generation technologies for development areas chosen under the Least (orange) and Most (blue) Stringent environmental scenarios. Columns indicate the technology used as totals in percentage calculations. For example, in the Least Stringent, High RE scenario, 13% of all CSP development areas overlap with selected wind development areas and 9% of all wind development areas overlap with CSP development areas. Values in grey show percentage overlap between the two environmental exclusion scenarios for each technology. For example, there is 45% overlap in High RE CSP development areas between the Least and Most Stringent scenarios. Wind percentage overlaps are not provided because not enough wind potential exists within California to meet the demand in the build-out cases.

Interactions between technologies

In some cases, land is suitable for multiple generation technologies (Figure 2.4). As environmental stringency increases, the overlapping area between technologies increases, which demonstrates that developers and planners may be faced with trade-offs between technology options under increasingly constrained build-outs (Figure 2.3). In the Least Stringent, High RE build-out scenario, 420 km^2 of development areas overlap between wind and CSP and 770 km^2 between PV and CSP, significant portions of each technology's total area. In this scenario, overlap between wind and CSP account for 9% and 13% of each technology's total, and for PV and CSP overlap is 55% and 23%, respectively (Figure 2.3). CSP's 13% overlap with wind represents an area exceeding the additional CSP land (3% of all CSP) required under the Most Stringent, High RE build-out scenario (vs. the Least Stringent). Thus, even if co-location of wind and CSP is pursued for 3% of all installed CSP capacity, it would offset the additional land use requirements that arise under the Most Stringent scenario.

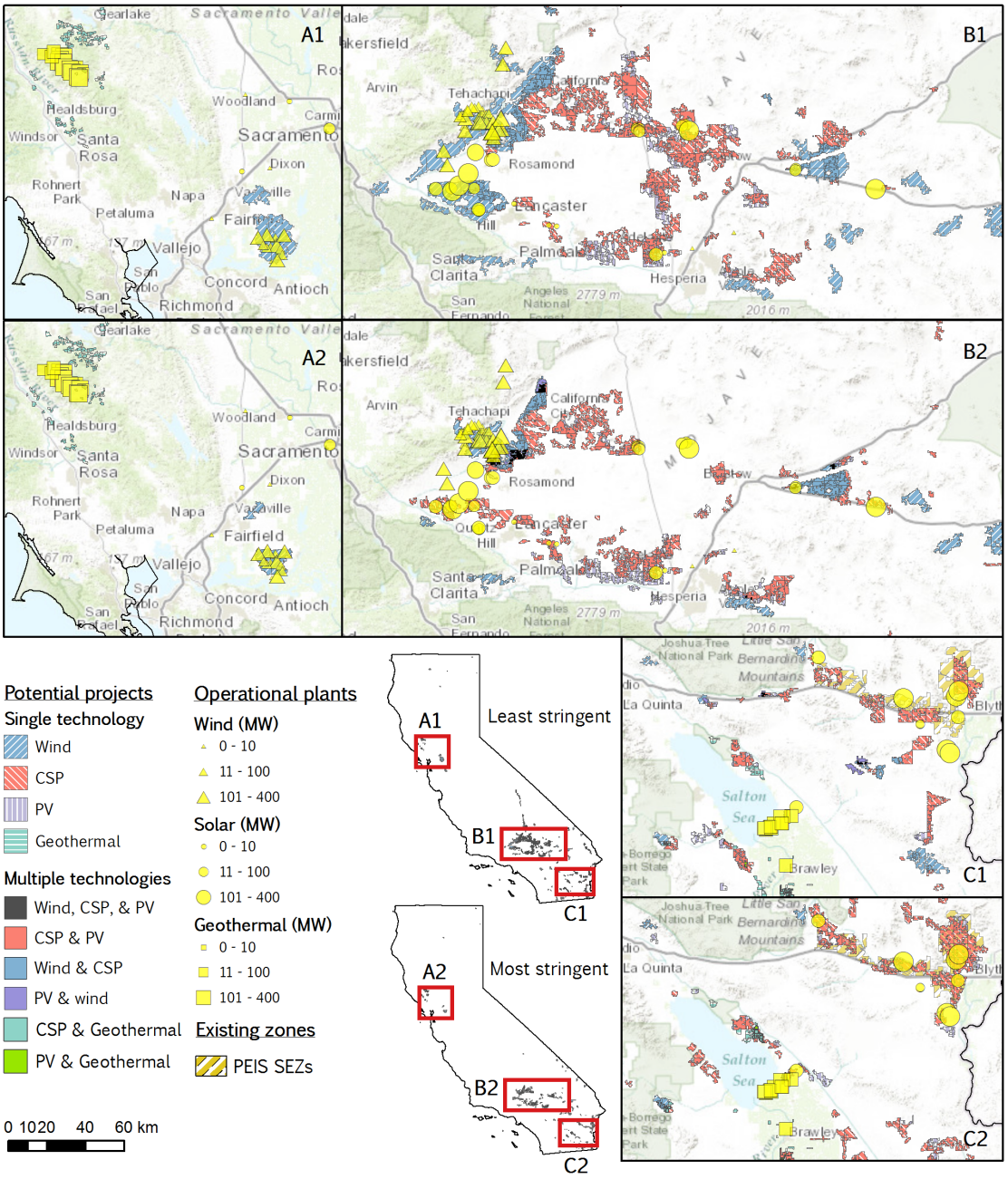

Figure 2.4: Maps of renewable energy build-out for the High-Renewable Energy scenario

Potential renewable energy development areas under the Least (A1-C1) and Most Stringent (A2-C2) environmental scenarios for the High Renewable Energy (RE) build-out. Areas of overlap between technologies are shown in solid colors (quantified in Figure 2.3). Sites suitable for single technologies are shown in diagonal lines. Yellow symbols indicate locations of operational wind, solar, and geothermal power plants, with symbol size specifying online capacity in megawatts (Source: California Energy Commission; California Energy Commission-Siting, Transmission and Environmental Protection Division, 2012). The Department of Energy and Bureau of Land Management's Programmatic Environmental Impact Statement (PEIS) Solar Energy Zones (SEZs; U.S. BLM and U.S. DOE, 2012) for California are shown in yellow diagonal lines. Percentage overlap by technology between maps (A1-C1) and (A2-C2) are provided within the grey boxes in Figure 2.3.

2.4 Discussion

The recent suite of studies on low-carbon energy transitions at state, national, and international levels (Sustainable Development Solutions Network (SDSN) and Institute for Sustainable Development and International Relations (IDDRI), 2013) has been complemented by renewable resource potential assessments, but there has not been spatially-explicit consideration of the land-use challenges as technologies are scaled up (California Public Utilities Commission [CPUC], 2009; Black & Veatch Corp. and NREL, 2009; Cameron, Cohen, and Morrison, 2012; Aydin, Kentel, and Duzgun, 2010; Lopez et al., 2012; Haaren and Fthenakis, 2011; Ramachandra and Shruthi, 2007; J. Clifton and Boruff, 2010). To inform policies that mitigate trade-offs between environmental and economic goals, our study investigates potential conflicts and opportunities by accounting for multiple land-use values, energy technologies, and generation scenarios.

Land use in low-carbon scenarios

Annual average land requirements for the four low-carbon scenarios of approximately 250 km^2 were not significantly different given the variability in published land-use factors and lack of consistent metrics for comparison of both direct and total land use. Wind had limited generation potential in California in our analysis, but it was based on current average assumptions about land-use efficiency and minimum resource requirements. With recent developments in wind technologies achieving higher performance at lower wind speeds and enabling installations at greater hub heights and on steeper slopes, innovation is increasing the generation achievable from the same land footprint as well as expanding areas suitable for wind development (R. H. Wiser and Bolinger, 2013). Even with innovation, some level of limitation on wind development by ecologically or recreationally valuable areas is likely to persist.

Fair comparisons of renewable and non-renewable technologies capture impacts over, at minimum, the lifetime of a power plant, often assumed to be 30 years in the LCA literature. The longer the time horizon examined, the more favorable renewable technologies' land-use efficiency becomes since total generation, which increases over time, is averaged over a consistent land footprint while non-renewable technologies require a continuous fuel supply (Fthenakis and Kim, 2009; Jordaan, 2010). The type of land impacts also differs by generation technology. For example, landscape fragmentation due to natural gas pipelines and dispersed wellheads is greater than that due to solar electricity (Jordaan, 2010). To improve overall land-use efficiency, policies can promote efficient, sustained use of land for RE development. For example, decommissioning policies could enforce removal of old equipment such that land can be released to other developers, and "re-powering" policies could encourage technical upgrades of (RE or conventional) power plants to increase installed capacity and capacity factors, and reduce environmental impacts.

Co-location of wind and solar technologies could address multiple siting challenges

A notable proportion of low-environmental-impact land in California is suitable for multiple RE technologies. Most studies have evaluated siting for only one technology at a time; yet applying results of independent studies without reconciling overlap would overestimate the available land resource. Moreover, we find that higher RE penetration and/or environmental constraints increase the magnitude of the overestimate. Therefore, resource assessments will be more accurate, and planning and permitting more efficient, if land value of all suitable technologies is considered simultaneously when evaluating different technology options, including technology-specific natural resource impacts such as habitat degradation and water consumption.

At the same time, suitability overlap presents an opportunity for co-location and increased land-use efficiency. Although research quantifying the efficiency gains from co-location is in the nascent stages (Sioshansi and Denholm, 2013), recent studies estimate that well-designed co-located wind-PV systems could double electricity generated on a given area, with shading from turbines resulting in a loss of only 1-2% of total PV production, and have better economies than single-technology plants (SolarPraxis and Reiner Lemoine Institute, 2013). Because transmission capacity and land can be shared, benefits include reduced transmission and substation footprint, reduced associated right-of-way challenges, and lower permitting costs and barriers per MWh produced (Loftis, 2013; Del Franco, 2014). Additionally, the seasonal and diurnal complementarity of wind and solar generation profiles would increase utilization of electricity infrastructure (Sioshansi and Denholm, 2013; Peterseim et al., 2014). In fact, we find that if co-location were achieved in just half of the identified overlapping areas, it would be possible for California to avoid development on valuable conservation areas (i.e., apply strict environmental constraints) and develop less land—compared with a no co-location outcome that applies the least environmental constraints (i.e., gives the most flexibility in location). Thus, co-location reconciles the potential land conflict between resource quality and conservation value at high RE penetrations. Because retrofitting existing single-technology plants, especially solar, is more difficult than constructing new co-located plants, these opportunities are most cost-effective when implemented sooner.

The need for consistently defined environmental exclusions

Inconsistencies among previous studies' designation of land area as restricting or allowing energy development, as well as in the definition of land types, create barriers to effective comparison across studies (Table A.4; California Public Utilities Commission [CPUC], 2009; Black & Veatch Corp. and NREL, 2009; WECC EDTF, 2011). We addressed existing discrepancies by (1) developing different levels of environmental constraints, (2) excluding areas with permanent legal protection, (3) using official management designations for biodiversity and landscape protection (GAP status) to inform what should be excluded from development but had not previously been excluded, and (4) applying environmental

datasets that have been identified through stakeholder processes (US. Geological Survey and National Gap Analysis Program, 2013). The DRECP represents a milestone in compiling and achieving consensus for biologically-informed datasets in the desert region of Southern California (Desert Renewable Conservation Plan, 2012). Replicating such an initiative state-wide would require generation of similar stakeholder-accepted conservation and management-based datasets.

Synergistic land-use and electricity planning for high RE penetration

Our findings are similar to other estimates of renewable generation potential on low-conservation-value land in California that report about 80 GW solar (Stoms, Dashiell, and Davis, 2013) and 6.2 GW wind (Kiesecker et al., 2011). These and other studies14 have highlighted the feasibility of "win-win" strategies for climate and conservation that restrict development to disturbed lands. However, ad hoc, market-driven development is more likely to result in environmental evaluation hurdles or additional transmission costs that increase expenses for developers, utilities, and ratepayers.

Our research reveals a trade-off between resource quality of energy and conservation interest for CSP, PV, and wind in a high RE penetration scenario. The low percentage of overlap between high and low environmental impact build-outs suggests that at some point (in time or in space), actions based on either conservation value or simple determinants of cost-effectiveness, (resource quality and transmission distance) could be at the cost of the other. This demonstrates that ecologically sensitive development must be actively pursued if California is to meet both its conservation and low-carbon goals, implying the need to encourage desired development patterns through coordinated energy and land-use planning. Analysis of economic and environmental spatial relationships could also help avoid conflict by identifying no-regret technology and siting choices, estimating the land and natural resource value of reallocation of generation capacity to distributed PV, or reducing demand through energy efficiency measures.44 Additionally, current electricity planning processes sequentially site generation and transmission, yet potential generation-transmission land-use trade-offs suggest that transmission-focused environmental recommendations (e.g., WECC Regional Transmission Expansion Planning30) should be incorporated in the prioritization scheme in RE zoning studies.

Limitations

This study does not spatially model land use of conventional generation or bioenergy, nor does it estimate the indirect land use associated with renewable technologies. Other criteria for site selection, such as how generation profiles vary spatially or the economic cost of land, were beyond the scope of the study. Also, differences in economic cost of infrastructure requirements between scenarios were not estimated, but would be useful better understand

the degree of conservation and economic trade-offs. Non-land resource requirements, particularly water, should also be considered for a fully comprehensive evaluation of resource constraints on low-carbon pathways.

Conclusion

With respect to the three objectives, we found that (1) California can meet high RE demands without the use of protected land, though wind energy may come from out-of-state. However, (2) because cost-effective development and conservation goals may conflict in some instances, we found that the most efficient and lower-impact build-out requires coordination of generation and transmission siting with conservation land-use priorities. (3) Because greater overlap between suitable areas for different RE technologies occurs with increasing environmental constraints, co-location of generation technologies could be an effective siting strategy to reduce conflicts between development and conservation. Spatially-explicit, forward-looking land-use models of multiple technologies, like that presented here, can anticipate the challenges and opportunities of electricity planning under multiple land-use constraints and inform official planning tools and processes. Hence, Outka (2011; Outka, 2011) gives a timely call to action, that "early in the expansion of renewable energy, when most of the infrastructure remains to be built, is the time to begin working as well as we can with the tools we have," for the immediate conservation benefits and because "siting well may be the most effective way to streamline power projects." (Outka, 2011).

Chapter 3

Integrating Land Conservation and Renewable Energy Goals in California: A Study of Costs and Impacts [1]

Currently, there is a lack of understanding of the environmental impacts and economic costs of potential renewable energy (RE) siting decisions that achieve ambitious RE targets. Such analyses are needed to inform policy recommendations that minimize potential conflicts between conservation and RE development. For these policies to be effective, they must be integrated into existing regulatory processes. The California Public Utilities Commission's (CPUC) Renewable Portfolio Standard (RPS) Calculator is a crucial first-order planning tool for RE procurement and transmission planning within the state. We developed the Optimal Renewable energy Build-out (ORB) model to generate input data for the RPS Calculator that reflects the renewable energy potential under various environmental constraints and to examine the land, conservation, water, and electricity cost impacts of the resulting environmentally constrained generation portfolios. We find that imposing environmental constraints on RE development achieves lower conservation impacts and results in development of more fragmented land areas. With increased RE and environmental exclusions, generation becomes more widely distributed across the state, which results in more development on herbaceous agricultural vegetation, grasslands, and developed urban land cover types. More ambitious RE targets result in higher water consumption, but under more environmental exclusions, this water demand is also more geographically dispersed. We find land

[1] This chapter was originally released as a report as:
Wu, G., N. Schlag, D. Cameron, E. Brand, L. Crane, J. Williams, S. Price. 2015. Integrating Land Conservation and Renewable Energy Goals in California: A Study of Costs and Impacts Using the Optimal Renewable Energy Build-Out (ORB) Model. Technical Report. 34 pages plus appendices.
The main content of the published paper has been placed in its entirety in the main body of the dissertation and the supporting information has been placed in its entirety in the Appendix of the dissertation.

use efficiencies of RE technologies are relatively inelastic to changes in environmental constraints, suggesting that cost-effective substitutions that reduce environmental impact and achieve RE goals is possible under most scenarios and exclusion categories. At very high RE penetration that is limited to in-state development, cost effectiveness decreases substantially under the highest level of environmental constraint due to the over-reliance on solar technologies. This additional cost is removed once the in-state constraint is lifted. Minimizing both negative conservation impacts and electricity costs at very high RE penetration will require California to utilize a combination of in-state and out-of-state RE resources, since it is possible to achieve 50% renewable energy generation by 2030 in the WECC-wide scenario under the most stringent set of environmental constraints while incurring only a 2% cost premium.

3.1 Background and Motivation

California has ambitious renewable energy targets, including a recently announced goal of 50 percent electricity derived from renewable sources by 2030. The state also has abundant undeveloped wind, geothermal, concentrating solar power (CSP) and solar photovoltaic (PV) resources. But many undeveloped landscapes with high renewable resource potential also have high conservation value, creating the potential for conflict between renewable energy development and conservation goals. These potential conflicts matter. If renewable energy projects proceed in environmentally sensitive areas, they can unnecessarily degrade the habitat, biodiversity and other values of natural landscapes. Conversely, environmental concerns can seriously impede renewable energy development by subjecting projects to multi-year delays, major cost increases and in some cases abandonment.

Despite these high stakes, the land use and water use implications of the state's renewable energy objectives have not been well characterized quantitatively or spatially. Information about these implications would help to clarify barriers to renewable energy development, evaluate the potential effects of proposed renewable energy policies and inform long-term energy planning. California has multiple long-term planning processes for transmission and renewable energy procurement, including the California Public Utilities Commission (CPUC) Long-Term Procurement Plan (LTPP), the California Independent System Operator (CAISO) Transmission Planning Process (TPP) and others. Although California and federal agencies have led multiple landscape-level planning initiatives to encourage environmentally-sensitive renewable energy development, the results from these studies have yet to be integrated into planning and procurement processes. Many transmission and long-term procurement planning decisions are informed by output from the California Renewable Portfolio Standard Calculator version 6.0 (RPS Calculator). Most importantly, CAISO uses the portfolio from the RPS Calculator to prioritize transmission investments necessary to meet renewable energy goals. Transmission availability is a critical factor for renewable energy developers when selecting potential project sites. Additional transmission availability through the planning of new lines or upgrades in turn encourages new generation projects

in those locations. As a result, the use of the Calculator in transmission planning has direct implications on the geographic regions where renewable energy projects will be proposed and developed, and, consequently, on the land and water impacts of those projects.

The RPS Calculator receives input data on transmission availability, renewable energy resource potential, and other factors. From this information, it produces the lowest-cost portfolio of future renewable energy projects—for multiple technologies and organized by Super Competitive Renewable Energy Zone (Super CREZ)[2]—that meets the renewable "net short" requirement, which is the difference between the RPS compliance target and the generation from existing and commercial[3] projects.

The RPS Calculator accounts for prohibitions on renewable energy development in some areas, such as national parks[4], but it does not account for the many areas where renewable energy development will impact sensitive resources and generate significant conflict with resource agencies and environmental stakeholders, increasing the risk of project delays or failure. As a result, the RPS Calculator may overstate the potential capacity for renewable energy development in areas where projects are likely to be infeasible due to, for instance, poor alignment with land-use planning designations or biodiversity conservation priorities. By the same token, overly conservative assumptions about land availability could lead the RPS Calculator to understate the potential for low-impact renewable energy development in some areas. While the RPS Calculator helps to analyze one policy goal—increased renewable energy development—it does not provide the information needed to improve planning by avoiding impacts to important natural habitats. Incorporating environmental constraints into the Calculator would provide a more realistic estimate of the potential for renewable energy generation in each Super CREZ. It also provides a basis for analyzing how to meet multiple state goals: RE development and protection of natural resources.

Objectives and Approach

To demonstrate how land conservation values can be integrated transparently into renewable energy procurement and transmission planning and examine the environmental outcomes of scenarios, we developed the Optimal Renewable energy Build-out (ORB) model. The model generates input data for the RPS Calculator that reflects the renewable energy potential in each Super CREZ when certain lands are excluded due to their conservation value. With this input, the RPS Calculator generates portfolios of future renewable energy production using the CPUC's "least-cost, best-fit" approach, given the resource availability and other constraints in each Super CREZ.

[2]Super Competitive Renewable Energy Zones are roughly county-scale energy planning units for which renewable resource potential, transmission capacity and renewable energy project costs have been estimated. The maps in this report show the Super CREZ boundaries.

[3]"Commercial" projects are those that have a CPUC-approved power purchase agreement (PPA).

[4]The full list of areas excluded from renewable energy development in the RPS Calculator has not been released for public review.

The ORB model then takes these environmentally-constrained portfolios from the RPS Calculator and models the spatially-specific optimal locations of the utility-scale wind, PV, CSP and geothermal projects that would make up each portfolio based on each possible project's resource quality and distance to nearest transmission line or substation.[5]

From this information and the RPS Calculator's outputs, we assess the following impacts of each portfolio:

1. The relative contribution of each RE technology in resulting RPS Calculator portfolios
2. Total land area required for renewable energy development and overall land-use efficiency;
3. Land cover type, conservation value, and geographic distribution of land developed for renewable energy;
4. Spatial distribution of water demand for renewable energy generation;
5. Relative cost of electricity production compared to the RPS Calculator base case.

This report presents portfolios generated at four different levels of environmental exclusion, from least restrictive to most restrictive. The exclusion categories are based on conservation interest, management designations and legal restrictions related to energy development. Each level of exclusion is evaluated under four 2030 renewable energy build-out scenarios: 33% of generation in-state; 40% in-state; 50% in-state; and 50% generation from a combination of in-state and out-of-state sources (anywhere within the Western Electricity Coordinating Council, or WECC, region).

This study is intended to be a proof of concept for integrating environmental exclusions into renewable energy planning models and decision-making in California. In order to demonstrate how this integration could be accomplished and why it may be valuable, the study employs a tool—the RPS Calculator—that the state currently uses to inform planning and long-term procurement decision-making. As of this writing, the RPS Calculator is under public review and active revision; this report is not meant to endorse the assumptions in the version of the RPS Calculator used in this study or to imply that the build-outs generated by the ORB model represent the full suite of options for achieving California's renewable energy goals.[6]

3.2 Methods

Data and scenarios

Site suitability and environmental impact data

Data representing the following categories of spatial characteristics were compiled from various sources: physical (slope, elevation, water bodies), socio-economic (population centers,

[5]By contrast, the RPS Calculator models only the total renewable generation and technology type within the boundaries of each Super CREZ; it does not specify project locations for generic future projects.

[6]The RPS Calculator Version 6.0 does not include load outside of the CAISO balancing authority area.

military zones, rail, roads, airports, mines), technical (renewable resources), agricultural (prime farmland), environmental (ecological, natural resources), and cultural (historic areas). Additionally, housing density, land cover type and water demand data were collected to estimate impacts of each build-out scenario. The sources of all exclusion and environmental impact data are listed in Appendix Table B.1.

Environmental exclusions and data

In order to assess the environmental and cost impacts of excluding RE development from areas with different levels of conservation value, we developed four environmental exclusion scenarios based on categories in Wu, Torn, and Williams (2015) (Chapter 2). The following categories increase in environmental stringency and level of administrative or legal protection, with Category 1 being the least stringent and Category 4 being the most stringent. The categories are additive in their use as exclusions levels—e.g., Category 3 Exclusion Level includes all Categories 1 and 2 lands.

Category 1 (Legally Excluded): Areas where legal restrictions preclude energy development. This category strictly follows exclusions from previous planning studies (i.e., Western Renewable Energy Zones (WREZ) Black & Veatch Corp. and NREL, 2009, Renewable Energy Transmission Initiative (RETI) California Public Utilities Commission [CPUC], 2009, Solar Programmatic Environmental Impact Statement (SPEIS) U.S. BLM and U.S. DOE, 2012).

Category 2: Areas with administrative and legal designations by public agencies in order to protect ecological and social values. In some cases these areas already have some restrictions on energy development. This category includes all "avoid" and "Category 2" areas identified in WREZ (Black & Veatch Corp. and NREL, 2009) and RETI (California Public Utilities Commission [CPUC], 2009) studies, respectively.

Category 3: Lands with ecological, economic or social value, including many conservation organizations' priority conservation areas, Prime Farmland, and lands proposed for designation as Wilderness.

Category 4: Lands with broad-scale ecological value based on regional models and studies, including contiguous high quality suitable habitat and ecologically intact lands. Datasets and sources that compose each Environmental Exclusion Category are listed in Appendix Table B.2.

Incorporating Environmental Constraints in the RPS Calculator

To assess cost impacts of imposing environmental constraints on RE development in California, we created environmentally-constrained RPS Calculator scenarios. To do so, we calculated the megawatts of potential installed capacity for each technology under each Environmental Exclusion Level by Super Competitive Renewable Energy Zone (CREZ) using

the site suitability models. Super CREZs are geographic areas within which resource potential, transmission capacity, and costs have been estimated (see Appendix Figure B.1 for a reference map showing labeled locations of Super CREZs). They are also the geographic unit at which PV generic projects are selected by the RPS Calculator. For each technology, we compared the estimated environmentally-constrained potential for each Super CREZ with the base case potential (no environmental exclusions) used in the unmodified RPS Calculator (v 6.0). These potential values are tabulated for each technology in the Appendix (Tables B.4, B.5, B.6, B.7). Because the environmentally-constrained potential estimates represent total potential, they needed to be corrected for existing and commercial RE power plants in each Super CREZs to create "net" resource potential. To create the 2030 portfolios, the Calculator selected generic projects to meet the renewable net short from this environmentally-constrained set of "net" resource potential. As an example of how this correction was performed, consider the following: the nearly 4 GW of operational or commercial wind projects that already exist in the Tehachapi Super CREZ were removed from the estimated total potential of 6.78 GW and 5.56 GW under the Category 1 and 2 Exclusion Levels, respectively, to create a net resource potential of 2.78 GW and 1.56 GW, respectively (Table B.4). For each Environmental Exclusion Level scenario, we modified the RPS Calculator using the lower of the environmentally-constrained and the unconstrained potential values (MW). For example, since the modeled potential under Category 4 wind exclusions (536 MW) for the Round Mountain Super CREZ was greater than the base case RPS Calculator potential (220 MW), the modified RPS Calculator Category 4 Exclusion Level scenario used 220 MW as the wind potential for Round Mountain.[7]

We generated technology-specific in-state portfolios for the following four unique 2030 RE targets in the RPS Calculator v6.0: 50% in-state, 40% in-state, 33% in-state, and 50% WECC-wide (Table 1). The RPS Calculator's least-cost, best-fit approach to portfolio creation may select different amounts of generation from each renewable energy technology, depending on its availability under different environmental exclusions. The resultant environmentally-constrained RPS Calculator portfolios (Table 1) and their contribution by Super CREZ were subsequently used as inputs for the optimal site selection process (see Figure 3.1 for the process flow diagram of analysis and data inputs/outputs). For assumptions and methods used in the RPS Calculator, refer to CPUC's published documentation.[8]

[7]However, an important caveat in the way the inputs to the RPS Calculator were modified is that the lower of the potential values (the RPS Calculator default and the ORB site suitability results) were used. As such, there may be more opportunities to develop in a low conservation value area than was made available to the Calculator in the present study. As such, the results reported here may be more conservative than what is possible. To accurately assess whether more opportunities for low impact development exist, a systematic comparison of the non-environmental exclusions will need to be conducted between the RPS Calculator's default potential inputs and ORB model's site suitability results.

[8]http://www.cpuc.ca.gov/PUC/energy/Renewables/hot/RPS+Calculator+Home.htm

Table 3.1: RPS Calculator technology-specific generation targets (GWh)

RPS Calculator scenario	Environmental Exclusion Level	Wind	PV	CSP	Geothermal	Total
50% in-state	Base	31288	38656	4095	19231	93270
40% in-state	Base	19779	26884	4095	16637	67395
33% in-state	Base	18469	21901	4040	8467	52877
50% WECC-wide	Base	30176	34267	4095	19231	87769
50% in-state	Category 1	25795	41123	3989	16114	87021
40% in-state	Category 1	19650	26540	3989	13431	63610
33% in-state	Category 1	17699	21885	3934	5718	49236
50% WECC-wide	Category 1	24899	30605	3934	13431	72869
50% in-state	Category 2	23198	42818	3989	16073	86078
40% in-state	Category 2	19043	26954	3989	13624	63610
33% in-state	Category 2	17587	21856	3934	5719	49096
50% WECC-wide	Category 2	21340	34210	3989	13624	73163
50% in-state	Category 3	18721	50077	3989	16341	89128
40% in-state	Category 3	16490	29451	3989	13892	63822
33% in-state	Category 3	16253	23079	3934	5718	48984
50% WECC-wide	Category 3	16837	30760	3989	16208	67794
50% in-state	Category 4	16266	50561	18234	8604	93665
40% in-state	Category 4	16068	33385	3989	8604	62046
33% in-state	Category 4	15235	23502	3989	6146	48872
50% WECC-wide	Category 4	15586	27382	3989	8604	55561

Optimal Renewable energy Build-out model (ORB model)

The Optimal Renewable energy Build-out (ORB) model is a spatially-explicit site selection model that identifies installation locations for each RE technology by minimizing total generation and transmission land area given a set of technology-specific generation targets and constraints. The ORB model consists of a spatial site-suitability model that identifies all land areas appropriate for renewable energy development and a linear integer optimization problem. To anticipate possible build-outs under multiple 2030 RPS Calculator scenarios and to assess their environmental impacts, we modified the original model Wu, Torn, and Williams (2015) for this present study to constrain the geographic selection of sites by Super CREZ, as specified by the RPS Calculator (Figure 3.1), and to account for overlapping suitable areas between multiple technologies.

Site suitability model

To identify all technically possible locations for renewable energy development in California, we created site suitability models for wind, PV, CSP, and geothermal using the methods established in Wu, Torn, and Williams (2015). Binary suitability maps were created using map algebra functions and datasets listed in Table B.2 by applying threshold and buffer specifications for each technology (Table B.3). The raster-based site suitability model was

programmed in Python using the arcpy module (ESRI ArcGIS 10.2, Redlands, CA) and ran using a spatial resolution of 500 m. We created a site suitability model for each technology for each of four Environmental Exclusion Levels, generating a total of 16 model outputs. The resulting potential estimates (MW) for each Super CREZ were estimated using the land use factors in Table 3.2, without applying any discounts to account for unforeseen development restrictions or for areas that may already have RE development. These values are tabulated in Appendix Tables B.4 - B.7.

Development zone creation. To prepare the site suitability outputs for the site selection process, we overlaid the technology-specific site suitability areas under each Environmental Exclusion Level and determined areas where four, three, and two technologies' suitability overlapped. All non-overlapping areas were identified and designated as those suitable for only one type of generation technology. All contiguous areas suitable areas greater than 20 km^2 were divided using a 4 km x 4 km grid, and contiguous areas smaller than 2 km^2 were excluded from further analysis since these fall below minimum area specifications for utility-scale projects. We refer to the resulting areas ranging from 2 to 20 km^2

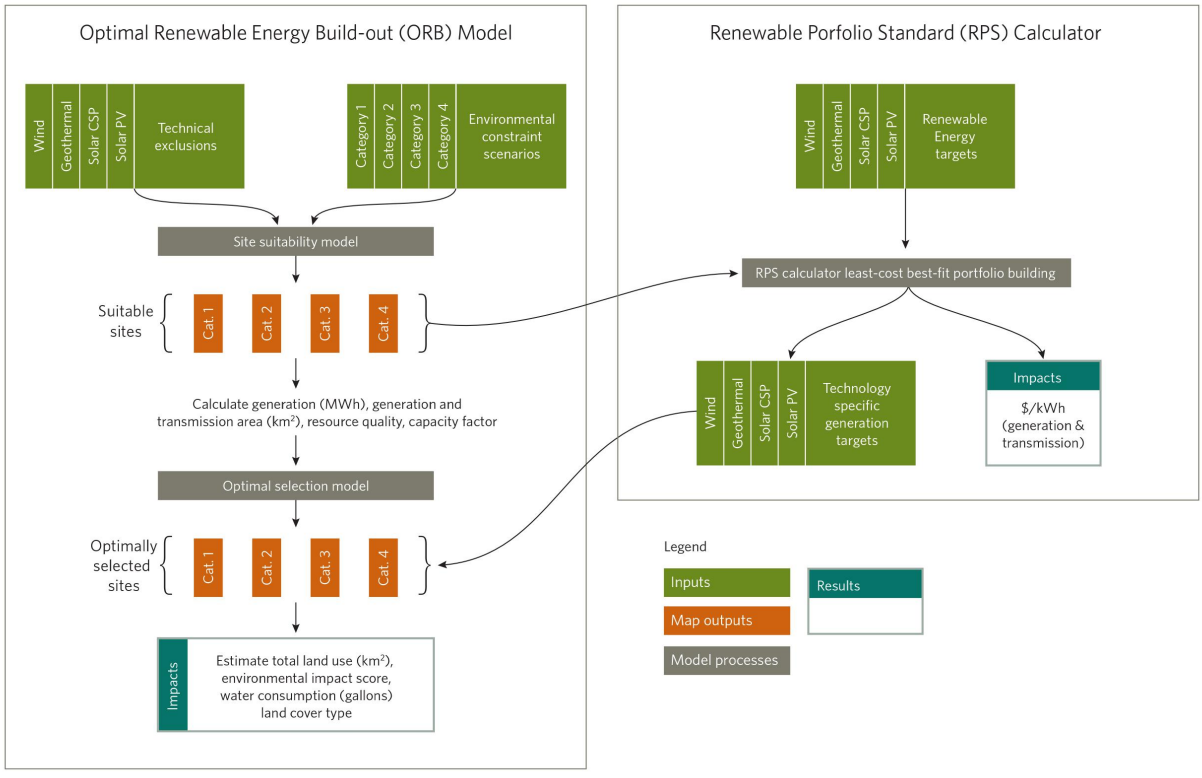

Figure 3.1: Methods flowchart
The flowchart shows the complementary roles of the ORB and RPS Calculator models in assessing the impacts of environmental constraints on renewable energy development.

Table 3.2: Technology-specific parameters

	Wind	PV	CSP	Geothermal
Land use factor (MW km^{-2}) – average literature values	6.1 [9]	30 [10]	30[11]	25.5[12]
Water demand (gal MWh^{-1}) – median literature values	0	26 [13]	78 [14]	135 [15] (binary or $\leq$ 80% CF); 10 [16] (flash or $>$ 80% CF)

as "development zones," which serve as the spatial unit of analysis and site selection. We merged all overlapping and single-technology development zones to create a feature class of all possible development zones with attributes that indicate the technologies for which a development zone are suited.

Development zone criteria. We calculated the following criteria for each development zone and for each technology: generation land area (km^2), Euclidean distance to nearest transmission line (km), Euclidean distance to nearest substation (km), interconnection land area (km^2), total land area (km^2), area-weighted resource quality (insolation, geothermal feasibility score), capacity factor (CF; %), annual average generation (MWh). The Wind Integration National Dataset (WIND) Toolkit from the National Renewable Energy Laboratory provides direct estimates of annual average capacity factors.[17] (J. King, A. Clifton, and Hodge, 2014), See Appendix Section B.1 for equations and details about estimating capacity factors for solar PV, solar CSP, and geothermal and estimating annual average electricity generation for each development zone and technology (Eq 4 in Appendix section B–2) using the zone and technology-specific CF and land use factor (Table 3.2).

Whether a development zone interconnects to the nearest substation or nearest transmission line is determined using the following heuristic: if the distance to the nearest substation is less than 37.5 km,[18] a new project would interconnect to the nearest substation; if it is greater than 37.5 km, it would connect to the nearest transmission line. Distances to either substation or transmission line were scaled up by a rule-of-thumb factor of 1.3, to account

[9](Denholm and Margolis, 2008)
[10](Ong, Campbell, Denholm, et al., 2013)
[11](Ong, Campbell, Denholm, et al., 2013)
[12](Ong, Campbell, and Heath, 2012)
[13](Macknick et al., 2011)
[14](Macknick et al., 2011)
[15](Macknick et al., 2011)
[16](Macknick et al., 2011)
[17]The WIND Toolkit data are in the form of point locations representing the average capacity factor of a 2 km x 2 km area around the point. To transform these data into the form usable as an input to the raster-based site suitability model, we generated a raster with 500 m cell size using inverse distance weighted interpolation of the data points.
[18]Typically the range for connecting to an existing substation is 25 – 50 km, beyond which a new line would be extended or a new substation built. The figure of 37.5 km is simply the median distance of this range. These values and the rule-of-thumb transmission line multiplication factor were provided by Jack Moore at Energy and Environmental Economics, San Francisco, California, USA.

for additional length resulting from topography, and then multiplied by a line width of 0.076 km to estimate interconnection land area (km^2). To avoid systematically reducing the total land use efficiency (MWh km^{-2}) of smaller development zones as a result of a fixed interconnection area, we applied a correction factor to the interconnection area using the ratio of the development zone area (as small as 2 km^2) to the largest possible development zone area (20 km^2). This correction results in a fixed generation-to-interconnection area ratio for development zones of different sizes that are the same distance from the nearest transmission line or substation and have the same resource quality

Site-selection using integer linear optimization

Relaxing site suitability estimates. The installed capacity of existing and commercial RE projects in a subset of Super CREZs exceeded the estimated potential under the more restrictive Environmental Exclusion Levels. For example, no potential installed capacity of solar CSP remain in the Kramer Super CREZ under the Category 4 Exclusion Level, but 1150 GWh of solar CSP generation need to be sited in Kramer due to existing or commercial power plants that cannot be excluded from the portfolio. We chose to model the entire build-out (both existing and commercial, as well as generic) for two key reasons. First, the electricity costs estimated in the RPS calculator reflect the entire portfolio, not just the "net short" build-out. Impacts (land use efficiency, environmental impact score) modeled using the net short build-out would not correspond to the electricity costs. Second, because locations of existing and commercial projects could not be made publicly available, we could not exclude them from the site suitability models. As a result, modeling only the net short build-out (i.e., generic projects) could select sites where current existing and commercial projects may be located.

In order to model the entire build-out of an RPS Calculator portfolio, including existing or commercial projects, we relaxed the environmental exclusions only for those Super CREZs with insufficient modeled potential to meet its RPS Calculator specified generation requirements. Exclusions were relaxed to the category that would allow sufficient generation to be sited. For example, a total of eight Super CREZs under the Category 4 Exclusion Level needed to be relaxed to Category 3 and three needed to be relaxed to Category 2 Exclusion Levels, in order to model the Super CREZ-specific generation portfolio (Figure 3.3). We prevented any additional generation from being sited in Super CREZs where the environmentally constrained potential was less than the generation from existing and commercial projects within those Super CREZs (see section 2.2 for a description of how these environmentally constrained portfolios were generated). We excluded from the site selection process Super CREZs with minimal (<5 GWh) generation targets in the RPS Calculator scenarios and that had no potential under any Environmental Exclusion Levels based on our site suitability models. These Super CREZs include: Los Angeles County, San Diego County, Orange County, and Santa Clara County. Additionally, due to the lack of geothermal potential in our site suitability model even under the most relaxed Environmental Exclusion Level, RPS Calculator-specified geothermal targets in Lassen North, Mono County, and Owens Valley

Super CREZs were not modeled in this study. The overlap of legal environmental exclusions with areas of high geothermal feasibility preclude identification of suitable sites in Owens Valley. Mono County geothermal site suitability is precluded by the slope exclusion (>1500 m).

Optimization problem construction. We constructed an integer linear optimization problem in order to optimally select development zones that meet the 2030 RE targets. Solving the optimization problem identifies both the sites and the technology for each site that minimizes total (generation and transmission) area used for electricity generation in each scenario, as shown in the objective function (Eqn. (B.1)). By specifying binary decision variables ($x_{t,z}$), constraint (Eqn. (B.2)) restricts the development status of each development zone to "no development" ($x_{t,z} = 0$) or "complete development ($x_{t,z} = 1$). Because each development zone (z) may be suitable for any combination of examined technologies (t), the optimization problem must choose to develop no more than one technology per zone, as enforced with constraint (Eqn. (B.4)), while ensuring that the build-out meets technology-specific targets (d_t), as enforced with constraint (Eqn. (A.4)). To align the geographic-specificity of the RPS Calculator with the ORB site selection process, constraint (Eqn. (A.5)) restricts the total MWh of generation for each technology within each Super CREZ to be greater than or equal to 90% of the Super CREZ-specific RPS Calculator targets ($g_{c,t}$). We restricted development by Super CREZ using a minimum generation equal to 90% of the values specified by the RPS calculator, but imposed no maximum generation, in order to provide some flexibility to account for the following differing assumptions between the ORB model and the RPS calculator: 1) differences in capacity factors that result in differences in generation estimates, 2) the overlap of suitable sites between technologies that could not be accounted for in creating environmentally constrained potential values for the RPS calculator, which could have the effect of over-estimating the technology-specific potential in a given Super CREZ, and 3) differences in minimum project size that would prevent the ORB model from finding a solution if a maximum generation value were imposed from the RPS calculator that was less than the minimum project size in the ORB model.

We programmed the integer optimization problem in the optimization programming language (OPL) using the IBM © CPLEX Optimization Studio. We solved the optimization problem for each of the four RPS Calculator build-out scenarios (Table 1) under each Environmental Exclusion Level (Section 2.1.2). However, we only report results for maintaining the current California RPS target of 33% by 2030 and the newly announced target of 50% by 2030 for both in-state and WECC-wide.

Nomenclature

Indices:

z	development zone index where $z \in 0...Z$
t	technology where $t \in wind, PV, CSP, geothermal$
c	Super CREZ index where $c \in 0...C$

Variables:

$x_{t,z}$	selection status $\in 0, 1$ of development zone z, technology t

Parameters:

$a_{z,t}$ total generation and transmission area of development zone z,technology t
$e_{z,t}$ electricity generation (MWh) of development zone z, technology t
d_t annual generation target (MWh) for technology t from the RPS Calculator
$g_{c,t}$ annual generation target (MWh) for technology t within super CREZ c
$i_{z,c}$ assignment $\in 0, 1$ of zone z to super CREZ c

Objective function and constraints

Minimize: total (generation and transmission) land use

$$f(x_{t,z}) = \sum_{z=1}^{Z} \sum_{t=1}^{T} a_{z,t} x_{z,t} \tag{3.1}$$

Subject to:

$$x_{t,z} \in 0, 1 \tag{3.2}$$

$$\sum_{t=1}^{T} x_{z,t} \leq 1 \qquad \forall z \in 1, ..., Z \tag{3.3}$$

$$\sum_{z=1}^{Z} e_{z,t} x_{z,t} \geq d_t \qquad \forall t \in 1, ..., T \tag{3.4}$$

$$\sum_{z=1}^{Z} i_{z,c} e_{z,t} x_{z,t} \geq 0.9 g_{c,t} \qquad \forall t \in 1, ..., T, \forall c \in 1, ..., C \tag{3.5}$$

Impact analysis

In addition to estimating total generation and land area characteristics of each scenario, the following impact metrics were estimated: area-weighted average environmental impact score, total water consumption by scenario (annual household-equivalents) and disaggregated by groundwater basin, average housing density (households km^{-2}), and land cover type. See Table B.1 for sources of datasets used to estimate impacts.

Environmental impact score. We created an environmental impact scoring system by assigning each of the environmental exclusion categories a score that is the inverted value of its category (section 2.1.2), such that Category 1 areas were assigned a value of 4 and Category 4 areas assigned a value of 1. This scoring is based on the assumption that siting in areas with less legally stringent conservation values (e.g. Category 4) will be lower impact than if development occurred on land areas with more stringent values (e.g. Category 2). All areas outside of Categories 1-4 exclusions were assigned an environmental impact score of 0. Since all Category 1 areas are legally protected and excluded from all environmental scenarios, possible environmental impact scores (EIS) range from 3 to 0.

We calculated the average EIS for the build-out of an RPS Calculator portfolio by area-averaging the EIS of all selected development zones. The average environmental impact score is a measure of the ecological and social conservation value of the land developed. It ranges from 0 to 3 with a score of 3 indicating that development projects have high conservation impact. An average EIS of zero implies no development in areas of environmental concern, whereas an average EIS score of 2 implies that on average, the selected build-out occupies areas with "medium environmental impact." For example, an average EIS of 2 could result from the ORB model siting 25% of development zones on land with "high environmental conflict" (score 3), 55% on land with "medium environmental conflict" (score 2), 15% on land with "low environmental conflict" (score 1), and 5% on land with "no environmental conflict" (score 0). The environmental impact score under Category 4 Exclusion Level could never actually be zero due to the relaxations of environmental constraints for existing and commercial RE projects. Additionally, we calculated the total area (km^2) of each EIS for each scenario.

Water consumption. Total water consumption estimates rely on the literature compilation of technology-specific water consumption values reported in Macknick et al. (2011) (Table **??**). Using the median value (gallons MWh^{-1}) and the annual MWh generated per technology, we estimated annual water consumption values in gallons, which were converted to annual average household water demand-equivalents (HWDeq). A unit of HWDeq is equal to 146,000 gallons of water, which is calculated using the average household water use of 400 gal d^{-1} (U.S. EPA: WaterSense). We report HWDeq values across the entire state and spatially disaggregated for each groundwater basin.

Landscape fragmentation and land cover. Average housing density is used as a proxy for landscape and habitat fragmentation (Radeloff et al., 2010). According to Radeloff et al. (2010) housing growth is one of the best indicators of threat to the biodiversity and ecosystem health of protected areas in the U.S. In order to understand how habitat and vegetative communities impacted change under different sets of environmental exclusions, we used the U.S. Geological Survey's GAP land cover data, which follows the National Vegetation Classification System, to determine the area of land cover type converted under each build-out scenario.

3.3 Results

Site suitability and optimal build-out

The site suitability models show the spatial distribution of technically and environmentally feasible resources across the state, and the optimally selected build-outs show areas of highest resource quality and close to existing or planned transmission. As the area of environmental exclusions increase from Category 1 to 3, the area of suitable sites reduce in a spatially homogenous fashion throughout the state (Figure 3.2). Under the Category 4 Exclusion Level, suitable sites are largely located in the Central Valley, particularly the Westlands, Los

Banos, Central Valley North, and Solano Super CREZs. Areas in Southern California with the largest areas of remaining potential under Category 4 Exclusion Level are the Riverside East, Imperial, Palm Springs, and San Bernardino Lucerne Super CREZs (see Appendix Figure B.1 for a reference map showing labeled locations of Super CREZs).

Using the relaxed site suitability areas in Figure 3.3, the ORB model identified selected sites to meet the Super CREZ-specific and state-wide generation targets for each technology. We constrained this site selection process in order to produce a build-out that best spatially represents the RPS Calculator portfolio within the limitations of the ORB model. That is, the ORB model attempts to spatially allocate generation to each Super CREZ according to RPS Calculator portfolio specifications. Figure 3.4 shows the optimally selected sites to meet the 50% in-state by 2030 target in the RPS Calculator. For selected sites of all RPS Calculator scenarios, see the accompanying layered PDF map that allows toggling of individual layers, including transmission lines and substation locations (Map B. 1). Under the Category 4 Exclusion Level in the 50% in-state, with solar PV replacing most of the reduced wind generation in the overall RE portfolio, the distribution of solar PV extends much more into the Central Valley (Carrizo North Super CREZ) and northern California (Solano, Central Valley North, and Sacramento River Valley Super CREZs) and out of the Mojave (Tehachapi, Kramer Super CREZs; Figure 3.4). Wind development in the Solano and Tehachapi Super CREZs remain relatively unchanged across environmental exclusion categories, but is significantly reduced in the Sacramento River Valley Super CREZ in Categories 3 and 4 Exclusion Levels. These technology-specific trends are similar for the 50% WECC-wide 2030 scenario (Map B. 1), except significantly less solar PV is required within California under Category 4 Exclusion Level (Table 1). For 33% in-state, almost no wind is sited in the Sacramento River Valley Super CREZ across all environmental exclusion scenarios, and solar PV is more widely distributed in the Central Valley region under Category 3 and 4 Exclusion Levels (Map B. 1).

Electricity generation and land use efficiency

Generation mix—Overall results show that the more ambitious the RE integration target, the stronger the effect of environmental constraints on the in-state generation mix. In RPS Calculator portfolios that achieve 33% in-state RE generation by 2030, environmental constraints had little impact on the in-state electricity generation of each technology (Figure 3.5A). The reduction in wind generation with increasing environmental constraints is offset by a proportional increase in solar PV generation (Figure 3.5A). In the 50% by 2030 in-state and WECC-wide scenarios, generation portfolios change more dramatically in response to the environmental exclusions imposed. If out-of-state (WECC-wide) imports are allowed, increasing the area of environmental exclusions drives down in-state wind generation, which under the Category 2 Exclusion Level, can be addressed cost-effectively with additional in-state solar PV. Under Category 3 and 4 Exclusion Levels, out-of-state wind generation is able to compensate for reduction in in-state wind and solar PV, as observed in the drop in solar PV generation and the overall in-state generation decline (Figure 3.5A). If electricity must

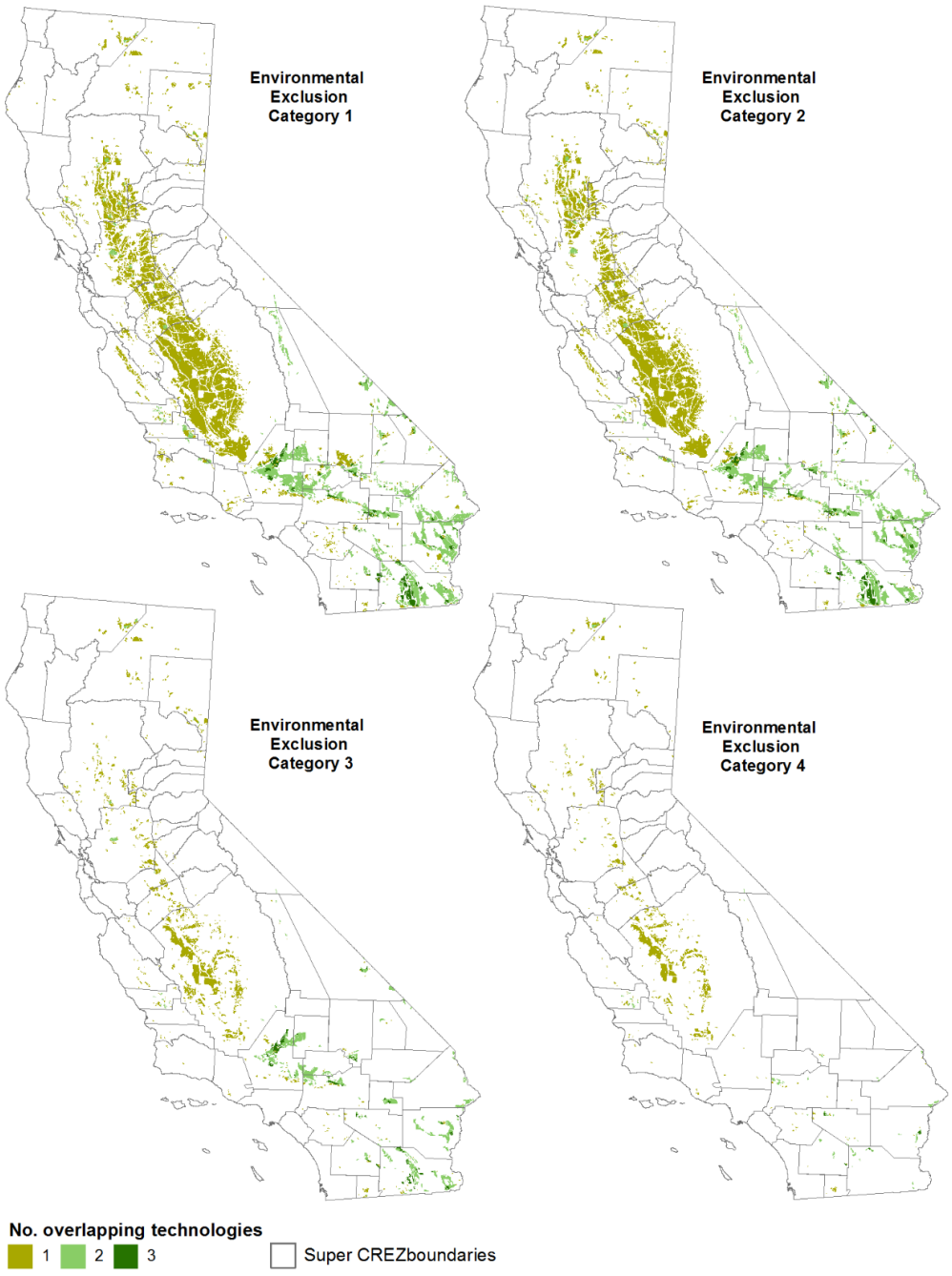

Figure 3.2: Suitable sites for the development of wind, solar PV, solar CSP, and geothermal Colors indicate the number of technologies for which an area is suitable. For example, dark green areas are those that are suitable for any possible combination of three out of the four technologies (i.e., wind, solar PV, solar CSP). The maps show suitable sites for Category 1 through 4 Environmental Exclusion Levels, with Category 1 being legal baseline exclusions and Category 4 having the most extensive exclusion criteria.

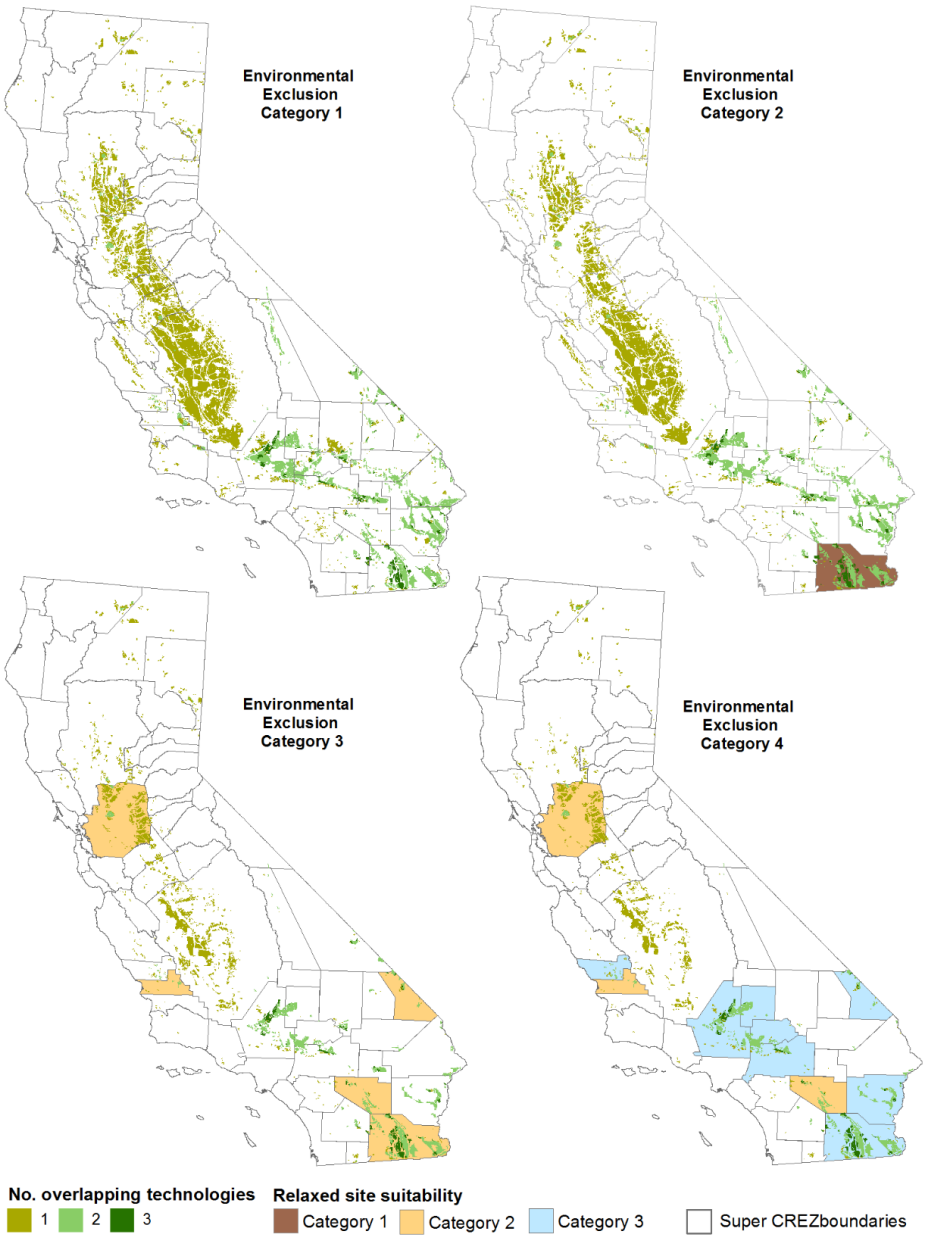

Figure 3.3: Suitable sites for the development of wind, solar PV, solar CSP, and geothermal under relaxed environmental exclusions.

Colors indicate the number of technologies for which an area is suitable. The maps show suitable sites under Category 1 through 4 Environmental Exclusion Levels. The difference between these maps and those in Figure 3.2 is the relaxation of particular Super CREZs in order to meet the generation targets of existing or commercial projects in the RPS Calculator portfolio. The color of each Super CREZ indicates the Environmental Exclusion Level to which the site suitability has been relaxed, with white fill being no relaxation. The suitable area within relaxed Super CREZs corresponds to the Exclusion Level to which it has been relaxed.

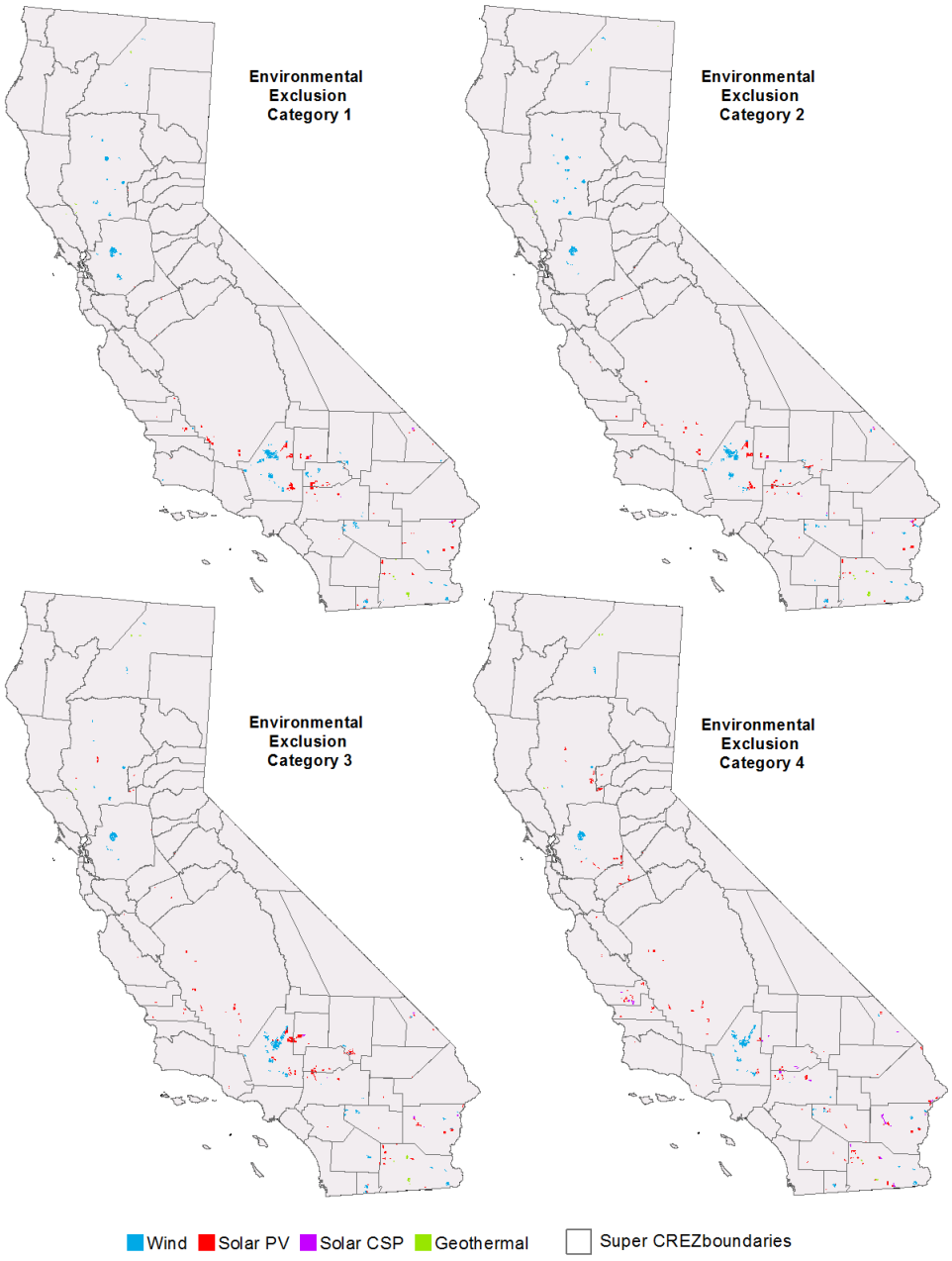

Figure 3.4: Development zones selected to meet the RPS Calculator's 2030 "50% in-state" renewable energy target

Maps show the optimally selected build-out for each technology using the relaxed site suitability models under the Category 1 through 4 Environmental Exclusion Levels (Figure 3.3). The ORB model selects development zones from the site suitability model by minimizing the total generation and transmission land area while meeting the RPS calculator portfolio's Super CREZ-specific technology generation requirements.

be generated within California (in the 50% in-state scenario), the same reduction in available wind generation under Category 2 and 3 Exclusion Levels must be offset by in-state solar PV. Under Category 4 Exclusion Level in the 50% in-state scenario, a dramatic increase in solar CSP generation largely compensates the reduction in both wind and geothermal generation (Figure 3.5A).

Land area—The total California land area needed for wind generation decreases at the higher exclusion levels, as generation mixes shift to more solar PV and CSP, and to out of state wind in the WECC-wide scenario (Figure 3.5C). The area in the in-state 50% scenario for solar PV increases with exclusion levels, and for CSP at the Category 4 Exclusion Level due to the need for over-development of solar technologies beyond demand resulting in solar generation curtailment. However, it may be acceptable to develop more areas of lower conservation value in exchange for avoided impacts in higher quality areas.

Land use efficiency—Reductions in generation land use efficiency (GWh km^{-2}) across Environmental Exclusion Levels and RPS scenario targets are gradual and low, with a few exceptions at high RE penetration and under high environmental constraints (Figure 3.5C). The decrease in land use efficiency is most notable for solar PV, solar CSP, and geothermal between Category 3 and 4 Exclusion Levels in achieving 50% in-state targets. Land use efficiency for wind decreases most drastically between Category 2 and 3 Exclusion Levels to meet the 33% in-state target. The relative inelasticity of land use efficiency across combinations of RPS targets and environmental exclusion categories is in large part due to the way the RPS Calculator builds portfolios. The Calculator selects the generation mix that minimizes costs, which is directly and largely determined by a development zone's renewable resource quality and thus the zone's land use efficiency. Higher resource quality translates into higher capacity factors and more generation per unit land area (e.g., GWh km^{-2}). Despite the gradual reduction in land use efficiency for each technology as RE penetration and environmental constraints increase, the overall—"all technologies"—land use efficiency increases (Figure 3.5C) since solar PV generation increasingly substitutes wind generation (Figure 3.5A), and the land use factor (e.g., MW km^{-2}) of solar PV is significantly greater than that of wind (Table 3.2). However, the land use areas reported for each technology represent the "total" project land use, which represents the entire area of a wind or solar power plant, as opposed to the direct land use, which represents the land transformed or altered from its natural state due to the presence of the power plant (i.e., just the land footprint of the infrastructure). The direct land use for wind power is significantly lower than that of solar power due to the footprint of wind turbines and roads

Conservation, water, and land cover impacts

Conservation impacts—To compare the conservation impacts of imposing environmental constraints on RE build-out, we developed an area-weighted average environmental impact score (EIS) and calculated the area of land falling within each EIS, where higher EIS values indicate greater conservation impact (Figure 3.6B, Figure 3.7). See methods section 2.4 for an explanation of the EIS metric. Across all generation technologies as well as an entire

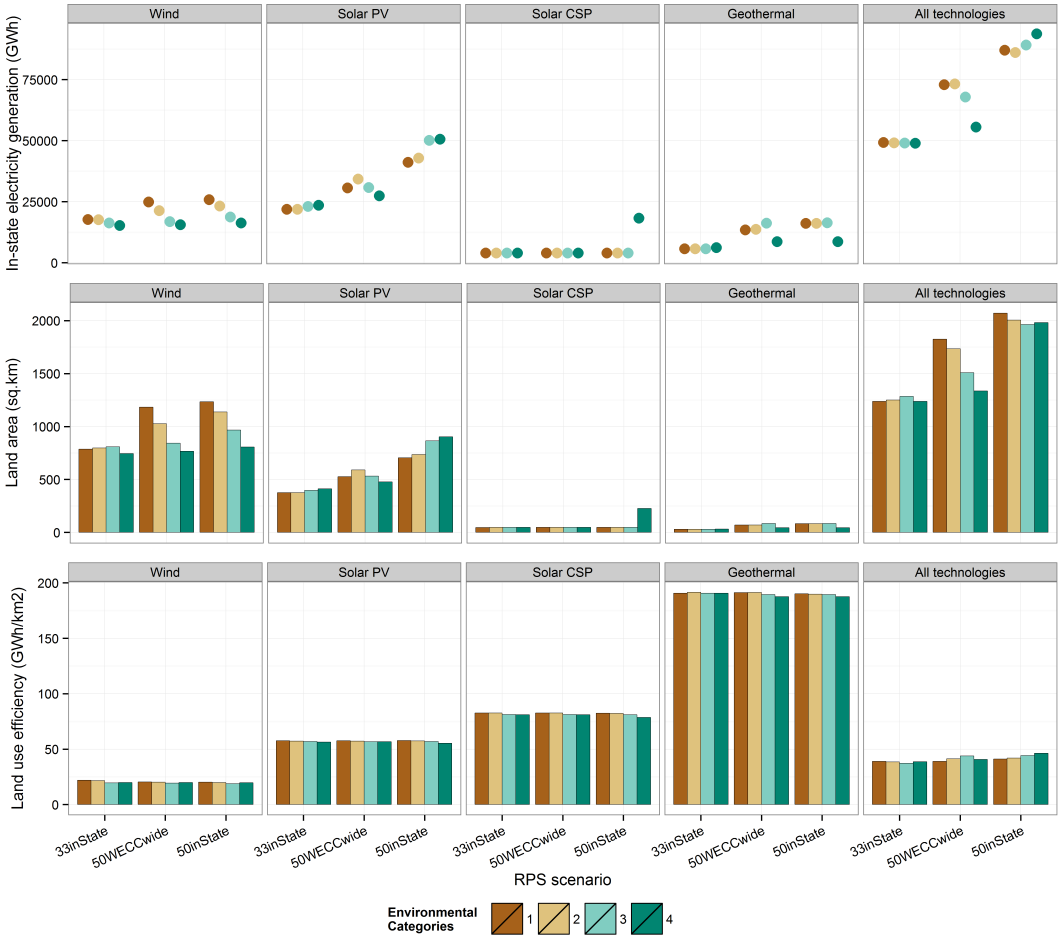

Figure 3.5: In-state generation and potential land area impacts of 2030 modeled build-out scenarios

The ratio of in-state electricity generation in GWh (A) to in-state generation land area in km^{-2} (B) is the land use efficiency in GWh km^{-2} (C). These generation and land area metrics are provided for each renewable energy technology or for "all technologies" combined within a particular scenario (e.g., 33% in-state RPS target under Category 1 Environmental Exclusion Level). Generation values and land areas do not include distributed solar PV or distributed wind.

RPS portfolio ("All technologies"), results show a decline in average EIS with increasing environmental constraints, which suggests that fewer environmentally sensitive areas would be selected for RE development (Figure 3.6B). This trend is also clearly observed in the reduction of land areas rated as EISs 3, 2, and 1 with increasing environmental exclusions (Figure 3.7). The entire RE build-out under the Category 4 Exclusion Level to meet the 50% in-state target has less than 200 km^2 in EIS 2 areas and nearly 1000 km^2 in EIS 0 areas compared to nearly 600 and 360 km^2, respectively, under the Category 1 Exclusion Level (Figure 3.7).

For solar PV in particular, average EIS decreases substantially and consistently with increasing environmental exclusions, indicating that for solar PV, land impacts can be largely avoided by applying development exclusions. Under the Category 4 Exclusion Level for all RPS scenarios, more than half of all solar PV land areas are sited on land with low conservation value (EIS 0). The average EIS of a large solar PV build-out, such as in the 50% in-state scenario, can be less than that of any other RE technology. The differences in average EIS between Category 3 and 4 Exclusion Levels for wind and solar CSP are negligible, but these scores are significantly lower than those under Category 1 and 2 Exclusion Levels (Figure 3.6B). Solar CSP under the Category 4 Exclusion Level and in the 50% in-state scenario has a large share of development on EIS 1 land areas (due to the need to relax constraints described in section 2.3.2) but also substantially more development is sited on EIS 0 land area compared to other Environmental Exclusion Levels (Figure 3.7).

Environmental constraints appear to have lower impacts on geothermal resource quality compared to other technologies, as the ORB model sited geothermal in areas with lower conservation value (average EIS is less than 1) even under the more relaxed environmental constraints. This indicates that some of the highest quality geothermal resources are also in locations that have lower conservation value. The average EIS for geothermal was relatively invariant to changes in environmental constraints, until Category 4 Exclusion Level, an observation that is also consistent with a previous study.4 Also, geothermal did not experience the same intensity of environmental constraints, since the Imperial Super CREZ, in which a large share of total in-state geothermal generation is sited by the RPS Calculator, needed to be relaxed for three of the four Environmental Exclusion Levels due to the insufficient wind and solar generation (Figure 3.3).

Landscape fragmentation—Trends in housing density, which is used as a proxy metric for landscape fragmentation (see methods section 2.4), are consistent with and complement trends observed in environmental impact scores (Figure 3.6C). Across all technologies, an increase in the area of environmental exclusions generally results in development on more fragmented land, which is consistent with environmentally sensitive or high conservation value lands as being more intact and less disturbed by human development (Figure 3.6C).

Water use—Water consumption is directly proportional to the amount of generation, with the exception of geothermal, which differs by sub-technology depending on the capacity factor of the site (Table 3.2). Total water consumption across the state will be less than 13,000 annual household-water-demand-equivalents (HWDeq) for all but the most environmentally constrained and highest RE penetration scenario (Figure 3.6D). Results of spatially

disaggregating all technologies' water demand by groundwater basin are shown in Figure B.2. Spatial disaggregation shows that no groundwater basin will sustain more than 3,000 HWDeq of demand from RE development. As RE penetration increases, additional basins—Salinas, Sacramento Valley, Modoc Plateau, Lucerne Valley, and Lower Mojave River Valley—may begin to experience water demand from RE generation (Figure B.2). Due to the multi-fold increase in solar CSP generation under the Category 4 Exclusion Level in the 50% in-state generation scenario, several basins experience a significant shift in water demand, with basins like Imperial Valley, Chuckwalla Valley, San Joaquin and Upper Mojave River Valley doubling in water demand, but basins like Antelope Valley reducing water demand by 50% due to a reduction in estimated renewable energy generation in this region. However, under the 50% WECC-wide scenarios, in-state water consumption is reduced across the state, with no single groundwater basin experiencing more than 1000 HWDeq from all RE development (Figure B.3). Though water demand increases under the Category 4 Exclusion Level in the 50% in-state scenario, the additional demand is distributed across more ground water basins (Figure B.3).

Land cover type—Analysis of land cover types impacted in each modeled build-out shows that development of wind, solar PV, and solar CSP will predominantly be on warm semi-desert scrub and grassland (Figure 3.8). However, the dominance of solar PV development on warm semi-desert scrub and grassland declines gradually with increasing environmental constraints in the 33% in-state and 50% WECC-wide scenarios. This results in more development on herbaceous agricultural vegetation, Mediterranean grassland and forb meadow, and developed and urban land cover types as we exclude more areas of conservation value. Due to the increase in solar PV generation targets, solar PV in the 50% in-state scenario even more strongly demonstrates this trend of shifting spatial development patterns from highly concentrated in the southern deserts to greater state-wide dispersion as we impose more environmental constraints (Figure 3.9). The largest changes in land cover type for wind occur in herbaceous agricultural vegetation, Mediterranean grassland and forb meadow, and warm temperate forest, all of which experience less land transformation from wind development with increasing environmental constraints at 50% in-state and WECC-wide targets. Geothermal is largely sited in agricultural and cool temperate forest lands, which is consistent with the locations of existing geothermal projects.

Electricity cost impacts Results of applying environmental exclusions in the RPS Calculator show that the level of in-state RE targets is what largely dictates the economic cost impact of increasing environmental constraints (Figure 3.10). As California's grid integrates more RE, the greater the electricity cost premium of applying environmental constraints becomes. Total revenue requirement is invariant to increases in environmental constraints in the 33% in-state scenario, with only a 0.2% cost premium under the Category 4 Exclusion Level. The maximum cost premium for the 50% WECC-wide scenario—under the Category 4 Exclusion Level—is still only 2%, with Category 1 through 3 Exclusion Levels resulting in no greater than a 0.6% electricity cost increase. It is only at the most environmentally constrained and highest in-state RE target scenario that the cost premium increases dramatically—from 2% to 12% between Category 3 and 4 Exclusion Levels.

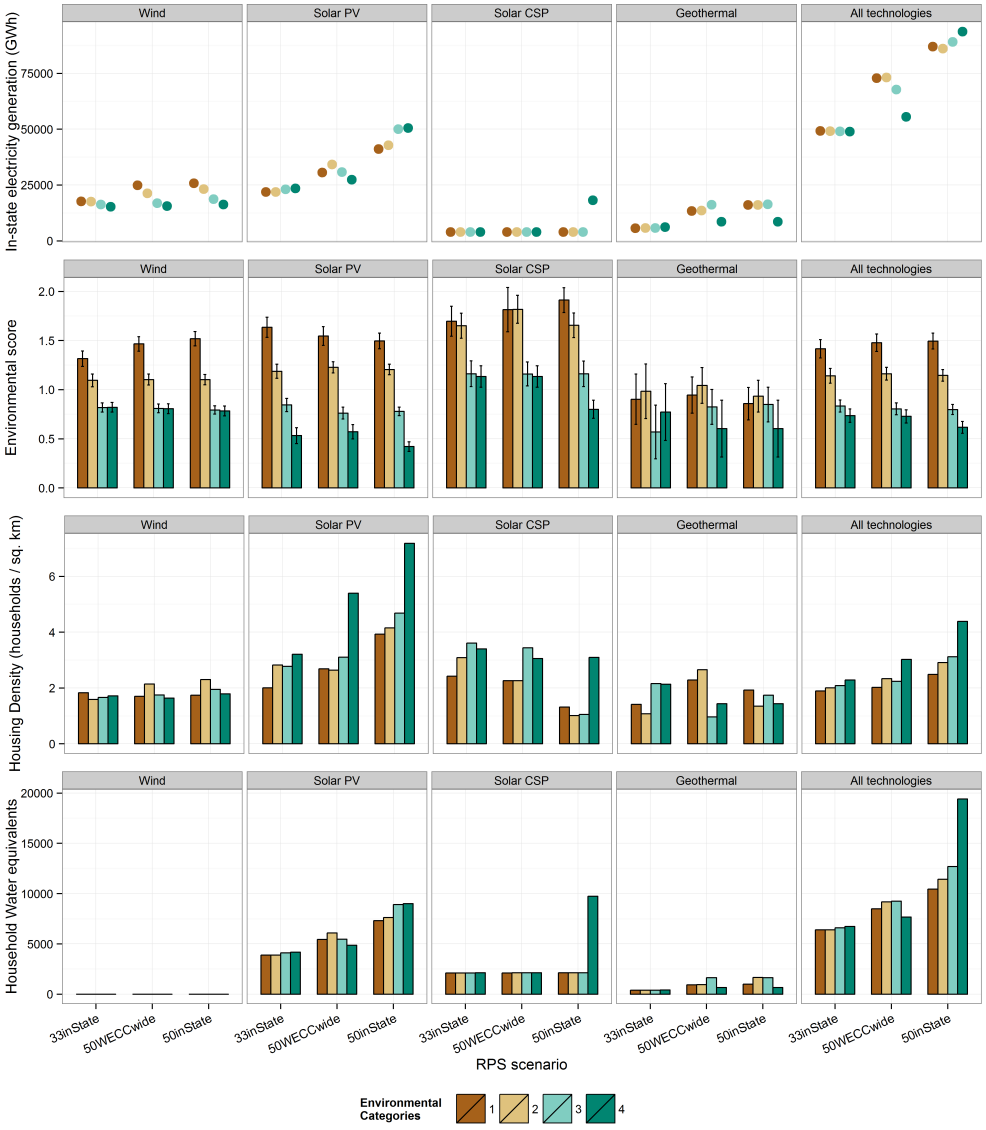

Figure 3.6: Environmental impacts of 2030 modeled build-out scenarios
In-state generation (A) is provided as another possible explanatory variable for the trends observed across environmental exclusion categories, RPS scenarios, and technologies. The average environmental impact score (EIS) (B) of a build-out scenario is the area-weighted average EIS occupied by the selected development zones. Average EIS values closer to zero indicate lower conservation impact; larger values indicate higher conservation impact. Error bars show each scenario's standard deviation. Average housing density (C) is used as a proxy for the degree of fragmentation, with areas of higher housing density having greater landscape fragmentation. Household water demand equivalents (D) is the annual water consumption of an average household in the U.S., or 146,000 gal. See section 2.4 for a description of impact metrics.

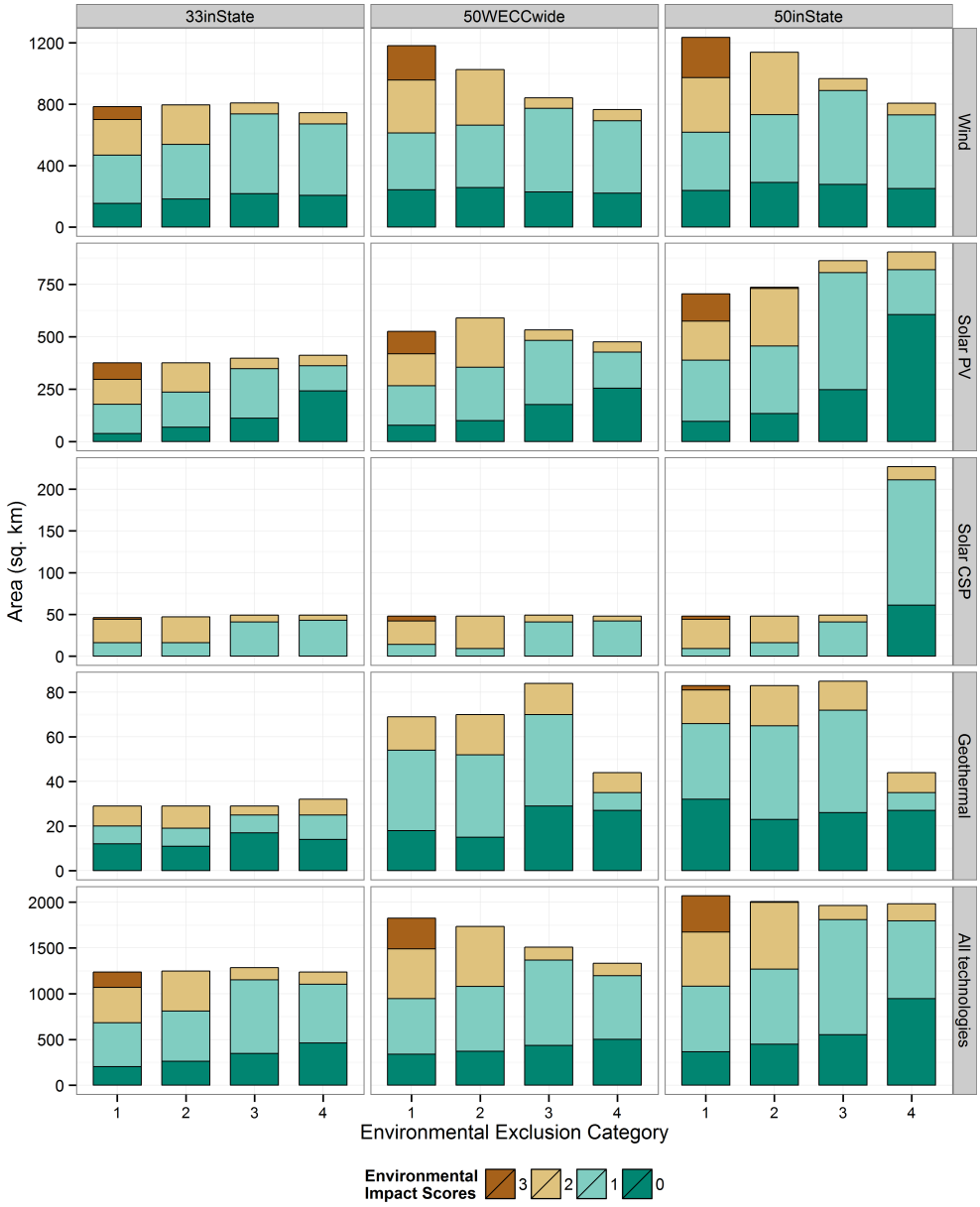

Figure 3.7: Environmental impact scores of 2030 modeled build-out scenarios' generation land area

Stacked bars show the area of land falling within each environmental impact score. EIS values closer to zero indicate areas with lower conservation impact; larger values higher conservation impact. The average environmental impact score reported in Figure 3.6B is the area-weighted average of an entire scenario.

Changes in electricity costs, which reflect both in-state and out-of-state generation and transmission costs incurred by the utility (but do not include mitigation or permitting costs that are specific to particular sites), can be in part explained by changes in total in-state RE generation (Table 1, Figure 3.5A). The amount of in-state generation steadily increases in the 50% in-state scenario, as more environmental constraints are imposed. This growth is almost entirely attributed to solar PV, which comprises a larger part of the generation portfolio as a result of reduced wind generation. Under Category 4 Exclusion Level in the 50% in-state scenario, curtailment of solar PV during low-demand hours explains the need for overall generation increase to meet the same amount of demand in 2030. Additionally, distributed PV generation (i.e., small scale) contributes approx. 12,000 GWh in the Category 4 Exclusion Level 50% in-state scenario and is not included in the RE generation values reported in Table 1, Figure 3.5A, or Figure 3.6A since the ORB model was not designed to model the build-out of distributed generation. As such, the combination of adding more costly distributed solar PV generation, curtailing utility-scale solar PV generation, and large increases in more costly solar CSP generation explains the large cost premium of the Category 4 Exclusion Level, 50% in-state scenario. The 50% WECC-wide scenario avoids the need for a large build-out

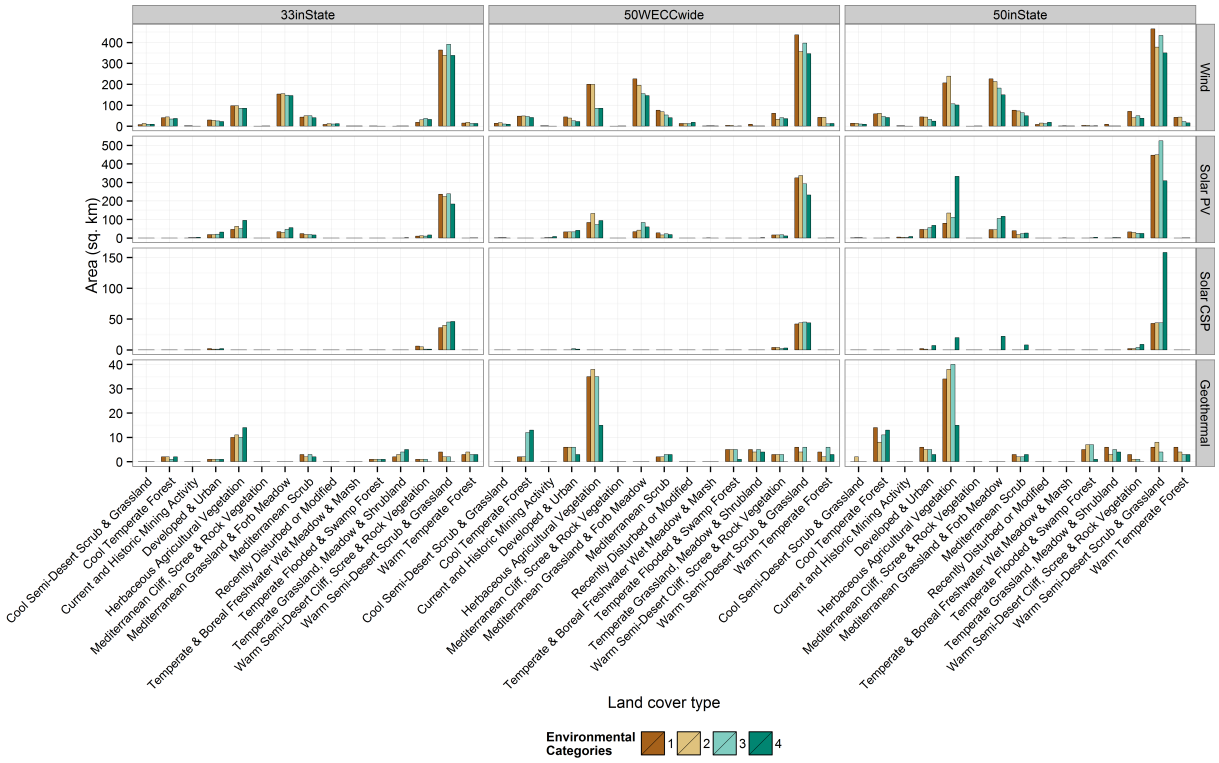

Figure 3.8: Area of land cover type impacted in each modeled build-out scenario Note that the limits of the y-axis differ between generation technologies. Land cover types follow the National Vegetation Classification System (NVCS). Figure 3.9 depicts the land cover types as they occur throughout California.

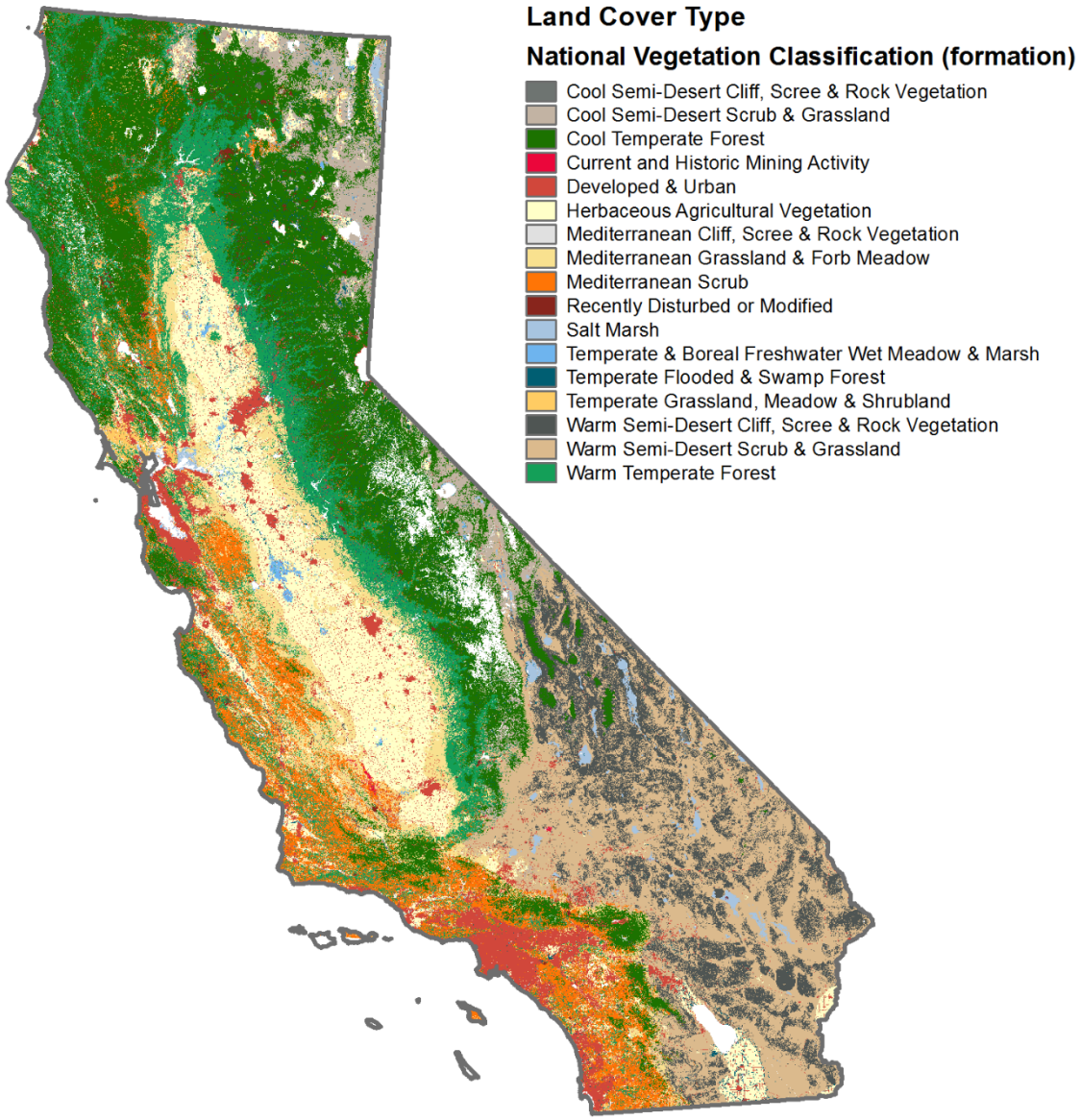

Figure 3.9: Land cover types in California
This map is a reference for Figure 3.8. As such, it only depicts land cover types impacted by modeled renewable energy build-out scenarios.

of solar electricity under the Category 4 Exclusion Level by taking advantage of out-of-state wind resources with higher marginal production value compared to in-state solar.

Additional transmission expansion and upgrade costs also contribute to cost increases, since the share of transmission in the total revenue requirement increases steadily from approximately 10.5% (Category 1) to 11.2% (Category 4) for the 50% in-state target. However, this rate of increase does not keep pace with the rate of increase of total electricity costs between Category 1 and 4 Exclusion Levels for the 50% in-state target. With increasing environmental constraints, transmission costs account for a smaller share of the cost differences between scenarios—it accounts for 32% of the cost difference between Category 1 and 2 Exclusion Level, 17% between Categories 2 and 3, and 16% between Categories 3 and 4.

3.4 Discussion of key results

RPS Calculator generation portfolios: The RPS target within California largely determines the extent to which the generation mix changes as a result of environmental constraints. Increasing the area of environmental exclusions reduces both the availability and cost of wind generation more consistently and substantially than any other technology examined (Figure 3.5).

By modifying the available potential under different tiers of environmental constraints within each Super CREZ, we created "environmentally preferred" generation portfolios within the RPS Calculator. Depending on the availability and cost of resources under each set of environmental constraints, these portfolios differ in their generation mix. The percentage target of RE largely determines the extent to which a portfolio changes as a result of environmental constraints. For the 33% in-state target, there is little variation in the generation of each technology except for wind, which consistently declines with increasing environmental exclusions. To achieve 50% in-state and WECC-wide targets, wind generation reduces in response to increasing environmental constraints. If all generation must be in-state, geothermal generation also decreases under the Category 4 Exclusion Level, with the difference largely made up by solar PV and solar CSP. The overall RE generation also increases with greater environmental constraints in this scenario due to the curtailment of solar electricity. However, if WECC-wide generation can be sourced to meet the 50% by 2030 target, in-state wind and solar PV generation that would be excluded under increasing environmental constraints would be substituted by out-of-state wind. As such, the most salient impact of imposing environmental constraints for California land areas in a 50% WECC-wide scenario is the overall reduction in within-state RE generation. This may result in a shift of environmental impact to out of state resources as creating environmentally constrained suitable sites for the entire WECC region was beyond the scope of the study. This suggests the need to coordinate land use and electricity planning at a regional scale to ensure the best climate and conservation outcomes.

Land area and land use efficiency: High renewable resource quality exists in environmentally sensitive areas, which results in a slight reduction in each

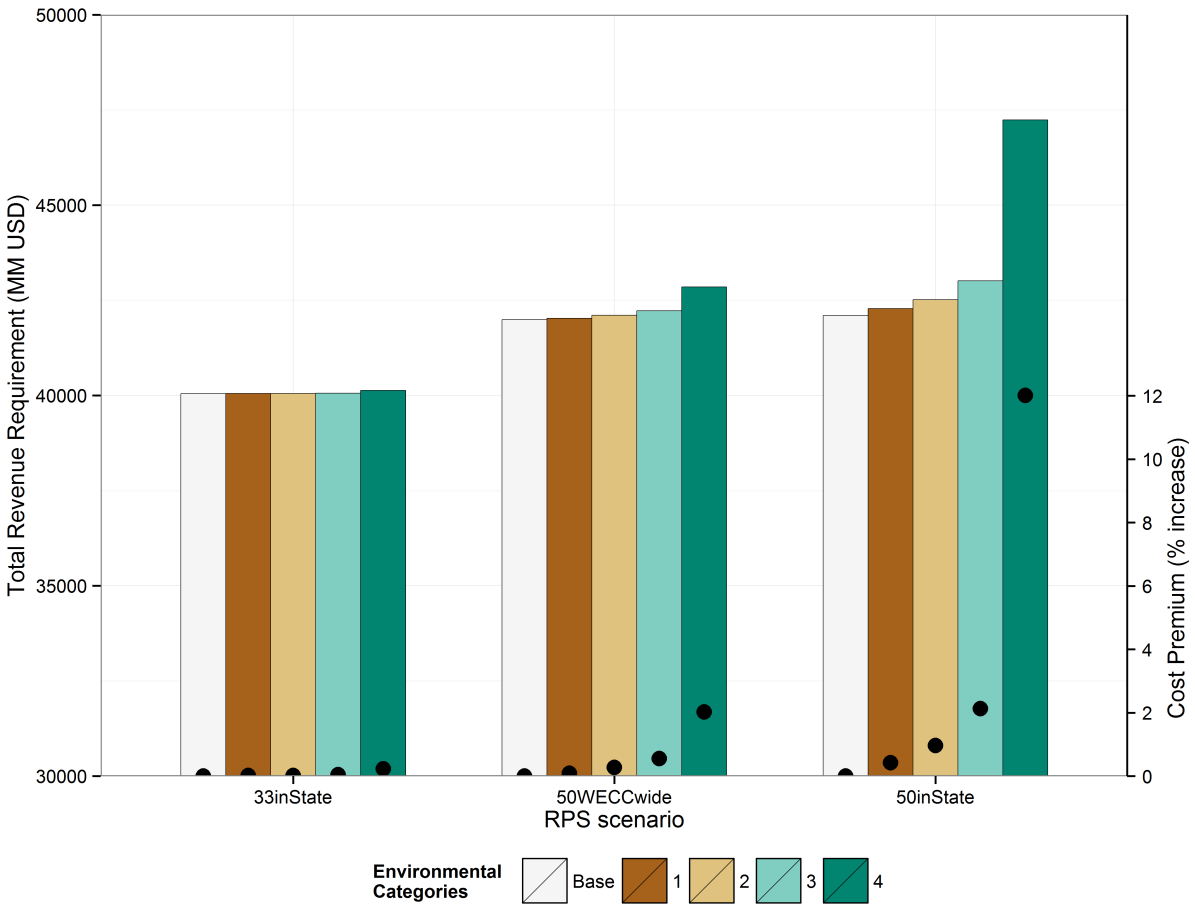

Figure 3.10: RPS Calculator estimated electricity costs of each Environmental Exclusion Level

The bar plot corresponds to the primary (left) y-axis indicating the total revenue requirement (total electricity costs) of each RPS Calculator portfolio (note that the left y-axis begins at 30,000 MM USD). The x-axis shows each Environmental Exclusion Level for each RPS target scenario—33% in-state, 50% WECC-wide, 50% in-state by 2030—in increasing order of in-state RE generation. The secondary (right) y-axis and the scatterplot show the electricity cost premium (in percent increase) of imposing an environmental exclusion above the base case. The RPS Calculator's environmental base case is the unmodified Calculator v6.0, which does not incorporate environmental exclusions developed in this present study.

generation technology's land use efficiency as more environmental exclusions are imposed. However, the relative inelasticity of land use efficiencies to additional environmental constraints suggests that cost-effective substitution of RE technologies is possible under most scenarios and environmental Exclusion Levels (Figure 3.5).

The general trend is a reduction in land use efficiency with increasing environmental constraints and higher electricity generation. However, the decline in land use efficiency is typically slight, which is likely an effect of the cost-minimizing method in which the RPS Calculator builds a generation portfolio, but is also importantly indicative of the ability for different RE technologies to cost-effectively substitute each other to meet RPS targets, at least until the most stringent Environmental Exclusion Level at highest RE penetration. Within a particular RPS target, the greatest decline (1 GWh km^{-2}) in total land use efficiency occurs between Category 3 and 4 Exclusion Levels for solar PV. That is, after the Category 3 Exclusion Level in the 50% in-state scenario, it becomes increasingly more costly to substitute the reduction in wind and geothermal with solar PV and CSP.

While the differences in land use efficiency have been quantified and compared, a better comparison would be of the resultant economic costs of these differences. It is otherwise difficult to meaningfully understand the impact of a 1 GWh km^{-2} loss in land use efficiency or a particular amount of additional area required to meet targets.

Conservation and land use benefits of environmental exclusions: Imposing environmental constraints on RE development achieves lower environmental impacts and results in development of more fragmented land areas (Figure 3.6, Figure 3.7).

Sites optimally selected under only legal exclusions (Category 1 Exclusion Level) are associated with higher environmental impact compared to sites selected under more environmental exclusions. Given that the RE build-outs are spatially modeled by minimizing generation and transmission land area, this result suggests that opportunities for development of high quality resources close to transmission and substations exist within environmentally sensitive areas, a finding that agrees with Wu, Torn, and Williams (2015) recent study using different sets of environmental exclusions. These areas of high conservation value and high quality resources are likely to be developed if they are not actively protected. Thus, the incorporation of environmental constraints in RPS planning and siting will be necessary to achieve both conservation and clean energy goals.

Land cover types and geographic diversity: With increased renewable energy generation and environmental exclusions, generation becomes more widely distributed across the state, which results in more development on herbaceous agricultural vegetation, grassland and forb meadow, and developed and urban land cover types (Figure 3.8).

For solar PV and CSP, which increase in generation under more ambitious RPS 2030 targets, the general trend with increased environmental constraints is a geographic shift of modeled installations from the desert south to other parts of the state, largely northern Mojave, the Central Valley, and Northern California. This geographic dispersion of RE development

is more favorable compared to spatially concentrated development from conservation, grid reliability, and system cost standpoints, since geographic heterogeneity reduces aggregate variability of generation and additional generation capable of ramping (Mills, 2010). Also, a shift towards disturbed land areas (agricultural vegetation and developed and urban land cover types) reduces the burden of development on fragile and intact desert and scrubland ecosystems.

Water consumption: Since renewable energy water demand is directly proportional to increases in generation, more ambitious renewable energy targets result in higher water consumption from renewable generation. However, overall electricity water demand will likely reduce due to the substitution of natural gas combined cycle, which is a more water-intensive generation technology. Under more environmental exclusions, this demand is also more geographically dispersed (Figure 3.6).

Water demand for electricity generation in any single groundwater basin does not exceed the annual water demand equivalent to 3,000 households, with most groundwater basins experiencing no more than 1000 household water demand equivalents. Under the Category 4 Exclusion Level, the water demand for WECC-wide and 33% in state scenarios of any single groundwater basin does not exceed the annual water demand equivalent to approximately 1000 households. Although water requirements from the four technologies examined in this study do increase with increasing RE penetration, the total water demand from electricity generation is likely to decrease since RE displaces conventional thermal technologies such as nuclear and natural gas that are much more water intensive per MWh of generation.

Electricity costs and balancing the benefits of land conservation: Minimizing both negative conservation impacts and electricity costs at high renewable energy penetration may require California to utilize WECC-wide renewable energy resources (Figure 3.10).

Meeting the 50% in-state target by 2030 under the Category 4 Exclusion Level is possible and would result in a 60% reduction in average environmental impact score or a 40% reduction in development on land areas with EIS 1, 2, and 3, compared to the build-out under the Category 1 Exclusion Level. However, doing so would incur an 82% increase in water consumption and a 12% increase in costs over the Category 1 Exclusion Level case. If environmental exclusions were reduced to Category 3 Exclusion Level to achieve the same 50% in-state target, the water and cost impacts would drop dramatically—to 20% increase in water consumption and a 2% cost premium—but it would only achieve a 47% reduction in average EIS or a 17% reduction in development on EIS 1-3 land areas. If the RPS portfolio could include WECC-wide resources, it would be possible to meet the most ambitious RPS target of 50% under the most stringent set of in-state environmental exclusions for only a 2% cost premium. The 50% WECC-wide build-out under the Category 4 Exclusion Level also uses less water and achieves more than 50% reduction in average environmental impact score or a 44% reduction in development on EIS 1-3 land areas, compared to the build-out under the Category 1 Exclusion Level.

Selecting the appropriate set of environmental constraints, which may be a combination of

technology-specific stringencies, will need to balance cost impacts with conservation, water, and grid benefits. Without monetary valuation of the total avoided ecosystem, ecological, and land use costs, as well as costs associated with permitting, delays, and mitigation, under each set of environmental exclusions, it is difficult to objectively determine whether the economic value of the environmental benefits justify a 2% or a 12% premium in electricity costs—i.e., whether the benefits exceed the costs in each scenario. As such, the results as they are presented in this study are inadequate for an objective decision within a traditional cost-benefit framework. Using a cost-effectiveness framework (e.g., USD per unit conservation value) could improve the tangibility of these conservation benefit vs. electricity cost comparisons.

Chapter 4

Strategic renewable energy siting using multi-criteria spatial analysis[1]

Recent forecasts suggest that African countries must triple their current electricity generation by 2030. As the first multi-criteria assessment of wind and solar potential for large regions of Africa, our study is the first to show how economically-competitive and low-environmental-impact renewable resources can significantly contribute to meeting this demand. We created the Multi-criteria Analysis for Renewable Energy (MapRE) framework to map and characterize solar and wind energy zones in 21 countries in the Southern and Eastern Africa Power Pools (SAPP and EAPP) and find that potential is several times greater than demand in many countries. "No-regrets" options—or zones that are low-cost, low-environmental impact, and highly accessible—exist such that significant fractions of demand can be quickly served with low-impact resources without large cost impacts. Because "no-regrets" options are spatially heterogeneous, international interconnections are necessary to help achieve low-carbon development for the region as a whole, and interconnections that support the best renewable options may differ from those planned for hydropower expansion. Additionally, interconnections and selecting wind sites to match demand reduces the need for SAPP-wide conventional generation capacity by 9.5% in a high-wind scenario, resulting in a 6-20% cost savings depending on the avoided conventional technology. Strategic selection of low-impact and accessible zones is more cost-effective with interconnections compared to solutions without interconnections. Overall results are robust to multiple load growth scenarios. Together, results show that multi-criteria site selection and deliberate plan-

[1]This chapter was originally published as:

Wu, G.C.*, R. Deshmukh*, K. Ndhlukula, T. Radojicic, J. Reilly-Moman, A. Phadke, D. Kammen, D.S. Callaway. 2017. Strategic siting and grid interconnection key to Africa's low-carbon electricity future. *Proceedings of the National Academy of Sciences.* doi: 10.1073/pnas.1611845114

*authors contributed equally.

The main content of the published paper has been placed in its entirety in the main body of the dissertation and the supporting information has been placed in its entirety in the Appendix of the dissertation.

ning of interconnections may significantly increase the economic and environmental competitiveness of renewable alternatives relative to conventional generation.

4.1 Introduction

As a region, Africa has the lowest per capita electricity consumption in the world, due in large part to lack of generation and transmission infrastructure development at both the national and regional levels (Eberhard et al., 2011). Yet, the average cost of electricity in most African countries is at least twice that of other non-OECD countries (Eberhard et al., 2011). For the region to successfully meet goals to increase affordable electricity access and reduce demand curtailment, electricity generation will need to grow exponentially. By some estimates, demand in the Eastern and Southern African Power Pools (EAPP and SAPP), which encompass more than 50% of the continent's population, may collectively exceed 1000 terawatt-hours by 2030, or nearly triple their electricity consumption in 2010 (Eastern Africa Power Pool et al., 2011; Southern Africa Power Pool and Nexant, 2007).

To meet energy goals, decision-makers are looking to fossil-fuel and hydropower as familiar and under-tapped resources (Eastern Africa Power Pool et al., 2011; Southern Africa Power Pool and Nexant, 2007; Eberhard et al., 2011). With the insecurity and high costs of fossil fuels, the planning paradigm has become increasingly hydropower-centric (Eastern Africa Power Pool et al., 2011; Southern Africa Power Pool and Nexant, 2007; Eberhard et al., 2011). Yet climate vulnerability (Cervigni et al., 2015), international cooperation barriers and transboundary water rights issues, large cost overruns (Sovacool, Gilbert, and Nugent, 2014), and high socio-environmental impacts (Winemiller et al., 2016) plague this paradigm and perpetuate risks of hydro-dependence. Among the alternatives, geothermal is considered under-developed but geographically limited with long lead times, and wind and solar have historically been dismissed as too expensive and temporally variable (Collier and Venables, 2012; Eberhard et al., 2011).

However, costs of utility-scale wind and solar generation are rapidly declining (Taylor et al., 2015). Levelized cost of wind energy is competitive with that of hydropower in Kenya and Ghana (A. Pueyo, Bawakyillenuo, and Osiolo, 2016). Wind and solar photovoltaics (PV) are now South Africa's cheapest and third cheapest form of generation, respectively (Bofinger, Mushwana, and Bischof-Niemz, 2015). As a result of these competitive costs, renewable energy deployment is growing in a handful of African countries (South Africa Department of Energy, Eskom, and National Energy Regulator of South Africa, 2016; Renewable Energy Policy Network for the 21st Century, 2015; Lake Turkana Wind Power, 2015). Yet, contribution of wind and solar in each power pool remains below 1%, likely due to multiple perceived risks of resource quality, interconnection availability, and high investment costs.

Multi-criteria resource mapping can minimize risk by enabling strategic site selection. To identify 'no-regrets' siting options–or those that are low-cost, low-impact, highly-accessible and thus can be justified from multiple stakeholder perspectives of risk–large amounts of data across large spatial scales must be synthesized (Black & Veatch Corp. and RETI Coor-

dinating Committee, 2009) and incorporated in a multi-criteria framework. Comprehensive wind and solar energy assessments and integration analyses have highlighted their potential to contribute to energy transitions in many countries (McElroy et al., 2009; Davidson et al., 2016), yet roughly half of the EAPP and SAPP countries lack even the most basic spatially-explicit wind and solar assessments. Existing studies typically omit critical cost, interconnection, socio-environmental impact information (Hermann, Miketa, and Fichaux, 2014).

To address this gap, we developed the first large-scale multi-criteria resource assessment of grid-connected wind, solar PV, and concentrating solar power (CSP) and integrated it into a new suite of tools—Multi-criteria Analysis for Planning Renewable Energy (MapRE). The resource mapping approach is based on techno-economic criteria, generation profiles (for wind), and socio-environmental constraints. The suite of MapRE spatial models and tools (`http://mapre.lbl.gov`) give any stakeholder the ability to weigh multiple siting criteria—e.g., generation cost, distance to transmission lines and load centers, and possible conservation impact—and examine their trade-offs. Siting using these criteria reduces difficult-to-monetize barriers, such as ecological impacts or challenging transmission extensions and upgrades, which often stall projects (Fischlein et al., 2013).

In addition to these factors, strategic siting of wind and solar energy can address the temporal variability of generation, a major challenge for grid integration, particularly in countries without strong institutional capacity and infrastructure. Technological solutions for balancing variability—such as excess reserve generation capacity, fast generators, and battery storage—are expensive (Cochran et al., 2012) and are significant barriers to economies with limited access to capital. Strategic spatial diversification of sites is an alternative, potentially more cost-effective strategy for managing variability (Mills and Ryan Wiser, 2012; Katzenstein, Fertig, and Apt, 2010; Drake and Hubacek, 2007; Reichenberg, Johnsson, and Odenberger, 2014; Roques, Hiroux, and Saguan, 2010); however, no study has examined the grid value of geographic diversification in large regions of Africa.

Studies in other parts of the world suggest that extensive interconnections can strengthen spatial diversification (MacDonald et al., 2016), and other studies have found that it is significantly cost-effective to support energy trade in Africa (Graeber, Spalding-Fecher, and Gonah, 2005; Bowen, Sparrow, and Yu, 1999; Rosnes and Vennemo, 2012; Sanoh et al., 2014; Saadi, Miketa, and Howells, 2015). However, those studies that examined renewable energy (Sanoh et al., 2014; Saadi, Miketa, and Howells, 2015) lacked the spatial (country-level) and temporal (annual) resolutions necessary for modeling integration of highly temporally and spatially variable renewable energy. The EAPP and SAPP are considering new interconnections, but to exchange future conventional and hydroelectric generation (Eastern Africa Power Pool et al., 2011; Southern Africa Power Pool and Nexant, 2007). Those required to support renewables may be substantially different.

We provide the first comprehensive multi-criteria assessment of wind and solar resources in EAPP and SAPP and identify 'no-regrets' options. We also examine the importance of strategic siting for managing temporal variability of generation by increasing hourly correlation between aggregate wind production and electricity demand, specifically whether in-

ternational interconnections enable cost-effective deployment of wind capacity in the SAPP. The power pools include the following 21 countries: Angola, Botswana, Burundi, Djibouti, Democratic Republic of Congo, Egypt, Ethiopia, Kenya, Lesotho, Libya, Malawi, Mozambique, Namibia, Rwanda, South Africa, Sudan, Swaziland, Tanzania, Uganda, Zambia, and Zimbabwe.

We apply the MapRE approach to examine trade-offs between wind and solar resource quality and multiple siting criteria, including transmission connectivity, distance to the nearest demand center, and ecological intactness of potential project areas. Using a unique dataset of hourly demand profiles for nine SAPP countries and hourly wind profiles, we optimally select wind sites to minimize conventional capacity, with and without interconnections and with and without consideration of multiple siting criteria. We examine wind specifically because it is currently more cost competitive than solar in Africa and exhibits more spatio-temporal variability. We compare this approach with the prevailing practice of selecting sites to minimize the levelized cost of wind electricity.

4.2 Methods

MapRE model overview

To estimate renewable resource potential and spatially-specific criteria important for site selection, we developed the Multi-criteria Analysis for Planning Renewable Energy (MapRE) spatial model using Python and R programming languages and the arcpy spatial analysis module (Appendix C, Fig. C.5). The framework is founded in previous resource assessment and zoning studies (Lopez et al., 2012; Black & Veatch Corp. and RETI Coordinating Committee, 2009; Black & Veatch Corp. and NREL, 2009), but improved and adapted to account for data availabilities of the study region. We used a combination of global or continental data and country-provided datasets that can be broadly categorized into the following: physical (slope, elevation), socio-economic (population density, built-areas), technical (resource quality), and environmental (land cover, protected areas) (Appendix C, Table C.2). We applied thresholds and buffer distances used in previous studies (Lopez et al., 2012; Black & Veatch Corp. and RETI Coordinating Committee, 2009; Black & Veatch Corp. and NREL, 2009) (Appendix C, Table C.2), but adjusted within an economically viable range for each country depending on the projected demand and the resource quality (Appendix C, Table C.3). We created maps of suitable areas for renewable energy development and further divided large areas into 5x5 km spatial units, or project opportunity areas (POA). For each POA, we estimated multiple siting criteria values, including component and total levelized cost of electricity (LCOE). Using a statistical regionalization technique (Spatial Kluster Analysis by Tree Edge Removal), we spatially clustered POAs into "zones" (30 km^2 to 1000 km^2 in size) based on the homogeneity of resource quality (W/m^2) of each POA. We then area-weighted averaged POA siting criteria to generate zone criteria values.

Criteria estimates

We estimated the following site selection criteria for each POA and zone: slope; elevation; population density; resource quality; distance to nearest major load center, transmission line, substation, road, surface water body, existing and proposed wind, solar, and geothermal energy projects; land cover type; total land area, human footprint score (Appendix C, S1.2.1 and Table C.4). We collected country-specific transmission and substation spatial data, and where unavailable, we used the continental dataset from the African Infrastructure Country Diagnostic initiative (Appendix C, Table C.4). In addition, load center locations were collected from countries individually. These criteria values were then used to calculate the following additional criteria for each POA and zone: capacity factor (Appendix C, S1.2.2), annual electricity generation, transmission or substation LCOE, generation LCOE, road LCOE, and total LCOE. Cost estimates relied on various assumptions about fixed and variable specific to the technology and subtechnology (Appendix C, S1.2.3, Table C.6).

Wind build-out scenarios for 2030

To understand the implications of different zone selection approaches and availability of interconnections, we modeled various wind energy build-out scenarios for SAPP in 2030 (Appendix C, S1.3). We acquired hourly wind speed profiles from Vaisala Inc. for 233 wind locations and solicited at least one year's (2013) worth of hourly electricity demand data from each country to create 2030 load forecasts (Appendix C, S1.3.1, Table C.7). Using these two datasets, we constructed a linear optimization problem to select wind zones that minimize the hourly peak net demand (*min-net-demand*) with and without interconnections. We compared the results of this approach to a scenario that minimizes wind LCOE. For each scenario, we compared the maximum net demand (i.e., the installed capacity required in addition to wind power), total annual net demand (i.e., the generation required in addition to wind power), average wind LCOE, and approximate system costs (Appendix C, S1.3.3).

4.3 Results and Discussion

Wind and solar resources are heterogeneous in quality and quantity, but sufficient 'no-regrets' potential exist in each power pool

After excluding areas on the basis of physical, technical, and socio-economic suitability for large-scale renewable energy development (Appendix C, Table C.2), the resulting quantity (TWh) of wind, solar PV, and CSP resources that exist within the EAPP and SAPP collectively exceed the projected 2030 demand 2-5 fold (Fig. 4.1, Appendix C, Fig. C.1 for power pool supply curves). However, these resources, particularly high-quality resources (e.g., high insolation or wind speed) that meet multiple siting criteria, are unevenly distributed between and within countries.

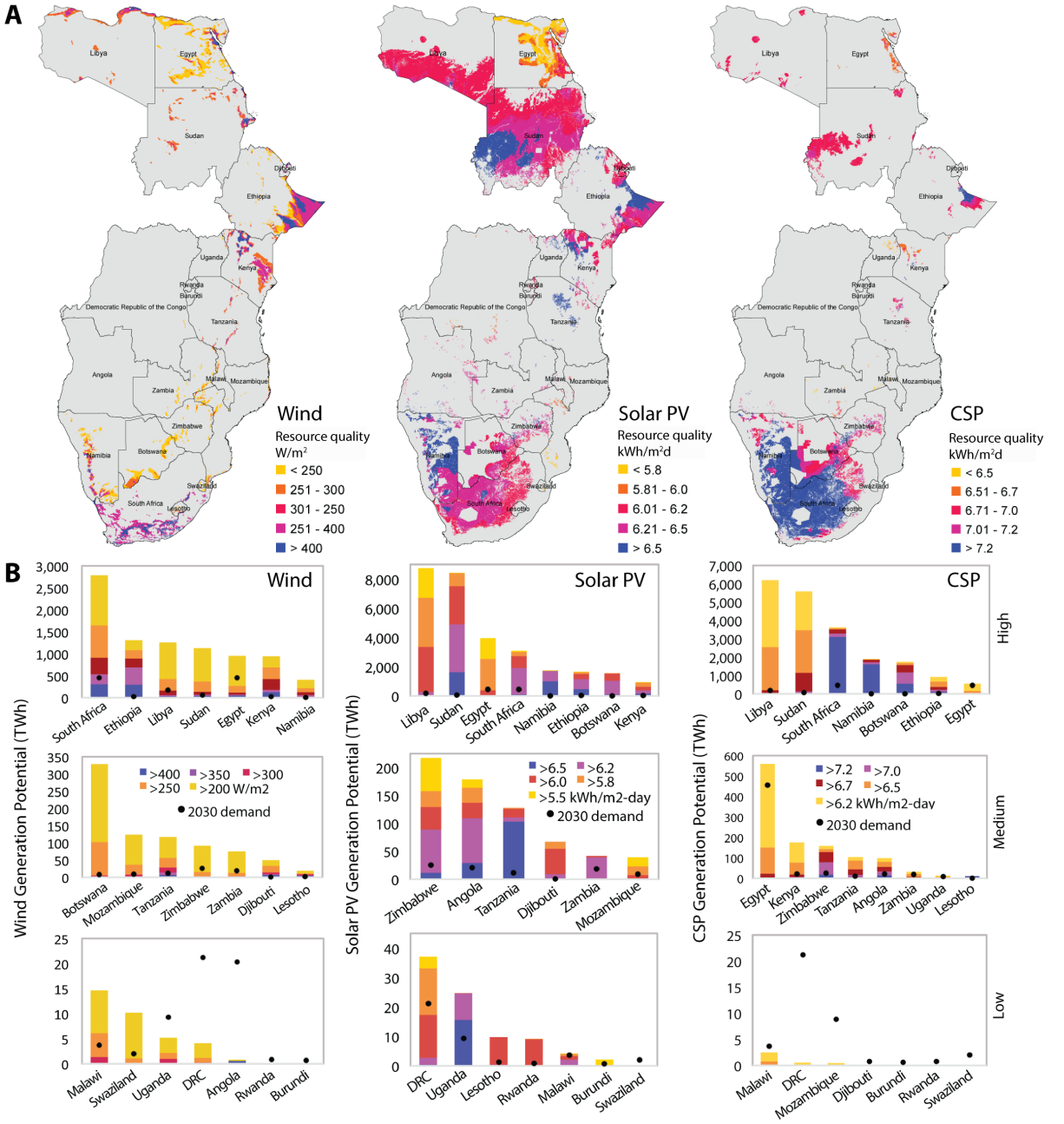

Figure 4.1: Location and potential (TWh) of each country's renewable resources within the Southern and Eastern Africa Power Pools.
(A) Maps show the location and quality of renewable energy potential. **(B)** Corresponding bar charts for each technology show the generation potential (TWh) of each resource quality range (in kWh/m^{2}d for insolation and m/s for wind speed) for each country. Countries are sorted by the total abundance of generation potential (high, medium, low). The 2030 demand for each country, as projected by the EAPP and SAPP Master Plans, is provided as a reference point (Southern Africa Power Pool and Nexant, 2007; Eastern Africa Power Pool et al., 2011).

Examining just resource quality and quantity alone, results show that high-quality resources in a majority of countries are one or two orders of magnitude greater than their projected 2030 demand (Fig. 4.1B). Although about one-fifth of all countries in the study region (Angola, Democratic Republic of Congo, Rwanda, and Burundi) lack sufficient high quality wind resources, their neighboring countries have wind resources that exceed their projected demand (Tanzania, Zambia, and Namibia). Nearly all countries have large and high quality solar PV potential (Fig. 4.1B). CSP is the most spatially limited of the three technologies, with potential significantly less than the projected 2030 demand in at least six countries. The distribution of resource availability and quality support the need for resource sharing to cost-effectively achieve low-impact electricity development regionally.

To examine trade-offs between economic costs and other siting barriers, we selected resource areas across the entirety of each power pool that are in the top 20% and 50% of areas closest to transmission infrastructure, closest to load centers, and that have the highest human footprint score. The multiple dimensions to consider in prioritizing energy projects–resource sufficiency, cost, and other siting barriers–are represented in the shape of each supply curve (Fig. 4.2; Appendix C, Fig. C.1).

Distances to load centers and transmission infrastructure account for the institutional and time barriers associated with connecting multiple distributed generation projects, which are often not fully captured in the transmission component of the levelized cost of electricity. Transmission availability is often cited as the greatest challenge to greater wind energy development (Fischlein et al., 2013), with some studies showing that it is often more cost- and time-effective to develop lower wind speed projects closer to transmission than attempt to interconnect high quality sites far from existing lines and load centers (Hoppock and Patiño-Echeverri, 2010). The distance to load center is a proxy for investments in transmission infrastructure required to deliver electricity from generators to load centers. Lastly, we used the human footprint score as a proxy for the degree of human "disturbance" from natural, unaltered states (Sanderson et al., 2002).

For solar PV, numerous countries have sufficient potential for 'no-regrets'—low-cost, low-impact, easily accessible—development, but a subset of these countries would require domestic or international transmission infrastructure to achieve 2030 targets. Specifically, Tanzania, Zimbabwe, Botswana, and Lesotho can meet 30% of their projected 2030 demand with low-impact solar PV (thick lines represent the top 20% of all sites), with Tanzania able to export up to 20 TWh of inexpensive and low-impact solar electricity to neighboring countries (Fig. 4.2A). In the EAPP, Ethiopia, Sudan, Uganda, and Tanzania can most favorably achieve 30% solar PV generation targets domestically (Fig. 4.2B). For these countries, sites with the lowest ecological impact and are closest to load centers and existing infrastructure also have high resource quality. This is not the case for all countries. Democratic Republic of Congo, Zambia, Angola, South Africa, Egypt, Kenya, and Libya possess some cost-effective sites that should receive high prioritization, but are not in the top 20% primarily due to limited transmission access. For these countries, meeting an ambitious 2030 target would require investing in transmission extensions to access lower cost PV resources or importing from neighbors. For CSP, the pattern of project prioritization is very similar to that of

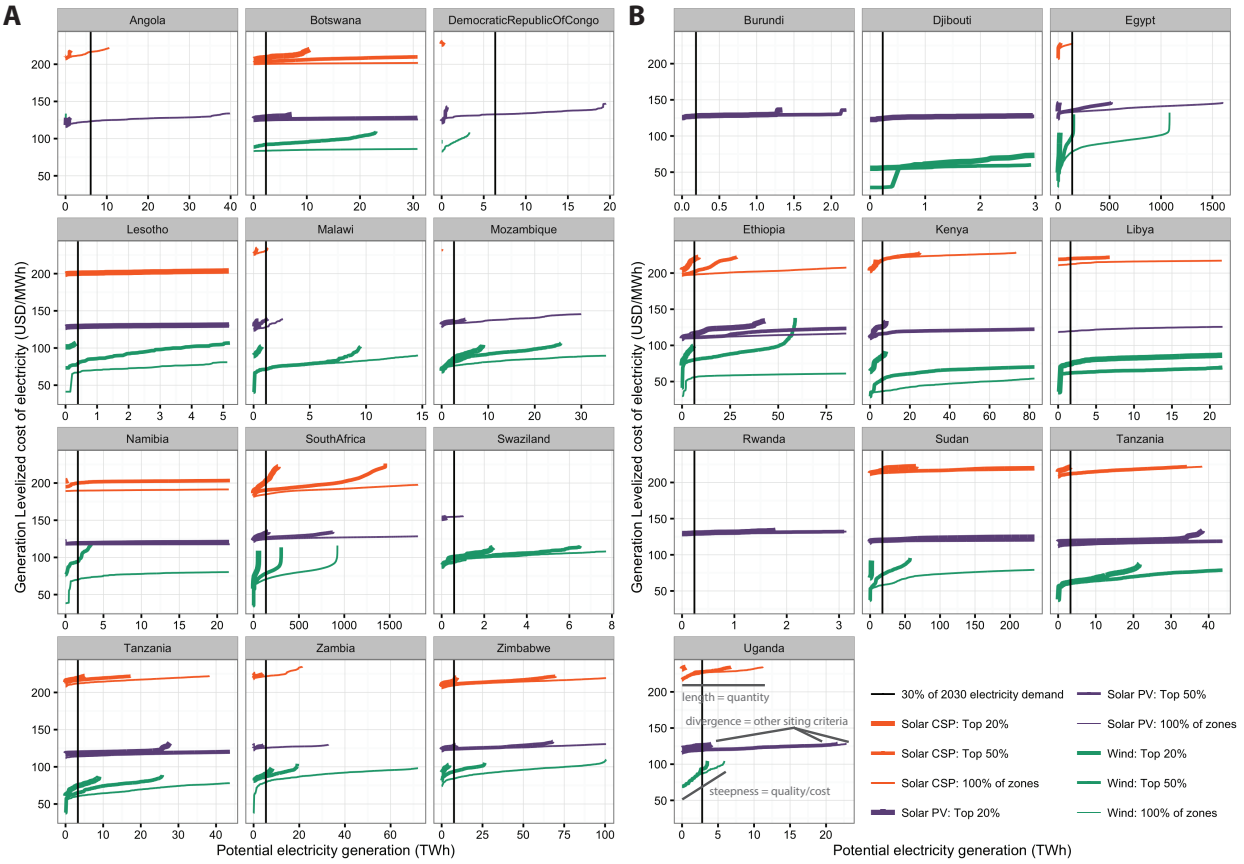

Figure 4.2: Multi-criteria project opportunity area supply curves for countries in the Southern and Eastern Africa Power Pools.
Supply curves show the cumulative potential of wind, solar PV, and CSP project opportunity areas that meet the top 20% and 50% of criteria values and all available zones within the Southern (A) and Eastern (B) Africa Power Pools. Project opportunity areas are sorted by generation levelized cost of electricity (LCOE). Vertical lines show 30% of each country's projected electricity demand in 2030. Criteria values include transmission distance, distance to nearest load center, and human footprint score. For example, the quantities of CSP potential in the top 50% and all sites in Uganda meet 2030 targets, and the difference between solar PV supply curves shows that though the top 20% of sites are limited in Uganda, they are sufficient to meet 2030 targets. Note that the x-axis varies between countries whereas the y-axis is fixed. For countries with large potential, the maximum value of the y-axis is six times the anticipated 2030 demand. Tanzania is a member of both power pools. The top 20 or 50% of zones are selected relative to other zones within the power pool. Assumptions for LCOE, including discount rate, are consistent across countries.

solar PV, but with fewer countries meeting all sufficiency, low-cost, and other siting criteria dimensions.

Wind resource supply curves are generally steeper and more divergent than those for solar technologies, indicating larger within-country cost and quality heterogeneity (Fig. 4.2). The

least-cost wind resource areas are distributed across several countries, including Malawi, Lesotho, Zambia, Djibouti, Ethiopia, Kenya, Libya, South Africa, Egypt, and Tanzania. However, these low-cost, high-quality wind sites generally score low in other siting criteria, as is seen in the large divergence between the supply curves within these countries. Tanzania, Swaziland, Djibouti, and Libya are exceptions in being able to meet 30% of their demand with accessible, low-impact, and cost-effective wind sites. Although trade-offs between cost and other siting factors appear to be greater for wind power leaving fewer 'no-regrets' areas, generation cost is not the only important determinant of wind resource quality. Selecting sites with wind speed regimes that generate most during the highest demand hours will increase their value (Mills and Ryan Wiser, 2012), a consideration we address in the following section.

International transmission interconnections enable least-cost wind deployment and greater displacement of conventional generation by wind

With hourly electricity demand data for nine countries in the SAPP (Appendix C, S1.3.1), we selected wind zones using four approaches: (1) *min-net-demand*: minimizing the maximum hourly net electricity demand (i.e., demand remaining after accounting for wind generation) across an entire year using *all zones* (Appendix C, S1.3.2); (2) *min-LCOE*: minimizing the annual average generation LCOE of wind using *all zones*; and (3, 4) *top 50%*: performing approaches (1) and (2) using a subset of zones that meet the top 50% of siting criteria within a power pool, as described in the previous section. For a given investment or installed capacity target, the *min-LCOE* approach maximizes wind generation, which reduces the need for conventional energy, whereas the *min-net-demand* approach reduces integration costs by minimizing need for non-wind, typically conventional generation capacity. We selected wind zones with and without international interconnections, referred to as *Interconnected* and *Isolated* scenarios, respectively. Each scenario installs a total of 61 GW of wind capacity, the amount needed to meet a 30-33% wind energy target by 2030 across the SAPP (Appendix C, Table C.6).

We compared the distribution of selected wind zones and found that the *min-net-demand, Interconnected, top 50%* scenario results in the most even distribution of capacity across countries (Fig. 4.3A). Instead of meeting South Africa's large demand domestically, a fully *Interconnected* SAPP allows for a large portion of its demand to be met internationally, in areas where wind generation profiles are better matched to SAPP's demand profile. When using the *top 50%* approach, many countries—Swaziland, South Africa, Malawi, Zambia, and Zimbabwe—see an increase in their share of wind capacity because of their more favorable sites, while others—Namibia, Mozambique, Tanzania—reduce their share relative to the *all zones* approach (Fig. 4.3A). With interconnections, the prevailing *min-LCOE* approach significantly increases capacity in Tanzania at the expense of capacity in other countries with lower capacity factors (Fig. 4.3A).

Results show a trade-off between selecting sites to maximize wind generation (*min-*

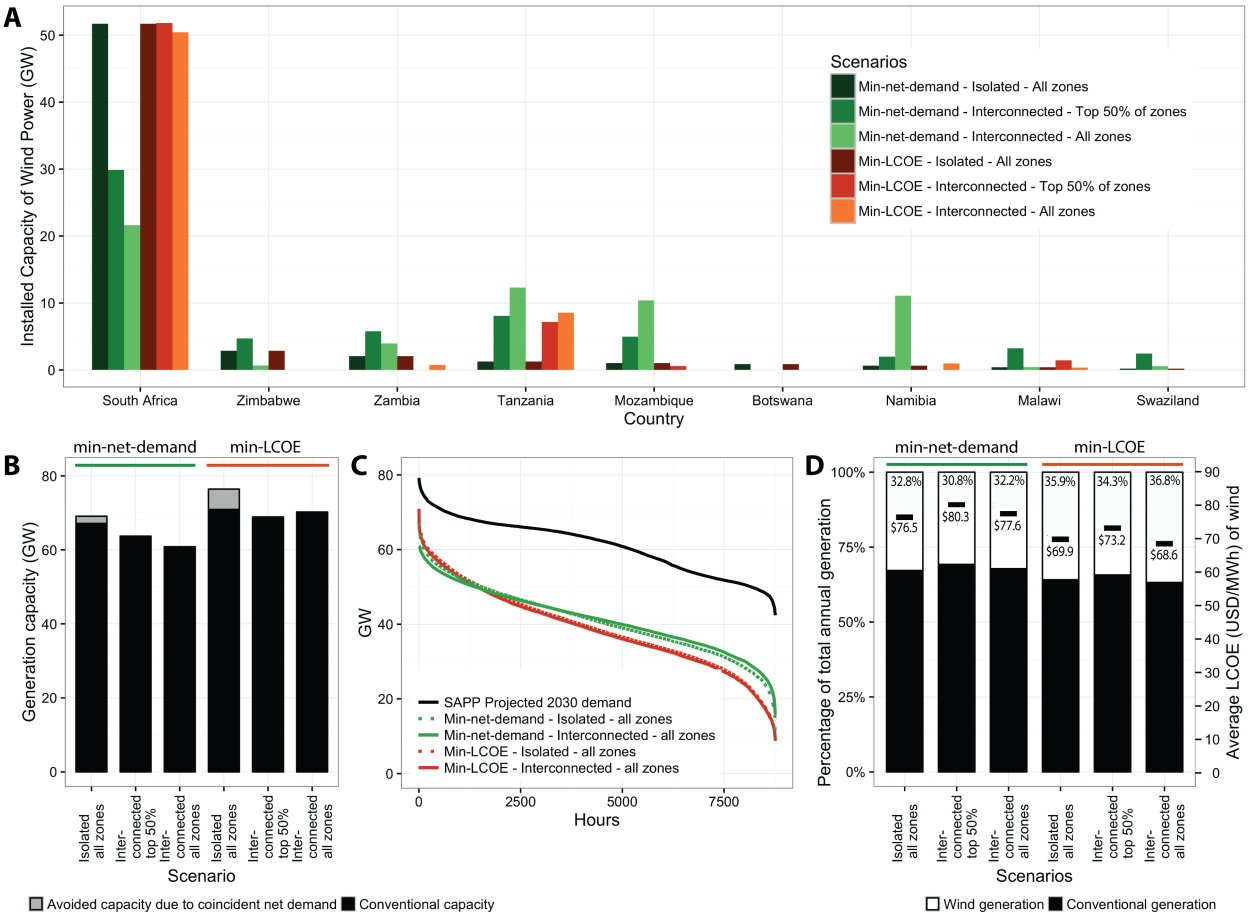

Figure 4.3: Wind build-out scenarios for the Southern African Power Pool (SAPP) in 2030. (A) Distribution of installed wind capacity among countries in the SAPP. (B) Conventional installed capacity needed to meet the highest hourly net demand within a year. (C) The hourly net electricity demand in gigawatts (GW) sorted from highest to lowest compared to the projected 2030 electricity demand. (D) The percentage of annual electricity from wind and non-wind generation (primary y-axis and bar plot) compared with the average levelized cost of electricity (LCOE) of wind generation (secondary y-axis and horizontal lines).

LCOE) and minimize additional conventional capacity (*min-net-demand*; Fig. 4.3A), though system costs are on the whole lower for the *min-net-demand* approach. (Fig. 4.4A). With interconnections, the *min-LCOE, all zones* approach generates 12% (24.5 TWh) more wind energy than the *min-net-demand, all zones* approach, resulting in 11% reduction in average wind LCOE (Fig. 4.3D), yet it requires 15% more, or 9.4 GW, conventional capacity (Fig. 4.3B). We estimated system costs assuming the extra conventional capacity needed would be met by natural gas combustion turbine (CT), scrubbed coal, or hydropower, as these are the technologies that have high priority status in the SAPP (Appendix C, S1.3.3). Costs show that the *min-net-demand, Interconnected, all zones* scenario leads to 0.4 - 2.5 billion

Table 4.1: Coefficient of variation of hourly net-demand and hourly site-averaged wind capacity factor for all site selection approaches and interconnection scenarios.

	Site selection approach			
	min-net-demand		*min-LCOE*	
	Hourly time series			
Interconnection scenario	Net-demand	Wind capacity factor	Net-demand	Wind capacity factor
Integrated, all zones	0.197	0.320	0.283	0.426
Integrated, top 50%	0.199	0.334	0.258	0.426
Isolated, all zones	0.224	0.354	0.280	0.440
Isolated, top 50%	0.223	0.357	0.256	0.442

USD/yr in cost savings over the *min-LCOE, Interconnected, all zones* approach depending on the technology assumption (Fig. 4.4A, Fig. 4.5). These costs savings account for 3.5% - 19% of the total annual costs of wind capacity (Fig. 4.4A). Assuming hydropower or coal capacity would be avoided, selecting sites to minimize peak net demand is more cost effective from the systems perspective than selecting sites to minimize wind LCOE.

Other, non-monetized system benefits of the *min-net-demand* approach include reduction in the temporal variability of hourly wind capacity factors and net demand (20% - 30% reduction in the coefficients of variation; Table 4.1). In contrast, there are little or no differences in the coefficient of variation between *Interconnected* and *Isolated* scenarios when selecting sites to minimize LCOE (Table 4.1). That is, the main factor determining temporal variability of wind generation is the site selection approach, not the presence or absence of interconnections. For example, two countries with existing wind farms sited based on minimizing LCOE that later interconnect may not see reductions in the variability of generation or net demand. Interconnections, however, do increase the diversity of available sites, allowing a *min-net-demand* siting approach to further reduce variability. This finding that increasing the geographic diversity of wind sites decreases coefficient of variation is consistent with empirical studies examining interconnection scenarios of wind plants (Fertig et al., 2012).

Lower aggregate net demand variability reduces the need to ramp up or down conventional generators to balance the variability (see Appendix C, Fig. C.2 for hourly ramp rate distributions), and a flatter load curve allows for more efficient use of base-load generators (Fig. 4.3C). Therefore, a site selection process based only on minimizing wind LCOE may not minimize system-wide costs and may not maximize the cost-savings of interconnections compared to a site selection approach that best matches wind generation with electricity demand.

Comparisons between *Interconnected* and *Isolated* scenarios show that interconnections reduce system costs regardless of site selection approach or assumptions about the conventional generation technology wind may displace (Fig. 4.4B). Compared *Isolated*, the *Inter-*

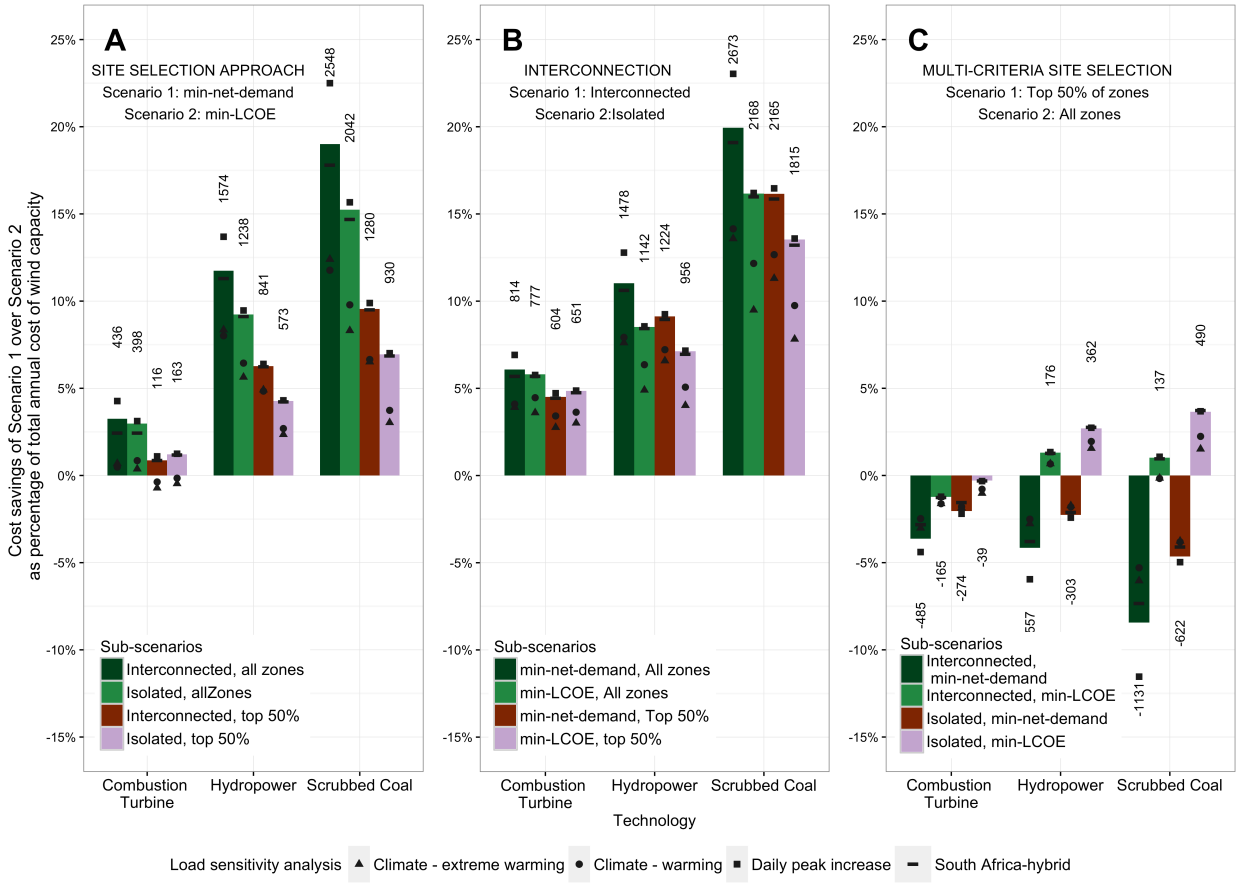

Figure 4.4: Cost differences between wind build-out scenarios.
Cost differences are expressed as percentage of total annual wind capacity cost, which is consistent across scenarios. Actual cost differences in millions USD per year are labeled above each bar for the base case. Positive percentage and cost values indicate cost savings of Scenario 1 compared with Scenario 2, and negative values indicate additional costs of the Scenario 1 compared with Scenario 2 in each panel. Costs were estimated assuming three different possible conventional capacity technologies—natural gas combustion turbine, hydropower, and scrubbed coal (x-axis). **(A)** The cost savings of the *min-net-demand* over the *min-LCOE* site selection approach. Positive values indicate that *min-net-demand* is more cost-effective. **(B)** The cost savings of the *Interconnected* over the *Isolated* scenario. Positive values indicate that the *Interconnected* scenario is more cost-effective. **(C)** The cost savings of the *top 50%* over the *all zones* site selection. Positive values indicate that the *top 50%* scenario is more cost-effective. The set of points for each bar shows results from load sensitivity analyses of four plausible future load growth scenarios: "Climate - extreme warming", "Climate - warming", "Daily peak increase", and "South - Africa hybrid". See Appendix C, section S1.3.4 and Figs. C.10 and C.11 for descriptions of the load growth scenarios.

connected scenario using the *min-net-demand, all zones* approach results in avoiding close to 10% or 6.3 GW of conventional generation capacity in the SAPP (Fig. 4.3B, Fig. 4.3C). The annual cost savings of interconnections combined with the *min-net-demand* approach is particularly large when assuming additional coal (2.2 - 2.6 billion USD or 14-20% of annual wind capacity costs) or hydropower capacity (1.2 - 1.5 billion USD, 9-12%; ranges represent *top 50%* and *all zones* approaches, respectively; see Fig. 4.4B).

Using SAPP's recent wheeling charges as a proxy for transmission capital costs per MWh traded (Appendix C, section 1.3.3), we find that interconnection costs in the *Interconnected* scenario are 1.6-1.8% of the amortized annual cost of wind capacity for the *min-net-demand, all zones* site selection approach, and 0.4 – 0.44% for the *min-LCOE, all zones* approach (Appendix C, Table C.1). These percentage cost ranges are less than the range of potential savings from avoided conventional capacity under these same scenarios (6-20% for *min-net-demand* and 4-16% for *min-LCOE*; Fig 4.4B). When international interconnection costs are included, interconnections would save 4.3% at worst (assuming combustion turbine capacity) and 18% at best (assuming scrubbed coal capacity) in avoided conventional capacity, represented as percentage of amortized annual wind capacity costs (Fig. 4.4B).

Multi-criteria site selection is not significantly more costly, and for the *min-LCOE* scenarios assuming hydropower or scrubbed coal capacity displacement, yield cost-savings (Fig. 4.4C). This is because sites selected using multiple siting criteria (*top 50%*) and the *min-LCOE* approach result in lower net peak demand compared to the *all zones* approach, reducing conventional capacity costs. Nearly all cost differences between the *top 50%* and *all zones* site selection scenarios are <5% of the annual cost of wind capacity (Fig. 4.4C). When examining ranked cost differences across all scenarios, results show that the *min-net-demand, Interconnected, top 50%* scenario is the second-most cost-effective option by a large margin when the avoided conventional technology is hydropower or coal (approx. 1 billion USD; Fig. 4.5). Regardless of the conventional technology, interconnections reduce the system costs of multi-criteria selection relative to all scenarios without interconnections (Fig. 4.5).

Load sensitivity analysis and limitations

Because only one year of load data were available and load profiles in 2030 are highly uncertain, we performed a sensitivity analysis using four future load growth trajectories that represent load responsiveness to climate change, economic structural changes, and grid-connected electrification and reduced load curtailment (see Appendix C, Fig. C.10-C.11 and section S1.3.4 for detailed scenario descriptions). Results show that the cost-effectiveness of *Interconnected* scenarios and the *min-net-demand* site selection approaches are sensitive to different load growth trajectories, but the range of results suggests that the baseline load scenario is in the middle (Fig. 4.4-4.5). Despite the trajectories being fairly extreme scenarios of load growth, on the whole, they do not change the conclusion that interconnections are very likely to reduce system costs from avoided conventional capacity (Fig. 4.4B, Fig. 4.5).

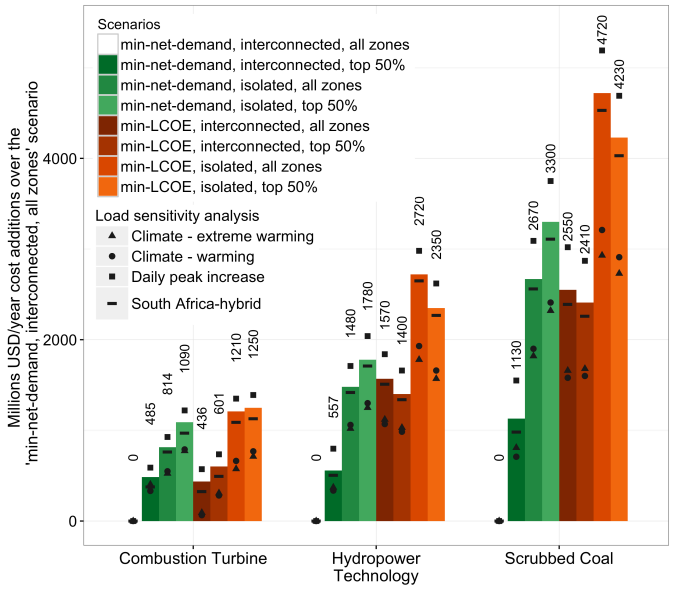

Figure 4.5: System cost additions compared to least-cost scenario.
For each technology, the bars show the difference in system costs between each scenario and the least-cost scenario (*min-net-demand, Interconnected, all zones*). System costs include the additional energy and/or conventional capacity required in each scenario. The set of four points for each bar shows results from load sensitivity analyses of four plausible future load growth scenarios (Appendix C, Fig. C.10 and C.11).

The "South Africa-hybrid" scenario, which represents economic structural changes, is very similar to that of the baseline (unmodified) load growth profile. The two "climate-warming" scenarios increase the conventional generation capacity requirements for the *Interconnected* scenario, but decrease it for the *Isolated* scenario, with a smaller yet still positive avoided capacity difference between interconnected and isolated scenarios compared to baseline (Appendix C, Fig. C.4). For the "Daily peak increase" load growth scenario, both the *Interconnected* and *Isolated* capacity requirements increase, but the avoided capacity of the *Interconnected* scenario is larger relative to baseline (Appendix C, Fig. C.4). These results suggest that the cost-effectiveness of the *Interconnected* scenario is highly dependent on the annual peak demand. We posit that the two climate load growth scenarios represent fairly extreme load responses to climate change such that the entire seasonal pattern disappears or inverts (Appendix C, Fig. C.10C and Fig. C.10D), without the counterbalancing likelihood of increased electrification or reduced curtailment, which has the effect of elevating demand during the daily peak hours. On the whole, the *Interconnected* scenario remains the more cost-effective choice, with load growth uncertainty reducing the confidence of this result only if natural gas combustion turbine were to be the avoided conventional technology under the "Climate-warming" load growth scenario (Fig. 4.5). Otherwise, for hydropower and coal, the differences in additional costs of the *Isolated* scenario remain large even under "Climate-warming" scenarios (1 – 3 billion USD/yr; Fig. 4.5) and the differences would be

very significant under the "Daily peak increase" scenario (1.9 – 5.6 billion USD/yr; Fig. 4.5). These costs would be adjusted downward by 0.04 – 0.24 billion USD/year, depending on site selection approach) due to transmission costs (Appendix C, Table C.1).

Currently, hydropower and coal appear to be the marginal generation technologies in the SAPP, though recent discoveries of natural gas in Mozambique may change this trend. However, transport of natural gas through a pipeline network would add significant capital costs that have not been considered in the cost estimates for combustion turbine capacity.

This study does not examine the effect of solar generation in the SAPP on system costs, but it is expected to alter net demand patterns. We relied on one year of modeled wind speed data, which may have interannual variability. However, previous analysis using 10 years of meso-scale wind data shows that the wind regime during peak hours in the region is stable (Wu, Deshmukh, et al., 2015), though wind patterns may change in the future. Such potential changes underscore the importance of incorporating multi-criteria analysis in siting decisions on an ongoing basis. Due to limited power systems data availability across multiple countries, our model examines only the extreme ends of SAPP's future–either complete grid isolation with no energy trade or complete interconnection such that the entire SAPP region operates like a coordinated, single balancing area without transmission constraints. Because generator-specific time series and constraint data needed for a production cost model and capacity expansion model could not be acquired across multiple countries, our model does not account for flexibility or responsiveness of other generators in the system. For the same data limitation reasons, we could use a capacity expansion model or a model that minimizes system costs to generate a scenario that balances conventional capacity and energy trade-offs.

4.4 Conclusions

Results demonstrate the large potential for utility-scale wind and solar energy development in many EAPP and SAPP countries, with particular countries possessing sufficient low-cost, accessible, and low-impact potential sites that can rapidly provide 'no-regrets'–or low-cost, low-impact, and highly accessible–low-carbon electricity. However, spatial heterogeneity of the most competitive resources that reduce system costs underpins the need for regional coordination and transmission infrastructure to enable resource sharing. Our study demonstrates how spatio-temporal models can be used to assess opportunities and address barriers for renewable energy development in countries where data are limited and where the load growth trajectory is highly uncertain.

By providing the institutional structure for electricity trade, the power pools in Africa can lay the groundwork for power plant siting to minimize regional system costs. Currently, the emphasis on large hydropower in a small handful of EAPP and SAPP countries could result in a set of interconnection plans that fail to support the development of plentiful 'no-regrets' solar and wind options across multiple countries. Our results show that wind and solar electricity can be cost competitive and have a much larger role to play in Africa's energy

transition, especially if the benefits of strategic siting and international interconnections are considered.

Chapter 5

Deforestation and agricultural expansion resulting from hydropower development in the Brazilian Amazon

Hydropower is often favored as a low cost, low carbon, and high return technology for meeting rising electricity demand and fueling economic growth. Despite the magnitude and pace of hydropower expansion in the Brazilian Amazon, there is a lack of understanding of land use and land cover change (LULCC), particularly indirect LULCC, resulting from hydropower development. This study uses remote sensing, and quasi-experimental matching and panel regression methods to estimate the effect of hydropower development on indirect deforestation and agricultural land use in the Brazilian Amazon. Using gathered data on existing hydropower plants in the Brazilian Amazon and their matched control sites >1MW, we estimate an 11.3% - 59% percent increase in indirect forest loss due to hydropower siting, in any given year for any given site. Hydropower development increased agricultural land use by 7% - 50% percent, though these estimates are weakly statistically significant, and insignificant in some regression models. These results suggest that continued hydropower development is likely to cause significant unintended indirect forest conversion, aiding in the advancement of the arc of deforestation in the Brazilian Amazon.

5.1 Introduction

Hydropower development in the Brazilian Amazon

The capacity of new hydropower being planned or under construction globally—1,700 GW, or nearly double the current installed capacity of 930 GW—is anticipated to affect one-fifth of all remaining free-flowing large rivers (Zarfl et al., 2015). Much of this new capacity is concentrated in the most biodiverse river and terrestrial ecosystems on earth, including the

Amazon, which sustains more than half of the world's remaining tropical forest area (Winemiller et al., 2016). The Amazon also contains the largest remaining hydropower potential capacity in Brazil (Machado et al., 2004). The history of Brazilian hydropower development shows an unprecedented explosion of hydropower projects in the Brazilian Amazon in the 2010s (Moretto et al., 2012), and if government energy plans proceed as documented (MMA 2012) to meet the projected 2.2% annual increase in energy demand (EPE, 2016), the Amazon will continue to be the frontier of hydropower development. In the Brazilian Amazon alone, there are more than 100 planned, proposed, or inventoried dams with capacity greater than 30 MW (ANEEL 2016, Major Dams database).

Hydropower projects have long been vexed by a wide range of environmental and social impacts including fisheries reduction (Barthem, Brito Ribeiro, and Petrere, 1991; Fearnside, 2014), flooding of indigenous and rural community lands, carbon dioxide and methane emissions (Fearnside and S. Pueyo, 2012), and loss of terrestrial and freshwater habitat and biodiversity (Magalhães and F. Hernandez, 2009). Yet, river regulation, inundation, and economic activity associated with or enabled by a hydro-power project could also generate a cascade of changing socio-economic conditions and hence trigger changes in land use, land cover, and hydrological dynamics in the watershed. These resulting indirect LULCC effects are poorly studied, though anecdotal evidence and the few empirical studies in the literature on mining activities strongly suggests that they have a disproportionate impact relative to the direct land use requirements (Sonter, Herrera, et al., 2017; Edwards et al., 2014; Weng et al., 2013).

Most research underestimates the land use change resulting from small-scale, "intensive land use" activities (Sonter, Barrett, et al., 2015). Sonter, Barrett, et al. (2015) defined intensive land uses as those that "occupy a small proportion of the landscape but indirectly drive land use change dynamics through their operation." While the authors find significant indirect land use associated with mining, hydropower can also be expected to have similar indirect LULCC impacts. Because hydropower is often sited in intact, relatively undeveloped areas due to specific and requisite hydrological and topographic characteristics, its potential to impact sensitive ecosystems and biodiversity can be disproportionate to the land area directly and indirectly affected. This phenomenon has been well documented, frequently through remote sensing and statistical methods, for road extensions and upgrades (Mertens and Lambin, 2000; Cropper, Puri, and Griffiths, 2001; Chowdhury, 2006).

Like roads, indirect land use change resulting from hydropower is likely to occur through spatial dependence and within some proximity of the dam itself. Agricultural activity can be increased through irrigation, and resettlement of displaced communities is often in the same watershed but typically at higher elevation. Hydropower's disruption of livelihoods previously dependent on river-provided ecosystem services could lead to environmental impacts from the substitute livelihood. For example, the lost fish protein from disruption of fisheries due to anticipated dam construction in the Mekong Basin is projected to cause a 19-63% increase in land usage for agriculture in affected countries (Orr et al., 2012). Hydropower reservoirs can also encourage increased urbanization of downstream areas due to reduced flood risk and increased development activity. These direct and indirect land use changes

can be directly observable, and with quasi-experimental methods, could be ascribed to hydropower development. However, depending on the causal mechanism, LULCC impacts may occur across multiple temporal and spatial scales.

Deforestation in the Brazilian Amazon and causal mechanisms linking hydropower and deforestation

Barbier, Burgess, and Grainger (2010) lay out a three-phase process of agricultural land expansion and forest loss in the frontier. The first phase involves the opening up of the frontier by large-scale, typically short-term extractive activities such as logging, mining, commercial agriculture, and the objective is to maximize short-term profits. The second phase is marked by opportunistic forest clearing by smallholders or migrants, since previously inaccessible areas are now open. Lack of land rights and enforcement in this phase leads to widespread forest clearing. Finally, in the third phase, wealthier land owners begin to establish property rights. These larger land owners benefit from government agriculture subsides, access to markets, and credit, and they drive out early settlers, who then migrate to other frontier regions. In this three-phase process, hydropower projects can play a role in frontier development as key actors in the first and third phases—first, as greenfield development projects to harness hydropower potential in remote areas, and third, through the continued provision of services that enable economic growth such as electricity, flood control, and river navigation.

The drivers of deforestation in tropical countries, and specifically in Amazonia, have been well studied (Pfaff, 1999; W. F. Laurance, Albernaz, et al., 2002; Barber et al., 2014; Hargrave and Kis-Katos, 2013). Key proximate drivers and predictors of deforestation include human population density, highways, dry season severity, and navigable rivers. The earliest of these studies identified the importance of roads, but also clearly distinguished "development projects" as having independent effects that significantly increased deforestation, though the study does not specify the types of development projects more likely to cause deforestation (Pfaff, 1999). Certainly, hydropower projects, as part of larger development schemes, have intentional land use and land cover impacts that are associated with economic development. However, many unintended, inter-related social and LULCC consequences of hydropower development have been documented. The best documented cases of this are consequences resulting from opportunistic migration.

As an example, the Tucuruí dam along the Tocantins River constructed in the late 1970s and early 1980s in the Amazon aggravated social dynamics in the surrounding region by accelerating territorial occupation and triggering a flood of migration (Fearnside, 1999). Valeça (1992) noted that the dam attracted new activities and changed the regional structure of the value of land, effectively causing new patterns of land use including new urban spaces upstream of the dam. As noted by Tundisi, Santos, and Menezes (2003), "small-scale navigation was substituted by road transportation; there was also a change in the macro economy: large scale industrial and forestry projects, agribusiness projects." In a recent news article about deforestation due to hydropower planning, a Brazilian researcher provides the follow-

ing cause of forest loss during and after the construction of the Tucuruí dam: "There is a great inflow of laborers looking for work, but not all are taken in...This intensifies conflicts, with the sprawling of [squatters into formerly rural] locations that have no infrastructure to support them" (Farah, 2016). In the same article, another Brazilian researcher interviewed comments on plans to construct a large hydropower plant—São Luiz do Tapajós—on the Tapajós river:

> On the one hand, the hydropower plant brings progress. On the other, it attracts people interested in illegal logging. It is inevitable. But the overseeing bodies have to be prepared for more intense [criminal] activity...[should the hydropower plant become a reality] it would heat up the market for land, which is regulated by violence and predatory exploitation of natural resources, which is in and of itself frightening.

In yet another documented example of possible widespread LULCC resulting from hydropower development, Fearnside (2005) describes how the temporary exception to a law prohibiting export of raw logs for the flooding of the Samuel reservoir in Rondônia coincided with a boom in illegal logging throughout the Western Amazon region.

Research questions and approach

The tendency has been to allow locations of "untapped" potential to guide siting practice and development planning. Yet, mitigation actions in the past that have failed to compensate for direct, let alone diffuse and indirect damages. A better understanding of the unintended social and environmental consequences associated with LULCC induced by hydropower development can help inform more comprehensive and low-impact model for energy planning in countries with transitioning or growing energy portfolios.

This study examines the indirect land use and land cover impacts of siting hydropower projects in the Brazilian Amazon. We ask the following questions: What is the proximate effect of hydropower development on indirect forest loss and agricultural land use in the Brazilian Amazon within 50 km of hydropower plant locations? How does the effect vary spatially and temporally? Using a quasi-experimental design, we combine statistical matching approaches to identify "control" sites, remote sensing classification methods to detect forest loss 1984-2017, and panel regressions to control for long-term unobserved drivers of LULCC. For assessing agricultural land use, we rely on a spatially-explicit longitudinal dataset based on agricultural census data (Dias et al., 2016).

5.2 Methods

We combined remote sensing, spatial analysis, and causal inference methods to estimate indirect forest-loss resulting from hydropower development in the Brazilian Amazon. Our approach consisted of the following key steps: (1) Data collection and preprocessing; (2)

statistical matching of existing hydropower sites (treatment) with planned, proposed, and inventoried sites (controls); (3) forest loss detection 1984 - 2017 within 50 km of existing (treatment) and planned/proposed (control) hydropower locations using scalable remote sensing techniques; (4) regression analyses to estimate the average forest-loss and agricultural land use effect of siting a hydropower plant. Forest loss estimates are directly calculated using image compositing and classification methods, whereas agricultural area estimates rely on a secondary, published dataset (Dias et al., 2016). See Figure 5.1 for a visual overview of the methods.

Data and preprocessing

We collected the following three categories of data: (1) existing and proposed hydropower plant locations; (2) spatially-explicit covariates; (3) remote sensing imagery (Landsat 4-8) and the Hansen Global Forest Change dataset.

Hydropower locations. Several country-specific, regional, and global hydropower plant locations datasets are publicly available. Since no single dataset was complete in either the power plant location or other attribute information, we compared and combined four such datasets (Table 5.1). Where the operational start year or installed capacity was missing for a hydropower plant, we manually filled these gaps by searching on the internet for articles, press releases, or government or corporate information. If the name of a hydropower plant appeared more than once across the datasets, we chose the location and attribute information from the Brazilian power regulatory agency, Agência Nacional de Energia Elétrica (ANEEL), but also visually inspected the location and attribute information (e.g., name of river) by overlaying the data on high resolution Google Earth imagery. After data cleaning and quality assessment, we identified 66 existing hydropower plants over 1 MW (51 over 20 MW), and 277 proposed or inventoried plants over 1 MW in the Legal Amazonian Area. After removing all proposed and inventoried sites within 80 km of an existing hydropower plant, 180 sites over 1 MW remained available for matching. Due to challenges of automating land cover change detection using satellite imagery in the Cerrado, the tropical open savanna biome, we restricted regression analyses to just the 29 existing power plants in the Brazilian Amazon biome. For each hydropower plant with less than 1 GW of installed capacity, we created a 50 km radius circular buffer around the dam site within which we estimated forest-loss. For power plants greater than or equal to 1 GW in capacity, we used a 100 km radius.

Covariate and ancillary data. We collected spatially explicit datasets to be used as matching variables, chosen based on their ability to predict the likelihood that a particular location would be developed for hydropower or deforested. Such datasets include protected and indigenous areas, and locations of urban areas (Table 5.1). We could not include other potentially useful predictors such as road network or population density as these datasets were not available for multiple time periods or for before 1990. However, we used a secondary dataset as a proxy for human settlement and development—a unique spatial annual time-series dataset of cropland and pastureland area per 1 km x 1 km grid-cell for all of Brazil from 1950-2014 (Dias et al., 2016). It uses 30 m remote sensing data for year 2010 to spatially

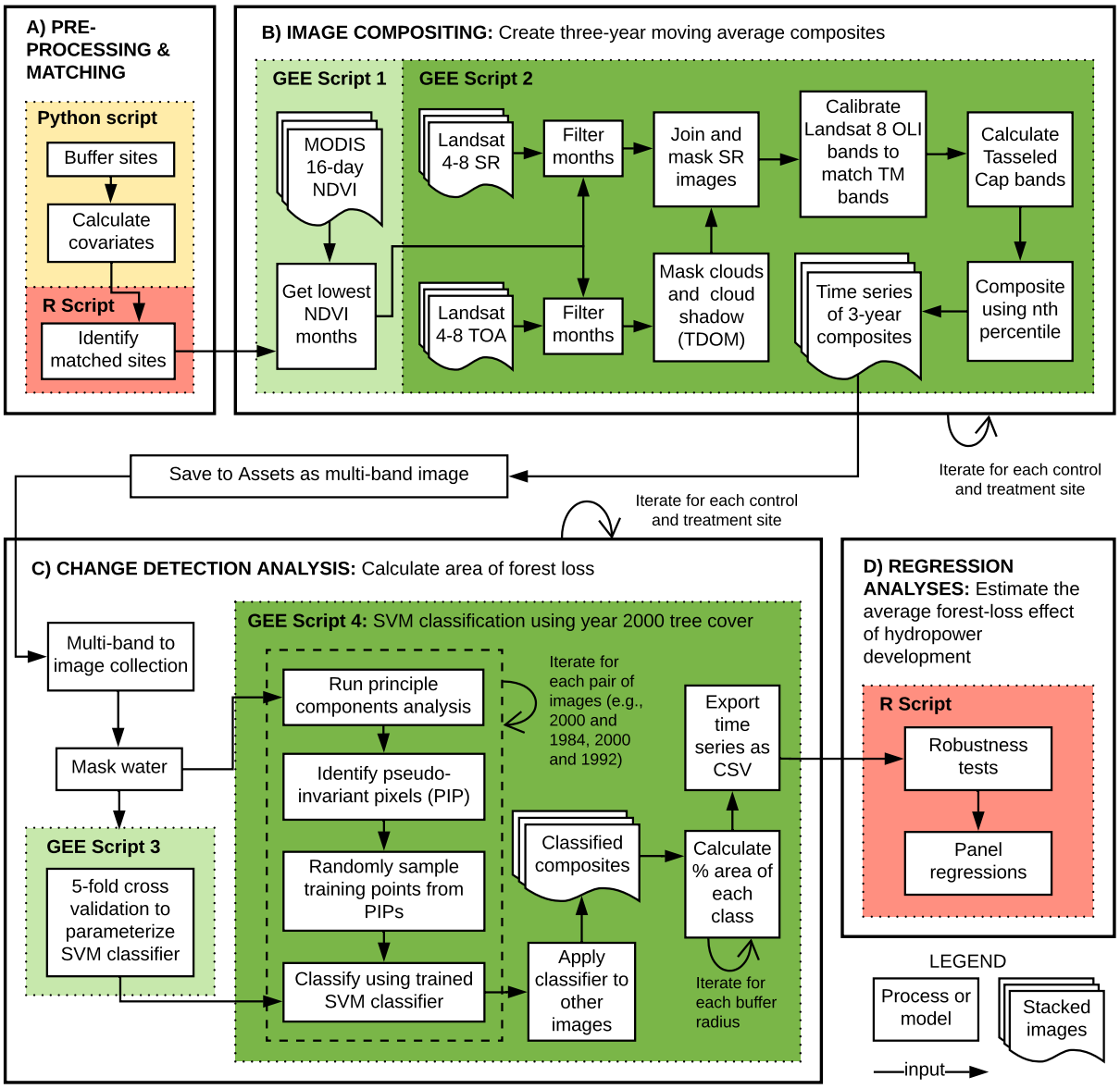

Figure 5.1: Workflow overview.

Green boxes indicate key remote sensing processes performed using Google Earth Engine (GEE), red boxes indicate statistical analyses performed using R, and yellow boxes indicate processes using Python modules.

disaggregate to 1 km resolution a time series of agricultural census data reported at the municipal level. We used the Dias et al. (2016) dataset both as a matching variable and as the response variable in a set of regression models (see Matching section below).

Table 5.1: Datasets used in the analyses

Data category	Source	Description	Datatype	Use
Hydropower locations	Agência Nacional de Energia Elétrica (ANEEL)	Government records of utility-scale hydropower plants in Brazil.	Points	control or treatment sites
Hydropower locations	dams-info.org	Location and attribute data were compiled by Fundación Proteger, International Rivers, and ECOA, to provide a database on dams in operation, under construction or planned for the Amazon basin. Planned locations have either had a feasibility study started, or for which "clear indications of a government's intentions to move forward with the project."	Points	control or treatment sites
Hydropower locations	Major dams (International Rivers)	This dataset of dam location and attribute data was distributed in 2014. International Rivers compiled the data from multiple sources and corrected it for location errors. Available on `http://data.globalforestwatch.org/`	Points	control or treatment sites
Hydropower locations	The Global Reservoir and Dam Database (GRanD) (WWF)	This database contains locations of dams and reservoirs globally and was compiled in 2011.	Points	control or treatment sites
Protected areas	Brazil's Ministério do Meio Ambiente (MMA)	Officially recognized conservation and indigenous areas	Polygon	matching variable
Urban areas	Schneider, Friedl, and Potere (2009)	urban area	Polygon	matching variable
Biomes	WWF	Biome	Polygon	matching variable
Agricultural areas	Dias et al. (2016)	This is a 1 km x 1 km gridded time series of hectares of agricultural area in Brazil. Total cropland data area available for 1950 - 2014, and pasturelands (natural and planted) are available for 1940 - 2012.	Raster	matching variable and response variable

Matching

Matching is a suite of methods that aims to balance the distribution of covariates between the treated group and the observational "control" group (Stuart, 2010). It essentially attempts to replicate randomized trial conditions using observational (non-randomized) data by selecting or weighting individuals based on their covariate values. We developed our own customized routines and used various packages in the R statistical software (R. Core Team, 2017) to produce matched controls using various distance and matching methods.

Variable selection

The general guidance on variable selection in matching is to include variables associated with treatment assignment (suitability for hydropower development) and/or the outcome (forest or other land use change). By limiting the range of possible control units to proposed, planned, or inventoried hydropower projects in the Brazilian Amazon, we effectively performed an exact match on variables determining treatment assignment; that is, proposed, planned, and inventoried projects meet several suitability criteria for development (e.g., hydraulic head, accessibility). For addressing bias related to the outcome (land use change), we matched on the following variables (short-hand covariate names are provided in quotation marks):

1. *Generation capacity in MW ("capacity"):* The size of the hydropower plant affects the ancillary infrastructure (e.g., roads, transmission lines), the construction duration and scale (e.g., staging area, laborers), the reservoir and flooded area (depending if the power plant is a run-of-river or reservoir), and the amount of services provided (electricity generation). All of these could affect the amount of land use and land cover change in an area.
2. *Percent of agricultural land pre-hydropower-development ("pre-dam agricultural land"):* Human activity in an area, which is correlated with amount of deforestation some tropical countries (Harrison, 1991). Because we lacked historic spatially-explicit data for population or migrant density over our study time period, we use the amount of agricultural land as its proxy. We used the Dias et al. (2016) annual (1950 - 2014) gridded dataset of cultivated and pastured area to match on the percentage of 5- and 10-year pre-hydropower agricultural land in each study area. Because this covariate value changes for each set of controls, depending on the treatment unit being considered, we needed to apply a panel-matching approach. We describe the process of accounting for treatment-specific agricultural land use in selecting control units in the following section.
3. *Distance to the nearest conservation or indigenous area ("distance to nearest protected area"):* Protected areas (both conservation and indigenous areas) have been shown to inhibit deforestation in the Brazilian Amazon (Soares-Filho et al., 2010).
4. *Distance to the nearest urban area ("distance to nearest city"):* Proximity to commodity markets is a key driver of deforestation in tropical regions (Pfaff, 1999; Barbier and Burgess, 2001; Chomitz and Gray, 1995). We use the euclidean distance from each control and treatment unit to the nearest urban area (Schneider, Friedl, and Potere, 2009).
5. *Biome:* The biome is used as a gross proxy for vegetative cover type and density and climate. Within the Legal Amazon region, there are three biomes—Amazon, Cerrado, and Pantanal. Also, the remote sensing techniques developed for this study perform differently across these biomes, making this matching covariate important for reducing possible systemic bias from change detection methods.

6. *Spatial proximity to the matched treatment unit:* Given that deforestation and other land use changes are highly heterogeneous processes in the Brazilian Amazon, using spatial proximity as a proxy for these spatially-dependent processes may be important for reducing bias in our treatment effect estimate. We use spatial proximity as a proxy for regionally or locally-specific social and political forces that may not be adequately captured individually in spatially-explicit datasets (e.g., state-level or municipal-level land use or economic policies and their enforcement). We describe how spatial proximity is used in each matching approach below.

Though the role of roads is well documented in land use change and deforestation in the tropics (Chomitz and Gray, 1995), we did not include distance to roads as a matching variable because we lacked historic road-density data over our study time period and because variables that may be affected by the treatment (hydropower development) should not be included the matching process (Stuart, 2010).

Matching approaches

Given the importance of matching approaches for bias reduction in causal inference, we apply and compare three matching techniques that vary in their treatment of spatial proximity, time-dependent covariates, and distance measures, as described below. Additionally, given that existing hydropower plants in our sample have different operational start years, we needed to employ panel-matching methods in order to match on pre-intervention covariates with values specific to each treatment site.

1. Distance adjusted propensity score matching (DAPSm): DAPSm, developed by Papadogeorgou, Choirat, and Zigler (2018), incorporates spatial proximity in standard propensity score (p-score) matching. Papadogeorgou, Choirat, and Zigler (2018) developed this approach to use spatial proximity as a proxy for addressing unmeasured confounding effects in matching. Using the DAPSm package in R (Papadogeorgou, Choirat, and Zigler, 2018), we calculate p-scores and determine the spatial weights that best balance p-score matching with spatial proximity. In order to match using the "5- and 10-year pre-dam agricultural land" covariate, we performed DAPSm for treatment sites grouped by decade of their operational start year. For example, for hydropower plants which started generating electricity any year between 1981 and 1990, we used the percent of agricultural land in 1975 as the "5- and 10-year pre-dam agricultural land" matching covariate for both control and treatment units. We match without replacement in chronological sequence, such that controls units that were matched in an earlier decade were excluded from consideration in DAPSm for subsequent decades. We exclude distance to the nearest city and the percent of agricultural land 10-years pre-hydropower-development due to challenges of estimating p-scores with small sample sizes. Only two and three treatment units had operational start years in the 1971-1980 and 1981-1990 decades, respectively. The more variables that are included in calculating the p-score, particularly as the number of observations decreases, the more likely

the control p-scores will ratchet to zero. Recent studies have demonstrated that this phenomenon leads to greater, not less, imbalance of matches, resulting in the "p-score paradox" (G. King et al., 2011). Due to the imperfect temporal matching of pre-dam agricultural land from decadal binning and the p-score paradox, we developed our own routine based on Mahalanobis distance, which is more appropriate for pair-wise matching and does not suffer from the curse of dimensionality (G. King et al., 2011).

2. Mahalanobis distance with geographic covariates (MD): In order to match based on the 5- and 10-year pre-hydropower percentage of agricultural land, which varies between treatment sites, we developed a routine in R statistical software that sequentially calculates the Mahalanobis distances between each treatment site and all control sites. That is, we used the year of the treatment site's operational start to create two variables representing the 5- and 10-year pre-dam percentage of agricultural land for the site itself as well as all possible controls. We used all the covariates described in the previous section in calculating the Mahalanobis distance, but specifically included each site's geographic latitude and longitude coordinates. To simplify subsequent statistical analyses, once a control was matched to a treatment, the control was no longer eligible to be matched with another treatment (no replacement). As a result, the order with which we matched treatments to controls matters. To find the optimal set of control matches, we performed the Mahalanobis distance matching without replacement routine 200 times, each time randomizing the sequence of treatment dams (following the method of Nielsen and Sheffield, 2009). We chose the order of treatment dams that minimized the sum of Mahalanobis distances between all treatments and matched controls.
3. Optimal propensity score matching (Opt PS): We use 1-1 optimal propensity score matching through the MatchIt package in R (Ho et al., 2011). We use all the covariates described in the previous section, but do not include any geographic covariates or weights and do not dynamically match using each treatment site's pre-dam agricultural land area. We simply used the percentage of agricultural land in 1968 (before any of the hydropower plants in our sample were constructed) for all sites.

A comparison of the locations of matched pairs shows that the three matching approaches differ in terms of how spatial proximity was used in the matching process (5.2). Figures 5.2b and 5.2c show that the MH method, by giving geographic proximity equal weight in the matching process, generated pairs that were further apart compared to DAPSm matches, which considered spatial proximity independently of the p-score estimation, leading to more spatially proximate matched pairs. Figure 5.2d shows that for the most part, optimal p-score matches are geographically much further apart compared to either DAPSm or MH approaches. The means and standard deviations of the matched controls show that all three approaches improved the covariate balance compared to all controls (5.2). However, MD controls were better matched on generation capacity and percentage of agricultural land in 1968, while Opt PS controls were better matched on distance to protected areas (5.2).

Table 5.2: Summary of balance of covariates in matched controls

Comparison of mean and standard deviation of covariates across matching approaches indicating degree of covariate balance (DAPSm: distance-adjusted propensity score matching; MD: Mahalanobis distance with geographic covariates; Opt PS: optimal propensity score matching). Percentage of agricultural land in 1968 is shown here as a substitute for the pair-specific covariate, percent of agricultural land 5- and 10-year pre-hydropower-development. Percentage of agricultural land in 2014 was not used as a matching covariate and is provided here to indicate the effect of matching on the means of an outcome variable.

Dataset	Summary statistic	Generation capacity (MW)	Distance to conservation or indigenous area (m)	Percentage of agricultural land in 1968	Distance to nearest urban area (m)	Percentage of agricultural land in 2014
Treated	Mean	1123	21204	0.00555	282621	0.209
All controls	Mean	433	9269	0.00607	248681	0.137
DAPSm matches	Mean	626	16552	0.00481	290776	0.196
MD matches	Mean	971	16222	0.00515	268269	0.163
Opt PS matches	Mean	903	19627	0.00464	273605	0.132
Treated	Stdev	2635	21161	0.00539	237801	0.155
All controls	Stdev	981	15612	0.00730	94578	0.127
DAPSm matches	Stdev	2112	23844	0.00428	92351	0.145
MD matches	Stdev	2476	23340	0.00536	122880	0.133
Opt PS matches	Stdev	1719	22633	0.00498	108403	0.139

Forest-loss detection using remote sensing techniques

To quantify forest loss within the circular buffers of treatment and matched control sites, we used the Google Earth Engine remote sensing platform (GEE; Gorelick et al., 2017) to perform all processing and analysis of Landsat 4-8 satellite imagery. GEE's parallel processing on the cloud capabilities allowed us to increase the scalability of remote sensing analysis. The GEE team provided additional asset storage space, enabling analysis of more than 100 hydropower locations.

Image preprocessing and compositing

Due to frequent and heavy cloud cover in the Amazon, we created three-year moving average composites for each buffered study area using Landsat imagery for years 1984 - 2017. To reduce cloud contamination, reduce inter-annual differences due to phenology, and maximize change detection, we first identified the 3-5 months during which vegetation had the lowest scene-averaged normalized vegetation difference index (NDVI) using the MODIS 16-day average NDVI product. Because MODIS scenes are available daily, at least one cloud-free scene per month is available across all sites. For producing the composites, we used only Landsat scenes captured within the time frame of the months identified. We combined

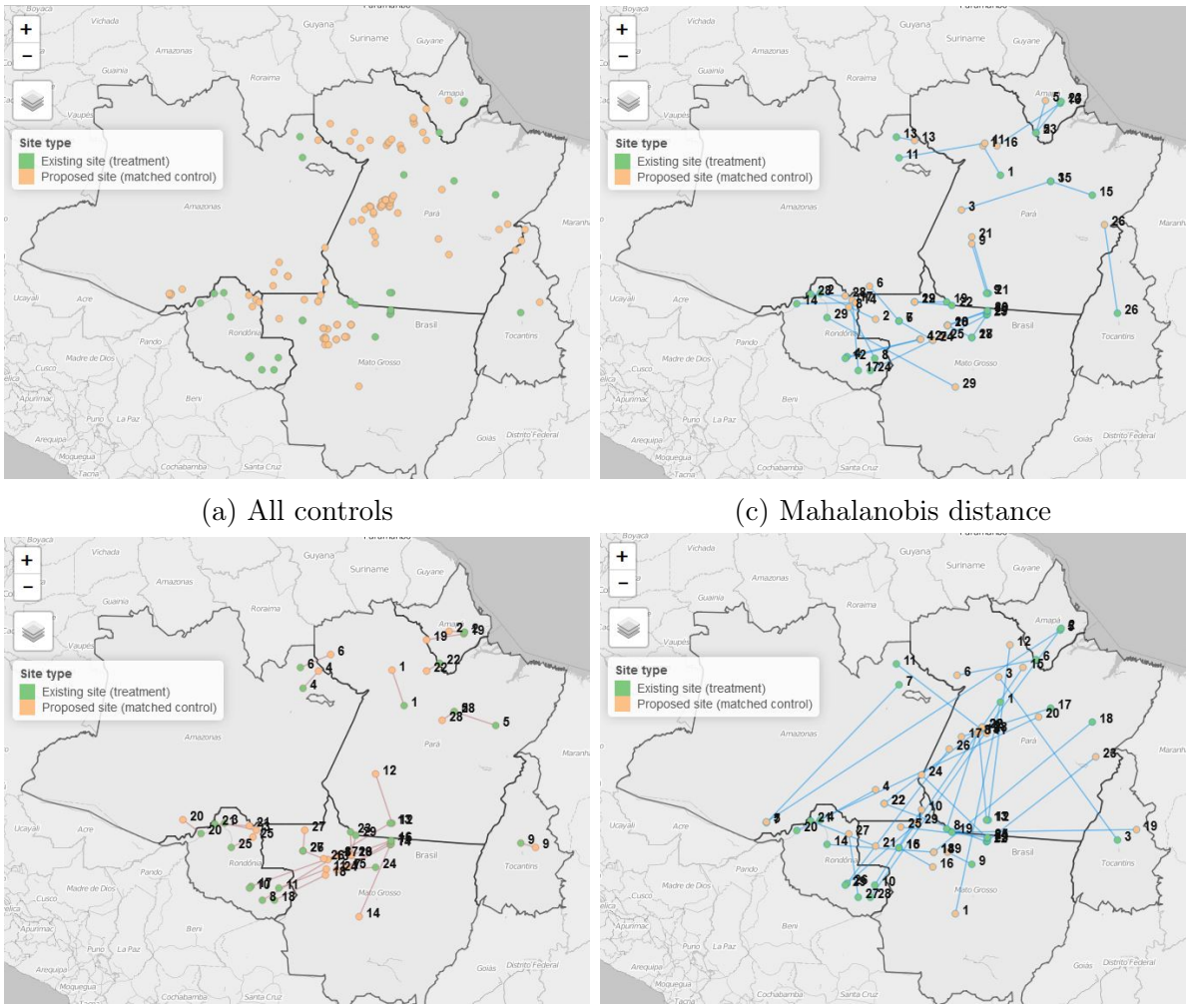

(a) All controls

(c) Mahalanobis distance

(b) DAPSm

(d) Optimal P-score

Figure 5.2: Map of matched treatment and control sites.

Map of matched treatment and control sites. We identified matched controls for 29 existing (treatment) sites using planned, proposed, and inventoried sites as possible controls within the Brazilian Amazon biome (a) using the following three matching approaches: distance-adjusted propensity score matching (DAPSm) (b), Mahalanobis distance (MD) matching using geographic coordinates as covariates (c), and propensity score using optimal matching with no consideration of geographic proximity (d). Lines indicate matched treatment and control sites and numerical labels indicate the match identification number unique to each matching approach. All proposed (control) sites shown and used for matching are greater than 80 km from any existing (treatment) site.

simple cloud score, FMask, and modified Temporal Dark Outlier Mask (TDOM) methods (Housman et al., 2015) to create cloud and cloud-shadow masks for each Landsat top-of-the-atmosphere (TOA) image. We then applied these mask to the corresponding Landsat

surface reflectance (SR) images for use in downstream analyses as SR images have been atmospherically corrected. Because Landsat 8 Operational Land Imager (OLI) bands capture comparable, but different, ranges of wavelengths with respect to Thematic Mapper (TM), we calibrated OLI images to match TM images (Landsat 4-7; Roy et al., 2016). Using the calibrated brands, we calculated the Tasseled Cap Indices (Kauth and Thomas, 1976) of all scenes using coefficients from the literature (Baig et al., 2014; Huang et al., 2002; Liu et al., 2015; Crist, 1985). Finally, we created a composite from the collection of processed Landsat images over a three-year time period using the median value per pixel.

Classification and change detection of composites

Despite using surface reflectance images, we observed differences in quality and radiometric correction over the long time series of composites. This reduces the accuracy of using band differencing for change detection (Song et al., 2001). As a result, we chose a post-classification approach for change detection (Tewkesbury et al., 2015). To train the classifier, we used the Hansen Global Forest Change v1.4 dataset's forest cover map for year 2000 (Hansen et al., 2013). After comparing Classification And Regression Tree (CART) and Support Vector Machine (SVM) classification methods, we determined that SVM produced more accurate results.

Parameterization of SVM classifiers. For each site, we used a 5-fold cross validation method to parameterize polynomial SVM classifiers. Using the composite image with median year 2000 (spanning 1999-2001), we sampled 1000 points from each of the two (forest and non-forest) land cover classes, randomly selected 80% of the points to train the classifier under a combination of hyperparameters, and used the remaining 20% to test the classifier and calculate a percent accuracy. We repeated this process five times per set of parameter values to calculate an average percent accuracy per set of hyperparameter values. We used these average percent accuracy values to select the best combination of hyperparameter values in the final classifier. We identified the best combination of values for the following hyperparameters and from the following parameter values: cost (0.01, 0.1, 1, 5, 10), gamma (0.01, 0.1, 1, 10, 50), and degree (1, 2, 3, 4, 5). For training the classifier, we chose the following band indices: un-normalized Tasseled Cap Disturbance Index (TC angle; Healey et al., 2005), Green Atmospherically Resistant Index (GARI; Gitelson, Kaufman, and Merzlyak, 1996), normalized difference between the short-wave infrared band (SWIR) 1 and SWIR band 2 (TM57), and the normalized difference between the near infrared (nir) and SWIR band 1 (TM54; Lu et al., 2004). These features' values range from -1 to 1, which means they are sufficiently "normalized" for use in SVM methods. We chose to use bands processed using a within-pixel normalizing approach, as opposed to subtracting the mean and dividing by the standard deviation of all pixels in the scene (or "soft" normalizing) more commonly used in preparing data for use in SVMs. This approach yields more accurate classified image time series because the mean and standard deviation of a band could vary or drift over time due to land use change.

Pseudo-invariant feature method for classification of time series composites.

We developed a pseudo-invariant feature method for classifying a time-series of image composites using a single year's training image (year 2000). The challenge of using only a single year to train many other years' composite also has to do with differences in quality and radiometric correction between images, and hence, between composites. Compared to applying a classifier trained using a different year's composite (i.e., 2000), a classifier trained using values from the composite year to be classified (the target) will naturally lead to better results. To do this using just one training image, we identified pixels that are spectrally similar (pseudo-invariant pixels or PIP) between pairs of composites (the training image and a target image) and limited random sampling of points for training the classifier to only these pixels. To automate the process of identifying PIPs, we conducted a principle components analysis (PCA) for each pair of images on an index-by-index basis, and selected the pixels where principle component 2 had values less than a certain threshold (Du, Teillet, and Cihlar, 2002). Only the pixels that overlapped better all the index-specific PIPs were used to randomly select points for training the classifier. Given the high variance of values for SWIR band 2, we used only TC angle, GARI, and TM54 to identify PIPs. To reduce computational demands, only four pairs of composites (year 2000 paired with years 1984, 1992, 2012, 2017) and were used to create PIPs and applied in classifying sub-groups of composites (1984-1991, 1992-1999, 2007-2012, 2013-2017). Composites for years 2000-2006 used the classifier trained with the composite and training image for year 2000.

After classifying each composite, the area of forest and non-forest was calculated at 10, 20, 30, 40, and 50 km (and 100 km for plants greater than 1 GW) buffer radii. To reduce the impacts of misclassification on the overall time trend, the forest area classified in the earliest composite was used a mask in all calculations of forest area loss in subsequent classified composite. As a result, our change detection method does not capture reforestation of areas deforested prior to 1984.

Panel regression analyses

Several methods are available for panel regression, and the choice between them rests on a battery of specification tests. Given the results of these specification and robustness tests, we use the following panel models: Random Effects (RE), Fixed Effects (FE), First Differences (FD), and Generalized Method of Moments (GMM).

First, we used a Random Effects model for estimating the forest-loss effect of hydropower development, as specified through the Hausman test. A RE model is also appropriate for examining the treatment effect when there is reason to believe that differences between individuals (hydropower plants) affect the outcome (forest loss)

$$y_{it} = \alpha + \beta X_{it} + \epsilon_{it} \tag{5.1}$$

Second, we used a two-way Fixed Effects model for estimating both forest-loss and agricultural-land-use effect of siting a hydropower plant, where the site (the existing or proposed hydropower plant) and the year are the two fixed effects. Effectively, a fixed-effects

model generates a dummy variable for each "fixed effect" or intercept—that is, for each site and for each year. The standard two-way fixed effects model is as follows:

$$y_{it} = \alpha_i + \beta X_{it} + \mu_{it} + \epsilon_{it} \tag{5.2}$$

To account for serial autocorrelation, we use a First Differences (FD) estimator for both forest loss and agricultural land use where $\Delta X_{it} = X_{it+1} - X_{it}$:

$$\Delta y_{it} = \beta \Delta X_{it} + \Delta \mu_i + \Delta \epsilon_i \tag{5.3}$$

Finally, to address serial autocorrelation directly using a dynamic panel regression, we use Generalized Method of Moments (GMM) estimator with two-step correction:

$$y_{it} = \gamma_1 y_{it-1} + \gamma_2 y_{it-2} + \beta X_{it} + \mu_i + \epsilon_i \tag{5.4}$$

As well as GMM with a lagged independent variables:

$$y_{it} = \gamma_1 y_{it-1} + \gamma_2 y_{it-2} + \beta_1 X_{it} + \beta_2 X_{it-1} + \mu_i + \epsilon_i \tag{5.5}$$

In all five regressions above, y_{it} is the percentage of forest loss since base year (1984) for site i and time t when fitting the model using the Landsat derived data, or the percentage of agricultural land (pasture and cultivated area) when fitting the model using Dias et al. (2016) data; X_{it} is a matrix of time varying explanatory variables, including a time-varying dummy variable indicating whether there is hydropower development on a site (i.e., the treatment variable); β is a vector of estimated coefficients; α_i is the individual or site-specific intercept term representing the time-invariant site-specific effect (otherwise known as unobserved heterogeneity between individuals); γ_1 and γ_2 are coefficients for the first and second order lagged dependent variables y_{it-1} and y_{it-2}; μ_i is the time-specific intercept term representing changes over time that affect all sites similarly (which can be thought of as disturbances); and ϵ_i is the error term.

We performed all regressions using R 3.4.3 (R. Core Team, 2017). We used the plm R package (Croissant and Millo, 2008) for fixed and random effects regressions and the sandwich package for standard error corrections. We performed a series of specification tests to determine whether the data meet each model's assumptions. Results of the Durbin-Wu-Hausman test for whether a random or fixed effects model is appropriate, determined that only the fixed effects model is consistent with the data. Using the F-test and Lagrange Multiplier Test, we determined the need to include a time fixed effect (i.e., two way model). The Augmented Dickey-Fuller Test established that the time series data residuals are stationary (i.e., there is no unit root). Both the Breusch-Pagan (B-P/LM) and Parsaran CD tests identified cross sectional dependence and heteroskedasticity. The Breusch-Godfrey/Wooldridge test identified serial correlation. We corrected the coefficients and standard errors for heteroskedasticity and serial correlation in the two-way fixed effects model using the Heteroskedasticity and Autocorrelation Consistent (HAC) covariance matrix estimator in the sandwich R package (Zeileis, 2006) by converting the fixed effects model into a linear model by de-meaning the

variables. We compared these estimates HAC clustered standard errors to the Heteroskedasticity Consistent (HC) covariance matrix estimator using the Arellano method that is robust to autocorrelation. We found that the HC-Arellano clustered errors are higher and thus report these in the results. To address the heteroskedasticity and the serial autocorrelation directly, we use a Generalized Method of Moments model with and without a lagged treatment variable.

A note about model specification. Each model has its strengths and weaknesses, based on the types of assumptions it requires about the data. For example, First Differences models assume that the "intervention" has an immediate effect on the outcome, in other words, it evaluates short-run effects. If the effect is leading or lagged, then taking first differences can result in biased estimates. There is reason to believe that hydropower projects can have a gradual, leading, or lagged effect on forest loss–and that these effects are may differ across individuals (examples provided in the Discussion section). It is possible to deal with the endogeneity arising from serial autocorrelation in two ways: (1) correcting for it in the error structure and estimating robust standard errors (bias correction) or (2) addressing it directly using dynamic panel models like GMM or lagged dependent variables. The factors that should determine the choice between these two general methods are ambiguous in the literature. It is known that endogeneity resulting from the error term being correlated with the dependent variable is an issue when the number of time periods (T) is small relative to the number of individuals (N), and the recommended way for addressing this is a GMM. However, if T gets larger relative to N, then GMM suffers from small sample properties (Baltagi, 2015). Breitung (in Baltagi, 2015) recommend that both methods—bias correction and GMM—can be appropriate for moderate T.

5.3 Results

Average effect of hydropower plant development on spatially proximal indirect forest loss

We find that the effect of hydropower plant development on forest cover loss as detected using Landsat imagery is significant—with the average effect size ranging from a 2.4% to 8.6% percentage point increase in forest-cover loss in any given year, depending on the estimator used (Tables 5.3, 5.4, D.1, D.3). Using the Hausman test for percent forest cover loss as the response variable, we find that both random and fixed effects are consistent, in which case, a random effects (RE) estimator is more efficient. However, given that the fixed effects model is more resistant to missing data, an issue in this study arising from frequent cloud cover, we also report the fixed-effects summary. Due to omitted-variable bias, we believe that the fixed-effect estimates may be more robust.

Using a two-way random effects (RE) estimator, we find that hydropower plant siting has a significant average effect of increasing forest loss by 5.4% (95% CI [0.1, 10.7]) and 6.8% points (95% CI [1.1, 12.5]) in any given year for the DAPSm and MD matching approaches,

respectively (Table 5.3 models (3), (4)). When the time trend is excluded from the RE regression, the coefficients increase to 7.7% (95% CI [1.1, 12.5]) and 8.6% (95% CI [2.0, 14.5]), respectively (5.3 models (1), (2). The robust standard errors are high for all RE estimates, resulting in large confidence intervals.

In univariate fixed effects (FE) regressions with only the treatment variable, the average effects of siting a hydropower plant are significant and very similar to estimates from the multivariate random effects model, with the key difference being lower Arellano clustered standard errors corrected for serial (time) and cross-sectional (individual) correlation (5.5% with 95% CI [2.0, 9.0] and 6.8% points (95% CI [3.5, 10.1]; Table 5.4 models (1), (2)). With time trend and other covariate interactions added, the coefficient does not change with DAPSm controls, though the standard errors are slightly higher, but the coefficient with MD controls reduces from 6.8% to 5.5% (95% CI[2.2, 8.8] (Table 5.4 models (3), (4)). The coefficient of the interaction of the treatment with the time trend is negative for both matching approaches, suggesting that the effect of hydropower siting on forest loss diminishes

Table 5.3: Random effects regression summary for percent loss of 1984 forest estimated from Landsat imagery.

"treatment_time" is a time-varying dummy variable for presence or absence of a hydropower plant. Its coefficient is the main treatment effect of hydropower development.

	Dependent variable:			
	Percent loss of 1984 forest cover			
	DAPSm	MD	DAPSm	MD
	(1)	(2)	(3)	(4)
treatment_time	0.077***	0.085***	0.054**	0.068**
	(0.029)	(0.029)	(0.027)	(0.029)
time_trend			0.009***	0.008***
			(0.001)	(0.001)
DistProtArea_km	0.002***	0.002***	0.002***	0.002***
	(0.001)	(0.001)	(0.001)	(0.001)
CapacityMW	0.00001*	0.00001***	0.00001**	0.00001***
	(0.00000)	(0.00000)	(0.00000)	(0.00000)
existingDam_dist_km	−0.0002	−0.0002	−0.0002	−0.0003
	(0.0002)	(0.0002)	(0.0002)	(0.0002)
city_dist_km	−0.00004	−0.0001	−0.00005	−0.0001
	(0.0001)	(0.0001)	(0.0001)	(0.0001)
Constant	0.124***	0.132***	−0.008	0.011
	(0.033)	(0.034)	(0.031)	(0.029)
Observations	1,631	1,760	1,631	1,760
R^2	0.174	0.215	0.458	0.452
Adjusted R^2	0.172	0.213	0.456	0.450
F Statistic	67.660***	95.480***	228.187***	239.350***
Note:				*p<0.1; **p<0.05; ***p<0.01

Table 5.4: Fixed effects regression summary for percent loss of 1984 forest cover estimated from Landsat imagery

"treatment_time" is a time-varying dummy variable for presence or absence of a hydropower plant. Its coefficient is the main treatment effect of hydropower development.

	Dependent variable:					
	Percent loss of 1984 forest cover					
	DAPSm	MD	DAPSm	MD	DAPSm	MD
	(1)	(2)	(3)	(4)	(5)	(6)
treatment_time	0.055***	0.068***	0.055***	0.055***	0.101**	0.096*
	(0.018)	(0.017)	(0.020)	(0.017)	(0.049)	(0.053)
treatment_time:time_trend					−0.002	−0.002
					(0.002)	(0.002)
time_trend:DistProtArea_km			0.0001***	0.0001***	0.0001***	0.0001***
			(0.00003)	(0.00003)	(0.00003)	(0.00003)
treatment_time:CapacityMW			−0.00000	0.00000	−0.00000	0.00000
			(0.00001)	(0.00000)	(0.00001)	(0.00000)
time_trend:existingDam_dist_km			0.00000	−0.00001	−0.00000	−0.00001
			(0.00001)	(0.00001)	(0.00001)	(0.00001)
time_trend:city_dist_km			0.00000	−0.00000	−0.00000	−0.00000
			(0.00000)	(0.00000)	(0.00000)	(0.00000)
Observations	1,631	1,760	1,631	1,760	1,631	1,760
R^2	0.055	0.082	0.198	0.238	0.211	0.248
Adjusted R^2	0.004	0.034	0.153	0.196	0.166	0.206
F Statistic	89.451***	149.092***	76.394***	104.213***	68.627***	91.407***
Note:						*p<0.1; **p<0.05; ***p<0.01

over time, though the interaction is not significant (Table 5.3 models (5), (6)).

As a conservative approach, we also fit the data using First Differences (FD) and Generalized Method of Moments (GMM) estimators which directly account for serial autocorrelation. The FD estimates of the average effect of the hydropower development on forest loss is positive and statistically significant for both matching approaches and regardless of whether a lagged dependent variable was included as a regressor (Table D.1, models (3), (4)). The effect size ranges from 1.3 - 1.6% percentage points, with very small standard errors (Table D.1. These coefficient estimates are much lower than either RE or FE estimates, though a comparison of coefficient values with their confidence intervals (CI) shows that the upper end of FD CIs are similar to the lower end of RE and FE CIs (Figure 5.6a). GMM coefficient estimates for hydropower development are all highly statistically significant and similar to, but slightly higher than FD estimates with lower standard errors (D.3 models (1) and (2); Figure 5.6a).

Pairwise comparisons of matched control and treatment sites show that for the majority of control-treatment pairs, treatment periods experienced visibly higher rates of forest loss compared to the matched control periods (15 out of 26 or more than half of the DAPSm

matches, and 19 out of 27 or more than two-thirds in the MD matches; Fig. 5.3a, 5.3b). For the remaining pairs, the control sites experienced higher rates of forest loss (3 out of 29 in both the DAPSm and MD matches) or experienced very similar rates of forest loss (8 out of 26 for DAPSm and 5 out of 28 for MH). When aggregated across pairs, forest loss trends over time show similar elevated levels for treatment sites (Fig 5.4a, 5.4b).

Other covariates. Of the four other site-specific covariates included in the RE models, only distance to protected area and generation capacity are statistically significant, with each kilometer further from a protected area resulting in 0.2% percentage points more forest loss and with each megawatt (MW) increase in generation capacity resulting in a small 0.001% percentage point increase in forest loss (Table 5.3). Time trend is also strongly significant, with each additional year resulting in a 0.9% percentage point increase in forest loss (Table 5.3). For the multivariate FE models with the time trend interacted with time-invariant covariates, only distance to the nearest protected area had a significant effect on forest loss over time, with each additional year and additional km away from a protected resulting in a 0.01% percentage point increase in forest loss (Table 5.4). There appears to be no time trend and generation capacity interaction. FD model estimates for regressors are similar to RE and FE estimates, though the effect of generation capacity is only significant for MD matches (Table D.1).

Effect differences due to distance from hydropower plant site. To understand whether hydropower development affects indirect land use in a spatially-dependent way, we compared FE estimates of hydropower effect size at the 50 km buffer radius baseline against estimates for study areas with 10 km, 20 km, 30 km, and 40 km buffer radii. For both DAPSm and MH matches, we find that the effect is positive and statistically significant across all buffer distances (Tables D.4, D.5). Estimates at 50 km radius are among the lowest, with the highest effect within 20-40 km of the dam location.

Average effect of hydropower plant siting on agricultural land expansion

Overall, we find that the effect of hydropower development on indirect agricultural land use change is lower and less statistically significant than that observed for forest loss. We report estimates from two-way fixed effects regressions (Table 5.5), given that results of the Hausman test suggest that a fixed effect model is more appropriate. However, due to the presence of serial autocorrelation, we also apply a First Differences (FD) with a lagged dependent variable as well as a Generalized Method of Moments (GMM) estimator.

In univariate FE regressions with only the treatment variable, the average effects of siting a hydropower plant on percentage of agricultural land is positive across all matching methods, but only significant for MD and Opt PS methods (Table 5.5, models (1-3)). However, when other covariates are included, only Opt PS remains statistically significant with a 2% percentage point increase (95% CI [-0.16, 4]) in agricultural land in any given year due to hydropower development (Table 5.5, models (4-5)). Like with forest loss, when hy-

Table 5.5: Fixed effects regression summary for Dias et al. (2016) estimated percent of agricultural land

	Dependent variable:									
	Percent of agricultural land									
	DAPSm	MD	Opt PS	DAPSm	MD	Opt PS	DAPSm	MD	Opt PS	
	(1)	(2)	(3)	(4)	(5)	(6)	(7)	(8)	(9)	
treatment_time	0.021	0.030**	0.039***	0.011	0.013	0.020*	0.073***	0.071***	0.063**	
	(0.014)	(0.013)	(0.014)	(0.013)	(0.012)	(0.011)	(0.023)	(0.024)	(0.025)	
treatment_time:time_trend							−0.003***	−0.003**	−0.002*	
							(0.001)	(0.001)	(0.001)	
time_trend:DistProtArea_km				0.0001***	0.0001***	0.0001***	0.0001***	0.0001***	0.0001***	
				(0.00002)	(0.00002)	(0.00002)	(0.00002)	(0.00002)	(0.00002)	
treatment_time:CapacityMW				−0.00000	−0.00000	−0.00000	−0.00000	−0.00000	−0.00000	
				(0.00000)	(0.00000)	(0.00000)	(0.00000)	(0.00000)	(0.00000)	
time_trend:existingDam_dist_km				−0.00001	−0.00001**	−0.00001***	−0.00001	−0.00001**	−0.00001***	
				(0.00001)	(0.00000)	(0.00000)	(0.00001)	(0.00000)	(0.00000)	
time_trend:city_dist_km				0.00000	−0.00000	−0.00000	−0.00000	−0.00000	−0.00000	
				(0.00000)	(0.00000)	(0.00000)	(0.00000)	(0.00000)	(0.00000)	
Observations	912	928	928	912	928	928	912	928	928	
R^2	0.016	0.040	0.059	0.312	0.400	0.511	0.356	0.445	0.534	
Adjusted R^2	−0.068	−0.042	−0.021	0.250	0.346	0.467	0.296	0.395	0.491	
F Statistic	13.939***	35.529***	53.913***	75.775***	113.425***	177.902***	76.818***	113.681***	162.013***	

Note: *p<0.1; **p<0.05; ***p<0.01

dropower development is interacted with the time trend, the coefficient for the interaction is significantly negative across all matching approaches, meaning that the effect of hydropower development on agricultural land expansion has reduced over time (Table 5.5 models (7-9)). With the treatment and time trend interaction term in place, the treatment coefficient also becomes significant (Table 5.5), which suggests that any significant effect of hydropower development on agricultural land use is not generalizable over time.

On the whole, FD estimates are nearly an order of magnitude lower than FE estimates of the effect of hydropower development on agricultural land use (Table D.2). However, only MD and Opt PS matches show significant effects, which become insignificant when lagged dependent variables were included as regressors (Table D.2 models (4)-(6)). GMM estimates, which include two lagged periods of the dependent variable and one lagged period for the treatment variable, show that the effect size of hydropower development on agricultural land use is similarly insignificant (Table D.3 models (3), (4)).

These trends in regression estimates are consistent with trends seen in plots of pairwise and aggregate changes in percent of agricultural land over time (Figures 5.3c, 5.3d, 5.5b). Several control and treatment pairs show nearly overlapping trends (10 out of 29 for both DAPSm and MD; 4 out of 29 for Opt PS), with a sizable number of treatment sites showing lower percent agricultural land than than its paired control (4 out of 29 for DAPSm; 7 out of 29 for MD; 6 out of 29 for Opt PS). In aggregate, the differences between treatment and control sites are not visibly pronounced (Figures 5.4c, 5.4d, 5.5d).

5.4 Discussion

Effect of hydropower development on land use and land cover

Our results suggest that hydropower development in the Brazilian Amazon results in significant indirect deforestation. There is inconsistent or poor evidence that hydropower development also causes expansion of agricultural land. Though it is unclear which estimator is most appropriate for modeling forest loss, past studies have suggested combining Fixed Effects and Lagged Dependent Variables (LDV) or another dynamic panel method as a bracketing strategy, with the the dynamic panel regression providing the lower-end estimates (Guryan, 2001). Using this guidance, the average effect of hydropower plant siting on indirect forest loss is 1.3 - 6.8% *percentage point* increase in any given year within a 50 km radius of the plant itself. Since the mean forest loss across all years for control sites is about 11.5 - 13% of 1984 forest cover (Appendix D Figure D.1), the effect range can be expressed as an 11.3% - 59% increase in indirect forest loss due to hydropower siting, in any given year for any given site. Though only weakly statistically significant, and insignificant in some models, hydropower development increases agricultural land use by 0.03 - 2.0% percentage points. This large range can be interpreted as a 0.7% - 50% increase in percent agricultural land use, assuming the average percent agricultural land use of all control values across all years, or about 4%. Inconsistency of results between forest loss and agricultural expansion are likely due

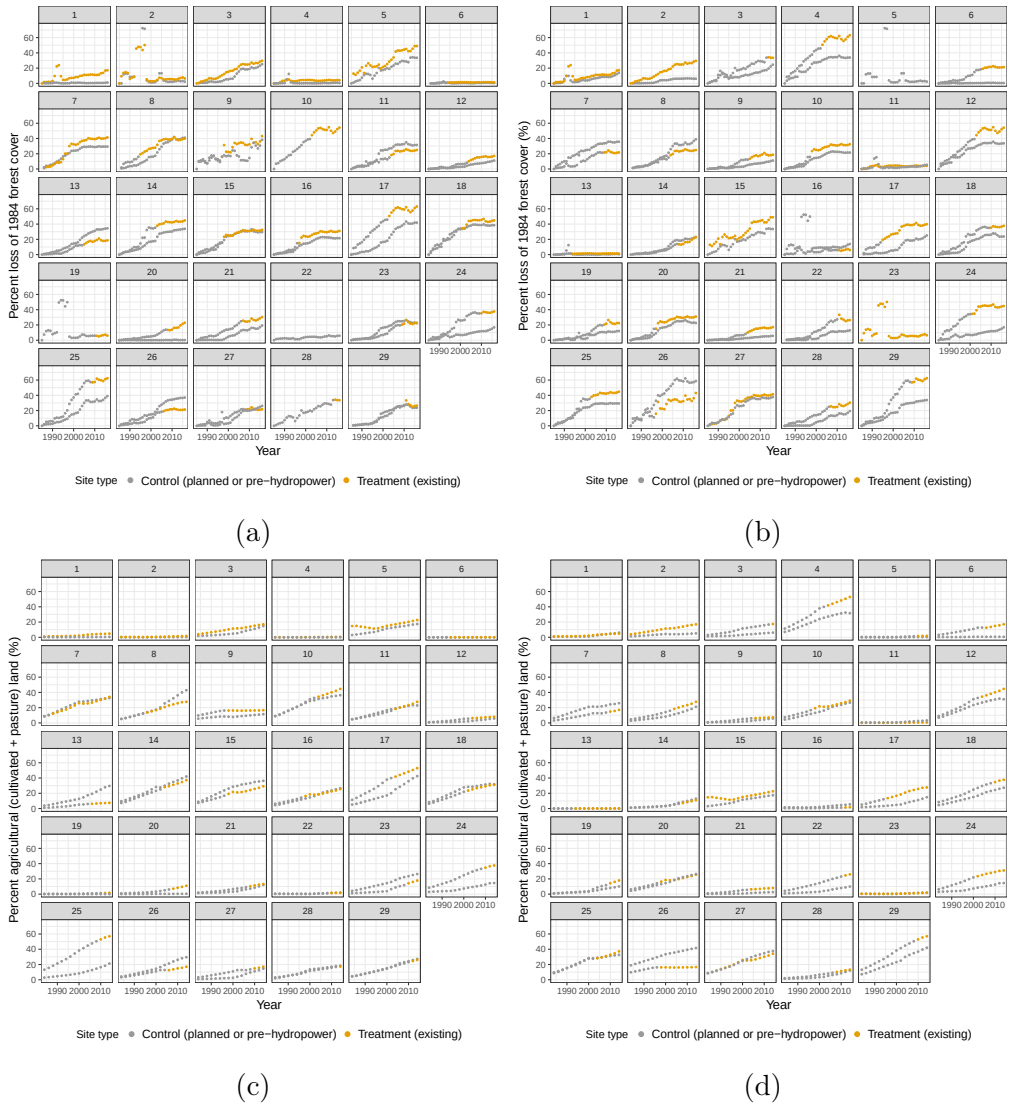

Figure 5.3: Pairwise control-treatment plots of changes in forest loss and agricultural land over time for DAPSm and MD matches.

Plots show the change in the dependent variables, percent of 1984 forest loss (a, b) and percent of agricultural land (c, d), over time of treatment and control pairs matched using the density adjusted propensity score matching (DAPSm; a,c) and Mahalanobis distance (MD; b,d) approaches. Yellow points indicate when a hydropower plant was developed in a treatment site. Grey points indicate locations without hydropower development across time. Though they are shown in the plots, points greater than 1.5 times the interquartile range are considered outliers and were removed from regression analyses. Sites missing data for its paired control or treatment site were excluded from regression analyses.

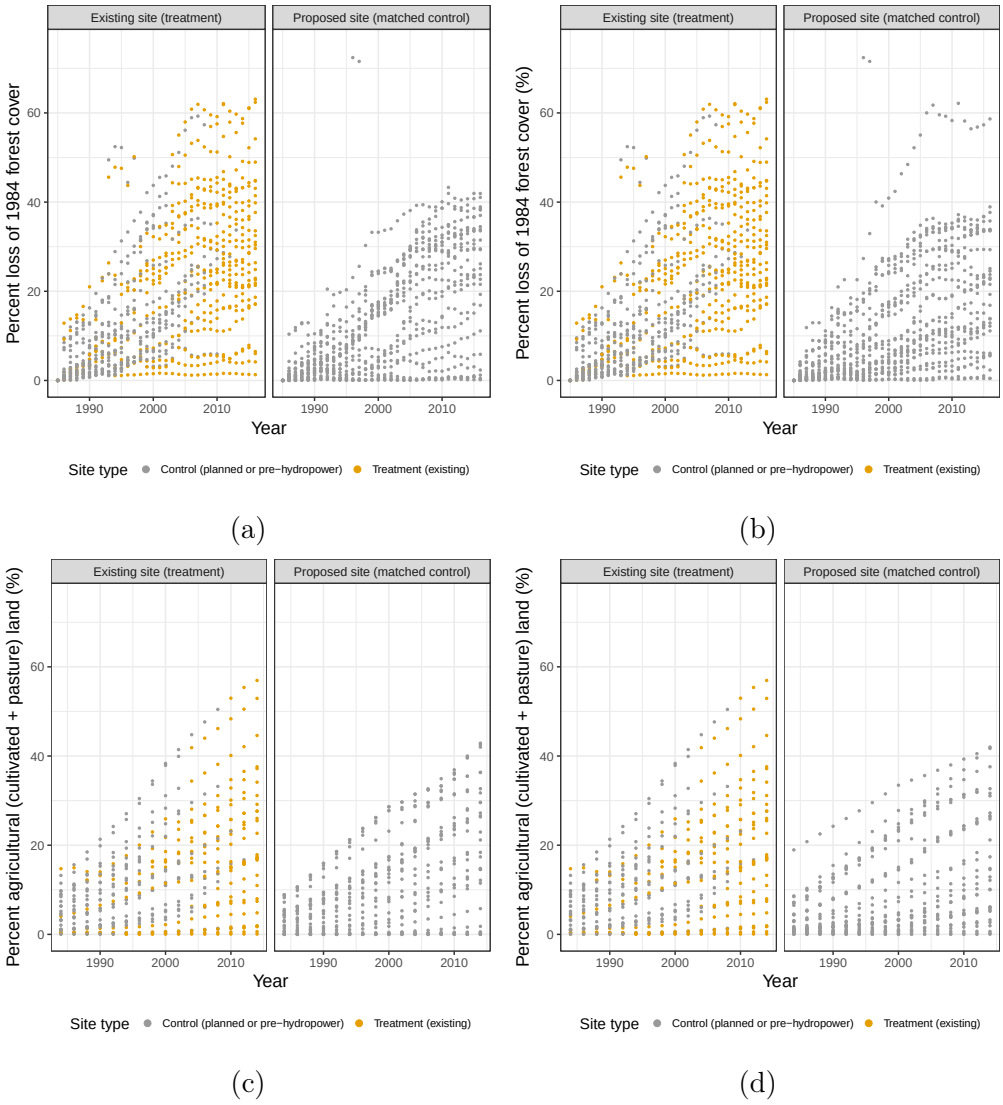

Figure 5.4: Aggregated plots of changes in forest loss and agricultural land over time for DAPSm and MD matches

Aggregated plots show the the change in dependent variables, percent of 1984 forest loss (a, b) and percent of agricultural land (c, d), over time of treatment and control units matched using the density adjusted propensity score matching (DAPSm; a,c) and Mahalanobis distance (MD; b,d) approaches. Panels compare existing sites against matched planned, proposed, and inventoried sites. The left hand "Existing site (treatment)" panel is the same for each dependent variable (a and b, c and d). Yellow points indicate when a hydropower plant was developed in a treatment site. Grey points indicate locations without hydropower development across time. Though they are shown in the plots, points greater than 1.5 times the interquartile range are considered outliers and were removed from regression analyses.

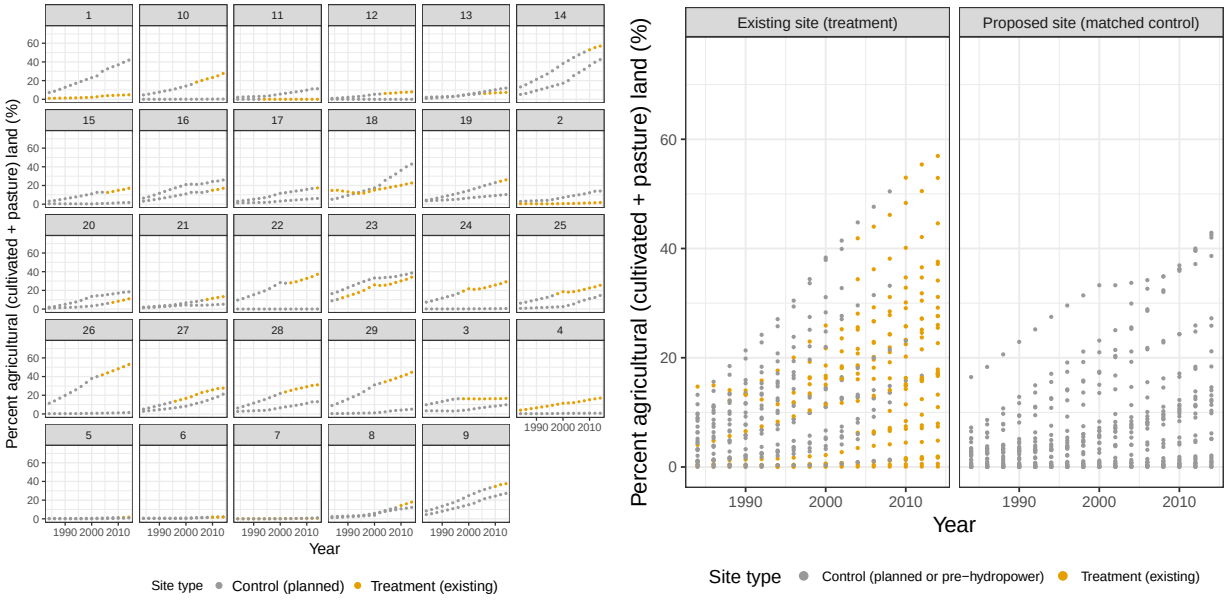

(b) (d)

Figure 5.5: Pairwise and aggregated plots of agricultural land use over time for optimal propensity score matches.

Pairwise (a) and aggregated plots (b) show the change in percent of agricultural land over time for treatment and control sites matched using optimal propensity score matching (Opt PS). These plots have similar properties as Figures 5.3 and 5.4.

to differences in the methods used to generate the two datasets—with forest loss estimated directly from imagery and agricultural area estimated from spatially disaggregated census data.

Heterogeneity between sites

The large standard errors for the average treatment effect, particularly for Fixed and Random Effects estimates, are largely explained by the significant spread of forest loss values within hydropower-developed sites, ranging from more than 60% to 1% loss of 1984 forest cover (Figure 5.4). A closer examination of those hydropower plants that experienced negligible indirect forest loss despite being developed pre-2000, provides case-specific explanations for their land use history. The development of the Balbina 250 MW hydropower plant (match ID 4 in Fig. 5.3a and match ID 11 in Fig. 5.3b) in 1985 created significant and highly controversial social and environmental damages, resulting in the establishment of a biological reserve to protect the reservoir and its islands as a mitigation strategy; the surrounding areas are protected by two other reserves established within a couple of years of Balbina's operational start date (Fearnside, 1989). Recent studies reveal that what happened with Balbina is more an exception than the norm; it is much more common for a hydropower

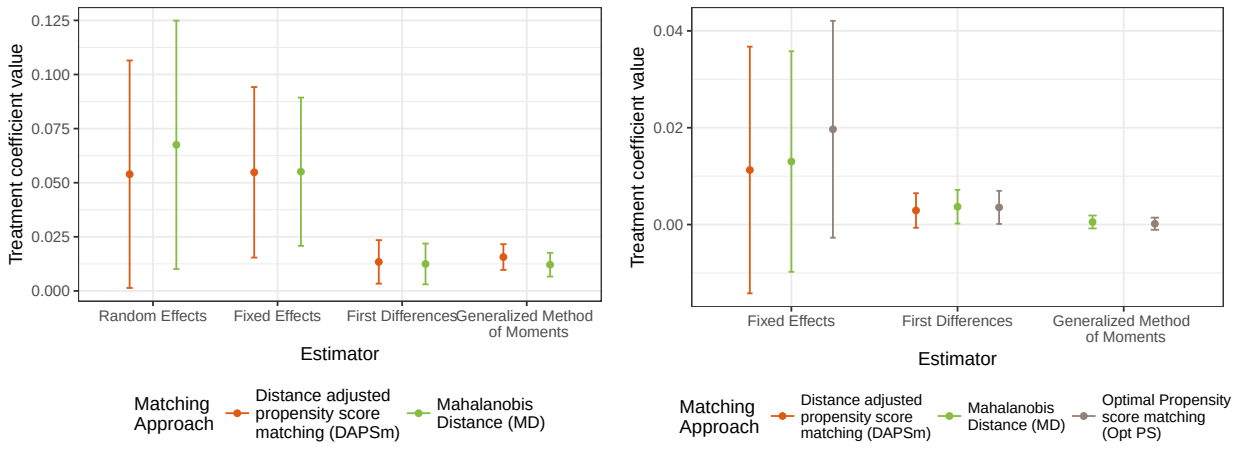

(a) (b)

Figure 5.6: Comparison of treatment coefficients for forest loss and agricultural land

Estimates of the treatment effect on percent of 1984 forest loss (a) and percent of agricultural land (b) are plotted for multiple estimators and matching approaches. 95% confidence intervals calculated using clustered standard errors are shown. Note that several coefficient estimates for hydropower development effects on percent of agricultural land are insignificant. Refer to Tables 5.5, D.2, and D.3 for p-values. GMM estimates are missing for DAPSm matches because collinearity issues with the data caused the model to fail to solve.

plant to cause protected area degazettement, downsizing, or downgrading (PADDD) (Pack et al., 2016). In fact, Pack et al. (2016) found that hydropower plant siting is the leading cause of all PADDD in Brazil, accounting for 39% of all enacted PADDD events. Pitinga (match ID 6 in Fig. 5.3a and match ID 13 in Fig. 5.3b), a 20 MW dam northeast of Balbina, was developed specifically to serve the needs of the large Pitinga tin mine. Two other existing dams with negligible forest loss in 2017 are Santo Antonio do Jari (not included in the plot or regressions due to the severity of cloud contamination in image composites) and Cachoeira Caldeirao (match ID 19 in Fig. 5.3a, match ID 16 in Fig. 5.3b) began operations in 2014 and 2016, respectively, with little time post-development to assess impacts. The final dam with negligible change over time is the first dam to be built in the Amazon, Coaracy Nunes (electricity generation started in 1975). The cloud contamination is severe for this site, with a handful of years in the 1990s missing images due to complete cloud cover. However, comparison of the earliest images in the mid 1980s show characteristic deforestation patterns emerging starting in the 1990s and steadily continuing into the 2000s, with pasture-land covering much of the southwestern portion of the study area before 1986 (Figures D.2)

Temporal and spatial dynamics

Findings suggest that the timing of hydropower development plays a role in its effect on forest loss. Since timing is largely related to the prevailing local or regional deforestation rates, this also suggests that the size of the impact of hydropower development on forest loss is related to background deforestation trends. We found significant negative coefficients for regression models with treatment interacted with the time trend, which indicate that the average effect of hydropower development on forest loss attenuates over time. We could interpret this at face value, meaning that more recently developed hydropower plants have had lower indirect deforestation impacts. However, the median operational start year is 2008, such that half of the existing hydropower plants in our sample were installed after 2008. If there is a delayed or gradual response of forest loss to hydropower development, then this trend over time could be explained by the relative lack of data during a power plant's operational years.

Other time-related dynamics can be observed from examining the data directly. The pairwise plots of forest loss indicates that significant forest loss appears to precede the estimated construction start in some cases. One plausible explanation for this is that in these cases, non-hydropower drivers of deforestation are more significant, and the added intervention of hydropower development only contributes rather than triggers forest loss. Another explanation could be that for larger dams, the estimated 5-year construction time is an underestimate, and the onset of the intervention actually occurred earlier in time. A recent study found that large dams take on average 8.6 years to construct (Ansar et al., 2014). Yet another plausible explanation is that just the impending construction of a hydropower plant in an area via an public announcement by the utility can lead to elevated human activity and deforestation. Media coverage of controversial planned dams in the Amazon have documented that just prioritizing dam construction projects in the planning phase can trigger illegal deforestation in the surrounding area. For example, plans for the São Luiz do Tapajós dam in Pará, Brazil have led to a rise in illegal squatting and deforestation, as reported by homestead farmers in the region who have been under increasing threat by illegal loggers seeking to appropriate their land (Farah, 2016). According to the article, "A network of illegal loggers is using the homestead projects to confer 'legitimacy' to their illicit cutting of trees in protected areas. The loggers claim homestead lands to be the source of illegally harvested timber to trick government enforcers."

The possibility of lagged or leading effects of hydropower development on forest loss is also consistent with the results of dynamic panel regressions. In the GMM regressions, both the dependent variable (forest loss) and the treatment variable (presence or absence of a hydropower plant) were lagged by two and one time-steps, respectively. We found that the non-lagged treatment effect is only significant in the presence of a lagged treatment variable, whose coefficient is also statistically significant. With no treatment variable lags, the treatment variable is no longer significant. This suggests that whether or not a site had hydropower development in the previous year significantly informs the effect of the dam in the current year. In other words, the history of development matters for its impact in a given

year. However, since the use of small samples with GMM models cause unstable regressions, results of GMM should be interpreted with caution (Baltagi, 2015).

Findings also suggest that the effects of hydropower development on forest loss is spatially dependent. Compared to The baseline treatment effects using a study area size with a 50 km radius, the treatment effect estimates for 20 - 40 km radii study areas are higher. Effects estimated at 10 km are more similar to the 50 km estimate, which could be due to the reservoir, which is excluded from deforestation change detection and in several existing sites, encompassing a significant area of a 10 km buffer study area. These spatial trends, with the exception of the 10 km radius, are consistent with previous studies' findings that deforestation has a distance-decay relationship around proximate drivers of deforestation such as roads (Barber et al., 2014; W. F. Laurance, Goosem, and S. G. W. Laurance, 2009).

We designed our matching approaches to vary the spatial similarity of matched control and treatment sites, as well as the quality of pairwise (vs. sample-wide) matching. We find that the DAPSm and MD matches yielded similar estimates of forest loss, with the MD matches yielding slightly higher treatment effect estimates or lower standard errors (Figure 5.6). The trend for Fixed and Random Effects regression coefficients show an increase in the treatment effect with reduced spatial constraints in matching, with the Opt PS, which has no spatial constraints, yielding the highest and only statistically significant treatment effect estimate (2% 95% CI [-0.16, 4]). Both sets of results suggest that the further control sites are from treatment sites, while increasing balance for other covariates, the higher the treatment effect estimates. Knowing that the balance on other covariates improved with relaxed spatial constraints (e.g., controls were more similar to treatments in terms of being further from protected areas and having lower initial agricultural land use; Table 5.2), this finding suggests that hydropower development on LULC changes may act across larger distances than examined in this study (50 km). The consequence is that the LULC histories of control sites close to existing hydropower plants may already be affected by hydropower development, thus reducing the estimated treatment effect.

Differences between forest loss and agricultural land area changes

In the Brazilian Amazon, typical land use patterns before the early 2000s were marked by a cascade of transitions, first from forest to clearing due to logging or subsistence agriculture, then from clearing or subsistence agriculture to large-scale pasture for cattle ranching (Fearnside, 2005). Since the early 2000s, pasture to mechanized cropland transitions and direct forest to mechanized cropland conversions have been the increasingly dominant land use patterns (Morton et al., 2006; Hecht and Cockburn, 2010; Arima et al., 2014). As such, we would expect our results for forest loss and agricultural land expansion to be very similar, albeit with a transitional lag for agricultural—pasture and cropland—expansion. The results are only weakly consistent this expectation. Without comparing the treatment effects themselves, since one dataset is measuring forest loss since 1984 and the other is measuring absolute percentage of agricultural land cover, we find that effect estimates on forest

loss are consistently significant across modeling approaches, whereas the effect estimates on agricultural land use is weakly significant or insignificant.

A close comparison of these two datasets reveals some disagreements within the same pairs of control and treatment sites. Several pairs in which the treatment site experienced distinctly higher loss of 1984 forest cover shows either the opposite relationship or overlapping trends for percent of agricultural land use (e.g., pairs 8, 14, 16, 18, 21 for DAPSm matches; pairs 9, 10, 20, 25, 28 for MD matches; Figure 5.3). However, differences in the ways that the two datasets were generated may be significant enough to prevent direct comparison. Because the Dias et al. (2016) dataset is derived from municipal level census data of land area under cultivation and pasture, the spatial disaggregation method will play a large role in how those hectares will be allocated across space. Thus, any limitations this dataset has stems largely from its spatial down-scaling process, and perhaps from possible inaccuracies of the underlying agricultural census data themselves. We generated the forest loss data specifically for this study and used spatially-explicit, native-resolution methods for assessing land cover change. Inaccuracies stemming from cloud contamination, phenology, and classification methods are its major limitations. Although the use of a three-year moving averages increase confidence in the overall time trend, it does not prevent noise from from increasing the standard errors of the regression estimates.

Limitations and remaining challenges

This study applied multiple matching approaches, datasets, and regression models to increase the robustness and certainty of the effect estimates. However, there are a number of limitations in our ability to capture and account for the variability of the effect of hydropower on LULC that may affect results. First, the LULC impacts of infrastructure development projects are temporally and spatially diffuse. This is particularly true when examining indirect land use changes. Given the anecdotal evidence for pre-construction human activity and forest loss due to planned hydropower projects, the use of planned projects as control units may underestimate the effect of hydropower development on forest loss. Secondly, given lack of information for half of the existing hydropower plants on construction start years, we relied on a five-year approximation, which could overestimate the effect for smaller dams and underestimate the effect for larger dams. Third, while the Landsat 5-8 missions provide 33 years of continuous land cover coverage (use of Landsat 1-3 requires manual processing and analyses, making them unsuitable for use in large scale studies), at least two of the more controversial hydropower projects, Samuel and Tucuruí, started construction before 1984. This means that we lacked pre-development forest loss data for these treatment sites, reducing their contribution to Fixed Effects estimates, which rely on "within" site variation in the treatment and response variables. Since these are treatment sites, this missing data issue could cause coefficients to be underestimated. Fourth, missing data due to poor Landsat imagery quality disproportionately affects treatment and control sites located "deeper" in the Amazon basin, which generally have lower rates of deforestation. This could bias the treatment effect estimate positively or negatively. Fifth, the choice of estimator strongly

affects the average treatment effect estimates. RE and FE coefficient values are similar, but they differ from FD and GMM coefficient values. The data is structured in a such a way that no one estimator is entirely apt.

Appendix A

Appendix for Chapter 2

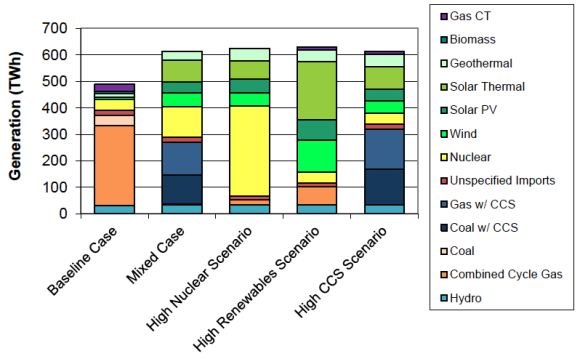

(a)

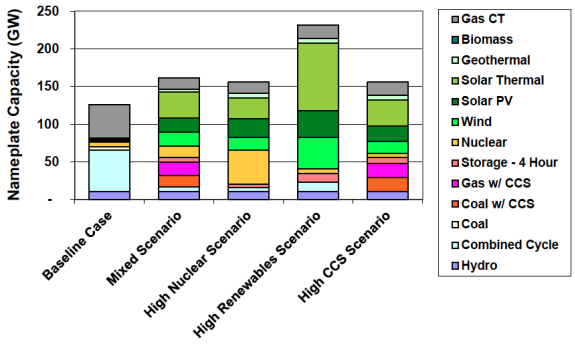

(c)

Figure A.1: Generation (A) and nameplate capacity (B) mix of each 2050 scenario in the California low carbon futures study chosen for this paper.

Figures 1a and 1b are reproduced Figures S20 and S22, respectively, in supplementary materials of Williams et al. (2012; Williams, DeBenedictis, et al., 2012).

Table A.1: Operational-phase life-cycle land-use factors based on 30-year plant lifetime

Technology	Design	Land-use metric	Land-use Factors (by generation in m^2 GWh^{-1})	Land use Factors (by capacity in MW km^{-2})	Reference and notes
Renewable					
Concentrating Solar Power (CSP)	Generic	Direct	364	31.7	Ong et al. (2012)[1]
CSP	Generic	Total	431	25	Ong et al. (2012)
Photovoltaic (PV)	Generic	Direct	432	34.3	Ong et al. (2012)
PV	Generic	Total	472	31	Ong et al. (2012)
Wind	Generic	Direct	26	353	Ong et al. (2012)
Wind	Generic	Total	3237	2.8	Ong et al. (2012)
Wind	California Generic	Total	1030[a]	Not Available	California-specific wind farm; Fthenakis and Kim (2009)[2]
Wind	California Generic	Direct	NA	460	Denholm et al. (2009)[3]: author calculated using values in appendix
Wind	California Generic	Total	NA	6.1[a]	Denholm et al. (2009): author calculated using values appendix
Wind	National Generic	Total	NA	3.0 (+/- 1.7)	Denholm et al. (2009)
Hydropower	Reservoir	Direct (NS)[b]	2350	NA	Fthenakis and Kim (2009) using Lake Powel reservoir (50-yr plant lifetime)
Biomass	Boreal forest	Direct (NS)	2000	NA	Jordaan (2010)[4] for Alberta, Canada
Geothermal	Generic	Direct	17.5	247	Ong et al. (2012)
Geothermal	Generic	Total	175	25.5	Ong et al. (2012)
Non-renewable					
Coal	U.S. Generic	Direct (NS)	410	NA	Fthenakis and Kim (2009)
Coal	With CCS	Direct (NS)	497[3]	NA	Fthenakis and Kim (2009) and Rochelle (2009)[5]
Nuclear	Generic	Direct (NS)	120	NA	Fthenakis and Kim (2009)
Natural gas combined-cycle (NGCC)	Generic	Direct (NS)	262	NA	Fthenakis and Kim (2009)
Natural gas	Alberta, Canada	Direct	100 - 400	NA	Jordaan (2010) for Alberta, Canada
NGCC	Generic	Direct (NS)	120	NA	NETL (2014)[6]

NGCC	With CCS	Direct (NS)	460	NA	NETL (2014)[6]
NGCC	With CCS	Direct (NS)	280[c]	NA	Fthenakis and Kim (2009) and applying Rochelle's (2009) parasitic load of 25%. This does not include land needed in the sequestration phase of NGCC-CCS.

Yellow cells indicate values used to compute land use demand results in Figure 1 A, B. Blue cells indicate values used to estimate total potential (Figure 2) and model build-out (Figure 4). "Direct" land use is land directly transformed by energy development. "Total" land use is land area of an entire project or power plant.

[a] California-specific values were adopted for both land use demand estimates (land-use factors by generation) and modeling of build-out (land-use factors by capacity).

[b] NS indicates that "total" vs. "direct" land use metric was not specified in the study, but description of methods strongly suggests "direct" land use.

[c] Coal-CCS and NGCC-CCS land use values were estimated using estimates of the average lowest achievable parasitic power load consumption (25%) due to CO2 extraction using amine scrubbing technology. This correction factor accounting for efficiency losses of CCS power plants was applied to the extraction and waste stages of relevant technologies.

Table A.2: GIS exclusion criteria and buffer distances to assess suitable sites

Criteria	Solar PV	Solar CSP	Wind	Geothermal	NG-CCS or Coal-CCS	Nuclear
PHYSICAL, TECHNICAL, SOCIO-ECONOMIC						
Raw renewable resource	Global Horizontal Insolation (GHI) < 5.0† kWh m^{-2} day^{-1}	Direct Normal Insolation (DNI) < 6.75 kWh m^{-2} day^{-1}	NREL Wind power class < 3 (max: 7)	USGS geothermal class < 9 (Max: 10)	IN‡: Natural Gas Plays IN: Coal reserves	N/A
Slope	> 3%	> 3%	> 20%	> 15%	> 12%	> 12%
Elevation (DEM)	> 1500 m	> 1500 m	> 1500 m	> 1500 m	> 1500 m	> 1500 m
Contiguous area	< 1 km^2	< 5 km^2	< 8 km^2	< 1 km^2	< 1 km^2	< 1 km^2
Water bodies and rivers	EX§	EX	EX	EX	EX	EX
Census urban zones	EX: 0.5 km	EX: 0.5 km	EX: 1 km	EX: 1 km	EX: 0.5 km	EX: 0.5 km
Population density (people km^{-2})	> 100	> 100	>100	>100	>100	>50
Surface mines (hazardous facility)	EX: 1 km	EX: 1 km	EX: 1 km	EX: 1 km	EX: 1 km	EX: 8 km
Airports (hazardous facility)	EX: 1 km	EX: 1 km	EX: 1 km	EX: 1 km	EX: 1 km	EX: 16 km
Roads	EX	EX	EX	EX	EX	EX: 1km
Rails	EX	EX	EX	EX	EX	EX: 1km
Military Installations (hazardous facility)	EX: 0.5 km	EX: 0.5 km	EX: 0.5 km	EX: 0.5 km	EX: 0.5 km	EX: 8 km
NATURAL DISASTERS						
Landslide risk areas: "high, suspected high, or combo-hi classifications"	EX	EX	EX	EX	EX	EX
Flood Risk Zones: A, AE, AH, AO, Open water, V	EX	EX	EX	EX	EX	EX
Fault lines: "ACODE"= 1 OR "SLIPRATE"= '1-5' OR "SLIPRATE"='>5'	IN	IN	IN	IN	EX: 10 km	EX: 16 km (1-5 mi line), 32 km (5 – 10 mi), 80 km (10-20 mi), 160 km (> 20 mi)
AGRICULTURAL						
Herbaceous agricultural land	EX	EX	IN	EX	EX	EX: 1 km
Prime agricultural land (just California)	EX	EX	IN	EX	EX	EX: 1 km
ENVIRONMENTAL						
All Layers	EX: 0.5 km	EX: 0.5 km	EX: 0.5 km	EX: 0.5 km	EX: 0.5 km	EX: 1 km

† Greater than or less than values indicate thresholds for exclusion.
‡ "IN" indicates inclusion of criteria and width of buffer if applicable.
§ "EX" indicates exclusion and width of buffer if applicable.

Table A.3: Data sources

Dataset	Source	Data type/ resolution
PHYSICAL, TECHNICAL, SOCIO-ECONOMIC		
Insolation (GHI and DNI)	National Renewable Energy Lab: Solar Maps http://www.nrel.gov/gis/data_solar.html	Feature/10km
Wind speed class	National Renewable Energy Lab: 50 m hub height (extrapolated to 80m for use in present analysis) http://www.nrel.gov/gis/data_wind.html	Feature
Geothermal: USGS Geothermal Favorability Map Derived From Logistic Regression Models and Identified Moderate and High Temperature Geothermal Systems of the Western US	http://certmapper.cr.usgs.gov/geoportal/rest/find/document?searchText =Geothermal&max=500&f=html&style=http://certmapper.cr.usgs.gov/ geoportal/catalog/skins/themes/erp/previewlittle.css	Feature
Elevation (DEM) and slope	U.S. Geological Survey: EarthExplorer: http://earthexplorer.usgs.gov/ SRTM dataset	Raster/d90m
Contiguous area	Lopez et al. (2012)[7], RETI[8], WGA[9]	Numerical values
Water bodies and rivers	Solar Energy Development Programmatic EIS (Solar PEIS): http://solareis.anl.gov/maps/gis/index.cfm	Polygon
Census urban zones	U.S. Tiger dataset: http://www.census.gov/cgibin/geo/shapefiles2011/main	Polygon
Population density (people/km^2)	Landscan: http://web.ornl.gov/sci/landscan/	Raster/1km
Surface mines (hazardous facility)	U.S. Geological Survey: Active mines and mineral plants in the U.S. http://mrdata.usgs.gov/mineplant/	Point
Airports (hazardous facility)	National Transportation Atlas Database: http://www.rita.dot.gov/bts/sites/rita.dot.gov.bts/files/publications/national_transportation_atlas_database/2013/points.html	Point
Roads	Solar PEIS and National Transportation Database: National Highway Planning Network. U.S. Tiger dataset for roads by county: http://www.census.gov/geo/maps-data/data/tiger-line.html	Polyline
Railway network	National Transportation Atlas Database: http://www.rita.dot.gov/bts/sites/rita.dot.gov.bts/files/publications/national_transportation_atlas_database/2013/polyline.html	Polyline
Military Installations (hazardous facility)	US-PAD (see below for environmental datasets)	Polygon
Coal reserves	USGS Energy Resources Program: Energy Data Finder: http://energy.usgs.gov/Coal/ AssessmentsandData/CoalAssessments.aspx	Polygon
Ground water (aquifers)	USGS aquifer database: http://nationalatlas.gov/atlasftp.html#aquifrp	polygon
Natural Gas Plays	Energy Information Association (EIA): http://www.eia.gov/pub/oil_gas/natural_gas/analysis_publications/maps/maps.htm	Polygon
Deep saline aquifers and other geologic carbon storage	National Carbon Sequestration Database and Geographic	Polygon
Transmission lines and corridors	- California Energy Commission - planned corridors: West Wide Energy Corridor Environmental Impact Statement, section 368 corridors: http://corridoreis.anl.gov/eis/fmap/gis/index.cfm	Polyline
Land ownership	Bureau of Land Management. Geospatial Data Downloads: "Federal and State managed lands in California" (LandStatus_v10.gdb) <http://www.blm.gov/ca/gis/>	Polygon
NATURAL DISASTERS		
Landslide risk areas: "high, suspected high, or combo-hi classifications"	USGS: National Atlas: Landslide incidence and susceptibility http://www.nationalatlas.gov/atlasftp.html#lsoverp	Polygon
Flood Risk Zones: A, AE, AH, AO, Open water, V	Federal Emergency Management Agency (FEMA): Map Service Center	Polygon

	https://msc.fema.gov/webapp/wcs/stores/servlet/FemaWelcomeView?storeId=10001&catalogId=10001&langId=-1	
Fault lines: "ACODE"= 1 OR "SLIPRATE"= '1-5' OR "SLIPRATE"= '>5'	U.S. Geological Survey: National Atlas: Quaternary Faults http://www.nationalatlas.gov/atlasftp.html#qfaultm	Polyline
AGRICULTURAL		
Herbaceous agricultural land	National Gap Analysis Program Land Cover Data (category: cropland): http://gapanalysis.usgs.gov/gaplandcover/data/download/	Raster/30m
Prime agricultural land and SUL farmland (state, local, and unique importance) in California	Williamson act –Farmland Mapping and Monitoring Program (FMMP) in CA: http://www.conservation.ca.gov/dlrp/fmmp/products/Pages/DownloadGISdata.aspx	Polygon
ENVIRONMENTAL		
U.S. Protected Area Database (US-PAD) v3.1	Protected Areas of the U.S. Database, Version v3.1: http://gapanalysis.usgs.gov/padus/data/download/	Polygon
Wetlands	US Fish and Wildlife Service: National Wetlands Inventory. http://www.fws.gov/wetlands/Data/State-Downloads.html	Polygon
BLM Roadless Areas	Solar PEIS dataset and USFS Inventoried Roadless Areas for contiguous US (Data Basin Dataset): http://www.arcgis.com/home/item.html?id=2dd4cfcf14e34bc8bd9d3bd7e13b1091	Polygon
BLM Critical Habitat for Endangered and Threatened species	Solar PEIS	Polygon
Important Bird Areas	Audubon Society	Polygon
Right of Way (exclude and avoid)	Solar PEIS	Polygon
Visual Management areas	Solar PEIS	Polygon
POWER PLANT LOCATIONS		
PV plants	California Energy Commission (CEC); EIA form 860: http://www.eia.gov/electricity/data/eia860/	Geographic coordinates
CSP plants	CEC; EIA	Geographic coordinates
Wind farms	CEC; EIA	Geographic coordinates
Geothermal	CEC; EIA; Geothermal Power Plants-USA: http://geo-energy.org/plants.aspx	Geographic coordinates

Table A.4: Comparison of environmental classifications in previous studies with chosen classifications in the present study

Land areas are classified as legally excluded (Ex) and the equivalent of Category 4 in the present study, or avoid (Av) with sensitivity score (corresponding to Categories 3.5, 3, 2, 1 in the present study; see Table 1 in main paper). Brackets in the first column indicate the studies in which the land area type was applied as an exclusion or avoidance layer.

LAND AREA TYPE	RETI	WREZ	WECC Transmission	The present study	Data Source
PROTECTED AREAS					
National park system (parks, preserves, historic parks, historical sites, lakeshores) [all studies]	Ex	Ex	4	Ex	PAD-US
National Recreation Areas [all studies]	Ex	Ex	3	Ex	PAD-US
National Wildlife Refuges (US FWS) & state (under "Habitat and Species Mgmt Areas" in PAD-US) [all studies]	Ex	Ex	4	Ex	PAD-US
Designated Federal Wilderness Areas and Wilderness Study Areas [all studies]	Ex	Ex	4	Ex	PAD-US and Solar PEIS
Recommended Federal Wilderness Areas and Wilderness Study Areas [WREZ]	-	Ex	4	Ex	PAD-US
USFS Inventoried Roadless areas (add separately to PAD-US) [all studies]	Ex	Ex	3	Ex	Solar PEIS
BLM National Conservation Areas (under "National Landscape conservation system" in PAD-US) (just King Range, Black Rock High Rock, Headwaters Forest Reserve) [RETI]	Ex	-	-	Ex	PAD-US
BLM National Conservation Areas (all others)	-	-	3	Av-3; Ex for geothermal as specified in data source	PAD-US; Geothermal: http://www.blm.gov/wo/st/en/prog/energy/geothermal/geothermal_nationwide/Documents/GIS_Data.html
(National Park) National Monument	Ex	Ex	3	Ex	PAD-US
(BLM) National Monument	Ex	Ex	3	Ex	PAD-US
National historic and scenic trails	Ex	-	3	Ex	PAD-US
National wild, scenic and recreational rivers	Ex	Ex	3	Ex	PAD-US
State Parks (CA, MT, OR, WA, WY)	Ex	Ex	3	Ex	
State Parks (all others)		Av	3	Av-3.5 if GAP statuses 1 or 2, Av-3 otherwise	PAD-US
California State Wilderness Areas [all studies]	Ex	Ex	4	Ex	PAD-US
State forest (CA) [WREZ]	-	Ex	3	Ex	PAD-US
State forest (other states) [WREZ]		Av	3	Av-3.5 if GAP statuses 1 or 2, Av-3 otherwise	PAD-US
DFG (now called Department of Fish and Wildlife) wildlife areas and ecological reserves [RETI]	Ex	-	3 (added)	Ex; Av-3 for non DFG wildlife areas	PAD-US
Existing conservation and mitigation banks under	Ex	Ex	3	Ex	PAD-US

conservation easements (CA) [all studies]					
Existing conservation and mitigation banks under conservation easements (for all other states) [WREZ]		Av	3	Av-3.5 if GAP statuses 1 or 2, Av-3 otherwise	PAD-US
Existing Conservation and Mitigation Bank	-	-	3	Ex	PAD-US
Moved to Cat 2: lands precluded from development in Habitat Conservation Plans [RETI]	Av	Ex- legally protected, Av-not legally protected	-	Unable to locate data	
Moved to Cat 2: Lands precluded from development under Natural Community Conservation Plans [RETI]	Av	Ex, Av depending on legal protection	-	Unable to locate data	
Wildlands Conservancy preserves [RETI]	Ex	-	-	Ex	
(State and national) wetlands [all studies]	Ex	Ex	3	Ex	USGS
Area of Critical Environmental Concern [all studies]	Av	Ex: geothermal, Av: wind, solar	3	Av-3.5 if GAP statuses 1 or 2, Av-3 otherwise	Solar PEIS; PAD-US
BLM landscape conservation system – Non-Wilderness [WREZ] OR National Conservation Areas [WECC] (same land area in PAD US)	-	Ex (except as specified for wind, geothermal), Av (solar)	3 (see National conservation area)	Ex	PAD-US
BLM Visual Resource Management class I and II [WREZ]	-	Av	3	Av-3	Solar PEIS-Visual management area byway buffer and EPA class 1 area
BLM ROW avoidance [WREZ & WECC]	-	Av	3	Av-3	Solar PEIS
BLM Special recreation management areas [WREZ & WECC]	-	Av	3	Av-3	Solar PEIS
BLM no surface occupancy restriction areas [WREZ & WECC]	-	Av	3	Av-3	Solar PEIS
BLM designated and proposed Research Natural Areas + Sikes Act Tracts [WREZ & WECC]	-	Av	3	Av-3.5 if GAP statuses 1 or 2, Av-3 otherwise	PAD-US
BLM Wildlife Management Areas [WREZ & WECC] Desert Wildlife Management Areas (DWMA) and Mojave Ground Squirrel (MGS) Conservation Areas [RETI]	Av (west Mojave)	Av	3	Av-3.5 if GAP statuses 1 or 2, Av-3 otherwise	Solar PEIS (does not consider flat tailed horned lizard); PAD-US
BLM land managed for wilderness characteristics [WREZ & WECC]	-	Av	3	Unable to locate data	
USFS Research Natural Areas [WREZ & WECC]	-	Av	3	Av-3	PAD-US
USFS Special interest areas [WREZ & WECC]	-	Av	3	Av-3	PAD-US
USFS congressional reserved areas	-	Av		Unable to locate data	

[WREZ]					
State wildlife areas (CA, ID, MT, NV, OR, WA, WY)	-	Ex	3	Ex	PAD-US
State wildlife areas (others)	-	Av	3	Av-3.5 if GAP statuses 1 or 2, Av-3 otherwise	PAD-US
NATURAL RESOURCE FACTORS					
USFWS Designated critical habitat for federally listed endangered and threatened species [RETI]	Av	-	3	Av-3.5 if GAP statuses 1 or 2, Av-3 otherwise	FWS critical habitat portal: http://ecos.fws.gov/crithab/
Lands purchased with private funds and donated to federal government [RETI]	Av	-	-	Unable to locate data	
Land in wilderness bills [RETI]	Av	-	-	Unable to locate data	
Areas which contain ecosystems or species that are at moderate risk [WECC]	-	-	2	Av-3	Solar PEIS; PAD-US (not exact match)
Areas with irreplaceable natural or cultural resources [WECC]	-	-	3	Unable to locate data	
Habitat areas for candidate or listed wildlife species mapped by State, Provincial or Federal Agencies [WECC]	-	-	3	Av-3.5 if GAP statuses 1 or 2, Av-3 otherwise	FWS critical habitat portal: http://ecos.fws.gov/crithab/
Audubon Society compiled Important bird areas (global) [WECC]	-	-	3	Av-3 for wind; Av-2 otherwise	Audubon Society
Audubon Society compiled Important bird areas (state) [WECC]	-	-	2 (3 for wind)	Av-3 for wind; Av-2 otherwise	Audubon Society
State Mapped Crucial big game winter range/severe winter range [WECC]	-	-	3	Av-3	PAD-US
State wildlife corridors [WECC]	-	-	3	Unable to locate data	
Marine Protected Areas [WECC]	-	-		Ex	PAD-US
LAND USE					
Agricultural Land [WECC]	-	-	2	Ex (for non-wind), Av-3 for wind	GAP analysis (cropland)
Williamson Act Prime Farmland (not in PAD)	Av (non-wind)	-	3	Ex (for non-wind) Av-3 for wind	Williamson Act data
Williamson Act Farmland of state and local importance, unique farmland	Av (non-wind)	-	-	Ex (for non-wind) Av-3 for wind	Williamson Act data
Native American land and Native Allotment [WECC]	Ex	-	2	Ex [2]	PAD-US
Other public land (state other, state trust land) [WECC]	-	-	2	1	PAD-US
Recreation Mgmt Areas with Gap statuses 3, 4				2	PAD-US
Historic/Cultural areas with Gap statuses 3,4				2	PAD-US
BLM resource management areas with Gap statuses 3,4				1	
Other water district land [WECC]	-	-	2	Av-2	PAD-US
Private non-profit land [WECC]	-	-	2	Av-3.5 if GAP statuses 1 or 2, Av-3 otherwise	PAD-US

Private Land- Unknown Restriction [WECC]	-	-	2	Av-3.5 if GAP statuses 1 or 2, Av-2 otherwise	PAD-US
Private Land- Unrestricted for development [WECC]	-	-	2	1	
Private Conservation Land (non-conservation easements in CA) (P_Des_type in PAD-US)				Av-3.5 if GAP statuses 1 or 2, Av-3 otherwise	PAD-US
Flood zones [WECC]	-	-	2	Ex (see Table S2)	FEMA
USDA Agricultural Research Center	-	-	2	Av-2	PAD-US
Watershed Protection Areas [WREZ]	-	Ex	-	Ex	PAD-US
Unknown land owner and no known mandate for protection	-	-	1	1	PAD-US

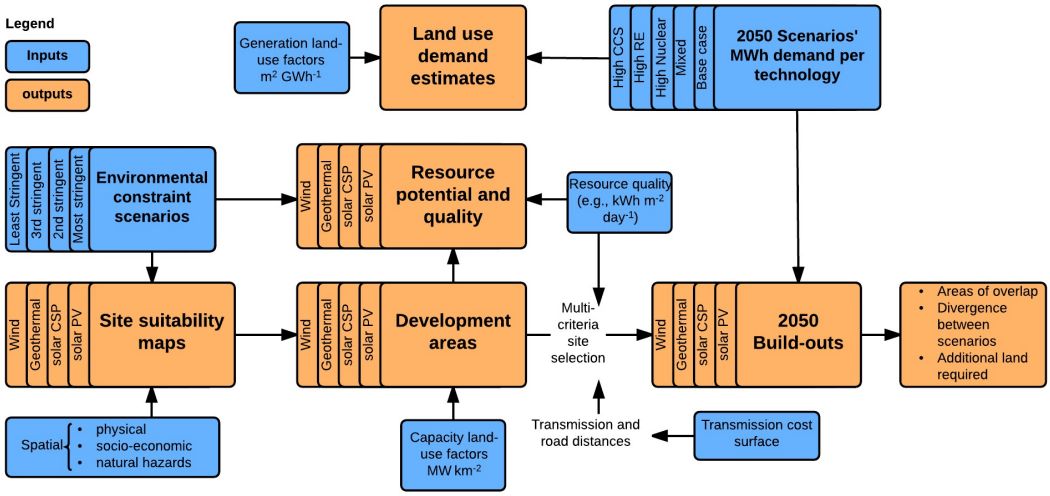

Figure A.2: Process flow diagram of methods.

Land use demand estimate results are shown in Figure 1, resource potential and quality results are show in Figure 2, site suitability maps are shown in Figure S4, build-outs maps are shown in Figure 3, overlapping area values are shown in Figure 4, and additional land requirements are tabulated in Table 2. Generation and capacity land-use factors are found in Table S1, Figure S1 shows the 2050 generation by technology, Figure S3B shows the transmission cost surface map, and Figure S3A shows the mapped environmental constraint scores.

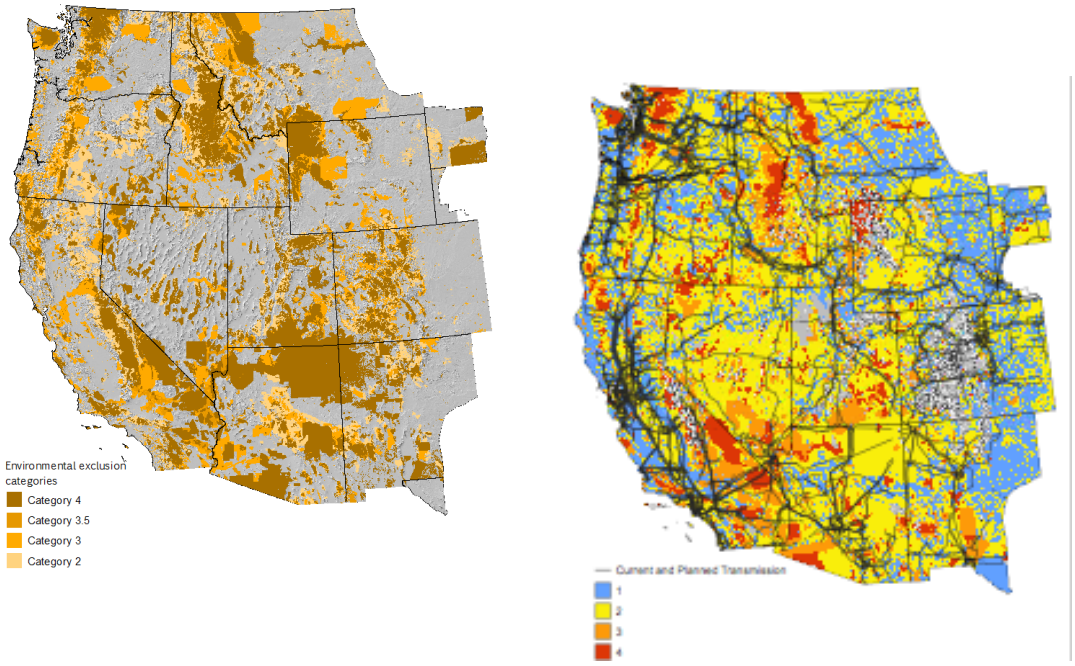

(a) (b)

Figure A.3: Generation (A) and nameplate capacity (B) mix of each 2050 scenario in the California low carbon futures study chosen for this paper.

Environmental scoring for generation (A) and transmission siting (B). Environmental (ecological, cultural, historical) areas were compiled from the USGS PAD-US database and various BLM sources. Each protected parcel was assigned an environmental score indicating suitability of land for generation (A) and transmission (B) infrastructure. The latter is also known as a "transmission cost surface." These layers were used as criteria for determining suitable sites for power plants and additional transmission requirements. Higher values indicate greater environmental impacts and risks.

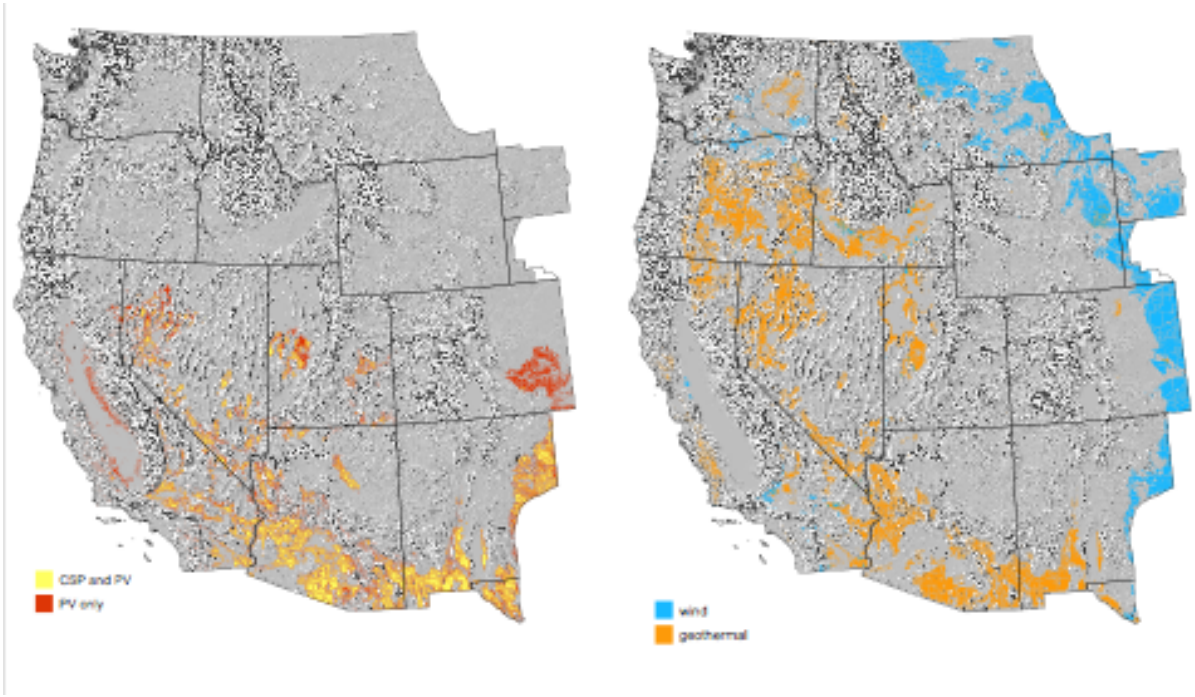

(a) (b)

Figure A.4: Site suitability maps for solar (A) and wind, geothermal (B) technologies in WECC under the Least Stringent environmental scenario.

A.1 Additional methods

Overview of environmental constraints used in previous studies

The high variability of assumptions amongst studies in environmental criteria and constraints for energy development is further confounded by the differences in designations and definitions of the same land criteria (see Table S4 for comparison of RETI and WREZ studies). This is in part due to the differing land use regulations across state and federal government agencies and the complexity of the way in which public land is owned, managed, and designated. Land parcels have primary designations that may not agree with secondary or local designations. State agencies oftentimes have state-specific land use regulations that are also specific to and differ between energy technologies. But in many of these studies—both academic and government mandated—-there appears to be a general mismatch between theory and practice in environmental criteria assumptions. With the exception two studies11,12 which focus on ecological siting criteria and specifically on "disturbed" land, many studies rely on legal "exclusion" areas—parcels of land for which there is a clear legal restriction against energy development—and generally include areas that are likely risky for project development, but can be achieved under mitigation arrangements. Moreover, notions of "legal protection" against development are inconsistent, particularly between what studies have considered legal exclusions and what government agency designations suggest are legal protections. The U.S. Protected Areas Database (PAD-US) compiled by the U.S. Geological Survey (USGS) assigns a "Gap Analysis Program" (GAP) Status code of 1-4, with Statuses 1 and 2 being areas with legal protection against permanent natural land cover disturbance and meet the definition of "protected" by the International Union for Conservation of Nature (IUCN) Thus, all Gap Status 1 or 2 land areas are also assigned an IUCN protection category. Below are the official USGS definitions for Statuses 1-4:

> Gap Status 1: An area having permanent protection from conversion of natural land cover and a mandated management plan in operation to maintain a natural state within which disturbance events (of natural type, frequency, intensity, and legacy) are allowed to proceed without interference or are mimicked through management.
>
> Gap Status 2: An area having permanent protection from conversion of natural land cover and a mandated management plan in operation to maintain a primarily natural state, but which may receive uses or management practices that degrade the quality of existing natural communities, including suppression of natural disturbance.
>
> Gap status 3: An area having permanent protection from conversion of natural land cover for the majority of the area, but subject to extractive uses of either a broad, low-intensity type (e.g. logging, OHV recreation) or localized intense type (e.g. mining). It also confers protection to federally listed endangered and threatened species throughout the area.

> Gap status 4: There are no know public or private institutional mandates or legally recognized easements or deed restrictions held by the managing entity to prevent conversion of natural habitat types to anthropogenic habitat types. The area generally allows conversion to unnatural land cover throughout or management intent is unknown.

There are land parcels that PAD-US has indicated as being Status 1 or 2, but are given either "avoidance" or no classification in the WREZ and RETI studies. Two notable examples of this are Areas of Critical Environmental Concern and non-California state forests, both considered "avoidance" categories by the WREZ study, but have GAP statuses of 1 or 2. Additionally, most private property owned by non-government organizations such as The Nature Conservancy, do not have federal legal protections, but are assigned GAP statuses of 1 or 2 because the property owners themselves manage those land parcels with the goal of permanent protection. The inconsistency of assumptions and the regional specificity of studies and available datasets is a challenge for producing future energy development scenarios of larger geographic scope.

Annual electricity generation calculations

Wind:

$$P_avg = 1.91(\frac{1}{2})pA_{blade}V_{s,i}^3)_{avg} \tag{A.1}$$

$$e_{w,s,i} = 8760P_{avg}EC_rP_r^{-1}a_{w,s,i} \tag{A.2}$$

Where P_avg = average power output of a turbine in Watts; p = air density (1.225 kg m^{-3} at 15 C and 1 atm), 1.91 is Rayleigh's correction factor for average wind speeds; A_{blade}= swept area of turbine blades in m^2; $v_{s,i}$ = wind velocity in m s-1; $e_{w,s,i}$= annual electricity generation of wind zone i of scenario s; E=average efficiency factor (30%); C_r = rated installed capacity per unit of land in MW km^{-2} , P_r = rated power per turbine in MW/turbine; and $a_{w,s,i}$ = area of zone i in scenario s in km^2 . All wind generation calculations assume a 1.5 MW turbine with 70 m blade diameter. Additionally, because turbines are now designed at a hub height of 80 m or higher, NREL wind speed data at 50 m hub height was extrapolated to 80 m using the 1/7 power rule of thumb, which states that the ratio of the unknown wind speed to known wind speed is equal to the ratio of the two sub heights, raised to the one-seventh power.

Solar PV

$$e_{pv,s,i} = 365I_{GHI,s,i}C_ra_{pv,s,i}(1-\eta) \tag{A.3}$$

Where $e_{pv,s,i}$ = annual electricity generation of each PV zone; $I_{GHI,s,i}$ = is the global horizontal insolation (instant solar radiation) in kWh m^{-1}d^{-1} of zone i in scenario s; C_r = rated installed capacity per unit of land in MW km^{-2} (see Table 1); and $a_{pv,s,i}$= area of

zone i in scenario s in km^2; η= the re-rating factor (difference between rated and actual performance). The de-rating factor used in this study is 20%. Though insolation is in units of kWh m^{-1}d^{-1}, it represents the number of "peak sun" hours per day, assuming a PV input rating and peak solar radiation of 1kW/m^2.

CSP:

$$e_{csp,s,i} = 365 I_{DNI,s,i} C_r a_{csp,s,i} (1 - \eta) \tag{A.4}$$

Where $e_{csp,s,i}$ = annual electricity generation of each CSP zone; $I_{DNI,s,i}$ = is the direct normal insolation in kWh m^{-1}d^{-1} or the number of peak sun hours per day of zone i in scenario s; C_r = rated installed capacity per unit of land in MW km^{-2} (see Table 1); and $a_{csp,s,i}$ = area of zone i in scenario s in km^2; η= the re-rating factor (10%). Note that this calculation assumes a solar multiple (ratio of solar field to nominal capacity) typical of CSP systems with no or little thermal storage, which is between 1-1.5. Even with greater prevalence of thermal storage, the total electricity generated should be the same per unit of land since the generator capacity will be smaller per unit of land due to the increasing solar multiple. Installed capacity per unit of land should diminish as the solar multiple increases, thus, while the capacity factor increases due to the solar multiple (thermal storage) for the plant, the installed capacity decreases, meaning the energy generated per unit of land should remain the same. The land use factor used in this study is derived from CSP systems in place today with a generation weighted average solar multiple closer to 1.5 (SI Table S1) (see Ong et al. 2013).13 While this calculation may underestimate the generation per project by assuming a lower capacity-based land use factor, this may compensate for the energy conversion losses involved in systems with more thermal storage and hence may still be an appropriate simplification for future CSP generation.

Geothermal:

$$e_{geo,s,i} = 8760 C_r a_{geo,s,i} CF \tag{A.5}$$

Where $e_{geo,s,i}$ = annual electricity generation of each geothermal zone; C_r = rated installed capacity per unit of land in MW km^{-2} (see Table 1); and $a_{geo,s,i}$= area of zone i of scenario s in km^2; CF= average capacity factor (Williams et al. 2012).

Additional methods for transmission estimates

In order to estimate associated transmission land use of each development project, we generated a transmission cost surface indicating each grid cell's difficulty or riskiness of obtaining right-of-way for transmission lines (SI Figure S2B). This was accomplished by assigning a "Null" classification to all physical exclusion areas and an environmental score of 3 or 4 to other technical, socio-economic, and natural hazard zones (SI Table S2). This output was then merged with a raster dataset of environmental transmission classification assignments compiled in WECC's ERTP report (SI Table S4), and all remaining non-classified, low-risk parcels of land were assigned a score of 1.

Appendix B

Appendix for Chapter 3

B.1 Methods: Estimation of capacity factors for PV, CSP, and geothermal development zones.

Solar PV:

$$CF = \frac{GHI}{I_{max}} do \tag{B.1}$$

Where GHI is the global horizontal insolation (average daily solar radiation) in kWh $m^{-2}d^{-1}$. I_max is the peak insolation or 2400 kWh $m^{-2}d^{-1}$, assuming a PV input rating and peak solar radiation of 1 kW m^{-2}. The efficiency loss factor is d and the outage rate is o; both are assumed to be 0.96 in this study.

CSP:

Assuming a no-storage system with a solar multiple of 1.3, we ran the National Renewable Energy Laboratory's System Advisor Model (SAM) generic CSP model for 22 locations in central and southern California and plotted the DNI of each location against the estimated CSP capacity factor (CF; Figure B.1). The logarithmic function that was fitted to the data (eq B.2) was used to predict the CF of each CSP development zone resulting from the site suitability models.

$$CF = 24.518 log(DNI) - 18.326 \tag{B.2}$$

We assumed no storage in this analysis due to the limitations of empirical studies quantifying the land use factor (MW km^{-2}) of existing CSP plants in the U.S. (Ong, Campbell, Denholm, et al., 2013). Only one or two CSP plants with storage were quantified, compared to more than a dozen CSP plants without storage. However, given that installed capacity and capacity factor are roughly inversely proportional, the total electricity generated of storage and no-storage system should be very similar per unit of land. This is because generator capacity of storage systems will be smaller per unit of land due to the increasing

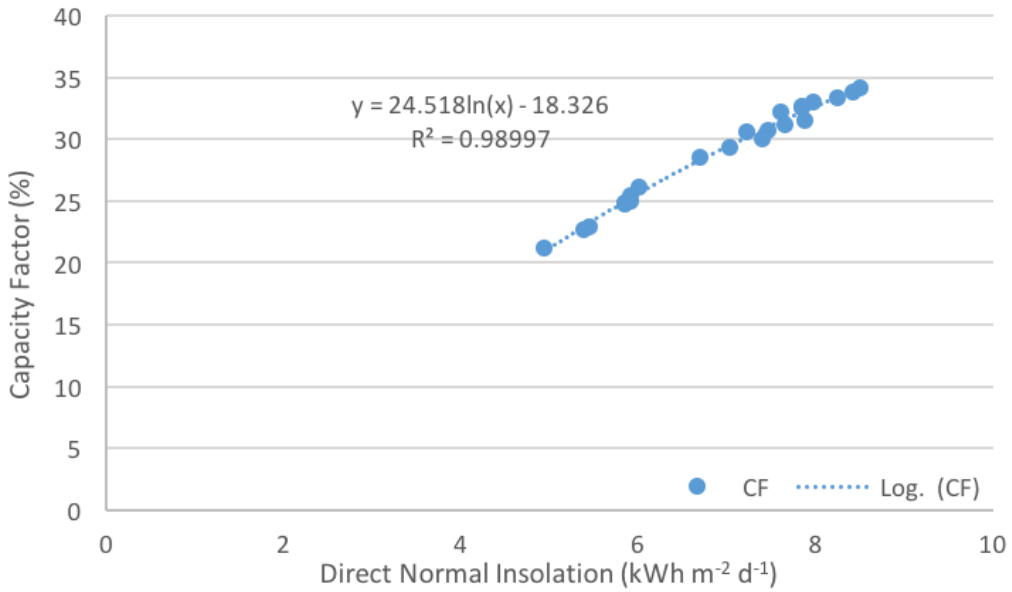

Figure B.1: Capacity factor of generic CSP power plant vs. DNI.

solar multiple necessary for storage systems, but the capacity factor increases since storage enables the generator to be used for many additional hours of the day.

Geothermal:

$$CF = 0.87\frac{RQ}{10} \tag{B.3}$$

RQ is the resource quality of geothermal and is a unit-less measure of geothermal feasibility that ranges from 1 to 10, where 10 represents the most feasible geothermal sites. 0.87 is the average capacity factor assumed for geothermal in Williams et al. (2012; Williams, DeBenedictis, et al., 2012)

Electricity generation estimation:

$$e_{t,z} = C_t a_z CF_{z,t} h \tag{B.4}$$

The annual average electricity generation $e_{z,t}$ for zone z and technology t. C_t is the rated installed capacity per unit of land or the land use factor in units of MW km^{-2} for technology t. The land area of zone z in km^2 is a_z, the capacity factor of zone z and technology t is represented by $CF_{z,t}$, and h is the number of hours in a year, or 8760.

Table B.1: Data sources

Dataset	Source	Data type/ resolution
PHYSICAL, TECHNICAL, SOCIO-ECONOMIC		
Insolation (GHI and DNI)	National Renewable Energy Lab: Solar Maps http://www.nrel.gov/gis/data_solar.html	Feature/10km
Wind capacity factors	National Renewable Energy Lab: The Wind Integration National Dataset (WIND) Toolkit	Point feature (2 km resolution)
Geothermal favorability	USGS Geothermal Favorability Map Derived From Logistic Regression Models and Identified Moderate and High Temperature Geothermal Systems of the Western US http://certmapper.cr.usgs.gov/geoportal/rest/find/document?searchText=Geothermal&max=500&f=html&style=http://certmapper.cr.usgs.gov/geoportal/catalog/skins/themes/erp/previewlittle.css	Feature
Elevation (DEM) and slope	U.S. Geological Survey: EarthExplorer: http://earthexplorer.usgs.gov/ SRTM dataset	Raster/d90m
Minimum contiguous area	Lopez et al. (2012)[13], RETI[3], WGA[5]	Numerical values
Water bodies and rivers	Solar Energy Development Programmatic EIS (Solar PEIS): http://solareis.anl.gov/maps/gis/index.cfm	Polygon
Census urban zones	U.S. Tiger dataset: http://www.census.gov/cgibin/geo/shapefiles2011/main	Polygon
Population density (people/km^2)	Landscan 2012: http://web.ornl.gov/sci/landscan/	Raster/1km
Surface mines (hazardous facility)	U.S. Geological Survey: Active mines and mineral plants in the U.S. http://mrdata.usgs.gov/mineplant/	Point
Airports (hazardous facility)	National Transportation Atlas Database: http://www.rita.dot.gov/bts/sites/rita.dot.gov.bts/files/publications/national_transportation_atlas_database/2013/points.html	Point
Roads	Solar PEIS and National Transportation Database: National Highway Planning Network. U.S. Tiger dataset for roads by county: http://www.census.gov/geo/maps-data/data/tiger-line.html	Polyline
Railway network	National Transportation Atlas Database: http://www.rita.dot.gov/bts/sites/rita.dot.gov.bts/files/publications/national_transportation_atlas_database/2013/polyline.html	Polyline
Military Installations (hazardous facility)	US-PAD (see below for environmental datasets)	Polygon
ENVIRONMENTAL – See Table A – 2 for data sources		
OTHER		
Land cover types	U.S. Geological Survey National Gap Analysis Program Land Cover Data http://gapanalysis.usgs.gov/gaplandcover/data/download/	Raster/30m
Super CREZ boundaries	California Public Utilities Commission RPS Proceeding Materials Version 6.0: http://www.cpuc.ca.gov/PUC/energy/Renewables/RPS+Proceeding+Materials+Version+6.htm	Feature
Housing density	USDA Forest Service and University of Wisconsin-Madison U.S. 2010 Block Level Housing Density- Public Land Adjusted http://silvis.forest.wisc.edu/maps/blk_pla/2010/download	Raster / 30 m
ENERGY INFRASTRUCTURE		
PV plants	California Energy Commission (CEC); EIA form 860: http://www.eia.gov/electricity/data/eia860/	Geographic coordinates
CSP plants	CEC; EIA	Geographic coordinates

Wind farms	CEC; EIA	Geographic coordinates
Geothermal	CEC; EIA; Geothermal Power Plants-USA: http://geo-energy.org/plants.aspx	Geographic coordinates
Transmission lines, substations, and corridors	- California Energy Commission Siting, Transmission, and Environmental Protection Division. - planned corridors: West Wide Energy Corridor Environmental Impact Statement, section 368 corridors: http://corridoreis.anl.gov/eis/fmap/gis/index.cfm	Polyline and points

Table B.2: Classification of environmental and ecological data into environmental exclusion categories.

See legend below table for explanation of color scheme.

Category 1	Data source
National park system (parks, preserves, historic parks, historical sites, lakeshores) [all studies]	**Organization**: U.S. Geological Survey **Name**: Protected Areas of the U.S. Database, Version v3.1: **Website:** http://gapanalysis.usgs.gov/padus/data/download/ Henceforth referred to as PAD-US **Notes**: PAD-US (search for "National Park System")
National Recreation Areas [all studies]	PAD-US ("National Recreation Areas")
National Wildlife Refuges (US FWS) & state (under "Habitat and Species Mgmt Areas" in PAD-US) [all studies]	PAD-US ("National and State Wildlife Refuge")
USFS Inventoried Roadless areas (add separately to PAD-US) [all studies]	**Organization**: Solar Programmatic Environmental Impact Statement **Name**: Core final solar PEIS data files **Website:** http://solareis.anl.gov/maps/gis/index.cfm Henceforth referred to as SPEIS
Designated Federal Wilderness Areas and Wilderness Study Areas [all studies]	From multiple sources: PAD-US ("Fed Wilderness Areas and Wilderness Study Areas"), SPEIS, WSEP **Organization**: Bureau of Land Management (BLM) **Name**: BLM Western Solar Energy Plan (WSEP) **Website**: http://blmsolar.anl.gov/maps/shapefiles/ Henceforth referred to as WSEP
BLM National Conservation Areas (under "National Landscape conservation system" in PAD-US) (just King Range, Black Rock, High Rock, Headwaters Forest Reserve) [RETI]	PAD-US ("Select BLM National Conservation Areas"), WSEP, SPEIS
(NPS) National Monument	PAD-US ("(NPS) National Monument"), WSEP, SPEIS
(BLM) National Monument	PAD-US ("(BLM) National Monument"), WSEP, SPEIS
National historic and scenic trails	PAD-US –none within CA, WSEP, SPEIS
National wild, scenic and recreational rivers	PAD-US ("National Wild, Scenic, and Recreational River"), WSEP, SPEIS
BLM ROW exclusion [WREZ & WECC] - all technologies	SPEIS
BLM Special recreation management areas [WREZ & WECC] - solar	WSEP
BLM no surface occupancy restriction areas [WREZ & WECC] - solar	WSEP
BLM designated and proposed Research Natural Areas + Sikes Act Tracts [WREZ & WECC] - solar	PAD-US ("BLM Research Natural Area")
Area of Critical Environmental Concern on BLM land ONLY [all studies] - for solar	WSEP
BLM Wildlife Management Areas [WREZ & WECC] - solar	PAD-US ("BLM Wildlife Management Areas")
State Parks (CA, MT, OR, WA, WY)	PAD-US ("State Parks")

State Wilderness Areas [all studies]	PAD-US ("State Wilderness Areas and Wilderness Study Areas")
State forest [WREZ]	PAD-US ("State Forest")
DFG (now called Department of Fish and Wildlife) wildlife areas and ecological reserves [RETI] and State wildlife areas	PAD-US ("DFW wildlife areas and ecological reserves")
Existing conservation and mitigation banks under conservation easements (CA) [all studies]	**Organization**: GreenInfo Network **Name**: California Conservation Easement Database (CCED) **Website**: http://www.calands.org/cced
Existing Conservation and Mitigation Bank	PAD-US ("Conservation and Mitigation Bank"); CADFW
Lands purchased with private funds and donated to federal government [RETI] (The Wildlands Conservancy)	TNC
(State and national) wetlands [all studies]	**Organization**: US Fish and Wildlife Service **Name**: National Wetlands Inventory. **Website**: http://www.fws.gov/wetlands/Data/State-Downloads.html
Watershed Protection Areas [WREZ]	PAD-US ("Watershed Protection Areas")
Marine Protected Areas [WECC]	PAD-US ("Marine Protected Areas")
Historic/Cultural areas with Gap statuses 3,4	PAD-US ("Historic or cultural areas")
Private Conservation Land (non-conservation easements in CA) (P_Des_type in PAD-US) and other Private non-profit land [WECC]	PAD-US ("Private Conservation Land")
Category 2	**Data source**
BLM National Conservation Areas (All others)	PAD-US ("BLM National Conservation Area"), WSEP, SPEIS
BLM Visual Resource Management class I and II [WREZ]	SPEIS
BLM ROW avoidance [WREZ & WECC] - all technologies	SPEIS
BLM Special recreation management areas [WREZ & WECC] - wind and geothermal	WSEP, SPEIS
BLM no surface occupancy restriction areas [WREZ & WECC] - wind and geothermal	WSEP and SPEIS
BLM designated and proposed Research Natural Areas + Sikes Act Tracts [WREZ & WECC] - wind and geothermal	PAD-US
BLM Wildlife Management Areas [WREZ & WECC] - wind and geothermal	PAD-US
Desert Wildlife Management Areas (DWMA) [RETI] - all technologies	WSEP and SPEIS
USFS Research Natural Areas [WREZ & WECC]	PAD-US ("Research Natural Areas")
USFS Special interest areas [WREZ & WECC]	PAD-US - none exist
Area of Critical Environmental Concern on BLM land [all studies] - for wind and geothermal	WSEP and SPEIS
Area of Critical Environmental Concern on non-BLM land [all studies] - all technologies	SPEIS
State reserves (State Natural Reserves, e.g., Torrey Pines Reserve, Antelope valley poppy reserve)	PADUS ("Reserves")
Other wildlife areas and ecological reserves(BLM, county, Bureau of reclamation)	PADUS (Other wildlife areas and ecological reserves)
LA county Significant Ecological Areas - existing	**Organization**: LA County Department of Regional Planning **Name**: Significant Ecological Areas

	Website: http://planning.lacounty.gov/sea/proposed Henceforth referred to as LACSEA
Moved to Cat 2: lands precluded from development in Habitat Conservation Plans [RETI]	**Organization**: RETI GIS data **Name**: GIS data for Phase 2B **Website**: http://www.energy.ca.gov/reti/documents/index.html Henceforth referred to as RETI GIS data
Moved to Cat 2: Lands precluded from development under Natural Community Conservation Plans [RETI]	RETI GIS data
Habitat areas for listed wildlife species mapped by State, Provincial or Federal Agencies [WECC]	**Organization**: Fish and Wildlife Service (FWS) **Name**: critical habitat portal **Website**: www.criticalhabitat.fws.gov
USFWS Designated critical habitat for federally listed endangered and threatened species [RETI] (includes Desert Tortoise, Peninsular BHS, FTL)	FWS critical habitat portal Fringed Toe Lizard: BLM West Mojave Plan from California PBHS: Essential Habitat from USFWS Department of Fish and Wildlife Service (DFWS)
USFWS Upland Species Recovery Units	**Organization**: U.S. Fish and Wildlife Service **Name**: San Jose kit fox core areas **Website**: http://www.fws.gov/ecos/ajax/docs/five_year_review/doc3222.pdf
USFWS Sage Grouse Core or Priority Areas	**Organization**: CA BLM and CA Fish and Game **Name**: "GRSG Preliminary PRIORITY Habitat (PPH) GIS Data as of 3/21/2012*" **Website**: http://www.blm.gov/wo/st/en/prog/more/sagegrouse/documents_and_resources.html) Multi-source dataset: WSEP and BLM/CAFG PPH
Mojave Ground Squirrel (MGS) Conservation Areas (core areas)	BLM West Mojave Plan 2005
Category 3 (terrestrial only)	**Data source**
Land in wilderness bills [RETI] - includes Sand to Snow, (Mojave Trails national Monument) National Trails Monument	TNC and WSEP
LA county Significant Ecological Areas- proposed	LACSEA
Habitat areas for candidate wildlife species mapped by State, Provincial or Federal Agencies [WECC]	TNC (FTHL, MGS)
Prime Farmland	**Organization:** California Department of Conservation **Name:** Williamson act –Farmland Mapping and Monitoring Program (FMMP) in CA **Website**: http://www.conservation.ca.gov/dlrp/fmmp/products/Pages/DownloadGISdata.aspx **Notes**: created a merged dataset using 2010, 2012
The Nature Conservancy Portfolio Areas	**Paper**: TNC Portfolio Areas – The Nature Conservancy, California Chapter Ecoregional Plans 1993 – 2004 Notes: Sonoran and Mojave Desert regions removed as they are superseded by other datasets
The Nature Conservancy Ecologically Core for CA deserts	**Organization**: The Nature Conservancy **Name**: Randall JM, Parker SS, Moore J, Cohen B, Crane L, et al. (2010) Mojave Desert Ecoregional Assessment. San Francisco, CA: The Nature Conservancy. 106 p. The Nature Conservancy. (2009) A framework for effective conservation management of the Sonoran Desert in California. Unpublished report. **Website:** http://www.drecp.org/meetings/2010-10-13_meeting/presentations/TNC_Mojave_Assessment.pdf Henceforth referred to as "TNC-Randall et al. 2010"

California Rangeland Conservation Coalition priority conservation areas- priority 1	**Organization**: California Rangeland Conservation Coalition **Name**: CRCC Focus Areas **Website**: http://www.rangelandtrust.org/index.php
Desert tortoise least cost path/ linkages - FWS Priority 1 == base (all costs considered)	**Paper**: Averill-Murray, R.C. 2013. Conserving Population Linkages for the Mojave Desert Tortoise (Gopherus agassizii). Herpetological Conservation and Biology 8(1): 1-15. **Website**: http://databasin.org/datasets/9a5f60c89e284606b3017954c1efebb1
Citizen's inventory wilderness data	**Organization**: California Wilderness Coalition **Name**: Citizen's inventory wilderness data **Website**: http://www.calwild.org/
Phil Leitner's MGS core areas	Leitner, P. 2008. "Current Status of the Mohave Ground Squirrel." *Transactions of the Western Section of the Wildlife Society* 44:11-29.
Category 3 (freshwater only)	**Data source**
Conservation value areas for freshwater species	TNC
Category 4 (terrestrial only)	**Data source**
The Nature Conservancy Ecologically Intact for CA deserts	TNC-Randall et al. 2010
California Rangeland Conservation Coalition priority conservation areas- priority 2	CRCC
Desert tortoise High quality contiguous habitat - FWS Priority 2 == binned1	See Averill-Murray et al. 2013 paper (above)
California Essential Habitat Connectivity Areas [TNC] and State wildlife corridors [WECC]	**Organization**: California Department of Transportation, California Department of Fish and Game, and Federal Highways Administration **Name**: Essential Connectivity areas of California **Website**: https://www.wildlife.ca.gov/Conservation/Planning/Connectivity/CEHC **Report**: Spencer,W.D.,P. Beier,K. Penrod,K. Winters,C. Paulman,H. Rustigian-Romsos,J. Strittholt,M. Parisi,and A. Pettler. 2010. California Essential Habitat Connectivity Project: A Strategy for Conserving a Connected California.
Mojave Ground Squirrel (candidate species) Maxent site suitability model at 0.438 cutoff	**Paper**: Inman RD, Esque TC, Nussear KE, Leitner P, Matocq MD, Weisberg PJ, Diltd TE, Vandergast AG. (2013) Is there room for all of us? Renewable energy and Xerospermophilus mohavensis. Endang Species Res 20:1-18 **Website**:http://databasin.org/datasets/063de529c9dd4635bb9f019cd0c0ca2a
Audubon Society compiled Important bird areas (state, continental, and global) [WECC]	**Organization**: Audubon California **Name**: California Important Bird Areas **Website**: http://ca.audubon.org/california-important-bird-areas-gis-data-and-methods
Category 4 (freshwater only)	**Data sources**
Groundwater dependent ecosystems	**Paper**: Howard J, Merrifield M (2010) Mapping Groundwater Dependent Ecosystems in California. PLoS ONE 5(6): e11249. doi:10.1371/journal.pone.0011249

LEGEND
Federal land
State land
Other or mixed
Criteria differs between solar and non-solar technologies

Table A – 3. GIS exclusion criteria and buffer distances to assess suitable sites.

Table B.3: GIS exclusion criteria and buffer distances to assess suitable sites.

Criteria	Solar PV	Solar CSP	Wind	Geothermal
PHYSICAL, TECHNICAL, SOCIO-ECONOMIC				
Raw renewable resource	Global Horizontal Insolation (GHI) < 5.0† kWh m^{-2} d^{-1}	Direct Normal Insolation (DNI) < 6.75 kWh m^{-2} d^{-1}	NREL Wind toolkit resource areas	USGS geothermal class < 9 (Max: 10)
Slope	> 5%	> 5%	> 25%	> 15%
Elevation (DEM)	> 1500 m	> 1500 m	> 2000 m	> 1500 m
Contiguous area	< 1 km^2	< 5 km^2	< 2 km^2	< 1 km^2
Water bodies and rivers	EX§	EX	EX	EX
Census urban zones	EX: 0.5 km	EX: 0.5 km	EX: 1 km	EX: 1 km
Population density (people km^{-2})	> 100	> 100	>100	>100
Surface mines (hazardous facility)	EX: 1 km	EX: 1 km	EX: 1 km	EX: 1 km
Airports (hazardous facility)	EX: 1 km	EX: 1 km	EX: 1 km	EX: 1 km
Roads	EX	EX	EX	EX
Rails	EX	EX	EX	EX
Military Installations (hazardous facility)	EX: 0.5 km	EX: 0.5 km	EX: 0.5 km	EX: 0.5 km
ENVIRONMENTAL				
All Layers	EX: 0.5 km	EX: 0.5 km	EX: 0.5 km	EX: 0.5 km

† Greater than or less than values indicate thresholds for exclusion.
¥ "IN" indicates inclusion of criteria and width of buffer if applicable.
§ "EX" indicates exclusion and width of buffer if applicable.

Table B.4: Wind potential (MW) within each Super CREZ under each Environmental Exclusion Level

Super CREZ	Cat. 1	Cat. 2	Cat. 3	Cat. 4	Cat. 3 (FW[1])	Cat. 4 (FW)	RPS Calc (base)
Barstow	3445	481	399	0	399	0	208
CarrizoNorth	0	0	0	0	0	0	67
CarrizoSouth	36	0	0	0	0	0	507
CentralValleyNorth	90	90	32	0	32	0	0
Cuyama	31	31	0	0	0	0	0
Distributed	0	0	0	0	0	0	253
El DoradoCounty	0	0	0	0	0	0	0
Fairmont	0	0	0	0	0	0	
Imperial East	321	315	230	0	0	0	
Imperial South	30	0	0	0	0	0	
ImperialNorth	0	0	0	0	0	0	
Imperial_N+S+E	351	315	230	0	230	0	361
Inyokern	0	0	0	0	0	0	0
IronMountain	686	120	0	0	0	0	0
Kramer	313	141	39	0	39	0	0
LassenNorth	2532	1387	968	435	648	146	2032
LassenSouth	0	0	0	0	0	0	0
Merced	0	0	0	0	0	0	0
MountainPass	590	393	0	0	0	0	0
NonCREZ	0	0	0	0	0	0	0
OwensValley	0	0	0	0	0	0	0
PalmSprings	746	442	371	263	265	181	212
Pisgah	346	48	0	0	0	0	0
RiversideEast	1712	1034	443	180	443	180	309
RoundMountain_A	342	290	231	117	0	0	
RoundMountain_B	512	512	419	419	0	0	
RoundMountain_A+B	854	801	650	536	221	107	220
SacramentoRiverValley	1997	1968	528	240	528	231	3248
SanBernardino_Baker	670	655	56	0	56	0	0
SanBernardino_Lucerne	1949	1729	992	155	992	155	82
SanDiegoNorthCentral	279	270	176	0	168	0	168
SanDiegoSouth	414	394	394	242	394	234	399
SantaBarbara	176	0	0	0	0	0	702
Solano	2601	1493	671	221	443	104	1354
Tehachapi	6785	5865	3437	104	3201	68	1131
TwentyninePalms	942	851	150	0	150	0	124
Victorville	1027	86	0	0	0	0	1093
Westlands	153	147	0	0	0	0	0
SUM	28,725	18,740	9,531	2,374	8,206	1,404	12,471

[1] FW indicates freshwater exclusions combined with terrestrial exclusions

Table B.5: Solar PV potential (MW) within each Super CREZ under each Environmental Exclusion Level

Super CREZ	Cat. 1	Cat. 2	Cat. 3	Cat. 4	Cat. 3 (FW[1])	Cat. 4 (FW)	RPS Calc (base)
Barstow	10487	7483	4973	615	4973	533	1740
CarrizoNorth	7420	5822	3773	3195	3773	3195	1519
CarrizoSouth	8800	2003	180	0	75	0	1321
CentralValleyNorth	45391	37449	6677	4392	6677	4362	1638
Cuyama	3783	2480	443	443	443	375	793
Distributed	0	0	0	0	0	0	15319
El DoradoCounty	248	248	0	0	0	0	0
Fairmont	0	0	0	0	0	0	
Imperial East	22140	18525	11325	510	0	0	
Imperial South	29700	29340	7928	0	0	0	
ImperialNorth	33517	32262	18559	2760	0	0	
Imperial_N+S+E	85357	80126	37811	3270	34687	3053	7509
Inyokern	0	0	0	0	0	0	981
IronMountain	44366	38821	7298	2260	7298	1900	3817
Kramer	21863	16864	10064	0	10064	0	2598
LassenNorth	5011	5011	4943	128	4291	128	5728
LassenSouth	0	0	0	0	0	0	0
Merced	0	0	0	0	0	0	0
MountainPass	5694	5694	1151	0	1151	0	560
NonCREZ	0	0	0	0	0	0	0
OwensValley	13068	9887	878	398	780	143	2003
PalmSprings	11989	10761	3546	2355	3546	2355	1276
Pisgah	17107	13867	829	362	829	354	470
RiversideEast	61618	57106	19047	3460	18799	3460	4691
RoundMountain_A	0	0	0	0	0	0	
RoundMountain_B	0	0	0	0	0	0	
RoundMountain_A+B	0	0	0	0	0	0	12246
SacramentoRiverValley	100624	95412	18340	12227	16356	10276	12468
SanBernardino_Baker	6566	6454	855	0	855	0	688
SanBernardino_Lucerne	23164	22976	14865	3510	14378	3158	2240
SanDiegoNorthCentral	7375	6095	4165	1808	3573	1583	991
SanDiegoSouth	459	395	395	195	395	195	268
SantaBarbara	7565	4995	345	345	158	158	1021
Solano	115899	69054	16356	9264	15666	8334	6162
Tehachapi	69833	59283	37363	360	36178	360	4888
TwentyninePalms	15864	15827	6195	83	6195	0	997
Victorville	21022	17749	10006	0	9983	0	2405
Westlands	475387	436721	146975	111733	146203	110690	13681
SUM	1,185,959	1,028,582	357,474	160,401	347,325	154,609	110,024

[1] FW indicates freshwater exclusions combined with terrestrial exclusions

Table B.6: Solar CSP potential (MW) within each Super CREZ under each Environmental Exclusion Level

Super CREZ	Cat. 1	Cat. 2	Cat. 3	Cat. 4	Cat. 3 (FW[1])	Cat. 4 (FW)	RPS Calc (base)
Barstow	9006	6884	4815	420	4815	405	2800
CarrizoNorth	3330	2408	1763	1763	1763	1763	3200
CarrizoSouth	4969	1395	0	0	0	0	6000
CentralValleyNorth	0	0	0	0	0	0	0
Cuyama	1929	1124	0	0	0	0	800
Distributed	0	0	0	0	0	0	0
El DoradoCounty	0	0	0	0	0	0	0
Fairmont	0	0	0	0	0	0	
Imperial East	21495	17813	10995	510	0	0	
Imperial South	27840	27310	6281	0	0	0	
ImperialNorth	31799	30711	17181	2520	0	0	
Imperial_N+S+E	81134	75834	34456	3030	31981	2955	13740
Inyokern	0	0	0	0	0	0	4290
IronMountain	43811	38469	7088	2065	7088	1705	9600
Kramer	21653	16864	9951	0	9951	0	12370
LassenNorth	0	0	0	0	0	0	0
LassenSouth	0	0	0	0	0	0	0
Merced	0	0	0	0	0	0	0
MountainPass	5244	5244	1083	0	1083	0	1560
NonCREZ	0	0	0	0	0	0	0
OwensValley	12359	8616	563	150	563	0	10000
PalmSprings	11090	10378	2894	1687	2894	1687	0
Pisgah	16004	12802	829	362	829	212	4200
RiversideEast	61109	57016	19047	3228	18799	3228	21100
RoundMountain_A	0	0	0	0	0	0	
RoundMountain_B	0	0	0	0	0	0	
RoundMountain_A+B	0	0	0	0	0	0	0
SacramentoRiverValley	0	0	0	0	0	0	0
SanBernardino_Baker	5501	5471	780	0	780	0	6350
SanBernardino_Lucerne	21904	21799	14265	2963	13913	2745	3080
SanDiegoNorthCentral	6595	5870	3828	1733	3498	1583	0
SanDiegoSouth	0	0	0	0	0	0	0
SantaBarbara	1366	1366	0	0	0	0	0
Solano	0	0	0	0	0	0	0
Tehachapi	69295	58753	36546	0	35481	0	17990
TwentyninePalms	15864	15827	6195	0	6195	0	3610
Victorville	20212	17509	9664	0	9641	0	2400
Westlands	818	818	465	0	293	0	10000
SUM	413,193	364,446	154,231	17,400	149,566	16,282	133,090

[1] FW indicates freshwater exclusions combined with terrestrial exclusions

Table B.7: Geothermal potential (MW) within each Super CREZ under each Environmental Exclusion Level

Super CREZ	Cat. 1	Cat. 2	Cat. 3	Cat. 4	Cat. 3 (FW[1])	Cat. 4 (FW)	RPS Calc (base)
Barstow	0	0	0	0	0	0	0
CarrizoNorth	0	0	0	0	0	0	0
CarrizoSouth	0	0	0	0	0	0	0
CentralValleyNorth	0	0	0	0	0	0	0
Cuyama	0	0	0	0	0	0	0
Distributed	0	0	0	0	0	0	0
El DoradoCounty	0	0	0	0	0	0	0
Fairmont	0	0	0	0	0	0	0
Imperial East	0	0	0	0	0	0	0
Imperial South	9283	9072	2724	0	0	0	0
ImperialNorth	10265	10055	4449	516	0	0	0
Imperial_N+S+E	19547	19128	7173	516	5072	363	1384
Inyokern	0	0	0	0	0	0	0
IronMountain	0	0	0	0	0	0	0
Kramer	0	0	0	0	0	0	24
LassenNorth	0	0	0	0	0	0	8
LassenSouth	0	0	0	0	0	0	0
Merced	0	0	0	0	0	0	0
MountainPass	0	0	0	0	0	0	0
NonCREZ	0	0	0	0	0	0	0
OwensValley	0	0	0	0	0	0	0
PalmSprings	1177	171	139	77	139	77	0
Pisgah	0	0	0	0	0	0	0
RiversideEast	0	0	0	0	0	0	0
RoundMountain_A	4364	3541	3277	1747	0	0	
RoundMountain_B	1785	1728	1288	1014	0	0	
RoundMountain_A+B	6149	5269	4565	2760	2187	1696	416
SacramentoRiverValley	4654	4494	2097	1995	325	325	0
SanBernardino_Baker	0	0	0	0	0	0	0
SanBernardino_Lucerne	0	0	0	0	0	0	0
SanDiegoNorthCentral	1943	1604	770	440	770	440	0
SanDiegoSouth	0	0	0	0	0	0	0
SantaBarbara	0	0	0	0	0	0	0
Solano	0	0	0	0	0	0	0
Tehachapi	0	0	0	0	0	0	0
TwentyninePalms	0	0	0	0	0	0	0
Victorville	0	0	0	0	0	0	0
Westlands	0	0	0	0	0	0	0
SUM	33,470	30,666	14,744	5,789	8,493	2,901	1,832

[1] FW indicates freshwater exclusions combined with terrestrial exclusions

Figure B.2: Location of Super Competitive Renewable Energy Zones (CREZ), counties, and partial counties in California

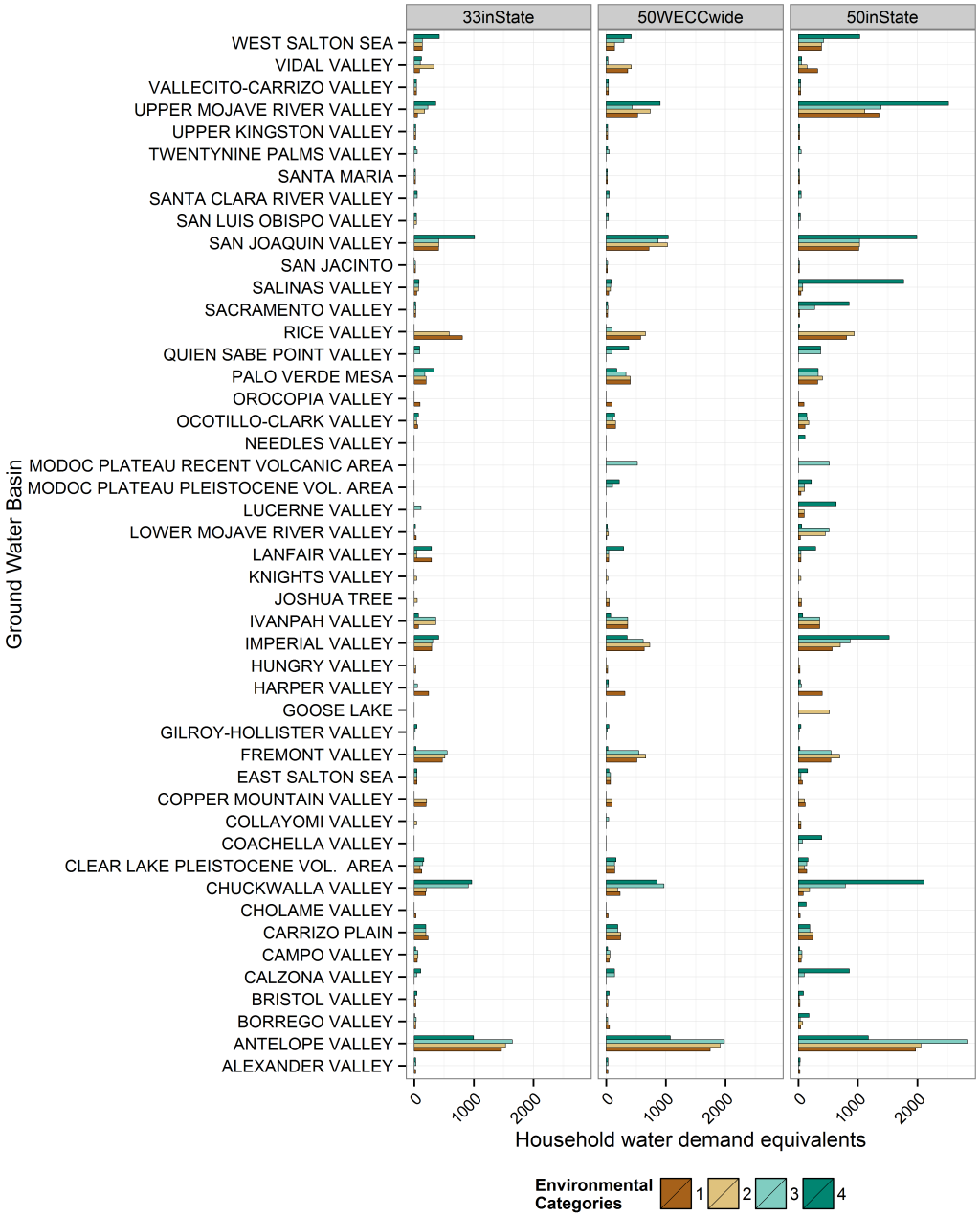

Figure B.3: Total water demand of each 2030 build-out scenario spatially disaggregated by ground water basin

Household water equivalents is the annual water consumption of an average household in the U.S., or 146,000 gallons.

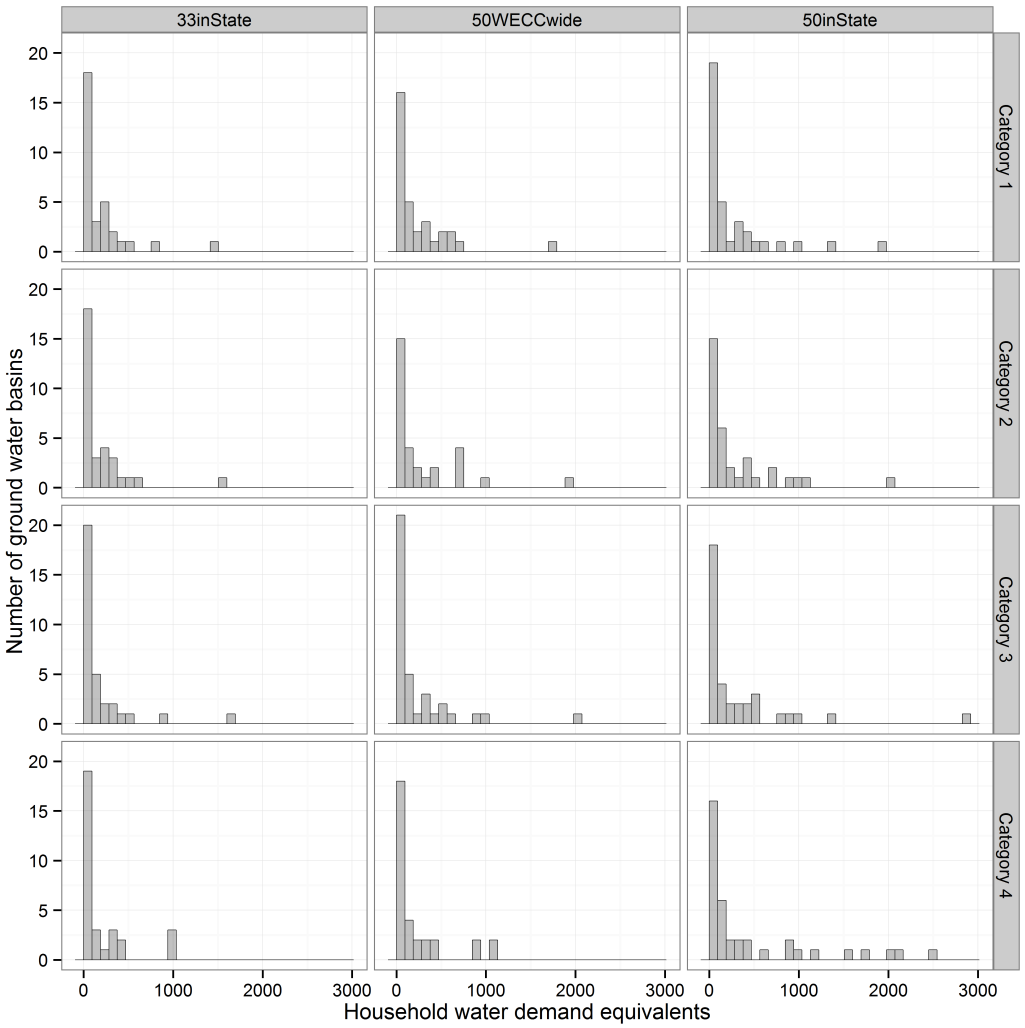

Figure B.4: Histogram of water demand (in household water demand equivalents) for each 2030 RPS target under each environmental Exclusion Level

Household water equivalents is the annual water consumption of an average household in the U.S., or 146,000 gallons.

Appendix C

Appendix for Chapter 4

C.1 Materials and Methods

Data inputs

A comprehensive zoning process requires various types of physical, environmental, economic, and energy data in both specific spatial and non-spatial formats. We relied on a combination of global or continental default spatial data (Table C.2) and country-provided datasets. The former serve the purpose of filling in missing country data and provide spatial uniformity for critical physical characteristics (e.g., elevation, wind speed). Country-specific datasets ensure consistency with similar past and ongoing national efforts, and in some cases, greater accuracy. We collected these data for 21 participating countries in the Eastern and Southern Africa Power Pools through a combination of stakeholders and country contacts at government agencies, utilities, and industries. The full zoning analysis could not be completed for Libya and Djibouti (both part of the Eastern Africa Power Pool) because these countries lacked requisite country-specific datasets (e.g., transmission infrastructure). As a result, we examined the Southern Africa Power Pool in more detail for the site selection process, using countries for which we could collect both transmission and demand data.

Data access Nearly all globally datasets in Table C.2 are freely available and downloadable using the website links provided. LandScan (gridded global population density) and Vaisala's hourly wind data are the two exceptions, but data may be purchased by contacting the vendor directly via the website links provided. A free and open source alternative to LandScan is Worldpop (http://www.worldpop.org.uk/). Hourly demand data and transmission or substation data were acquired for each country individually. Data availability and sources are tabulated for each country in Appendix A of the MapRE report (Wu, Deshmukh, et al., 2015) and Table C.5.

Project opportunity area and zone criteria estimates

Human Footprint Score

The Human Footprint Score is a metric for degree of human influence in a defined land area, and it is used in this study as a proxy for degree of human "disturbance" from natural, unaltered states (Sanderson et al., 2002). We estimated this metric following Sanderson et al. (2002) methods, using the following datasets that indicate the degree of human influence and access: population density, land use/land cover, road and railway access, and surface water (rivers and oceans). Datasets were coded into standardized scores ranging from 0 (least influenced) to 10 (most influenced) (Table C.4). We did not include the power infrastructure criteria in Sanderson et al. (2002), which relies on nighttime light visibility spatial data. Assumptions about electric power infrastructure's use as a proxy for population distribution and correlation with human settlements is based on developed countries' widespread electricity availability, which is not the case for many parts of our study region.

We summed the scores for each dataset to create a Human Influence Index. These scores were normalized within global terrestrial biomes (Olson et al., 2001), since absolute scores in one ecoregion may have a different effect compared to scores in another ecoregion. Within each ecoregion, the lowest Human Influence Index was assigned a Human Footprint Score of 0 and the largest index value a human footprint score of 100. The resulting Human Footprint Score represents the relative human influence within an ecoregion as a percentage of the maximum value. For example, a score of 1 within the Central Zambezian Miombo woodlands suggests that the area is the top 1% least disturbed or most wild area within the ecoregion. Since we calculated the human footprint score for each 500 m grid cell, we averaged the scores across every grid cell in each project opportunity area.

Capacity factor estimation

Solar PV To estimate solar PV capacity factors (r_{solar}), we extracted and spatially averaged the resource quality (q) (solar irradiance W/m^2) of each project opportunity area for solar PV (Eq. C.1). Since land use factors that we applied are specified for MW$_{\text{ac}}$, we further applied outage rates (η_o), and inverter and AC wiring efficiencies (η_ι) to estimate the capacity factor for solar PV (Table C.6). We assume an incident power density of 1000 W/m^2 to produce an output at the rated capacity of the plant.

$$r_{solar} = \frac{(1-\eta_o)\,(1-\eta_\iota)\,q}{1000} \tag{C.1}$$

Solar CSP Apart from the type of collector technology (parabolic trough, compact linear Fresnel reflector or heliostat solar tower), the capacity-based land use factor (e.g., MW/km^2) of solar CSP depends on two interdependent variables: the solar multiple and thermal storage. The design capacity of the solar CSP plant is based on the design output of the power turbine block. The solar multiple is the ratio of the actual size of the power plant's solar

field to the size of the solar field that would be required to drive the turbine at its nominal design capacity assuming standard solar irradiance of 1 kW/m^2 at standard temperature and pressure.

Thermal storage can significantly improve the capacity factor of the plant and its ability to generate when the value of electricity is greatest, which is the greatest advantage of thermal storage. Thermal storage can enable a CSP plant to store heat during high solar insolation hours and generate electricity during the evening, night or other hours when the sun is not shining. Power plants with thermal storage can have solar multiples of up to 3-5 (IRENA, 2013a). While such plants have a higher cost per MW due to the additional thermal storage equipment and a larger solar field (i.e., higher solar multiple), they have higher capacity factors compared to plants without thermal storage. CSP plants with no storage are typically designed to have a solar multiple between 1.1 – 1.5 (IRENA, 2013a), which is greater than 1 in order to generate electricity during the morning and evening hours when insolation is lower than threshold requirements, at the expense of losing some excess energy during the peak sun hours.

More thermal storage results in higher capacity factors (CF), but it reduces the land use factor (MW/km^2) due to the increasing solar multiple required. Given the near linear trade-off between thermal storage and land use factor, the generation-based land use factor (MWh/km^2) should be invariant to thermal storage assumptions. Nonetheless, we estimate CFs assuming both storage and no storage. Due to lack of empirical land use factor data for thermal storage systems, we use average empirical land use factors for no-storage CSP plants examined in the USA, which are more robust (as measured by number of data samples), and applied the ratio of storage to no-storage solar multiples to estimate land use factors for CSP plants with thermal storage (Table C.6) (Ong, Campbell, Denholm, et al., 2013).

Models of CSP power plant generation are complex and difficult to approximate using only design calculations and average direct normal insolation (DNI) values. Instead, we used the National Renewable Energy Laboratory's System Advisory Model to simulate the CF for 45 locations throughout the study region in Africa and five locations in California and Arizona (in order to achieve greater representation of higher DNI regions) for two generic CSP plants with the following assumptions: (1) no storage and a solar multiple of 1.2; (2) 6 hours of storage and a solar multiple of 2.1. Weather data for both U.S. and African locations were available from the U.S. Department of Energy Simulation Software database, a compilation of weather data from multiple sources (U.S. Department of Energy, n.d.). We linearly regressed each location's CF against its DNI, wind speed, temperature, and latitude, and determined that DNI was the only statistically significant explanatory variable for trends in CF. We plotted CF against DNI and chose to fit a logarithmic equation to the data because of known increased efficiency losses at the higher end of the DNI range (Figure C.6). We used these fitted equations (Figure C.6) to estimate the CF for the spatially averaged DNI in each project opportunity area for both no-storage and 6-hr-storage CSP power plant design assumptions.

Wind The capacity factor of a wind turbine installation depends on the wind speed distribution at the wind turbine hub height, the air density at the location, and the power curve of the turbine. We used spatially-averaged shape and scale parameters for the Weibull distribution provided by 3Tier Inc. (now Vaisala Inc.) to generate a wind speed probability distribution per 3.6 km grid cell (the resolution of 3Tier data).

Air density is inversely related to elevation and temperature. It decreases with increasing elevation or temperature, and as a result, can significantly affect the power in the wind for a particular wind speed regime. Wind turbine power curves provided by manufacturers typically assume an air density of 1.225 kg/m^3, which is the air density at sea level and 15°C. An increase in elevation from sea level to 2500 m can result in 26% decrease in air density. Changes in temperature produce a smaller yet significant effect on air density compared to elevation. A temperature increase from 0°C to 25°C can result in a drop of 8% in air density. To account for the effect of air density on power generation, we first estimated the air density for each grid cell, and then applied power curves modified for different air densities to the wind speed distributions.

For air density, we first estimated the pressure (p) for each grid cell from the elevation and temperature of those grid cells (see Table C.2 for data sources), the air pressure at sea level (p_o: 101325 Pa), the gravitational acceleration (g: 9.807 kg/m^3), and the gas constant (R: 287.04 J/kg-K) (Eq. C.2) (Gipe, 2004). We then estimated the air density (ρ) from the estimated pressure (p), the gas constant and temperature of the grid cell (Eq. C.3).

$$p = \rho \cdot e^{\frac{-Zg}{RT}} \tag{C.2}$$

$$\rho = \frac{p}{RT} \tag{C.3}$$

On-shore wind turbines are generally classified into three International Electrotechnical Commission (IEC) classes depending on the wind speed regimes. We used normalized wind curves for the three IEC classes developed by the National Renewable Energy Laboratory (J. King, A. Clifton, and Hodge, 2014) (see Figure C.7), and scaled these to a 2000 kW rated wind turbine. Adopting an approach similar to (R. Wiser et al., 2012), we assumed the IEC Class III and II turbines to be viable in sites up to the reference wind speeds of 7.5 m/s and 8.5 m/s respectively, as defined by the IEC. For sites with average wind speeds above 8.5 m/s, we assumed the IEC Class I turbine to be suitable. In reality, depending on the site-specific gust, turbulence, and air density, IEC Class II and III turbines could be placed at sites with higher average wind speeds than those assumed in our analysis, in order to extract more energy from the wind (R. Wiser et al., 2012).

For each of the three turbine classes, we adjusted the power curves for a range of air densities by scaling the wind speeds of the standard curves according to the International Standard IEC 61400-12 (IEC, 1998; Svenningsen, 2010). In Equation C.4, v_{adj} is the adjusted wind speed, v_{std} is the wind speed from the standard power curve, ρ_{std} is the standard air density of 1.225 kg/m^3, and ρ_{adj} is the estimated air density of the grid cell.

$$v_{adj} = v_{std} \left(\frac{\rho_{std}}{\rho_{adj}} \right)^{1/3} \tag{C.4}$$

Since the resulting power curve (v_{adj}, P_{std}) is evaluated at the adjusted wind speed values, v_{adj}, we needed to interpolate the P_{adj} at discrete wind speed values (v_{std}) in order to plot the air-density-adjusted power curve (v_{std}, P_{adj}) (Svenningsen, 2010). The resultant adjusted power curves show that air density can significantly affect the wind turbine power curves, and subsequently, the expected capacity factors at a site (Figure C.8).

To compute the capacity factor for each 3.6 km grid cell, we selected the appropriate air-density-adjusted power curve given the average wind speed, which determines the IEC class, and the air density, which determines the air-density adjustment within the IEC class. For each grid cell, we then discretely computed the power output at each wind speed given its probability (determined by the Weibull distribution parameters provided by 3Tier) and summed the power output across all wind speeds within the turbine's operational range to calculate the mean wind power output in W ($\overline{P}$). The capacity factor (r_{wind}) is simply the ratio of the mean wind power output to the rated power output of the turbine (P_r or 2000 kW), accounting for any collection losses (η_a) and outages (η_o) (Eq. C.5).

$$r_{wind} = \frac{(1 - \eta_a) \cdot (1 - \eta_o) \cdot \overline{P}}{P_r} \tag{C.5}$$

Levelized cost of electricity (LCOE) calculations

The LCOE is a metric that describes the average cost of electricity for every unit of electricity generated over the lifetime of a project at the point of interconnection. Using the size (km^2) (a_x) of the project opportunity area x and its associated land use factor (l_t) for technology t, land use discount factor (f_t) for technology t, distance to nearest substation (or transmission line; $d_{i,x}$) and road ($d_{r,x}$) from area x, and economic parameters listed in Table C.6, we calculated the generation, interconnection and road components of the levelized cost of electricity (LCOE in USD/MWh). Note that the size (km^2) of a project opportunity area (a) and its associated land use factor (l_t) and land use discount factor (f_t) cancel out in the LCOE equations, but are included for completeness to show the ratio of cost to electricity generation (Eqs. C.6 - C.8).

Road LCOE was estimated using a fixed capital cost per km of additional road needed to service the project, and is expressed per unit of electricity output from the project. Since road capital costs do not scale according to installed capacity of a project, unlike generation and interconnection costs which increase with each additional MW of capacity, the size of a project opportunity area affects the road cost. That is, a POA within 10 km of existing road infrastructure will have a higher road cost than another POA within the same distance of the nearest road if it is comparatively smaller in land area. In order to allow road LCOEs to vary only by each POA's road connection distance and resource quality, we assumed 50

MW of capacity per POA regardless of size (Eq. C.8). We assumed that one road will be built for every 50 MW capacity project, which is a reasonable size for a utility-scale project, and roughly equal to the potential capacity of a project opportunity area.

Total LCOE is simply the sum of the generation, interconnection, and road cost components. We prioritize distance to nearest substation in estimating transmission LCOE when high quality spatial data for substations were available, but we also estimated transmission LCOE costs based on distance to the nearest transmission line. Refer to Table C.6 for values used in LCOE calculations.

$$LCOE_{generation,t,x} = \frac{a_x l_t \left(1 - f_t\right) \left(c_{g,t} i_{cr} + o_{f,g,t}\right)}{8760 \cdot a_x l_t \left(1 - f_t\right) r_{t,x}} + o_{v,g,t} \tag{C.6}$$

$$LCOE_{interconnection,t,x} = \frac{a_x l_t \left(1 - f_t\right) \left(d_{i,x} \left(c_i i_{cr} + o_{f,i,t}\right) + c_s i_{cr}\right)}{8760 \cdot a_x l_t \left(1 - f_t\right) r_{t,x}} \tag{C.7}$$

$$LCOE_{road,t,x} = \frac{d_{r,x} \left(c_r i_{cr} + o_{f,r}\right)}{8760 \cdot r_{t,x} \cdot 50MW} \tag{C.8}$$

Where $c_{g,t}$ is the capital cost of generation for technology t; c_i is the capital cost of interconnection (i); c_s is the capital cost of substation (s); c_r is the capital cost of road; $r_{t,x}$ is the capacity factor of technology t and area x; $o_{f,g,t}$ is the fixed operations and maintenance cost of generation for technology t; $o_{f,i,t}$ is the fixed operations and maintenance cost of interconnection (i) for technology t; $o_{v,g,t}$ is the variable (v) operations and maintenance cost of generation (g) for technology t; $o_{v,i,t}$ is the variable (v) operations and maintenance cost of interconnection (i) for technology t; $o_{f,r}$ is the fixed (f) operations and maintenance cost of roads (r). The capital recovery factor (i_{cr}) converts a present value to a uniform stream of annualized values given a discount rate and the number of interest periods (Eqn. C.9). We have assumed a real discount rate (i) of 10% that reflects the high cost of capital in Africa. n is the number of years in the lifetime of a power plant.

$$i_{cr} = \frac{i \left(1 + i\right)^n}{\left(1 + i\right)^n - 1} \tag{C.9}$$

Although LCOE assumptions were selected to be as representative of current conditions and costs, these LCOE estimates are best used to compare costs within a single technology since LCOE values may be higher or lower than others reported in the literature given the dynamic nature of the industry. Further, the discount rate can significantly affect the LCOE, and can vary across countries.

System integration costs or balancing costs are not included in LCOE estimates. These can vary across countries based on their electricity generation mix. For example, hydro capacity with storage is considered more flexible than coal power plants that typically incur a higher penalty for cycling in order to balance both variable renewable energy and load (net load).

The LCOE does not account for differences in the value of electricity generated by different technologies in a particular location. Generation at different times of the day or year have different economic value depending on the demand and the available generation at that time.

LCOE estimates are based on present existing and planned transmission and road infrastructure. In this study, we did not value a project opportunity area sequentially based on the utilization of infrastructure that may be built earlier for another nearby planned project.

Wind build-out scenario analysis

Input load and wind generation data

We created load profiles for the year 2030 ($d_{2030,t}$) using the projected annual demand in 2030 (Eastern Africa Power Pool et al., 2011; Southern Africa Power Pool and Nexant, 2007) by multiplying the load in each hour t ($d_{2013,t}$) by the ratio of the 2030 annual load (D_{2030}; Table C.7) to the 2013 annual load (Eq. C.10). This simple load projection technique assumes that load profile shapes will remain the same between 2013 and 2030, with an equal proportional increase in energy demand across all hours. See section C.1 for methods used to conduct a sensitivity analysis of load profiles.

$$d_{2030,t} = d_{2013,t} \frac{D_{2030}}{\sum_{t=1}^{T} d_{2013,t}} \tag{C.10}$$

For the Southern Africa Power Pool (SAPP) countries, we procured mesoscale modeled hourly wind generation profiles for each of 233 wind locations, selected within zone extents based on resource abundance, resource quality, representation across countries, and spatial representation within a country. Using these profiles, we created hourly capacity factor ($c_{z,t}$) profiles for all 738 wind zones in the SAPP by adjusting the hourly wind capacity factor ($c_{m,t}$) of the mesoscale modeled profile using the ratio of zones' ($\overline{c_z}$) and modeled ($\overline{c_m}$) profiles' annual average capacity factors (Eq. C.11). We matched each zone to the nearest location for which we acquired mesoscale modeled wind profiles.

$$c_{z,t} = c_{m,t} \frac{\overline{c_z}}{\overline{c_m}} \tag{C.11}$$

Min-net-demand site selection approach

To select wind zones and the amount of capacity to install in each zone (x_z), we minimized the maximum hourly net demand, or the difference between the hourly load and the hourly wind generation (Eq. C.12). This hourly net demand is the amount of energy non-wind generators would need to supply each hour. Therefore, the maximum hourly net demand

within a year is the amount of non-wind installed capacity that must be available to ensure that demand is met across all hours of the year. The objective function (Eq. C.12) was minimized subject to installing a specified amount of wind capacity across the region or country (Eq. C.13) (Table C.7) and selecting no more than the available potential capacity of each zone (Eq. C.15). We used the projected 2030 demand (Table C.7) to calculate the target wind capacity (i), assuming wind will generate 30% of total annual electricity demand and have an average capacity factor of 30%. The resulting target installed capacity (i) of 61 GW across all of SAPP was consistent across scenarios.

The integer optimization problem was programmed in Python using the Pyomo module and solved using IBM CPLEX. We used this optimal wind site selection method for the following four scenarios: 30% wind penetration for each country in SAPP using only domestic wind zones (*Isolated* scenario), and 30% wind penetration across the entire SAPP region (*Interconnected* scenario), and the *Isolated* and *Interconnected* scenarios using only the top 50% of zones across three selection criteria (see the results section of the main text).

Linear optimization

Indicies

z	Zone identifier $\in \{z...Z\}$
t	Hour $\in \{1, ..., 8760\}$

Variables

x_z	Capacity to install (MW) in zone z

Parameters

$c_{z,t}$	Capacity factor of zone z hour t
$d_{2030,t}$	Electricity demand (MWh) of hour t in year 2030
p_z	Potential installed capacity (MW) of zone z
i	Target capacity (MW)

Objective function

Minimize

$$max(d_{2030,t} - \sum_{z=1}^{Z} c_{z,t} x_z) \tag{C.12}$$

Constraints

Subject to

$$\sum_{z=1}^{Z} x_z = i \tag{C.13}$$

$$x_z \geq 0 \quad \forall z \in \{z, ..., Z\} \tag{C.14}$$

$$x_z \leq p_z \quad \forall z \in \{z, ..., Z\} \tag{C.15}$$

Scenario comparisons

Peak net demand calculations. Typically, conventional generation capacity is sized to meet demand. Because wind power plants are "must-run" generators, conventional generation capacity is instead sized to meet the net demand, or the difference between the demand and amount of wind generation in each hour. Therefore, to meet demand in all hours, conventional generation capacity must equal the annual peak net demand. For the *Interconnected* scenario, the conventional generation capacity is simply the coincident peak net demand, W_c (Eq. C.17), or the peak net demand calculated by adding the net demand across all countries for each hour. For the *Isolated* scenarios, both coincident and non-coincident peak net demand were calculated (Eq. C.16, Eq. C.17). Non-coincident net demand, W_{nc}, represents the total amount of conventional capacity across the SAPP needed if each country met its net demand separately (C.16). Non-coincident net demand is always greater than or equal to the coincident net demand. The difference between these two values represents the avoided conventional capacity due to interconnection alone, as opposed to the balancing of wind variability through optimal site selection. This value is represented by the gray bars ("Avoided capacity due to coincident net demand") in Fig. 3B in the main text. Therefore, the coincident peak net demand represents the conventional capacity needed to balance the net demand due to the wind profile variability.

$$W_{nc} = \sum_{y=1}^{Y} [max(w_{y,t}) \quad \forall y \in \{y...Y\}] \tag{C.16}$$

$$W_c = max[\sum_{y=1}^{Y} w_{y,t} \quad \forall t \in \{1...8760\}] \tag{C.17}$$

where

$$w_{y,t} = d_{y,2030,t} - \sum_{z=1}^{Z} c_{y,z,t} x_{y,z} \tag{C.18}$$

y	country $\in \{y...Y\}$
$w_{y,t}$	net demand of country y for hour t
W_{nc}	non-coincident peak net demand across all countries in the SAPP

W_c	coincident peak net demand across all countries in the SAPP
$x_{y,z}$	Capacity installed (MW) in zone z in country y
$c_{y,z,t}$	Capacity factor of zone z hour t in country y
$d_{y,2030,t}$	Electricity demand (MWh) of hour t in year 2030 for country y

Cost difference calculations. To compare approximate system costs, we monetized differences in (1) energy needs and (2) conventional capacity needs between scenarios. For (1), we assumed that any additional energy needs would be generated using hydropower or coal technologies, using the marginal cost of electricity (Table C.8). Because additional energy is needed in the *min-net-demand* scenarios and its supply curve shows that the extra energy needed is during low-net-demand or baseload hours (Fig. 3C in the main text), it is more likely that coal or hydropower, rather than natural gas, will be used to supply the extra energy required. For (2), we assumed that any extra conventional capacity needed could be met using natural gas combustion turbine (CT), hydropower, or coal (see Table C.8 for cost inputs). We use the non-coincident net peak demand (see Eq. C.16) to represent the needed conventional capacity. We represent cost additions or savings relative to the amortized annual capital cost of wind power, which is consistent across scenarios.

Inteconnection cost estimates. A bottom-up estimate of interconnection infrastructure costs rely on knowing the lengths and voltages of new lines. A high resolution spatio-temporal 'capacity-expansion' model of the power pool's entire power system (current and future generators, their locations, and current and future transmission availability and capacity) would be needed to generate such estimates. To approximate these interconnection infrastructure costs given the lack of access to data needed to build a power systems model, we use a top-down approach that relies on the interconnection costs reported for energy trade within the SAPP. Using the MWh of energy traded in the SAPP and the revenue from wheeling charges reported in the SAPP annual reports (`http://www.sapp.co.zw/areports.html`), we calculated the wheeling cost per MWh. These wheeling costs are \$2.46/MWh for 2014 - 2015, \$2.31/MWh for 2012-2013, and \$2.62/MWh for 2011 - 2012. (Southern Africa Power Pool, 2014; Southern Africa Power Pool, 2015). Wheeling is the transport of electricity from within a grid to serve demand outside of the grid. One of the central reasons for wheeling charges is to recover the capital and maintenance costs of transmission infrastructure. For each *Interconnected* wind build-out scenario, we calculated the net energy traded in the SAPP by summing the difference between wind electricity generated under the *Isolated* and the *Interconnected* scenarios for each country and halving the total amount. We applied the range of wheeling fees charged by the SAPP (\$2.31/MWh - \$2.62/MWh) to calculate the wheeling charges per scenario. We then represented the wheeling charges as percentage of the amortized annual capital cost of wind power in order to compare interconnection costs with conventional energy and conventional capacity cost differences (see section C.1 above).

Load profile sensitivity analysis

We created four load growth scenarios that maintain the same level of energy consumption but differ in the load profile shapes. See Fig. C.10 for each scenario's hourly load profiles averaged across each month and Fig. C.11 for the load duration curve across an entire year for all four scenarios. A load duration curve is the load for each hour sorted from highest to lowest. We modified each country's load profiles separately and aggregated them to create the Southern Africa Power Pool-wide load profile. The scenarios are as follows:

- "Climate – warming": relative to baseline, peak summertime (November through March) demand increases by 5% and wintertime (May through September) demand decreases by an appropriate amount to maintain the same level of energy across the year. For most SAPP countries, the annual peak demand occurs in the winter, during the months of July or August, due to heating demand and other appliance usage. Previous studies have shown that load in South Africa is extremely sensitive to climate (Chikobvu and Sigauke, 2013), and under likely climate change scenarios, wintertime and summertime temperatures are expected to increase (Niang et al., 2014; Department of Environmental Affairs, South African National Biodiversity Institute, and GIZ, 2013). This scenario represents greater air conditioning load increase in response to rising summer temperatures under climate change. According to Eskom, South Africa's largest utility, air conditioning load is fairly uniformly across all day-time hours and some early evening hours. Therefore, we uniformly increased summertime load from 10:00 to 22:00 from November to March. These modifications create monthly hourly average profiles that have similar daily peak demand across the year (see Fig. C.10d) and reduce the annual peak demand (see Fig. C.11). Tanzania's and Mozambique's load profiles were not altered in this scenario because their load profiles do not show a seasonal pattern, unlike that of the remaining seven SAPP countries.

- "Climate – extreme warming": relative to baseline, peak summertime demand increases by 8% and wintertime demand decreases by an appropriate amount to maintain the same level of energy across the year. Like the "Climate - warming" scenario, this scenario also anticipates strong summertime warming and increased AC load. The greater increase in summertime load inverts the current, baseline seasonal trend of annual peak load occurring in the wintertime for most SAPP countries (Fig C.10a) to one that shows annual peak demand occurring in the summer (Fig C.10e). This has the effect of slightly reducing the annual peak demand relative to baseline, but not as significantly as in the "Climate - warming" scenario (Fig. C.11).

- "South Africa - hybrid": the daily hourly profiles averaged across a month for each country are combined with that of South Africa's using 50%-50% weighted averaging. This scenario represents economic structural growth in load curves to resemble that of South Africa's (Fig. C.10c and C.11). Although the monthly average hourly load profiles and the load duration curve do not appear to differ from that of the baseline

scenario, this is primarily because South Africa contributes 85% of the demand in the SAPP. Differences in load profiles at the country-level are more discernible.

- "Daily peak increase": Increase in daily peak hours by 5-7% across all days of the year (Fig. C.10b). This scenario represents increased electrification leading to increased load from appliance ownership and usage. It also represents reduced curtailment, as load shedding typically occurs during both summer and wintertime peak hours, despite summertime peak demand being less than wintertime peak demand. According to Eskom, this is because less capacity is available in the summer due scheduled maintenance. This scenario effectively increases the annual peak demand (Fig. C.11).

Each of the future load growth scenarios were generated by modifying each monthly average hourly demand profile. This was done by calculating the difference between each hour's demand and the unmodified monthly average for that hour and then adding this difference to the growth scenario's generated monthly average for that hour.

C.2 Supporting figures and tables

Figures and Tables for results

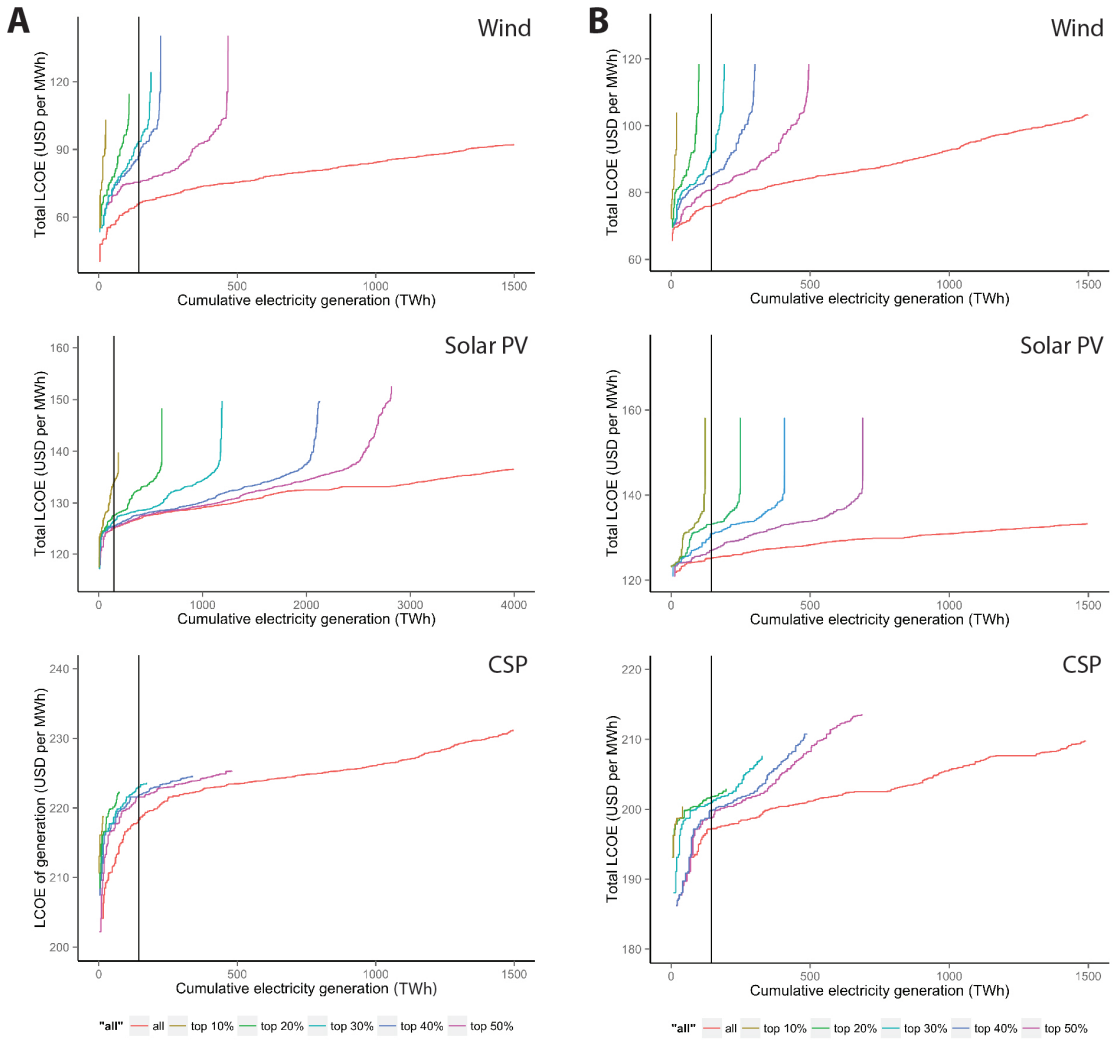

Figure C.1: Technology supply curves for the Eastern **(A)** and Southern **(B)** Africa Power Pools.

For each technology, each supply curve shows all project opportunity areas and those that meet the top 10% - 50% of siting criteria values (shortest distance to transmission infrastructure, shortest distance to load center, and greatest human footprint score). The black vertical lines show 25% of the projected demand in 2030 (Eastern Africa Power Pool et al., 2011; Southern Africa Power Pool and Nexant, 2007). Supply curves show whether it is possible to achieve a particular generation target in each power pool under particular levels of siting criteria constraints and at what marginal total levelized cost of electricity.

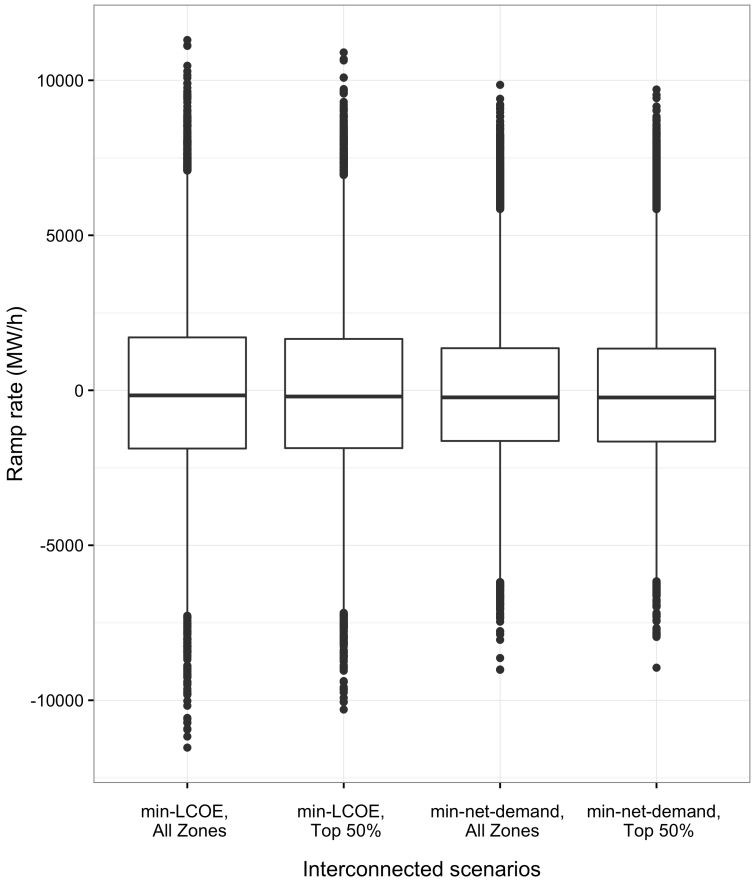

Figure C.2: Distribution of hourly ramp rates for the *Interconnected* wind build-out scenarios.
Ramp rates were calculated by taking the inter-hourly differences in net demand. They indicate the amount of energy that conventional generators need to produce or reduce hour-to-hour to balance the variability of wind generation. Given the range of ramp rates of conventional generators (2%/min for coal, 5% for combined cycle, and 8.3% for gas turbine (Veatch and NREL, 2012), 100% of available up-ramp capacity can be dispatched within an hour. If day-ahead scheduling commits enough capacity to meet the forecasted daily peak demand, there will be sufficient capacity to ramp up, regardless of the ramp requirement calculated for each scenario. However, a wider distribution of ramp rates indicates the need for more conventional generation flexibility and cycling, increasing the rate of wear-and-tear on conventional generators and increasing the system costs due to a higher demand for flexibility services.

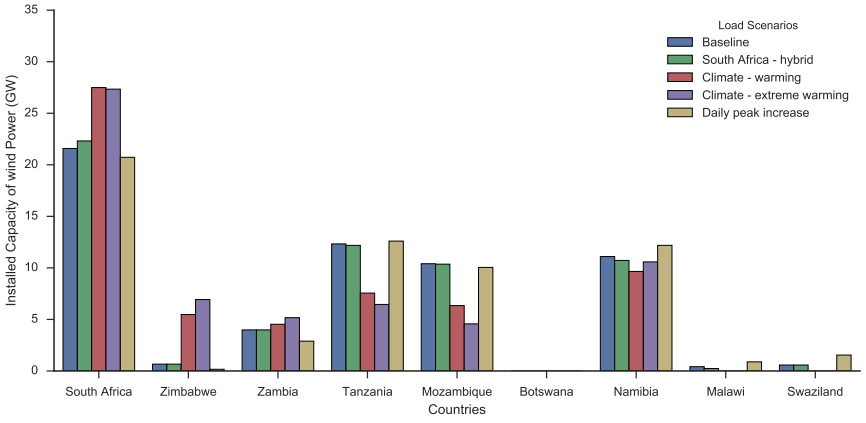

(a)

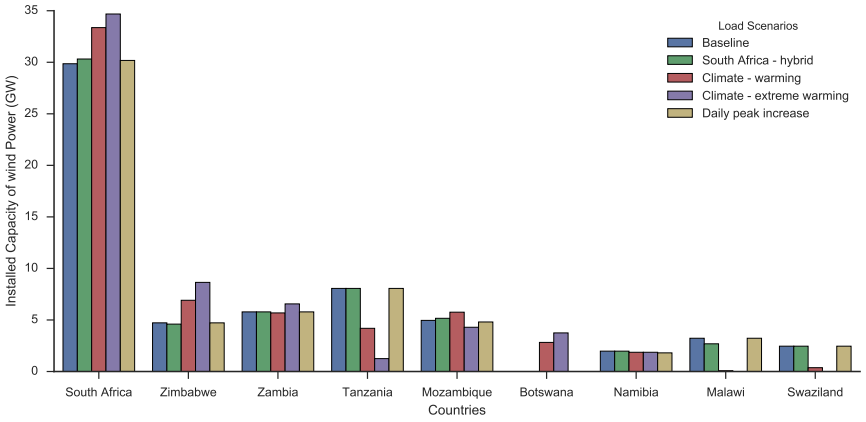

(b)

Figure C.3: Distribution of installed wind capacity among countries in the SAPP using the baseline load profile and four future load growth profiles for "*Interconnected, min-net-demand, all zones*" (a) and "*Interconnected, min-net-demand, top 50%*" scenarios (b). Figure C.10 and C.11 and section C.1 for descriptions of future load growth profiles.

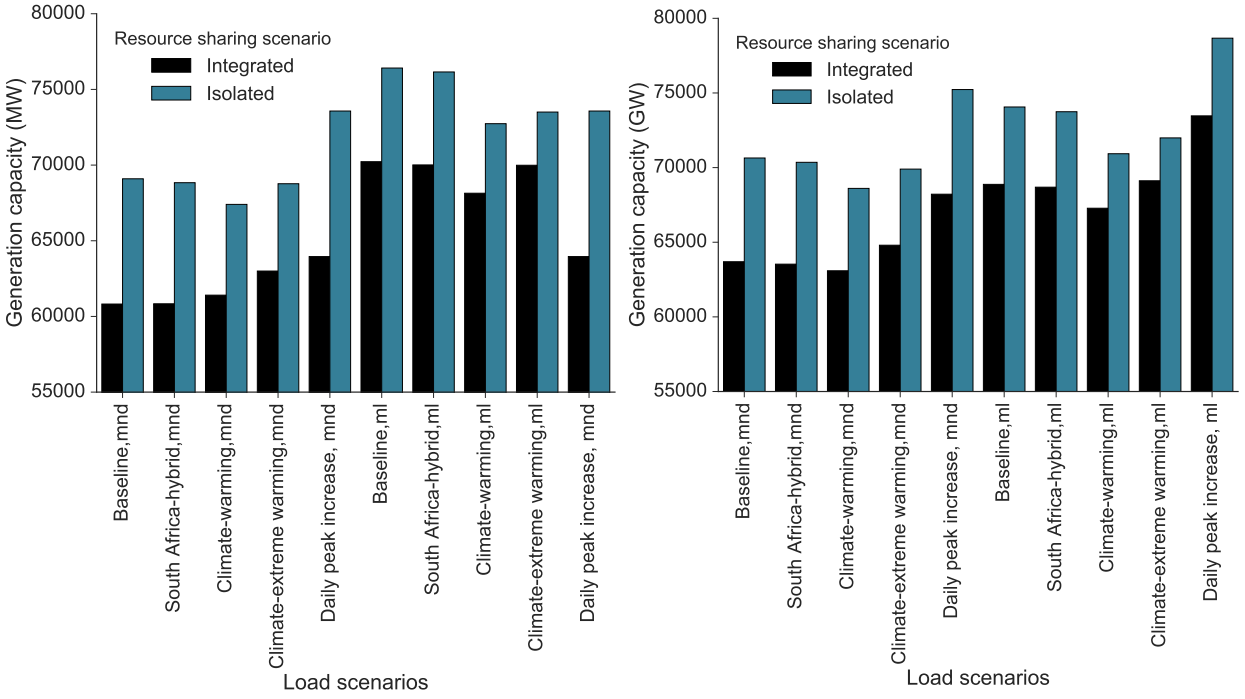

Figure C.4: Conventional installed capacity needed to meet the highest hourly net demand within a year using baseline load profiles and four load growth projections for "all zones" (a) and the "top 50%" of zones (b).
Note that the range of the y-axis does not begin at zero in order to highlight the differences between scenarios. See Figures C.10 and C.11 for details on the load growth scenarios.
"mnd" = "min-net-demand" and "ml" = "min-LCOE".

Table C.1: Transmission costs for "Interconnected" wind build-out scenarios

Scenario	**Annual wheeling fees (Million USD)**	**Wheeling fees as percentage of annual wind capital costs**	**Fraction of wind energy traded**	**Net energy traded (TWh)**
Min-net-demand, all zones	210 - 240	1.6 - 1.8%	40.4%	91
Min-net-demand, top 50% zones	140 - 160	1.0 - 1.2%	28.2%	60
Min-LCOE, all zones	52 - 59	0.40 - 0.44%	9.1%	23
Min-LCOE, top 50% zones	42 - 48	0.32 - 0.36%	8.2%	18

Figures and tables for methods

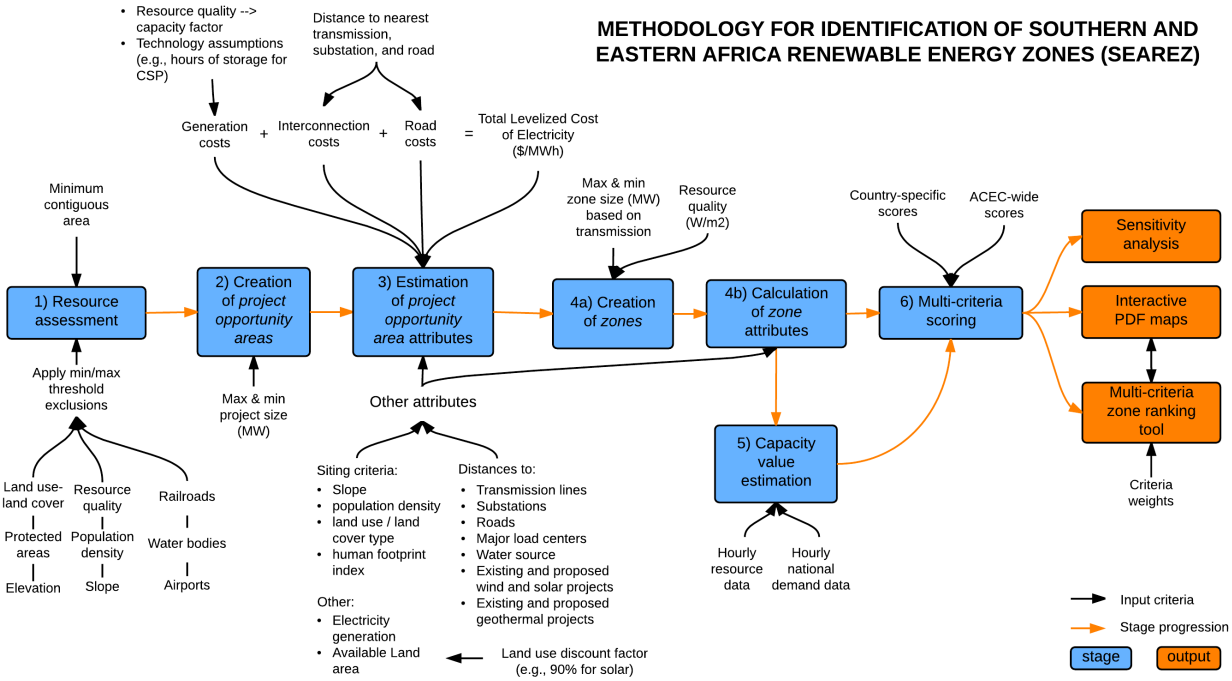

Figure C.5: The MapRE zoning methodology flow chart.
The chart shows the stages of analysis and the required inputs. Interactive PDF maps and zone ranking tool outputs are available on `http://mapre.lbl.gov`.

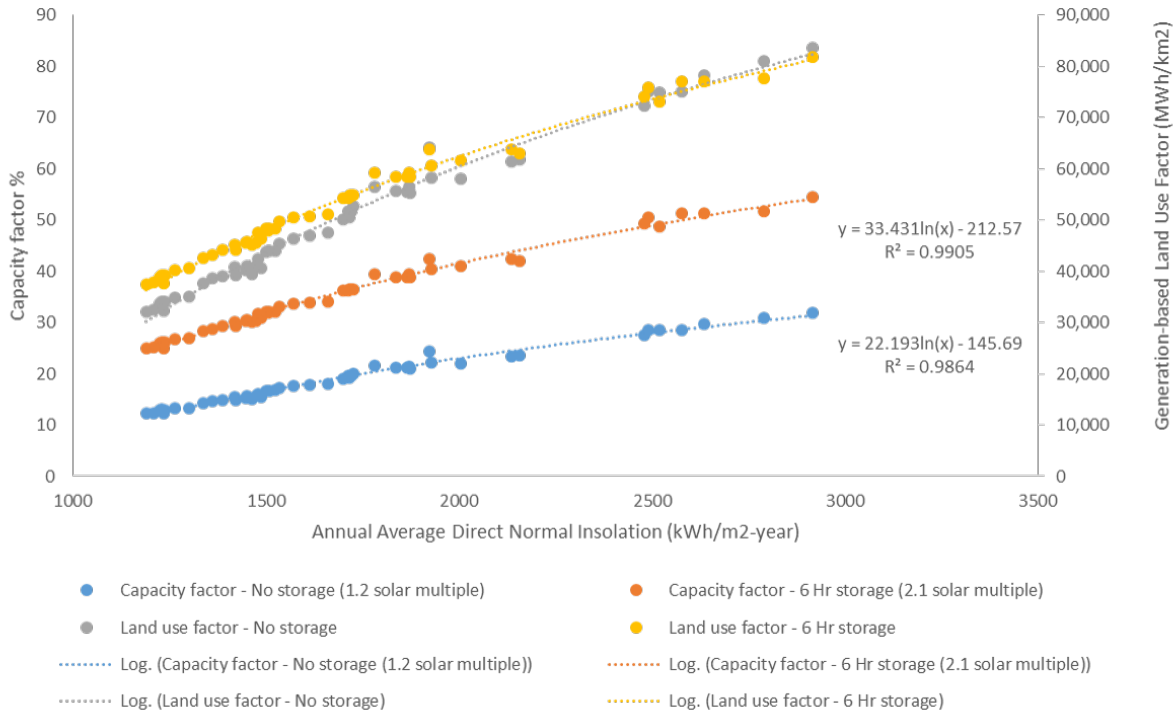

Figure C.6: Relationship between capacity factor, land use factor, and Direct Normal Insolation (DNI) for CSP.
Capacity factors were simulated using specifications for a generic CSP plant in the National Renewable Energy Laboratory's System Adviser Model for 45 locations throughout the study region in Africa and five locations in California and Arizona, USA. Logarithmic equations were fit to the simulated capacity factor data to statistically model the relationship between capacity factor and DNI. Land use factors (MW/km^2) on the secondary axis were estimated for each location's capacity factor assuming an installed capacity land use efficiency of 30 MW/km^2 for no storage and 17 MW/ km^2 for 6 hours of storage.

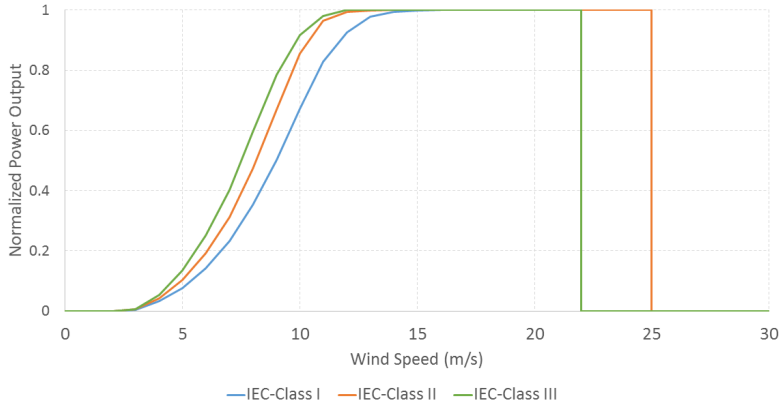

Figure C.7: Normalized wind turbine power curves for different IEC class turbines reproduced from (J. King, A. Clifton, and Hodge, 2014).

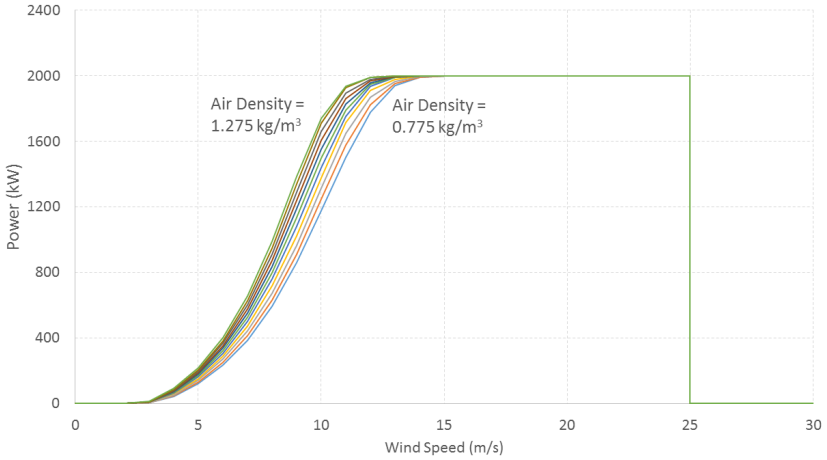

Figure C.8: Adjusted IEC Class II turbine wind power curves for air densities ranging from 1.275 kg/m^3 to 0.775 kg/m^3 (from left to right, respectively).

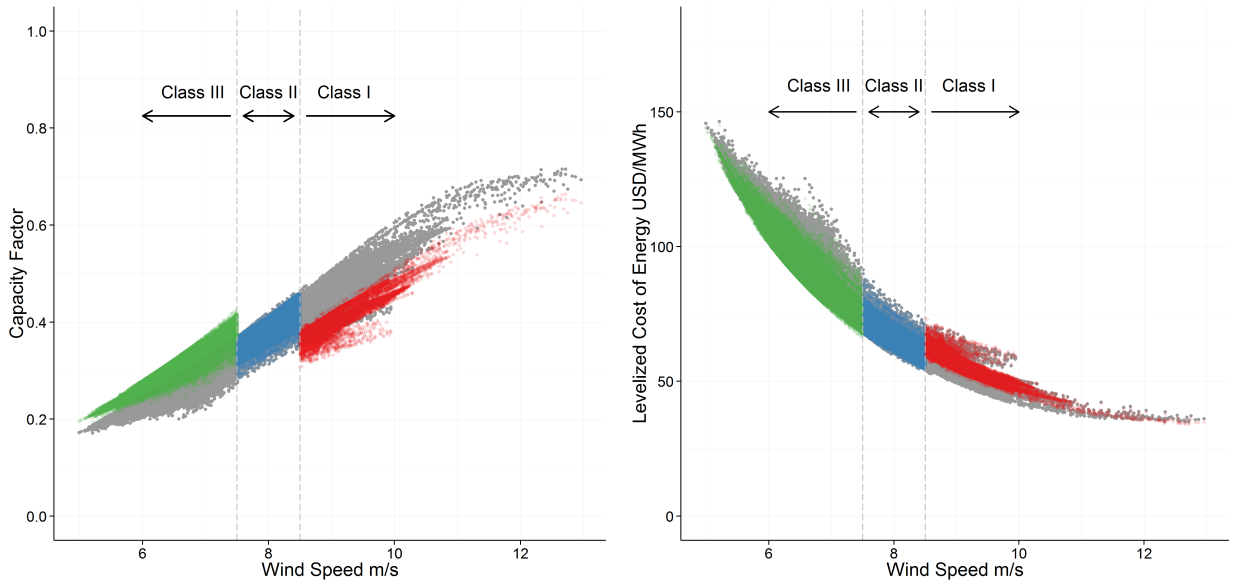

(a) (b)

Figure C.9: Relationship between average wind speed and estimated capacity factor (A) and levelized cost of energy for wind (B) across the Eastern and Southern Africa Power Pools. Capacity factors and LCOEs estimated using the wind-speed-appropriate Class I, II and III turbine power curves are represented by red, blue and green points respectively. Capacity factors and LCOEs estimated using just the Class II turbine power curve are also represented by grey points across the wind speed regimes.

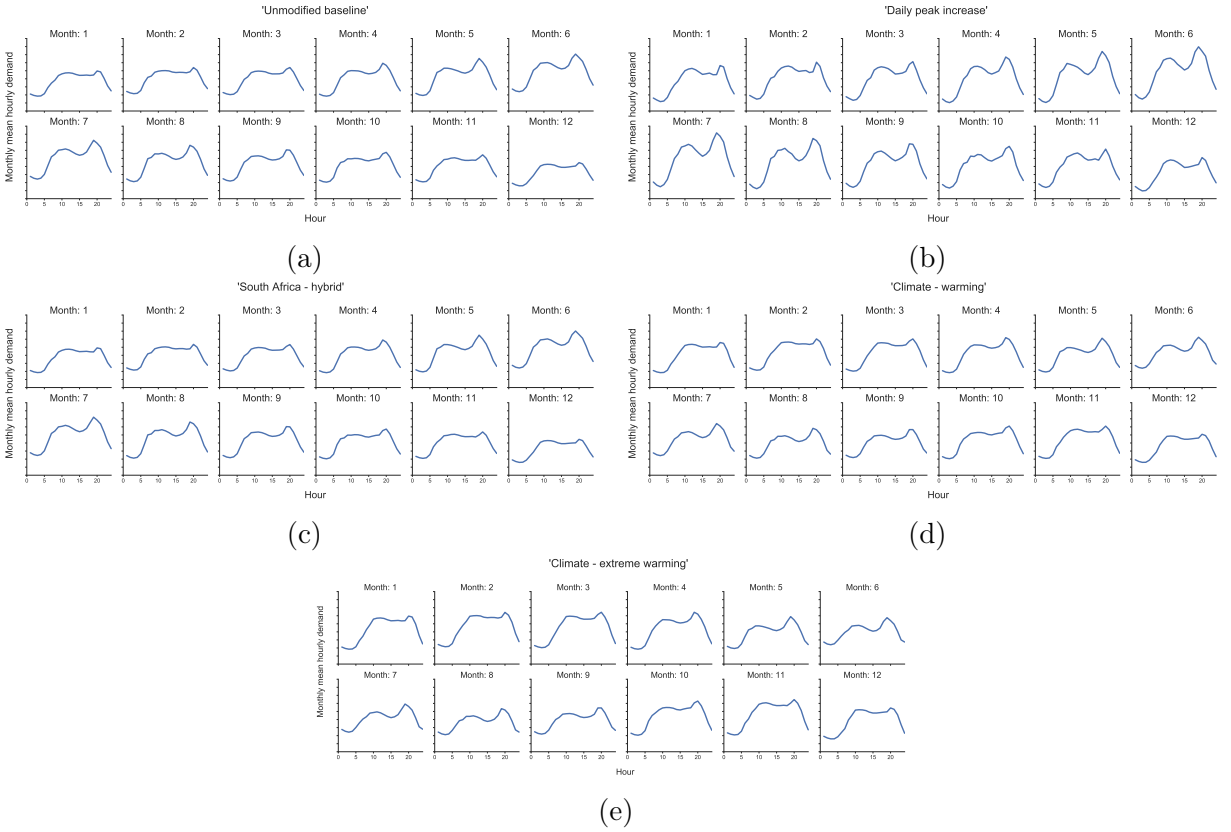

Figure C.10: Unmodified monthly mean daily load profiles of the Southern Africa Power Pool (A) and modified load profiles under the following growth scenarios.
Plots show the following modifications: (B) increase in the daily peak hours, (C) 50% structural shift in individual country load shapes to resemble South Africa's, (D) climate warming that increases peak summertime demand by 5%, (E) climate warming that increases peak summertime demand by 8%. The total demand is the same across load growth scenarios. The y-axis of all load curves have the same scale.

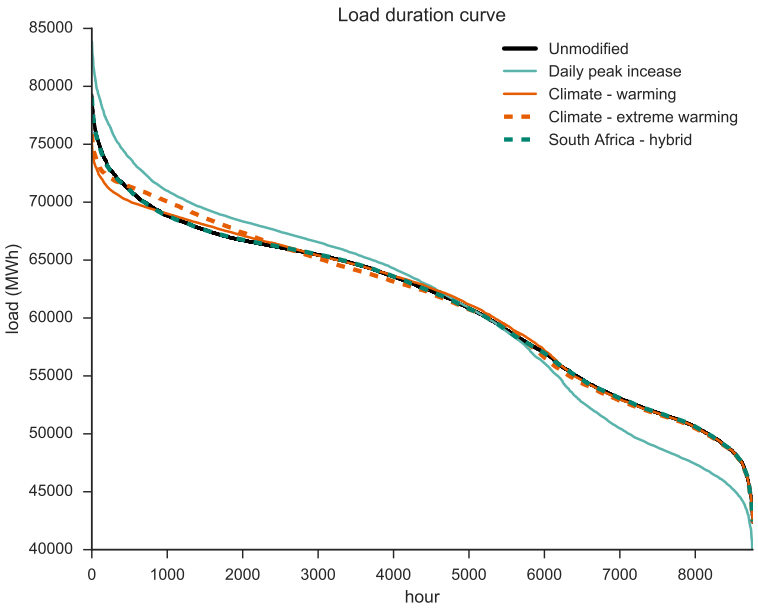

Figure C.11: Annual load duration curves for the Southern Africa Power Pool under various load growth scenarios.
A load duration curve is the load for each hour sorted from highest to lowest. "Daily peak increase" shows greater growth in the daily peak hours, "South Africa - hybrid" shows a 50% structural shift in individual country load shapes to resemble South Africa's, "Climate - warming" shows increases in peak summertime demand by 5%, "Climate- extreme warming" shows increases in peak summertime demand by 8% in countries that have seasonally varying load profiles. The total demand is the same across load growth scenarios.

Table C.2: Data sources and resource assessment thresholds

Stage of analysis	**Category**	**File type**	**Source**	**Description**	**Year**	**Default exclusion thresholds**
Resource assessment	Boundaries	Vector	Global Administrative Database (GADM) v2	GADM is a spatial database of the location of the world's administrative areas (or administrative boundaries) for use in GIS and similar software. Administrative areas in this database are countries and lower level subdivisions. http://www.gadm.org/country	2012	
Resource assessment	Elevation	Raster	Shuttle Radar Topographic Mission (SRTM) – CGIAR-CGI Digital Elevation dataset v4.1	Produced by NASA originally, the SRTM is a major breakthrough in digital mapping of the world and provides a major advance in the accessibility of high quality elevation data for large portions of the tropics and other areas of the developing world. 3 arc seconds (approx. 90 m) resolution. http://srtm.csi.cgiar.org/	2000	>1500 m (all technologies)
Resource assessment	Slope	Raster	SRTM - CGIAR	Created from elevation dataset using ArcGIS 10.2 Spatial Analyst.	2000	>5% (solar); >20% (wind)
Estimation of Project opportunity area attributes	Temperature	Raster	WorldClim	WorldClim is a set of global climate layers (climate grids) with a spatial resolution of about 1 square kilometer. Hijmans, R.J., S.E. Cameron, J.L. Parra, P.G. Jones and A. Jarvis, 2005. Very high resolution interpolated climate surfaces for global land areas. International Journal of Climatology 25: 1965-1978. http://www.worldclim.org/formats	1950 - 2000	
Resource assessment	Land use/land cover (LULC)	geotiff	ISGCM - Global Map V.2 (Global Version)	The Global Land Cover by National Mapping Organizations (GLCNMO) is the data of 500m (15 arc seconds) grid with 20 land cover items. The data were created by using MODIS data observed in 2008 (Terra & Aqua Satellites) with the cooperation of NMOs of the world in providing training data and validation. The classification is based on LCCS developed by FAO. Download data via: https://www.iscgm.org/gmd/	2008	See Table 2 in (Wu, Deshmukh, et al., 2015)
Resource assessment and Project oppor-tunity area attributes	Water bodies	vector	World Wildlife Federation Global lakes and wetlands database	Comprises lakes, reservoirs, rivers and different wetland types in the form of a global raster map at 30-second resolution. We excluded the following categories: lake, reservoir, river, freshwater marsh, floodplain, swamp forest, flooded forest, coastal wetland, brackish/saline wetland, and intermittent wetland/lake from.	2004	<500 m buffer

Stage of analysis	Category	File type	Source	Description	Year	Default exclusion thresholds
				http://www.worldwildlife.org/pages/global-lakes-and-wetlands-database		
Project opportunity area attributes	Rivers	vector	Natural Earth	Natural Earth is a public domain map dataset featuring both cultural and physical vector data themes. The rivers datasets are originally from the World Data Bank 2. All rivers received manual smoothing and position adjustments to fit shaded relief generated from SRTM Plus elevation data, which is more recent and (presumably) more accurate. http://www.naturalearthdata.com/downloads/	Unknown (version 3.0.0)	
Resource assessment	Population density	raster	LandScan (Oak Ridge National Laboratory)	ORNL's LandScanTM is the community standard for global population distribution. At approximately 1 km resolution (30" X 30"), it is the finest resolution global population distribution data available and represents an ambient population (average over 24 hours). https://www.ornl.gov/ornl/careerssci/landscan/	2012	>100 persons km^{-2}
Resource assessment	Wind	raster	3Tier/Vaisala	Data were created from computer simulations using a meso-scale numerical weather prediction model and validated using publicly available wind speed observations from 194 meteorological stations within Africa from the National Centers for Environmental Prediction (NCEP). Annual wind speed, wind power density, and wind power output were provided at 80 m hub height and 5 km resolution for a typical meteorological year. Data can be downloaded on the Global Atlas by searching for "Vaisala Global wind dataset": http://irena.masdar.ac.ae/	10-year model run	<300 Wm^{-2}
Resource assessment	Solar DNI	raster	3Tier/Vaisala	The dataset is based on actual, half-hourly, high-resolution visible satellite imagery observations via the broadband visible wavelength channel at a 2 arc minute resolution. Data can be downloaded on the Global Atlas by searching for "Vaisala Global solar dataset": http://irena.masdar.ac.ae/	15 years	<250 Wm^{-2}
Resource assessment	Solar GHI				(July 1998 – last quarter)	<280 Wm^{-2}

Stage of analysis	Category	File type	Source	Description	Year	Default exclusion thresholds
Resource assessment	Protected Areas	vector	World Database of Protected Areas (WDPA)	The World Database on Protected Areas (WDPA) is the most comprehensive global spatial dataset on marine and terrestrial protected areas available. The WDPA is a joint project of UNEP and IUCN, produced by UNEP-WCMC and the IUCN World Commission on Protected Areas working with governments and collaborating NGOs. Download data via https://www.protectedplanet.net/	2014	<500 m buffer
Resource assessment	Protected Areas	vector	Protected Planet	Open source database that includes most WDPA locations, but also include polygon representations of the WDPA point locations (those with unknown extents/boundaries). Download data via https://www.protectedplanet.net/	2014	<500 m buffer
Resource assessment	Rail	vector	Africa Infrastructure Country Diagnostic (AICD) - Africa Development Bank (AfDB) and World Bank (WB)	Primary data collection efforts covering network service infrastructures (ICT, power, water & sanitation, road transport, rail transport, sea transport, and air transport) from 2001 to 2006 in 24 selected African countries. Download data via: http://www.infrastructureafrica.org/about	Variable; compiled 2011	<500 m buffer
Project opportunity area attributes	Roads	vector	AICD – AfDB and WB	See above rail category	Variable; compiled 2008	
Project opportunity area attributes	Roads	vector	gROADSv1 - Columbia University	Global Roads Open Access Data Set, Version 1 was developed under the auspices of the CODATA Global Roads Data Development Task Group at Columbia University. The data set combines the best available roads data by country into a global roads coverage, using the UN Spatial Data Infrastructure Transport (UNSDI-T) version 2 as a common data model. Download data via: http://sedac.ciesin.columbia.edu/data/set/groads-global-roads-open-access-v1	Variable; compiled (1980-2010)	
Project opportunity area attributes	Transmission	vector	AICD – AfDB and WB	Transmission lines were only available for a subset of sub-Saharan African countries. In some cases, lines do not represent geographic footprint of transmission lines but are schematics depicting points of interconnection. See Appendix A of the MapRE report (Wu, Deshmukh, et al., 2015) for transmission infrastructure data sources for each country.	Variable - compiled 2010	

Stage of analysis	Category	File type	Source	Description	Year	Default exclusion thresholds
Project opportunity area attributes	Renewable energy locations	vector	AICD – AfDB and WB, Cross Border Information	Existing and proposed power plants for select sub-Saharan African countries where data were available.	Variable; compiled 2011	
Project opportunity area attributes	Load centers	Lat-long coordinates	Geonames	The GeoNames geographical database is available for download free of charge under a creative commons attribution license. It contains over 10 million geographical names and consists of over 9 million unique features including 2.8 million populated places and 5.5 million alternate names. Download data via www.geonames.org	2014	
Project opportunity area attributes	Wind speed time series	.csv	3Tier/Vaisala	Hourly wind speed, wind power density, and wind power output for 10 years (same simulated data that was used to create the typical meteorological year (TMY) average values); approximately 5 km resolution. Data must be purchased from Vaisala directly: http://www.vaisala.com/en/energy/Pages/default.aspx	10-year model run	

Table C.3: Adjusted resource quality thresholds for each country.

Country	**Wind W/m²**	**Solar PV GHI W/m²**	**Solar CSP DNI W/m²**	**Elevation**	**Slope**	**Population**	**LULC**
Angola	200 (lower)[1]	250 (PP)[2]	280 (PP)				
Botswana	200 (lower)	250 (PP)	280 (PP)				
Burundi	200 (lower)	230 (lower)	260 (lower)	2500 m	20% (wind and solar)	200 persons per km2	Include "Tree Open" category
DRC	200 (lower)	210 (PP)	260 (lower)	2500 m			
Djibouti	300 (PP)	250 (PP)	260 (lower)				
Egypt	200 (lower)	230 (lower)	270 (lower)				
Ethiopia	200 (lower)	250 (PP)	280 (PP)	3000 m			
Kenya	250 (lower)	250 (PP)	270 (lower)	2500 m			
Lesotho	200 (lower)	250 (PP)	280 (PP)	2500 m			
Libya	300 (PP)	250 (PP)	280 (PP)				
Malawi	200 (lower)	240 (PP)	260 (lower)	2500 m			
Mozambique	200 (lower)	230 (PP)	260 (lower)				
Namibia	200 (lower)	250 (PP)	280 (PP)				
Rwanda	200 (lower)	230 (lower)	260 (lower)	2500 m	10% (wind)	200 persons per km2	Include "Tree Open" and "Mixed Cropland" categories
South Africa	300 (PP)	250 (PP)	280 (PP)	2000 m			
Sudan	250 (lower)	250 (PP)	280 (PP)				
Swaziland	250 (lower)	210 (lower)	260 (lower)				
Tanzania	250 (lower)	250 (PP)	280 (PP)	2000 m			
Uganda	200 (lower)	250 (PP)	260 (lower)	2500 m			
Zambia	200 (lower)	250 (PP)	260 (PP)	2000 m			
Zimbabwe	200 (lower)	250 (PP)	280 (PP)				

[1]Threshold that is lower than the Power-Pool-wide (PP) resource threshold indicated in Table C.2
[2]Power-Pool-wide (PP) threshold values

Table C.4: Human Influence Index scoring system for Human Footprint datasets

Dataset	Scoring system
Population density	Score increased linearly from 0 to 10 persons/km2; all densities greater than 10 were assigned a score of 10.
Land use land cover	10 – built environments, 9 – cropland and paddy fields, 7 – cropland/mosaic vegetation, 0 – for all other land use land cover categories
Roads and railways	Areas within 1 km of roads and railways were assigned a score of 10, and those areas between 1 and 15 km assigned a score of 4.
Oceans and rivers	Areas within 1 km of rivers or the ocean oceans were assigned a score of 10, and those areas between 1 and 15 km assigned a score of 4.

Table C.5: Transmission and substation spatial data availability and sources

Country	Default transmission data	Country-specific substations	Country-specific transmission lines
Angola	AICD[3]	N/A	N/A
Botswana	AICD	Botswana Power Corporation	N/A
Burundi	AICD	N/A	N/A
Djibouti	N/A	N/A	N/A
DRC	AICD	N/A	N/A
Egypt	CBI[4]	N/A	N/A
Ethiopia	AICD	N/A	N/A
Kenya	AICD	KETRACO	KETRACO
Lesotho	AICD	N/A	N/A
Libya	N/A	N/A	N/A
Malawi	AICD	ESCOM	ESCOM
Mozambique	AICD	Ministry of Energy	N/A
Namibia	AICD	NamPower	NamPower
Rwanda	AICD	REDC	REDC
South Africa	AICD	Eskom	Eskom
South Sudan	CBI	N/A	N/A
Sudan	CBI	N/A	N/A
Swaziland	AICD	Swaziland Electricity Company (SEC)	Swaziland Electricity Company (SEC)
Tanzania	AICD	N/A	TANESCO (partially complete)
Uganda	AICD	UNEP	UNEP
Zambia	AICD	ZESCO	N/A
Zimbabwe	AICD	ZETDC	N/A

[3]Africa Infrastructure Country Diagnostic, an African Development Bank Initiative

[4]Cross Border Information and African Energy, 2015. African Energy Atlas 2015. http://www.africa-energy.com/african-energy-atlas

Table C.6: Parameters in levelized cost of electricity estimates

Parameters	**Wind**			**Solar PV**	**Solar CSP**	
					No-storage	**6 hr storage**
Land use factor [MW/km2](l)	9[1]			30[2]	30[2]	17[3]
Land use discount factor (f)	75%			90%	90%	
Costs	**Class I**	**Class II**	**Class III**		**No-storage**	**6 hr storage**
Generation – capital [USD/kW] (c_g)	1250[4]	1450[4]	1700[4]	2000[4]	3700[5]	7400[5]
Generation – fixed O&M [USD/MW/y] ($o_{f,g}$)	60000[4]			50000[4]	50000[4]	
Generation – variable O&M [USD/MWh] ($o_{v,g}$)	-			4[9]	-	
Transmission – capital [USD/MW/km] (c_i)	990[6]			990[6]	990[6]	
Transmission – fixed O&M [USD/km] ($o_{f,i}$)	-			-	-	
Substation – capital [USD / 2 substations (new transmission)] (c_s)	71000[6]			71000[6]	71000[6]	
Road – capital [USD/km] (c_r)	407000[7]			407000[7]	407000[7]	
Road – fixed O&M [USD/km] ($o_{f,r}$)	-			-	-	
Economic discount rate (i)	10%[8]			10%[8]	10%[8]	
Outage rate (h_o)	2%[9]			4%[9]	4%[9]	
Inverter efficiency and AC wiring loss (h_i)	-			4%[8]	-	
Array and collection loss (h_a)	15%[10]			-	-	
Lifetime [years] (n)	25[8]			25[8]	25[8]	

[1] Mean of U.S. empirical values (3 MW/km2) (Ong, Campbell, and Heath, 2012) and theoretical land use factors (Black & Veatch Corp. and RETI Coordinating Committee, 2009)

[2] (Ong, Campbell, and Heath, 2012)

[3] Estimated from no-storage land use factor by multiplying by the ratio of no-storage to 6-hr-storage solar multiples (2.1/1.2)

[4] For Class II turbine: (Veatch and NREL, 2012). See (Institute, 2011) for decrease in Class I turbine cost, and (Lantz, Ryan Wiser, and Hand, 2012; R. Wiser et al., 2012) for increase in Class III turbine costs, relative to Class I turbine costs.

[5] (IRENA, 2013a)

[6] (Veatch and NREL, 2012)

[7] (Africon, 2008)

[8] (IRENA, 2013b)

[9] Default value in the System Advisor Model (SAM) by NREL

[10] (Tegen et al., 2013)

Table C.7: Projected 2030 electricity demand

Country	**2030 Demand (GWh)**	**Peak demand (MW)**	**Wind capacity to install by 2030 to meet 30% RPS (MW)**[5]
Angola	20294	-	N/A [6]
Botswana	7730	578	882
Burundi	622	-	N/A
Democratic Republic Of Congo	21225	-	N/A
Djibouti	764	-	N/A
Egypt	455525	-	N/A
Ethiopia	21363	-	N/A
Kenya	20646	-	N/A
Lesotho	1309	-	N/A
Libya	5420	-	N/A
Malawi	3667	475.9	419
Mozambique	8840	761	1009
Namibia	5420	546	619
Rwanda	788	-	N/A
South Africa	453069	35360	51720
Sudan	58754	-	N/A
Swaziland	1952	223	223
Tanzania	10923	898.79	1247
Uganda	9313	-	N/A
Zambia	18003	1794.6	2055
Zimbabwe	25153	1621	2871

[5]Renewable Portfolio Standard, or a target amount of renewable energy
[6]N/A: Optimal wind site selection was not performed for this country
[7]All natural gas values are from (U.S. Energy Information Administration, 2016).
[8]All coal cost values are (U.S. Energy Information Administration, 2016).
[9]Costs used to calculate annual amortized cost of wind capacity assume Class II turbine using values from Table C.6
[10]From (Taylor et al., 2015) (Figure 7.3, pg 118). This value is the average capital cost of African hydropower plants.
[11]U.S. Energy Information Administration, 2016
[12](U.S. Energy Information Administration, 2016)
[13]Calculated using the above fuel inputs
[14](U.S. Energy Information Administration, 2016)

Table C.8: Cost inputs for comparing wind build-out scenarios

	Natural gas combustion turbine (CT)[7]	**Scrubbed Coal**[8]	**Hydropower**	**Wind**[9]
Capital cost ($/MW)	922,000	2,726,000	1,500,000 [10]	1450000
Fixed O&M ($/MW-yr)	5,260	31,160	15,150 [11]	60000
Variable O&M $/MWh	15.44	5	5 [12]	-
Heating value (BTU/lb)	-	10000	-	-
Fuel cost ($/MMBTU or $/MT)	-	50	-	-
Heat rate BTU/kWh	-	8800	-	-
Aux Consumption (%)	-	10	-	-
Discount rate (%)	10	10	10	10
Plant lifetime (yrs)	25	25	25	25
Marginal cost of generation ($/MWh)	-	23.2 [13]	5 [14]	-

Appendix D

Appendix for Chapter 5

D.1 Additional Figures

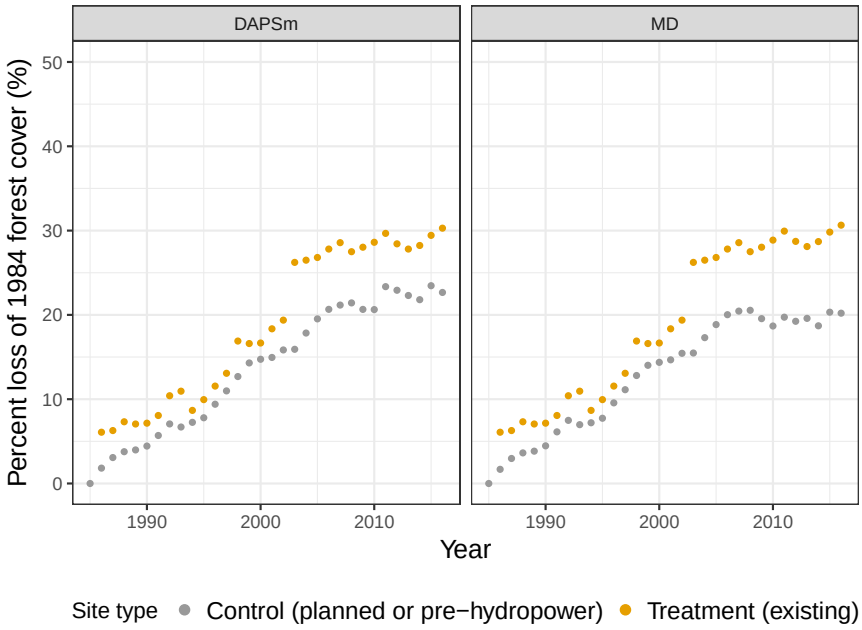

Figure D.1: Annual average percent loss of 1984 forest cover for control and treatment values

Plots show the annual average percent loss of 1984 forest cover for DAPSm and MD matched controls. Note the treatment averages are the same between panels.

D.2 Additional Tables

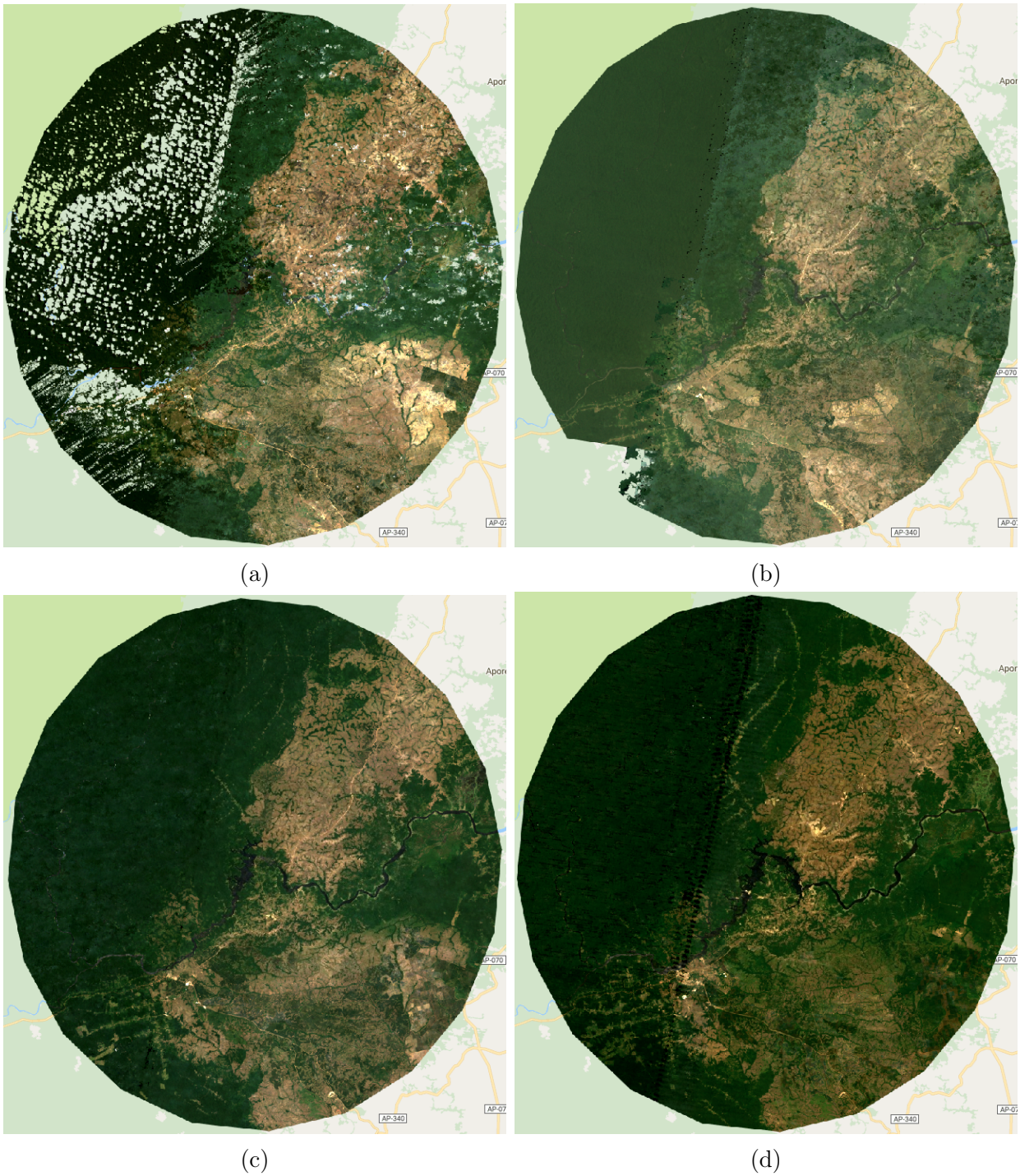

(a) (b)

(c) (d)

Figure D.2: Three-year Landsat composites of the Coaracy Nunes Dam

Composite correspond to the following median years: 1987 (a), 1991 (b), 2001 (c), 2016 (d). Composite quality is extremely poor in the earlier decades due to heavy cloud cover and contamination. Note the emerging deforestation patterns north of the dam visible in the 2000s.

Table D.1: First differences regression summary for Landsat estimated perfect loss of 1984 forest cover with and without a lagged dependent variable

	Dependent variable:			
	Percent loss of 1984 forest cover			
	DAPSm	MD	DAPSm	MD
	(1)	(2)	(3)	(4)
treatment_time	0.013***	0.012***	0.016***	0.015***
	(0.005)	(0.005)	(0.005)	(0.005)
lag(percent1984ForestLost_50km_R, 1:2)1			0.216***	0.210***
			(0.055)	(0.054)
lag(percent1984ForestLost_50km_R, 1:2)2			0.025	0.020
			(0.041)	(0.028)
time_trend	0.005*	0.006**	0.001	0.001
	(0.003)	(0.003)	(0.003)	(0.003)
treatment_time:CapacityMW	−0.00000	−0.00000**	−0.00000	−0.00000***
	(0.00000)	(0.00000)	(0.00000)	(0.00000)
time_trend:DistProtArea_km	0.0001***	0.0001***	0.0001*	0.0001*
	(0.00003)	(0.00003)	(0.00004)	(0.00004)
time_trend:existingDam_dist_km	0.00000	0.00000	0.00001	0.00001
	(0.00001)	(0.00001)	(0.00001)	(0.00001)
time_trend:city_dist_km	0.00000	−0.00000	0.00001	0.00001
	(0.00000)	(0.00000)	(0.00000)	(0.00000)
Observations	1,579	1,704	1,460	1,579
R^2	0.002	0.003	0.034	0.029
Adjusted R^2	−0.001	−0.0004	0.029	0.025
F Statistic	−4.059	−3.857	4.225***	3.384***
Note:				*p<0.1; **p<0.05; ***p<0.01

Table D.2: First differences regression summary for percent of agricultural land with and without a lagged dependent variable

	Dependent variable:					
	Percent of agricultural land					
	DAPSm	MD	Opt PS	DAPSm	MD	Opt PS
	(1)	(2)	(3)	(4)	(5)	(6)
treatment_time	0.003	0.004**	0.004**	0.001	0.001	0.001
	(0.002)	(0.002)	(0.002)	(0.001)	(0.001)	(0.001)
lag(percent_nonForested, 1:2)1				0.803***	0.811***	0.801***
				(0.038)	(0.045)	(0.041)
lag(percent_nonForested, 1:2)2				0.053	0.046	0.052
				(0.034)	(0.036)	(0.033)
time_trend:DistProtArea_km	0.0001***	0.0001***	0.0001***	0.00002***	0.00001***	0.00002***
	(0.00003)	(0.00003)	(0.00002)	(0.00001)	(0.00001)	(0.00001)
treatment_time:CapacityMW	−0.00000	−0.00000	−0.00000	−0.00000**	−0.00000**	−0.00000*
	(0.00000)	(0.00000)	(0.00000)	(0.00000)	(0.00000)	(0.00000)
time_trend:existingDam_dist_km	0.00001	0.00000	−0.00000	0.00000	0.00000	−0.00000
	(0.00000)	(0.00000)	(0.00000)	(0.00000)	(0.00000)	(0.00000)
time_trend:city_dist_km	0.00001***	0.00001**	0.00000***	0.00000***	0.00000***	0.00000***
	(0.00000)	(0.00000)	(0.00000)	(0.00000)	(0.00000)	(0.00000)
Observations	855	870	870	741	754	754
R^2	0.178	0.199	0.312	0.757	0.756	0.779
Adjusted R^2	0.174	0.195	0.309	0.755	0.754	0.777
F Statistic	30.543***	29.510***	80.223***	379.956***	382.724***	435.185***
Note:						*p<0.1; **p<0.05; ***p<0.01

Table D.3: Generalized Method of Moments (GMM) regression summary using both percent of forest loss and agricultural land as dependent variables

	Dependent variable:			
	Percent loss of 1984 forest cover		Percent of agricultural land	
	DAPSm	MD	MD	Opt PS
	(1)	(2)	(3)	(4)
lag(percent1984ForestLost_50km_R, 1:2)1	1.025***	1.005***		
	(0.043)	(0.043)		
lag(percent1984ForestLost_50km_R, 1:2)2	−0.080*	−0.061		
	(0.044)	(0.040)		
lag(percent_nonForested, 1:2)1			1.376***	1.306***
			(0.069)	(0.081)
lag(percent_nonForested, 1:2)2			−0.396***	−0.317***
			(0.071)	(0.087)
lag(treatment_time, 0:1)0	0.016***	0.013**	0.001	0.0003
	(0.006)	(0.005)	(0.001)	(0.001)
lag(treatment_time, 0:1)1	−0.011*	−0.011**	−0.0002	−0.0001
	(0.006)	(0.005)	(0.001)	(0.001)
Observations	52	56	58	58

Note: *p<0.1; **p<0.05; ***p<0.01

Table D.4: Fixed effects regression summary for Landsat estimated percent loss of 1984 forest cover at different buffer distances from the treatment or control site for DAPSm matched controls

	Dependent variable:				
	Percent loss of 1984 forest cover				
	10 km	20 km	30 km	40 km	50 km
	(1)	(2)	(3)	(4)	(5)
treatment_time	0.059**	0.072***	0.074***	0.067**	0.055***
	(0.026)	(0.027)	(0.027)	(0.027)	(0.020)
time_trend:DistProtArea_km	0.0001***	0.0001***	0.0001***	0.0001***	0.0001***
	(0.00004)	(0.00004)	(0.00003)	(0.00004)	(0.00003)
treatment_time:CapacityMW	0.00001	0.00000	0.00000	0.00000	−0.00000
	(0.00001)	(0.00001)	(0.00001)	(0.00001)	(0.00001)
time_trend:existingDam_dist_km	−0.00001	−0.00000	−0.00000	0.00000	0.00000
	(0.00001)	(0.00001)	(0.00001)	(0.00001)	(0.00001)
time_trend:city_dist_km	0.00000	0.00000	0.00000	0.00000	0.00000
	(0.00000)	(0.00000)	(0.00000)	(0.00000)	(0.00000)
Observations	1,664	1,664	1,664	1,664	1,631
R^2	0.139	0.134	0.134	0.134	0.198
Adjusted R^2	0.092	0.086	0.087	0.087	0.153
F Statistic	51.064***	48.843***	48.964***	48.899***	76.394***
Note:					*p<0.1; **p<0.05; ***p<0.01

Table D.5: Fixed effects regression summary for Landsat estimated percent loss of 1984 forest cover at different buffer distances from the treatment or control site for Mahalanobis matched controls

	Dependent variable:				
	Percent loss of 1984 forest cover				
	10 km	20 km	30 km	40 km	50 km
	(1)	(2)	(3)	(4)	(5)
treatment_time	0.051**	0.058**	0.064**	0.067***	0.055***
	(0.024)	(0.026)	(0.025)	(0.025)	(0.017)
time_trend:DistProtArea_km	0.0001**	0.0001***	0.0001***	0.0001***	0.0001***
	(0.00004)	(0.00004)	(0.00004)	(0.00003)	(0.00003)
treatment_time:CapacityMW	0.00001***	0.00001**	0.00000	0.00000	0.00000
	(0.00000)	(0.00000)	(0.00000)	(0.00000)	(0.00000)
time_trend:existingDam_dist_km	−0.00001	−0.00001	−0.00001	−0.00000	−0.00001
	(0.00001)	(0.00001)	(0.00001)	(0.00001)	(0.00001)
time_trend:city_dist_km	0.00000	−0.00000	−0.00000	−0.00000	−0.00000
	(0.00000)	(0.00000)	(0.00000)	(0.00000)	(0.00000)
Observations	1,792	1,792	1,792	1,792	1,760
R^2	0.129	0.121	0.134	0.144	0.238
Adjusted R^2	0.083	0.074	0.087	0.098	0.196
F Statistic	50.445***	46.885***	52.500***	57.045***	104.213***
Note:					*p<0.1; **p<0.05; ***p<0.01

Table D.6: Match identification numbers and the project names of the corresponding control and treatment hydropower plants for each matching approach (DAPSm, MD, Opt PS)

Match ID	treatment_DAPSm	control_DAPSm	control_MD	treatment_MD	treatment_OptPS	control_OptPS
1	Curua-Una	Sororoca	Berimbau	Curua-Una	alta_floresta	JatobA
2	coaracy_nunes	AguaBranca	IlhaSAPSoPedro	Samuel	altoe_2	MachadinhoI
3	Samuel	Jaburu	SAPSoLuizdoTapajos	BeloMonte	Balbina	CachoeiradoMeio
4	Balbina	Katuema	Erikpatsa	alta_floresta	BeloMonte	SAPSoLuizdoTapajos
5	Tucurui	BeloMonte	AguaBranca	SantoAntoniodoJari	braco_norte_1	SumaAoma
6	pitinga	Carona	Inferninho	Dardanelos	braco_norte_2	Itacaiunas2
7	braco_norte_2	Juara	castanheira	FaxinalII	braco_norte_3	ChacorAPSo
8	altoe_2	SAPSoJoAPSodaBarra-SecundArio	MachadinhoI	rondon2	braco_norte_4	QuebraRemo
9	Lajeado	NovoAcordo	JardimdeOuro	salto_tres_de_maio	CachoeiraCaldeirao	CachoeiraAguaPreta
10	saldanha	PEX-093	CabeASSadeBoi	braco_norte_3	chupinguaia	Sapopema
11	rondon2	SAN-020	Frieira	Balbina	coaracy_nunes	Sororoca
12	salto_curua	JardimdeOuro	JRN-530	saldanha	colider	SaltoApiacAs
13	salto_tres_de_maio	ARN-026	Katuema	pitinga	Curua-Una	BarradoClaro
14	braco_norte_1	BarradoClaro	ji-parana	jirau	Dardanelos	Prainha
15	braco_norte_3	ApiakAKayabi	BeloMonte	Tucurui	FaxinalII	castanheira
16	braco_norte_4	CabeASSadeBoi	Jutuarama	CachoeiraCaldeirao	Jamari	Perdida1
17	alta_floresta	SAPSoJoAPSodaBarra-PrimArio	Jaburu	altoe_2	jirau	Babaquara_Altamira
18	chupinguaia	JRN-577	SaltoApiacAs	colider	Lajeado	PancadaGrande
19	CachoeiraCaldeirao	UrucupatA	JRN-277	sao-manoel	pitinga	ManacA
20	jirau	CachoeiraSantoAntAnio	cabeca_de_boi	braco_norte_4	rondon2	SAPSoSimAPSoAlto
21	santo-antonio	Tabajara	CachoeiradosPatos	salto_curua	saldanha	SaltoAugustoBaixo
22	SantoAntoniodoJari	A41PA008	Escondido	teles-pires	salto_curua	Iara
23	sao-manoel	cabeca_de_boi	SantoAntoniodoJari	coaracy_nunes	salto_tres_de_maio	TrairAPSo
24	colider	Castanheira	Castanheira	chupinguaia	Samuel	IlhaSAPSoPedro
25	Jamari	MachadinhoI	Juara	braco_norte_1	santo-antonio	cachoeira-porteira
26	Dardanelos	TucumAPS	MarabA	Lajeado	SantoAntoniodoJari	A41PA008
27	FaxinalII	QuebraRemo	colider	braco_norte_2	sao-manoel	Candeia
28	BeloMonte	Babaquara_Altamira	Tabajara	santo-antonio	teles-pires	SAPSoJoAPSodaBarra-PrimArio
29	teles-pires	SaltoApiacAs	BarradoClaro	Jamari	Tucurui	SAPSoJoAPSodaBarra-SecundArio

Bibliography

Africon (2008). *Africa Infrastructure Country Diagnostic: Unit Costs of Infrastructure Projects in Sub-saharan Africa*. Tech. rep.

Alho, Cleber J.R. (2011). "Environmental Effects of Hydropower Reservoirs on Wild Mammals and Freshwater Turtles in Amazonia: A Review". en. In: *Oecologia Australis* 15.3, pp. 593–604. ISSN: 21776199. DOI: 10.4257/oeco.2011.1503.11. URL: https://revistas.ufrj.br/index.php/oa/article/view/8151 (visited on 04/20/2018).

Allison, Taber D., Terry L. Root, and Peter C. Frumhoff (2014). "Thinking globally and siting locally – renewable energy and biodiversity in a rapidly warming world". en. In: *Climatic Change* 126.1-2, pp. 1–6. ISSN: 0165-0009, 1573-1480. DOI: 10.1007/s10584-014-1127-y. URL: https://link.springer.com/article/10.1007/s10584-014-1127-y (visited on 04/17/2018).

Andrade Meireles, Antonio Jeovah de et al. (2013). "Socio-environmental impacts of wind farms on the traditional communities of the western coast of Ceará, in the Brazilian Northeast". In: *Journal of Coastal Research*, pp. 81–86. URL: http://ics2013.org/papers/Paper3867_rev.pdf (visited on 07/24/2015).

Ansar, Atif et al. (2014). *Should We Build More Large Dams? The Actual Costs of Hydropower Megaproject Development*. SSRN Scholarly Paper ID 2406852. Rochester, NY: Social Science Research Network. URL: http://papers.ssrn.com/abstract=2406852 (visited on 08/14/2015).

Arima, Eugenio Y. et al. (2014). "Public policies can reduce tropical deforestation: Lessons and challenges from Brazil". In: *Land Use Policy* 41, pp. 465–473. ISSN: 0264-8377. DOI: 10.1016/j.landusepol.2014.06.026. URL: http://www.sciencedirect.com/science/article/pii/S026483771400146X (visited on 05/09/2018).

Aydin, Nazli Yonca, Elcin Kentel, and Sebnem Duzgun (2010). "GIS-based environmental assessment of wind energy systems for spatial planning: A case study from Western Turkey". In: *Renewable and Sustainable Energy Reviews* 14.1, pp. 364–373. ISSN: 1364-0321. DOI: 10.1016/j.rser.2009.07.023. URL: http://www.sciencedirect.com/science/article/pii/S1364032109001610 (visited on 04/09/2013).

Baig, Muhammad Hasan Ali et al. (2014). "Derivation of a tasselled cap transformation based on Landsat 8 at-satellite reflectance". In: *Remote Sensing Letters* 5.5, pp. 423–431. ISSN: 2150-704X. DOI: 10.1080/2150704X.2014.915434. URL: https://doi.org/10.1080/2150704X.2014.915434 (visited on 05/09/2018).

Baltagi, Badi Hani (2015). *The Oxford Handbook of Panel Data*. en. Google-Books-ID: iHHDBAAAQBAJ. Oxford University Press. ISBN: 978-0-19-994004-2.

Barber, Christopher P. et al. (2014). "Roads, deforestation, and the mitigating effect of protected areas in the Amazon". In: *Biological Conservation* 177, pp. 203–209.

Barbier, Edward B. and Joanne C. Burgess (2001). "The Economics of Tropical Deforestation". en. In: *Journal of Economic Surveys* 15.3, pp. 413–433. ISSN: 1467-6419. DOI: 10.1111/1467-6419.00144. URL: http://onlinelibrary.wiley.com/doi/abs/10.1111/1467-6419.00144 (visited on 05/09/2018).

Barbier, Edward B., Joanne C. Burgess, and Alan Grainger (2010). "The forest transition: Towards a more comprehensive theoretical framework". In: *Land Use Policy*. Forest transitions 27.2, pp. 98–107. ISSN: 0264-8377. DOI: 10.1016/j.landusepol.2009.02.001. URL: http://www.sciencedirect.com/science/article/pii/S0264837709000131 (visited on 05/09/2018).

Barthem, Ronaldo Borges, Mauro César Lambert de Brito Ribeiro, and Miguel Petrere (1991). "Life strategies of some long-distance migratory catfish in relation to hydroelectric dams in the Amazon Basin". In: *Biological Conservation* 55.3, pp. 339–345. ISSN: 0006-3207. DOI: 10.1016/0006-3207(91)90037-A. URL: http://www.sciencedirect.com/science/article/pii/000632079190037A (visited on 05/08/2018).

Benchimol, Maíra and Carlos A. Peres (2015). "Widespread Forest Vertebrate Extinctions Induced by a Mega Hydroelectric Dam in Lowland Amazonia". en. In: *PLOS ONE* 10.7, e0129818. ISSN: 1932-6203. DOI: 10.1371/journal.pone.0129818. URL: http://journals.plos.org/plosone/article?id=10.1371/journal.pone.0129818 (visited on 04/20/2018).

Berrill, Peter et al. (2016). "Environmental impacts of high penetration renewable energy scenarios for Europe". en. In: *Environmental Research Letters* 11.1, p. 014012. ISSN: 1748-9326. DOI: 10.1088/1748-9326/11/1/014012. URL: http://stacks.iop.org/1748-9326/11/i=1/a=014012 (visited on 04/17/2018).

Bird, L and M.R. Milligan (2012). *Lessons from Large-Scale Renewable Energy Integration Studies*. Tech. rep. Golden, CO: National Renewable Energy Laboratory.

Black & Veatch Corp. and NREL (2009). *Western Renewable Energy Zones, Phase 1: QRA Identification Technical Report*. Tech. rep. NREL/SR-6A2-46877. Western Governor's Association.

Black & Veatch Corp. and RETI Coordinating Committee (2009). *Renewable Energy Transmission Initiative (RETI) Phase 1B Final Report*. Tech. rep. RETI-1000-2008-003-F. URL: http://www.energy.ca.gov/reti/documents/index.html.

Bofinger, Stefan, Crescent Mushwana, and Tobias Bischof-Niemz (2015). *Smoothing out the Volatility of South Africa's Wind and PV Energy Resources*. Cape Town, South Africa.

Bowen, Brian H., F. T. Sparrow, and Zuwei Yu (1999). "Modeling electricity trade policy for the twelve nations of the Southern African Power Pool (SAPP)". In: *Utilities Policy* 8.3, pp. 183–197. DOI: 10.1016/S0957-1787(99)00019-3. URL: http://www.sciencedirect.com/science/article/pii/S0957178799000193 (visited on 07/08/2015).

California Energy Commission-Siting, Transmission and Environmental Protection Division (2012). *Map of Power Plants in California*. URL: http://www.energy.ca.gov/maps/powerplants/power_plant_statewide.html (visited on 11/20/2013).

California Public Utilities Commission [CPUC] (2009). *Renewable Energy Transmission Initiative (RETI) Phase 1B*. Tech. rep. URL: http://www.energy.ca.gov/reti/documents/index.html.

Cameron, D. Richard, Brian S. Cohen, and Scott A. Morrison (2012). "An Approach to Enhance the Conservation-Compatibility of Solar Energy Development". In: *PLoS ONE* 7.6, e38437. DOI: 10.1371/journal.pone.0038437. URL: http://dx.doi.org/10.1371/journal.pone.0038437 (visited on 03/06/2014).

Cervigni, Raffaello et al. (2015). *Enhancing the Climate Resilience of Africa's Infrastructure: The Power and Water Sectors*. Tech. rep. Washington, DC: World Bank.

Chikobvu, Delson and Caston Sigauke (2013). "Modelling influence of temperature on daily peak electricity demand in South Africa". In: *Journal of Energy in Southern Africa* 24.4, pp. 63–70. ISSN: 1021-447X. URL: http://www.scielo.org.za/scielo.php?script=sci_abstract&pid=S1021-447X2013000400008&lng=en&nrm=iso&tlng=en (visited on 10/21/2016).

Chomitz, Kenneth M. and David A. Gray (1995). "Roads, lands, markets, and deforestation: a spatial model of land use in Belize". In: *World Bank Policy Research Working Paper* 1444.

Chowdhury, Rinku Roy (2006). "Driving forces of tropical deforestation: The role of remote sensing and spatial models". In: *Singapore Journal of Tropical Geography* 27.1, pp. 82–101.

Clifton, Julian and Bryan J. Boruff (2010). "Assessing the potential for concentrated solar power development in rural Australia". In: *Energy Policy*. Special Section on Carbon Emissions and Carbon Management in Cities with Regular Papers 38.9, pp. 5272–5280. ISSN: 0301-4215. DOI: 10.1016/j.enpol.2010.05.036. URL: http://www.sciencedirect.com/science/article/pii/S0301421510004076 (visited on 05/09/2018).

Cochran, J et al. (2012). *Integrating Variable Renewable Energy on the Electric Power Markets: Best Practices from International Experience*. Tech. rep. National Renewable Energy Laboratory.

Collier, Paul and Anthony J. Venables (2012). "Greening Africa? Technologies, endowments and the latecomer effect". In: *Energy Economics*. Green Perspectives 34, Supplement 1, S75–S84. ISSN: 0140-9883. DOI: 10.1016/j.eneco.2012.08.035. URL: http://www.sciencedirect.com/science/article/pii/S0140988312002058 (visited on 05/28/2016).

Copeland, Holly E. et al. (2009). "Mapping Oil and Gas Development Potential in the US Intermountain West and Estimating Impacts to Species". In: *PLoS ONE* 4.10, e7400. DOI: 10.1371/journal.pone.0007400. URL: http://dx.doi.org/10.1371/journal.pone.0007400 (visited on 04/12/2013).

Crist, Eric P (1985). "A TM Tasseled Cap equivalent transformation for reflectance factor data". In: *Remote Sensing of Environment* 17.3, pp. 301–306. ISSN: 0034-4257. DOI: 10.

1016/0034-4257(85)90102-6. URL: http://www.sciencedirect.com/science/article/pii/0034425785901026 (visited on 05/09/2018).

Croissant, Yves and Giovanni Millo (2008). "Panel Data Econometrics in R : The plm Package". en. In: *Journal of Statistical Software* 27.2. ISSN: 1548-7660. DOI: 10.18637/jss.v027.i02. URL: http://www.jstatsoft.org/v27/i02/ (visited on 05/09/2018).

Cropper, Maureen, Jyotsna Puri, and Charles Griffiths (2001). "Predicting the location of deforestation: The role of roads and protected areas in North Thailand". In: *Land Economics* 77.2, pp. 172–186.

Davidson, Michael R. et al. (2016). "Modelling the potential for wind energy integration on China's coal-heavy electricity grid". In: *Nature Energy* 1.7, p. 16086. ISSN: 2058-7546. DOI: 10.1038/nenergy.2016.86. URL: http://www.nature.com/articles/nenergy201686 (visited on 07/14/2016).

Dawson, Lucas and Peter Schlyter (2012). "Less is more: Strategic scale site suitability for concentrated solar thermal power in Western Australia". In: *Energy Policy* 47, pp. 91–101. ISSN: 0301-4215. DOI: 10.1016/j.enpol.2012.04.025. URL: http://www.sciencedirect.com/science/article/pii/S0301421512003254 (visited on 04/09/2013).

Del Franco, Mark (2014). "North American Windpower: Piggybacking Wind And Solar: Can Two Renewable Energy Sources Peacefully Co-Exist?" In: *North American Wind Power*. URL: http://www.nawindpower.com/e107_plugins/content/content.php?content.13003 (visited on 10/15/2014).

Denholm, Paul, Maureen Hand, et al. (2009). *Land-use requirements of modern wind power plants in the United States*. Tech. rep. National Renewable Energy Laboratory Golden, CO. (Visited on 03/16/2015).

Denholm, Paul and Robert M. Margolis (2008). "Land-use requirements and the per-capita solar footprint for photovoltaic generation in the United States". In: *Energy Policy* 36.9, pp. 3531–3543. ISSN: 0301-4215. DOI: 10.1016/j.enpol.2008.05.035. URL: http://www.sciencedirect.com/science/article/pii/S0301421508002796 (visited on 09/23/2012).

Department of Environmental Affairs, South African National Biodiversity Institute, and GIZ (2013). *Climate Trends and Scenarios Factsheet for South Africa*. URL: http://www.sanbi.org/sites/default/files/documents/documents/ltas-factsheetclimate-trends-and-scenarios2013.pdf.

Desert Renewable Conservation Plan (2012). *Primary Features of DRECP Alternatives*. URL: http://www.drecp.org/documents/docs/2012-12-21_DRECP_Alternatives_Primary_Features.pdf.

Dias, Lívia C. P. et al. (2016). "Patterns of land use, extensification, and intensification of Brazilian agriculture". en. In: *Global Change Biology* 22.8, pp. 2887–2903. ISSN: 1365-2486. DOI: 10.1111/gcb.13314. URL: http://onlinelibrary.wiley.com/doi/abs/10.1111/gcb.13314 (visited on 05/09/2018).

Drake, Ben and Klaus Hubacek (2007). "What to expect from a greater geographic dispersion of wind farms?—A risk portfolio approach". In: *Energy Policy* 35.8, pp. 3999–4008. ISSN:

0301-4215. DOI: 10.1016/j.enpol.2007.01.026. URL: http://www.sciencedirect.com/science/article/pii/S030142150700033X (visited on 05/12/2016).

Du, Yong, Philippe M. Teillet, and Josef Cihlar (2002). "Radiometric normalization of multitemporal high-resolution satellite images with quality control for land cover change detection". In: *Remote sensing of Environment* 82.1, pp. 123–134.

Eastern Africa Power Pool et al. (2011). *Regional Power System Master Plan and Grid Code Study*. Tech. rep. URL: http://eac.int/energy/index.php?option=com_docman&task=cat_view&gid=81&Itemid=70.

Eberhard, Anton et al. (2011). *Africa's power infrastructure : investment, integration, efficiency*. Tech. rep. Washington, DC: The World Bank. URL: http://www.ppiaf.org/sites/ppiaf.org/files/publication/Africas-Power-Infrastructure-2011.pdf.

Edwards, David P. et al. (2014). "Mining and the African Environment". en. In: *Conservation Letters* 7.3, pp. 302–311. ISSN: 1755-263X. DOI: 10.1111/conl.12076. URL: http://onlinelibrary.wiley.com/doi/abs/10.1111/conl.12076 (visited on 05/08/2018).

Electricity Reliability Council of Texas (ERCOT) (2008). *Competitive Renewable Energy Zones Transmission Optimization Study*. Tech. rep. ERCOT System Planning. URL: http://www.ercot.com/news/presentations/ (visited on 03/06/2014).

Ellis, Erle C. (2011). "Anthropogenic transformation of the terrestrial biosphere". en. In: *Philosophical Transactions of the Royal Society of London A: Mathematical, Physical and Engineering Sciences* 369.1938, pp. 1010–1035. ISSN: 1364-503X, 1471-2962. DOI: 10.1098/rsta.2010.0331. URL: http://rsta.royalsocietypublishing.org/content/369/1938/1010 (visited on 05/09/2018).

EPE (2016). *Demanda de Energia 2050*. NOTA TÉCNICA DEA 13/15. Empresa de Pesquisa Energética. URL: http://www.epe.gov.br/sites-pt/publicacoes-dados-abertos/publicacoes/PublicacoesArquivos/publicacao-227/topico-202/DEA%2013-15%20Demanda%20de%20Energia%202050.pdf (visited on 05/07/2018).

[EWIS] European Wind Integration Study (2010). *Towards a Successful Integration of Large Scale Wind Power into European Electricity Grids. Final Report*. Tech. rep. Brussels: European Network of Transmission System Operators for Electricity. URL: http://www.wind-integration.eu/downloads/library/EWIS_Final_Report.pdf (visited on 03/05/2014).

Farah, Tatiana (2016). *Proposed Amazon dam attracts illegal loggers, threatens local farmers*. en-US. URL: https://news.mongabay.com/2016/05/proposed-amazon-dam-attracts-illegal-loggers-threatens-local-farmers/ (visited on 05/09/2018).

Fearnside, Philip M. (1989). "Brazil's Balbina Dam: Environment versus the legacy of the Pharaohs in Amazonia". en. In: *Environmental Management* 13.4, pp. 401–423. ISSN: 0364-152X, 1432-1009. DOI: 10.1007/BF01867675. URL: http://link.springer.com/article/10.1007/BF01867675 (visited on 05/09/2018).

— (1999). "Social Impacts of Brazil's Tucuruí Dam". en. In: *Environmental Management* 24.4, pp. 483–495. ISSN: 0364-152X, 1432-1009. DOI: 10.1007/s002679900248. URL: http://link.springer.com/article/10.1007/s002679900248 (visited on 05/09/2018).

Fearnside, Philip M. (2005). "Deforestation in Brazilian Amazonia: History, Rates, and Consequences". In: *Conservation Biology* 19.3, pp. 680–688. ISSN: 0888-8892. DOI: 10.1111/j.1523-1739.2005.00697.x. URL: https://onlinelibrary-wiley-com.libproxy.berkeley.edu/doi/full/10.1111/j.1523-1739.2005.00697.x (visited on 05/09/2018).

— (2008). "The Roles and Movements of Actors in the Deforestation of Brazilian Amazonia". In: *Ecology and Society* 13.1. ISSN: 1708-3087. URL: http://www.jstor.org/stable/26267941 (visited on 04/20/2018).

— (2014). "Impacts of Brazil's Madeira River dams: Unlearned lessons for hydroelectric development in Amazonia". In: *Environmental Science & Policy* 38, pp. 164–172.

Fearnside, Philip M. and Salvador Pueyo (2012). "Greenhouse-gas emissions from tropical dams". en. In: *Nature Climate Change* 2.6, pp. 382–384. ISSN: 1758-678X, 1758-6798. DOI: 10.1038/nclimate1540. URL: http://www.nature.com/doifinder/10.1038/nclimate1540 (visited on 05/08/2018).

FERC (2016). "Energy Infrastructure Update For December 2016". en. In: p. 8.

Fertig, Emily et al. (2012). "The effect of long-distance interconnection on wind power variability". en. In: *Environmental Research Letters* 7.3, p. 034017. ISSN: 1748-9326. DOI: 10.1088/1748-9326/7/3/034017. URL: http://stacks.iop.org/1748-9326/7/i=3/a=034017 (visited on 11/04/2016).

Fischlein, Miriam et al. (2013). "States of transmission: Moving towards large-scale wind power". In: *Energy Policy* 56, pp. 101–113. ISSN: 0301-4215. DOI: 10.1016/j.enpol.2012.11.028. URL: http://www.sciencedirect.com/science/article/pii/S0301421512010105 (visited on 05/11/2016).

Fripp, Matthias (2012). "Switch: A Planning Tool for Power Systems with Large Shares of Intermittent Renewable Energy". In: *Environmental Science & Technology* 46.11, pp. 6371–6378. ISSN: 0013-936X. DOI: 10.1021/es204645c. URL: http://dx.doi.org/10.1021/es204645c (visited on 10/15/2013).

Fritsche, Uwe R. et al. (2017). *Energy and Land Use*. Tech. rep. UNCCD and IRENA. URL: https://static1.squarespace.com/static/5694c48bd82d5e9597570999/t/59ce3cb68fd4d2da17339c3c/1506688188502/Fritsche+et+al+%282017%29+Energy+and+Land+Use+-+GLO+paper-corr.pdf (visited on 04/16/2018).

Fthenakis, Vasilis and Hyung Chul Kim (2009). "Land use and electricity generation: A life-cycle analysis". In: *Renewable and Sustainable Energy Reviews* 13.6–7, pp. 1465–1474. ISSN: 1364-0321. DOI: 10.1016/j.rser.2008.09.017. URL: http://www.sciencedirect.com/science/article/pii/S1364032108001354.

Gipe, Paul (2004). *Wind Power*.

Gitelson, Anatoly A., Yoram J. Kaufman, and Mark N. Merzlyak (1996). "Use of a green channel in remote sensing of global vegetation from EOS-MODIS". In: *Remote Sensing of Environment* 58.3, pp. 289–298. ISSN: 0034-4257. DOI: 10.1016/S0034-4257(96)00072-7. URL: http://www.sciencedirect.com/science/article/pii/S0034425796000727 (visited on 05/09/2018).

Gorelick, Noel et al. (2017). "Google Earth Engine: Planetary-scale geospatial analysis for everyone". In: *Remote Sensing of Environment*. Big Remotely Sensed Data: tools, applications and experiences 202, pp. 18–27. ISSN: 0034-4257. DOI: 10.1016/j.rse.2017.06.031. URL: http://www.sciencedirect.com/science/article/pii/S0034425717302900 (visited on 05/09/2018).

Graeber, Bernhard, Randall Spalding-Fecher, and Brian Gonah (2005). "Optimising transnational power generation and transmission investments: a Southern African example". In: *Energy Policy* 33.18, pp. 2337–2349. DOI: 10.1016/j.enpol.2004.04.025. URL: http://www.sciencedirect.com/science/article/pii/S0301421504001557 (visited on 07/08/2015).

Guryan, Jonathan (2001). *Desegregation and Black Dropout Rates*. NBER Working Paper 8345. National Bureau of Economic Research, Inc. URL: https://econpapers.repec.org/paper/nbrnberwo/8345.htm (visited on 05/09/2018).

Haaren, Rob van and Vasilis Fthenakis (2011). "GIS-based wind farm site selection using spatial multi-criteria analysis (SMCA): Evaluating the case for New York State". In: *Renewable and Sustainable Energy Reviews* 15.7, pp. 3332–3340. ISSN: 1364-0321. DOI: 10.1016/j.rser.2011.04.010. URL: http://www.sciencedirect.com/science/article/pii/S136403211100147X (visited on 09/11/2013).

Hansen, M. C. et al. (2013). "High-Resolution Global Maps of 21st-Century Forest Cover Change". en. In: *Science* 342.6160, pp. 850–853. ISSN: 0036-8075, 1095-9203. DOI: 10.1126/science.1244693. URL: http://science.sciencemag.org/content/342/6160/850 (visited on 05/09/2018).

Hargrave, Jorge and Krisztina Kis-Katos (2013). "Economic Causes of Deforestation in the Brazilian Amazon: A Panel Data Analysis for the 2000s". en. In: *Environmental and Resource Economics* 54.4, pp. 471–494. ISSN: 0924-6460, 1573-1502. DOI: 10.1007/s10640-012-9610-2. URL: http://link.springer.com/article/10.1007/s10640-012-9610-2 (visited on 05/09/2018).

Harrison, S (1991). "Population growth, land use and deforestation in Costa Rica, 1950-1984. Crecimiento de la población, uso de la tierra y deforestación en Costa Rica, 1950-1984." In: *Interciencia* 16.2. URL: http://www.sidalc.net/cgi-bin/wxis.exe/?IsisScript=oet.xis&method=post&formato=2&cantidad=1&expresion=mfn=011579 (visited on 05/09/2018).

Healey, Sean P. et al. (2005). "Comparison of Tasseled Cap-based Landsat data structures for use in forest disturbance detection". In: *Remote Sensing of Environment* 97.3, pp. 301–310.

Hecht, Susanna B. and Alexander Cockburn (2010). *The fate of the forest : developers, destroyers, and defenders of the Amazon*. Chicago ; London: University of Chicago Press. ISBN: 0226322726.

Hermann, Sebastian, Asami Miketa, and Nicolas Fichaux (2014). *Estimating the renewable energy potential in Africa - A GIS-based approach, IRENA-KTH working paper*. Tech. rep. International Renewable Energy Agency (IRENA).

Hernandez, Rebecca R., Madison K. Hoffacker, and Christopher B. Field (2014). "Land-Use Efficiency of Big Solar". In: *Environmental Science & Technology* 48.2, pp. 1315–1323. ISSN: 0013-936X. DOI: 10.1021/es4043726. URL: http://dx.doi.org/10.1021/es4043726 (visited on 04/24/2014).

Hernandez, R.R. et al. (2014). "Environmental impacts of utility-scale solar energy". In: *Renewable and Sustainable Energy Reviews* 29, pp. 766–779. ISSN: 1364-0321. DOI: 10.1016/j.rser.2013.08.041. URL: http://www.sciencedirect.com/science/article/pii/S1364032113005819 (visited on 10/15/2013).

Ho, Daniel E. et al. (2011). "MatchIt: Nonparametric Preprocessing for Parametric Causal Inference". en. In: *Journal of Statistical Software* 42.8. ISSN: 1548-7660. DOI: 10.18637/jss.v042.i08. URL: http://www.jstatsoft.org/v42/i08/ (visited on 05/09/2018).

Hoppock, David C. and Dalia Patiño-Echeverri (2010). "Cost of Wind Energy: Comparing Distant Wind Resources to Local Resources in the Midwestern United States". In: *Environmental Science & Technology* 44.22, pp. 8758–8765. ISSN: 0013-936X. DOI: 10.1021/es100751p. URL: http://dx.doi.org/10.1021/es100751p (visited on 05/11/2016).

Housman, Ian et al. (2015). *Monitoring forest change in southeast Asia: case studies for USAID Lowering Emissions in Asia's Forests*. Tech. rep. RSAC-10108-RPT1. Salt Lake City, UT: U.S. Department of Agriculture, Forest Service, Remote Sensing Applications Center. URL: http://www.leafasia.org/sites/default/files/public/resources/USAIDLEAF-RSAC-ForestLossReport-November2015-Revised.pdf.

Huang, C. et al. (2002). "Derivation of a tasselled cap transformation based on Landsat 7 at-satellite reflectance". en. In: *International Journal of Remote Sensing* 23.8, pp. 1741–1748. ISSN: 0143-1161, 1366-5901. DOI: 10.1080/01431160110106113. URL: http://www.tandfonline.com/doi/abs/10.1080/01431160110106113 (visited on 05/09/2018).

IEA (2017). *World Energy Outlook 2017*. URL: https://www.iea.org/weo2017/ (visited on 04/18/2018).

IEC (1998). *International Standard IEC 61400-12- Wind Turbine Generator Systems - Part 12: Wind turbine power performance testing*.

Institute, Vaasa Energy (2011). *Choice of Turbine*. URL: http://www.vindkraft.fi/.

IRENA (2013a). *Concentrating Solar Power - Technology Brief*. Tech. rep. International Renewable Energy Agency (IRENA).

— (2013b). *Renewable power generation costs in 2012: An overview*. Tech. rep. International Renewable Energy Agency (IRENA).

Jordaan, Sarah M. (2010). "The land use footprint of energy extraction in Alberta". PhD thesis. Calgary, Alberta: University of Calgary. URL: http://www.keith.seas.harvard.edu/Thesis/TH9_Jordaan_2010.pdf (visited on 04/09/2013).

Kahn, Robert D. (2000). "Siting Struggles: The Unique Challenge of Permitting Renewable Energy Power Plants". In: *The Electricity Journal* 13.2, pp. 21–33. ISSN: 1040-6190. DOI: 10.1016/S1040-6190(00)00085-3. URL: http://www.sciencedirect.com/science/article/pii/S1040619000000853 (visited on 04/09/2013).

Katzenstein, Warren, Emily Fertig, and Jay Apt (2010). "The variability of interconnected wind plants". In: *Energy Policy* 38.8, pp. 4400–4410. ISSN: 0301-4215. DOI: 10.1016/j.

enpol.2010.03.069. URL: http://www.sciencedirect.com/science/article/pii/S0301421510002594 (visited on 09/16/2016).

Kauth, R J and G S Thomas (1976). "The Tasselled Cap – A Graphic Description of the Spectral-Temporal Development of Agricultural Crops as Seen by LANDSAT". en. In: *IEEE: Symposium on Machine Processing of Remotely Sensed Data*, p. 13. URL: https://docs.lib.purdue.edu/cgi/viewcontent.cgi?referer=https://scholar-google-com.libproxy.berkeley.edu/&httpsredir=1&article=1160&context=lars_symp.

Kaza, Nikhil and Marie Patane Curtis (2014). "The Land Use Energy Connection". en. In: *Journal of Planning Literature* 29.4, pp. 355–369. ISSN: 0885-4122. DOI: 10.1177/0885412214542049. URL: https://doi.org/10.1177/0885412214542049 (visited on 04/17/2018).

Kiesecker, Joseph M. et al. (2011). "Win-Win for Wind and Wildlife: A Vision to Facilitate Sustainable Development". In: *PLoS ONE* 6.4, e17566. DOI: 10.1371/journal.pone.0017566. URL: http://dx.doi.org/10.1371/journal.pone.0017566 (visited on 04/09/2013).

King, Gary et al. (2011). "Comparative Effectiveness of Matching Methods for Causal Inference". URL: https://gking.harvard.edu/publications/comparative-effectiveness-matching-methods-causal-inference.

King, J, A Clifton, and Bri-Mathias Hodge (2014). *Validation of Power Output for the WIND Toolkit*. Tech. rep. NREL/TP-5D00-61714. National Renewable Energy Laboratory.

Lake Turkana Wind Power (2015). *The Lake Turkana Wind Power Project – Fact Sheet*. URL: http://www.ltwp.co.ke/the-project/overview (visited on 05/01/2016).

Lantz, Eric, Ryan Wiser, and Maureen Hand (2012). *IEA Wind Task 26: The Past and Future Cost of Wind Energy*. Tech. rep. NREL/TP-6A20-53510. National Renewable Energy Laboratory. URL: http://www.nrel.gov/docs/fy12osti/54526.pdf (visited on 12/07/2014).

Laurance, William F., Ana K. M. Albernaz, et al. (2002). "Predictors of deforestation in the Brazilian Amazon". en. In: *Journal of Biogeography* 29.5-6, pp. 737–748. ISSN: 1365-2699. DOI: 10.1046/j.1365-2699.2002.00721.x. URL: http://onlinelibrary.wiley.com/doi/abs/10.1046/j.1365-2699.2002.00721.x (visited on 05/09/2018).

Laurance, William F., Miriam Goosem, and Susan G. W. Laurance (2009). "Impacts of roads and linear clearings on tropical forests". In: *Trends in Ecology & Evolution* 24.12, pp. 659–669. ISSN: 0169-5347. DOI: 10.1016/j.tree.2009.06.009. URL: http://www.sciencedirect.com/science/article/pii/S0169534709002067 (visited on 05/09/2018).

Liu, Qingsheng et al. (2015). "Comparison of tasselled cap transformations based on the selective bands of Landsat 8 OLI TOA reflectance images". In: *International Journal of Remote Sensing* 36.2, pp. 417–441. ISSN: 0143-1161. DOI: 10.1080/01431161.2014.995274. URL: https://doi.org/10.1080/01431161.2014.995274 (visited on 05/09/2018).

Loftis, Blair (2013). "Co-Location of Wind and Solar ... Anyone Want to Play Nice?" In: *Power Engineering*. URL: http://www.power-eng.com/articles/print/volume-

117/issue-2/departments/view-on-renewables/co-location-of-wind-and-solar-anyone-want-to-play-nice.html (visited on 10/15/2014).

Lopez, Anthony et al. (2012). *U.S. Renewable Energy Technical Potentials: A GIS-Based Analysis*. Tech. rep. NREL/TP-6A20-51946. Golden, CO: National Renewable Energy Laboratory.

Lovich, Jeffrey E. and Joshua R. Ennen (2011). "Wildlife Conservation and Solar Energy Development in the Desert Southwest, United States". en. In: *BioScience* 61.12, pp. 982–992. ISSN: 0006-3568. DOI: 10.1525/bio.2011.61.12.8. URL: http://academic.oup.com/bioscience/article/61/12/982/392612 (visited on 05/09/2018).

Lu, Dengsheng et al. (2004). "Relationships between forest stand parameters and Landsat TM spectral responses in the Brazilian Amazon Basin". In: *Forest Ecology and Management* 198.1, pp. 149–167. ISSN: 0378-1127. DOI: 10.1016/j.foreco.2004.03.048. URL: http://www.sciencedirect.com/science/article/pii/S0378112704003445 (visited on 05/09/2018).

MacDonald, Alexander E. et al. (2016). "Future cost-competitive electricity systems and their impact on US CO2 emissions". en. In: *Nature Climate Change* 6.5, pp. 526–531. ISSN: 1758-678X. DOI: 10.1038/nclimate2921. URL: http://www.nature.com/nclimate/journal/v6/n5/full/nclimate2921.html (visited on 05/11/2016).

Machado, José Alberto da Costa et al. (2004). *Determining factors in the construction of hydro electric power plants in the amazon: reasons for claiming damage payments*. En, En. UNESCO. ISBN: 978-92-9089-076-8. URL: http://bases.bireme.br/cgi-bin/wxislind.exe/iah/online/?IsisScript=iah/iah.xis&src=google&base=REPIDISCA&lang=p&nextAction=lnk&exprSearch=28249&indexSearch=ID (visited on 05/08/2018).

Macknick, Jordan et al. (2011). *A Review of Operational Water Consumption and Withdrawal Factors for Electricity Generating Technologies*. Tech. rep. NREL/TP-6A20-50900. Golden, CO: National Renewable Energy Laboratory.

Magalhães, SMSB and Francisco Hernandez (2009). "Painel de especialistas: análise crítica do Estudo de Impacto Ambiental do Aproveitamento Hidrelétrico de Belo Monte". In: *Belém:[sn]* 29.

Mai, Trieu et al. (2012). *Exploration of High Penetration Renewable Electricity Futures, Volume I of Renewable Energy Futures Study*. Tech. rep. NREL/TP-6A20-52409-1. Golden, CO: National Renewable Energy Laboratory. URL: http://www.nrel.gov/analysis/re_futures/.

McDonald, Robert I. et al. (2009). "Energy Sprawl or Energy Efficiency: Climate Policy Impacts on Natural Habitat for the United States of America". In: *PLoS ONE* 4.8, e6802. DOI: 10.1371/journal.pone.0006802. URL: http://dx.doi.org/10.1371/journal.pone.0006802 (visited on 03/07/2014).

McElroy, Michael B. et al. (2009). "Potential for Wind-Generated Electricity in China". en. In: *Science* 325.5946, pp. 1378–1380. ISSN: 0036-8075, 1095-9203. DOI: 10.1126/science.1175706. URL: http://www.sciencemag.org/content/325/5946/1378 (visited on 08/13/2015).

Mertens, Benoit and Eric F. Lambin (2000). "Land-cover-change trajectories in southern Cameroon". In: *Annals of the association of American Geographers* 90.3, pp. 467–494.

Mills, Andrew (2010). "Implications of Wide-Area Geographic Diversity for Short- Term Variability of Solar Power". In: *Lawrence Berkeley National Laboratory*. URL: http://escholarship.org/uc/item/9mz3w055 (visited on 01/26/2015).

Mills, Andrew and Ryan Wiser (2012). *Changes in the Economic Value of Variable Generation at High Penetration Levels: A Pilot Case Study of California*. Tech. rep. LBNL-5445E. Lawrence Berkeley National Laboratory.

Moretto, Evandro Mateus et al. (2012). "Histórico, tendências e perspectivas no planejamento espacial de usinas hidrelétricas brasileiras: a antiga e atual fronteira Amazônica". In: *Ambiente & Sociedade* 15.3, pp. 141–164. ISSN: 1414-753X. DOI: 10.1590/S1414-753X2012000300009. URL: http://www.scielo.br/scielo.php?script=sci_abstract&pid=S1414-753X2012000300009&lng=en&nrm=iso&tlng=pt (visited on 05/08/2018).

Morton, Douglas C. et al. (2006). "Cropland expansion changes deforestation dynamics in the southern Brazilian Amazon". en. In: *Proceedings of the National Academy of Sciences* 103.39, pp. 14637–14641. ISSN: 0027-8424, 1091-6490. DOI: 10.1073/pnas.0606377103. URL: http://www.pnas.org/content/103/39/14637 (visited on 05/09/2018).

Mulvaney, Dustin (2017). "Identifying the roots of Green Civil War over utility-scale solar energy projects on public lands across the American Southwest". en. In: *Journal of Land Use Science* 12.6, pp. 493–515. ISSN: 1747-423X, 1747-4248. DOI: 10.1080/1747423X.2017.1379566. URL: https://www.tandfonline.com/doi/full/10.1080/1747423X.2017.1379566 (visited on 04/17/2018).

National Energy Technology Laboratory (2014). *Life Cycle Analysis of Natural Gas Extraction and Power Generation*. Tech. rep. DOE/NETL-2014/1646. URL: http://www.netl.doe.gov/File%20Library/Research/Energy%20Analysis/Life%20Cycle%20Analysis/NETL-NG-Power-LCA-29May2014.pdf (visited on 10/15/2014).

National Research Council (2007). *Environmental Impacts of Wind-Energy Projects*. ISBN: 978-0-309-10834-8. URL: http://www.nap.edu/catalog.php?record_id=11935 (visited on 10/15/2013).

Nelson, James et al. (2012). "High-resolution modeling of the western North American power system demonstrates low-cost and low-carbon futures". In: *Energy Policy* 43, pp. 436–447. ISSN: 0301-4215. DOI: 10.1016/j.enpol.2012.01.031. URL: http://www.sciencedirect.com/science/article/pii/S0301421512000365 (visited on 11/01/2015).

Niang, I. et al. (2014). "Africa". In: *Climate Change 2014: Impacts, Adaptation, and Vulnerability. Part B: Regional Aspects. Contribution of Working Group II to the Fifth Assessment Report of the Intergovernmental Panel on Climate Change*. http://www.ipcc.ch/report/ar5/wg2/. Cambridge, United Kingdom and New York, NY, USA: Cambridge University Press, pp. 1199–1265. URL: http://www.ipcc.ch/pdf/assessment-report/ar5/wg2/WGIIAR5-Chap22_FINAL.pdf.

Nielsen, Rich and John Sheffield (2009). "Matching with Time-Series Cross-Sectional Data".

Olson, David M. et al. (2001). "Terrestrial Ecoregions of the World: A New Map of Life on Earth A new global map of terrestrial ecoregions provides an innovative tool for conserving biodiversity". en. In: *BioScience* 51.11, pp. 933–938. ISSN: 0006-3568, 1525-3244. DOI: 10.1641/0006-3568(2001)051[0933:TEOTWA]2.0.CO;2. URL: http://bioscience.oxfordjournals.org/content/51/11/933 (visited on 03/06/2015).

Omitaomu, Olufemi A. et al. (2012). "Adapting a GIS-based multicriteria decision analysis approach for evaluating new power generating sites". In: *Applied Energy* 96, pp. 292–301. ISSN: 0306-2619. DOI: 10.1016/j.apenergy.2011.11.087. URL: http://www.sciencedirect.com/science/article/pii/S0306261911007938 (visited on 10/24/2012).

Ong, Sean, Clinton Campbell, Paul Denholm, et al. (2013). *Land-Use Requirements for Solar Power Plants in the United States*. Tech. rep. NREL/TP-6A20-56290. Golden, CO: National Renewable Energy Laboratory.

Ong, Sean, Clinton Campbell, and Garvin Heath (2012). *Land Use for Wind, Solar, and Geothermal Electricity Generation Facilities in the United States*. A report from the National Renewable Energy Laboratory to the Electric Power Research Institute. National Renewable Energy Laboratory.

Orr, Stuart et al. (2012). "Dams on the Mekong River: Lost fish protein and the implications for land and water resources". In: *Global Environmental Change* 22.4, pp. 925–932.

Outka, Uma (2011). "The Renewable Energy Footprint". In: *Stanford Environmental Law Journal* 30, p. 241. URL: http://heinonline.org/HOL/Page?handle=hein.journals/staev30&id=247&div=&collection=journals (visited on 03/05/2014).

Pack, Shalynn M. et al. (2016). "Protected area downgrading, downsizing, and degazettement (PADDD) in the Amazon". In: *Biological Conservation* 197, pp. 32–39. ISSN: 0006-3207. DOI: 10.1016/j.biocon.2016.02.004. URL: http://www.sciencedirect.com/science/article/pii/S0006320716300386 (visited on 05/09/2018).

Papadogeorgou, Georgia, Christine Choirat, and Corwin M. Zigler (2018). "Adjusting for unmeasured spatial confounding with distance adjusted propensity score matching". en. In: *Biostatistics*. DOI: 10.1093/biostatistics/kxx074. URL: http://academic.oup.com/biostatistics/advance-article/doi/10.1093/biostatistics/kxx074/4818356 (visited on 05/09/2018).

Peterseim, Juergen H. et al. (2014). "Concentrating solar power hybrid plants – Enabling cost effective synergies". In: *Renewable Energy*. Renewable Energy for Sustainable Development and Decarbonisation 67, pp. 178–185. ISSN: 0960-1481. DOI: 10.1016/j.renene.2013.11.037. URL: http://www.sciencedirect.com/science/article/pii/S0960148113006150 (visited on 05/09/2018).

Pfaff, Alexander S. P. (1999). "What Drives Deforestation in the Brazilian Amazon?: Evidence from Satellite and Socioeconomic Data". In: *Journal of Environmental Economics and Management* 37.1, pp. 26–43. ISSN: 0095-0696. DOI: 10.1006/jeem.1998.1056. URL: http://www.sciencedirect.com/science/article/pii/S0095069698910567 (visited on 05/08/2018).

Pueyo, Ana, Simon Bawakyillenuo, and Helen Osiolo (2016). *Cost and Returns of Renewable Energy in Sub-Saharan Africa: A Comparison of Kenya and Ghana*. Tech. rep. Institute of Development Studies.

R. Core Team (2017). *R: A language and environment for statistical computing. R Foundation for Statistical Computing, Vienna, Austria. 2016*.

Radeloff, Volker C. et al. (2010). "Housing growth in and near United States protected areas limits their conservation value". In: *Proceedings of the National Academy of Sciences of the United States of America* 107.2, pp. 940–945. ISSN: 0027-8424. DOI: 10.1073/pnas.0911131107. URL: http://www.ncbi.nlm.nih.gov/pmc/articles/PMC2818924/ (visited on 01/11/2015).

Ramachandra, T.V. and B.V. Shruthi (2007). "Spatial mapping of renewable energy potential". In: *Renewable and Sustainable Energy Reviews* 11.7, pp. 1460–1480. ISSN: 1364-0321. DOI: 10.1016/j.rser.2005.12.002. URL: http://www.sciencedirect.com/science/article/pii/S1364032106000050 (visited on 02/19/2013).

Reichenberg, Lina, Filip Johnsson, and Mikael Odenberger (2014). "Dampening variations in wind power generation—the effect of optimizing geographic location of generating sites". en. In: *Wind Energy* 17.11, pp. 1631–1643. ISSN: 1099-1824. DOI: 10.1002/we.1657. URL: http://onlinelibrary.wiley.com/doi/10.1002/we.1657/abstract (visited on 05/12/2016).

Renewable Energy Policy Network for the 21st Century (2015). *REN21 Status of Renewables Interactive Map*. URL: http://www.ren21.net/status-of-renewables/ren21-interactive-map/ (visited on 05/01/2016).

Roques, Fabien, Céline Hiroux, and Marcelo Saguan (2010). "Optimal wind power deployment in Europe—A portfolio approach". In: *Energy Policy*. Large-scale wind power in electricity markets with Regular Papers 38.7, pp. 3245–3256. ISSN: 0301-4215. DOI: 10.1016/j.enpol.2009.07.048. URL: http://www.sciencedirect.com/science/article/pii/S030142150900545X (visited on 07/15/2015).

Rosnes, Orvika and Haakon Vennemo (2012). "The cost of providing electricity to Africa". In: *Energy Economics* 34.5, pp. 1318–1328. ISSN: 0140-9883. DOI: 10.1016/j.eneco.2012.06.008. URL: http://www.sciencedirect.com/science/article/pii/S0140988312001144 (visited on 06/01/2016).

Roy, D. P. et al. (2016). "Characterization of Landsat-7 to Landsat-8 reflective wavelength and normalized difference vegetation index continuity". In: *Remote Sensing of Environment*. Landsat 8 Science Results 185, pp. 57–70. ISSN: 0034-4257. DOI: 10.1016/j.rse.2015.12.024. URL: http://www.sciencedirect.com/science/article/pii/S0034425715302455 (visited on 05/09/2018).

Saadi, Nawfal, Asami Miketa, and Mark Howells (2015). "African Clean Energy Corridor: Regional integration to promote renewable energy fueled growth". In: *Energy Research & Social Science*. Special Issue on Renewable Energy in Sub-Saharan AfricaContributions from the Social Sciences 5, pp. 130–132. DOI: 10.1016/j.erss.2014.12.020. URL: http://www.sciencedirect.com/science/article/pii/S2214629614001546 (visited on 08/14/2015).

Sanderson, Eric W. et al. (2002). "The Human Footprint and the Last of the Wild". In: *BioScience* 52.10, pp. 891–904. ISSN: 0006-3568. DOI: 10.1641/0006-3568(2002)052[0891:THFATL]2.0.CO;2. URL: http://www.bioone.org/doi/abs/10.1641/0006-3568(2002)052[0891:THFATL]2.0.CO%3B2 (visited on 03/06/2015).

Sanoh, Aly et al. (2014). "The economics of clean energy resource development and grid interconnection in Africa". In: *Renewable Energy* 62, pp. 598–609. DOI: 10.1016/j.renene.2013.08.017. URL: http://www.sciencedirect.com/science/article/pii/S0960148113004199 (visited on 07/06/2015).

Schneider, A., M. A. Friedl, and D. Potere (2009). "A new map of global urban extent from MODIS satellite data". en. In: *Environmental Research Letters* 4.4, p. 044003. ISSN: 1748-9326. DOI: 10.1088/1748-9326/4/4/044003. URL: http://stacks.iop.org/1748-9326/4/i=4/a=044003 (visited on 05/09/2018).

Shirley, Rebekah, Yuliya Shmidt, and Nika Rogers (2012). *Crossing the Finish Line: An Assessment of Contract Failure Rates in California's Race to 33 Percent Renewable Energy*. Tech. rep. Division of Ratepayer Advocates, California Public Utilities Commission.

Sioshansi, Ramteen and Paul Denholm (2013). "Transmission Benefits of Co-Locating Concentrating Solar Power and Wind". In: *IEEE Transactions on Sustainable Energy* 99, pp. 1–9.

Smil, Vaclav (2005). *Energy at the Crossroads: Global Perspectives and Uncertainties*. The MIT Press. ISBN: 0-262-69324-0.

Soares-Filho, Britaldo et al. (2010). "Role of Brazilian Amazon protected areas in climate change mitigation". en. In: *Proceedings of the National Academy of Sciences* 107.24, pp. 10821–10826. ISSN: 0027-8424, 1091-6490. DOI: 10.1073/pnas.0913048107. URL: http://www.pnas.org/content/107/24/10821 (visited on 05/09/2018).

SolarPraxis and Reiner Lemoine Institute (2013). *Study Reveals Solar and Wind Power Plants to be A Perfect Combination: Minimal shading losses and yields up to twice as high*. URL: http://www.solarpraxis.de/en/company/news-media/detailview/article/Studie_Solar_und_Windkraftanlagen_ideal_als_Komb/ (visited on 03/01/2014).

Song, Conghe et al. (2001). "Classification and change detection using Landsat TM data: when and how to correct atmospheric effects?" In: *Remote sensing of Environment* 75.2, pp. 230–244.

Sonter, L. J., D. J. Barrett, et al. (2015). "A Land System Science meta-analysis suggests we underestimate intensive land uses in land use change dynamics". In: *Journal of Land Use Science* 10.2, pp. 191–204.

Sonter, L. J., Diego Herrera, et al. (2017). "Mining drives extensive deforestation in the Brazilian Amazon". en. In: *Nature Communications* 8.1, p. 1013. ISSN: 2041-1723. DOI: 10.1038/s41467-017-00557-w. URL: http://www.nature.com/articles/s41467-017-00557-w (visited on 05/08/2018).

South Africa Department of Energy, Eskom, and National Energy Regulator of South Africa (2016). *South Africa Independent Power Producers Programme*. URL: http://www.ipprenewables.co.za/#page/303 (visited on 05/01/2016).

Southern Africa Power Pool (2014). *SAPP Annual Report - 2014*. Tech. rep.

Southern Africa Power Pool (2015). *SAPP Annual Report - 2015*. Tech. rep. URL: http://www.sapp.co.zw/areports.html.

Southern Africa Power Pool and Nexant (2007). *SAPP Regional Generation and Transmission Expansion Plan Study*. Tech. rep.

Sovacool, Benjamin K., Alex Gilbert, and Daniel Nugent (2014). "Risk, innovation, electricity infrastructure and construction cost overruns: Testing six hypotheses". In: *Energy* 74, pp. 906–917. ISSN: 0360-5442. DOI: 10.1016/j.energy.2014.07.070. URL: http://www.sciencedirect.com/science/article/pii/S0360544214008925 (visited on 08/21/2015).

Stoms, David M., Stephanie L. Dashiell, and Frank W. Davis (2013). "Siting solar energy development to minimize biological impacts". In: *Renewable Energy* 57, pp. 289–298. ISSN: 0960-1481. DOI: 10.1016/j.renene.2013.01.055. URL: http://www.sciencedirect.com/science/article/pii/S0960148113000943 (visited on 04/09/2013).

Stuart, Elizabeth A. (2010). "Matching methods for causal inference: A review and a look forward". In: *Statistical science : a review journal of the Institute of Mathematical Statistics* 25.1, pp. 1–21. ISSN: 0883-4237. DOI: 10.1214/09-STS313. URL: https://www.ncbi.nlm.nih.gov/pmc/articles/PMC2943670/ (visited on 05/09/2018).

Sustainable Development Solutions Network (SDSN) and Institute for Sustainable Development and International Relations (IDDRI) (2013). *The Deep Decarbonization Pathway Project*. URL: http://beta.unsdsn.org/what-we-do/deep-decarbonization-pathways/ (visited on 03/10/2014).

Svenningsen, Lasse (2010). *Power Curves Air Density Correction and Other Power Curve Options in WindPRO*.

Taylor, Michael et al. (2015). *Renewble Power Generation Costs in 2014*. Tech. rep. International Renewable Energy Agency (IRENA). URL: http://www.irena.org/DocumentDownloads/Publications/IRENA_RE_Power_Costs_2014_report.pdf (visited on 08/20/2015).

Tefera, Bezuayehu and Geert Sterk (2008). "Hydropower-induced land use change in Fincha'a watershed, western Ethiopia: Analysis and impacts". In: *Mountain Research and Development* 28.1, pp. 72–80.

Tegen, S. et al. (2013). *2011 Cost of Wind Energy Review*. Tech. rep. NREL/TP-5000-56266. National Renewable Energy Laboratory.

Tewkesbury, Andrew P. et al. (2015). "A critical synthesis of remotely sensed optical image change detection techniques". In: *Remote Sensing of Environment* 160, pp. 1–14. ISSN: 0034-4257. DOI: 10.1016/j.rse.2015.01.006.

Trainor, Anne M., Robert I. McDonald, and Joseph Fargione (2016). "Energy Sprawl Is the Largest Driver of Land Use Change in United States". en. In: *PLOS ONE* 11.9, e0162269. ISSN: 1932-6203. DOI: 10.1371/journal.pone.0162269. URL: http://journals.plos.org/plosone/article?id=10.1371/journal.pone.0162269 (visited on 05/09/2018).

Tundisi, José Galizia, Marco Aurélio Santos, and Carlos Frederico S. Menezes (2003). *Tucurui reservoir and hydroelectric power plant: Management experience brief*. URL: http://citeseerx.ist.psu.edu/viewdoc/summary?doi=10.1.1.459.2715 (visited on 05/07/2018).

UNEP (2017). "Green Energy Choices: the Benefits, Risks and Trade-Offs of Low-Carbon Technologies for Electricity Production". en. In: *Resource Panel*. URL: http://www.resourcepanel.org/reports/green-energy-choices-benefits-risks-and-trade-offs-low-carbon-technologies-electricity (visited on 04/17/2018).

U.S. BLM and U.S. DOE (2012). *Final Programmatic Environmental Impact Statement (PEIS) for Solar Energy Development in Six Southwestern States*. Tech. rep. FES 12-24; DOE/EIS-0403, Volumes 1–7. URL: http://solareis.anl.gov/documents/fpeis/index.cfm.

U.S. Department of Energy. *EnergyPlus Energy Simulation Software Weather Data*. Tech. rep. URL: http://apps1.eere.energy.gov/buildings/energyplus/cfm/weather_data2.cfm/region=1_africa_wmo_region_1.

U.S. Energy Information Administration (2016). *Cost and Performance Characteristics of New Generating Technologies, Annual Energy Outlook 2016*. Tech. rep. URL: http://www.eia.gov/forecasts/aeo/assumptions/pdf/table_8.2.pdf.

US. Geological Survey and National Gap Analysis Program (2013). *Standards and Methods Manual for State Data Stewards of the Protected Areas Databse of the U.S.*

Vajjhala, Shalini P. and Paul S. Fischbeck (2007). "Quantifying siting difficulty: A case study of US transmission line siting". In: *Energy Policy* 35.1, pp. 650–671. ISSN: 0301-4215. DOI: 10.1016/j.enpol.2005.12.026. URL: http://www.sciencedirect.com/science/article/pii/S0301421506000048 (visited on 04/09/2013).

VALENÇA, Waleska Floraci de Seixas (1992). "A Dimensão urbana dos impactos da hidrelétrica de Tucuruí." PhD thesis. Rio de Janeiro: COPPE UFRJ.

Veatch, Black & and NREL (2012). *Cost and performance data for power generation technologies*. Tech. rep. National Renewable Energy Laboratory.

WECC EDTF (2011). *Environmental Recommendations for Transmission Planning*. Tech. rep., p. 170. URL: http://www.wecc.biz/committees/BOD/TEPPC/SPSG/EDTF/default.aspx.

Wei, Max et al. (2013). "Deep carbon reductions in California require electrification and integration across economic sectors". en. In: *Environmental Research Letters* 8.1, p. 014038. ISSN: 1748-9326. DOI: 10.1088/1748-9326/8/1/014038. URL: http://iopscience.iop.org/1748-9326/8/1/014038 (visited on 10/15/2013).

Weng, Lingfei et al. (2013). "Mineral industries, growth corridors and agricultural development in Africa". In: *Global Food Security* 2.3, pp. 195–202. ISSN: 2211-9124. DOI: 10.1016/j.gfs.2013.07.003. URL: http://www.sciencedirect.com/science/article/pii/S2211912413000357 (visited on 05/08/2018).

Williams, James H., Andrew DeBenedictis, et al. (2012). "The Technology Path to Deep Greenhouse Gas Emissions Cuts by 2050: The Pivotal Role of Electricity". en. In: *Science* 335.6064, pp. 53–59. ISSN: 0036-8075, 1095-9203. DOI: 10.1126/science.1208365. URL: http://www.sciencemag.org/content/335/6064/53 (visited on 10/10/2012).

Williams, James H., Benjamin Haley, et al. (2014). *Pathways to Deep Decarbonization in the United State*. Tech. rep. Sustainable Development Solutions Network, Institute for Sustainable Development, and International Relations.

Winemiller, K. O. et al. (2016). "Balancing hydropower and biodiversity in the Amazon, Congo, and Mekong". en. In: *Science* 351.6269, pp. 128–129. ISSN: 0036-8075, 1095-9203. DOI: 10.1126/science.aac7082. URL: http://science.sciencemag.org/content/351/6269/128 (visited on 05/29/2016).

Wiser, R. H. and Mark Bolinger (2013). *2012 Wind Technologies Market Report*. Tech. rep. LBNL-6356E. Lawrence Berkeley National Laboratory.

Wiser, R. et al. (2012). *Recent Developments in the Levelized Cost of Energy from U.S. Wind Power Projects*.

World Bank (2014). "Africa's Growth Set to Reach 5.2 percent in 2014 With Strong Investment Growth and Household Spending". In: *The World Bank*. URL: http://www.worldbank.org/en/news/press-release/2014/04/07/africas-growth-set-to-reach-52-percent-in-2014-with-strong-investment-growth-and-household-spending (visited on 11/04/2015).

Wu, Grace C., Ranjit Deshmukh, et al. (2015). *Renewable Energy Zones for the Africa Clean Energy Corridor*. LBNL#187271. International Renewable Energy Agency and Lawrence Berkeley National Laboratory.

Wu, Grace C., Margaret S. Torn, and James H. Williams (2015). "Incorporating Land-Use Requirements and Environmental Constraints in Low-Carbon Electricity Planning for California". In: *Environmental Science & Technology*. ISSN: 0013-936X. DOI: 10.1021/es502979v. URL: http://dx.doi.org/10.1021/es502979v (visited on 02/08/2015).

Zarfl, Christiane et al. (2015). "A global boom in hydropower dam construction". en. In: *Aquatic Sciences* 77.1, pp. 161–170. ISSN: 1015-1621, 1420-9055. DOI: 10.1007/s00027-014-0377-0. URL: http://link.springer.com/article/10.1007/s00027-014-0377-0 (visited on 05/08/2018).

Zeileis, Achim (2006). "Object-oriented Computation of Sandwich Estimators". en. Paper. Department of Statistics, Mathematics, WU Vienna University of Economics, and Business, Vienna. URL: http://epub.wu.ac.at/1644/ (visited on 05/09/2018).